JOURNAL OF CAVE AND KARST STUDIES

August 2000
Volume 62 Number 2
ISSN 1090-6924
A Publication of the National Speleological Society

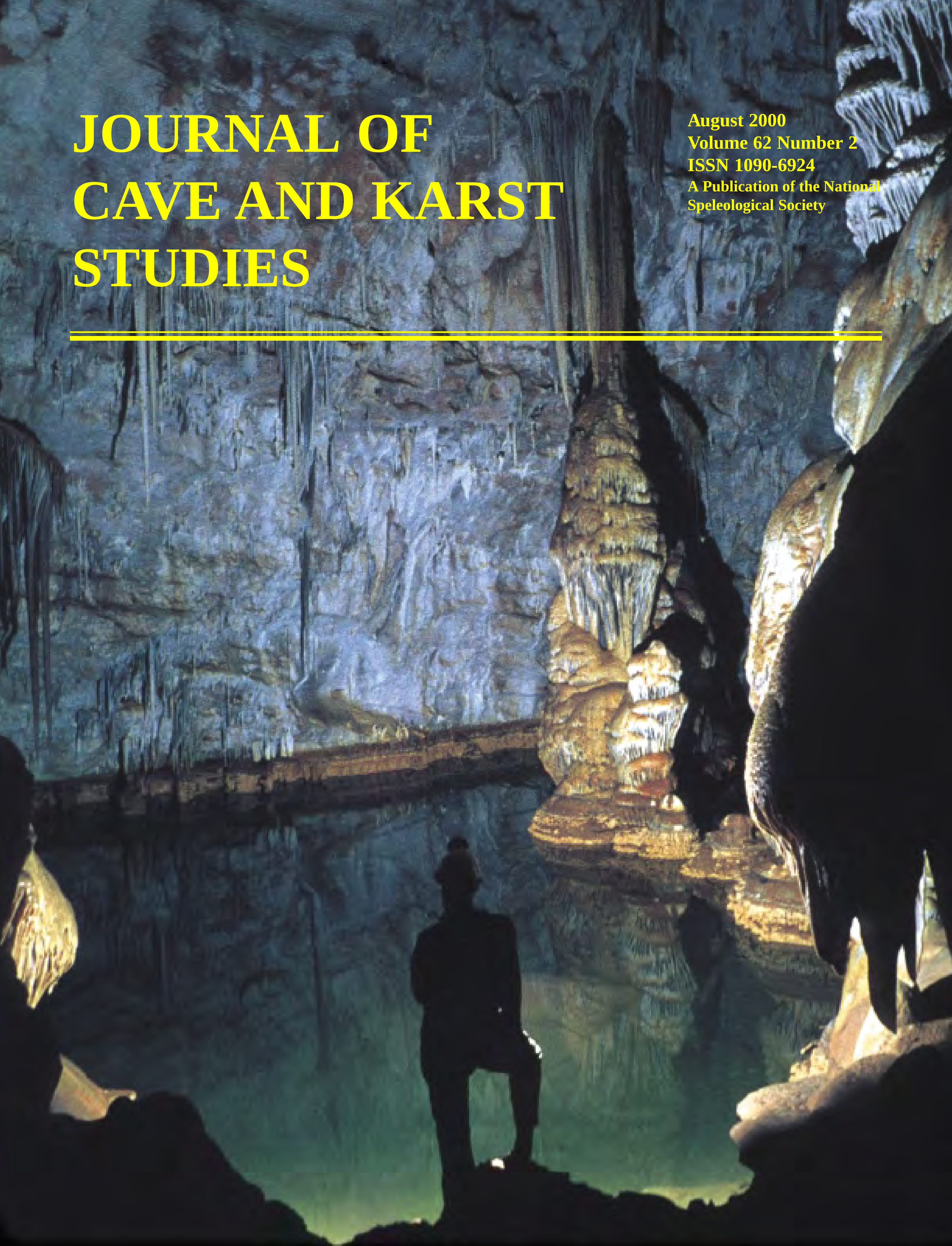

Journal of Cave and Karst Studies
of the National Speleological Society

Volume 62 Number 2 August 2000

CONTENTS

The *Journal of Cave and Karst Studies* (ISSN 1090-6924) is a multi-disciplinary, refereed journal published three times a year by the National Speleological Society, 2813 Cave Avenue, Huntsville, Alabama 35810-4431; (256) 852-1300; FAX (256) 851-9241, e-mail: nss@caves.org; World Wide Web: http://www.caves.org/~nss/. The annual subscription fee, worldwide, by surface mail, is $18 US. Airmail delivery outside the United States of both the *NSS News* and the *Journal of Cave and Karst Studies* is available for an additional fee of $40 (total $58); The *Journal of Cave and Karst Studies* is not available alone by airmail. Back issues and cumulative indices are available from the NSS office. POSTMASTER: send address changes to the *Journal of Cave and Karst Studies*, 2813 Cave Avenue, Huntsville, Alabama 35810-4431.

Covers: Virgin Cave, Guadalupe Mountains, New Mexico. Photos by J.A. Pisarowicz

INTRODUCTION TO THE CAVES OF THE GUADALUPE MOUNTAINS SYMPOSIUM

HARVEY R. DUCHENE
7216 East Bentley Circle, Englewood, Colorado 80112 USA hduchene@compuserve.com
CAROL A. HILL
17 El Arco Drive, Albuquerque, New Mexico 87123 USA carolannhill@cs.com

Over 25 years ago, in October of 1971, four young geology graduate students—Harvey DuChene, Carol Hill, Dave Jagnow, and Dwight Deal—sat on the floor of the Mystery Room in Carlsbad Cavern, chatting and wondering about the many puzzling features in this most enigmatic of caves. “Fingertips can be pushed ¼ - ¾” into the wall rock,” wrote Jagnow into Hill’s notebook. “Random thoughts on inadequate data,” began Deal’s rambling discourse. “Darndest things I ever saw,” was DuChene’s first remark on encountering some strange-looking krinkled wall blisters, followed by his thoughts on how these cornflake-like speleothems might have formed. Harv ended his comments with the entry: ‘Wild idea for today!’

As these remarks show, we didn’t have a clue as to what was going on—as to how the cave itself had formed; why the bedrock was so corroded and “punky”; why there was a “popcorn line” in certain sections of the cave; why large blocks of gypsum existed on the floor of the cave; what the bluish waxy clay deposits in the cave signified; and what the presence of the calcite spar meant and why it was so highly corroded, even down to a linoleum-like pattern over rock surfaces. We didn’t know it then, but this trip heralded the beginning of a remarkable 25+ year “journey” that would later be referred to by cavers as the “golden age of speleology in the Guads.” The ideas developed in the Guadalupe Mountains during this time span would change the course of speleology, and would also help bring it into the position of a “respectable” science, rather than an amateur effort by a “bunch of grubby cavers.” Now, after almost 30 years and at the beginning of the 21st Century, it seems most appropriate that these ideas should be consolidated into a single work. The result is this Caves of the Guadalupe Mountains Symposium issue.

The Guadalupe Mountains are located in southeastern New Mexico and west Texas, USA, in the Pecos River section of the Great Plains physiographic province (Fig. 1). The mountains are about 110 km long and 25 km wide. They start as low hills near Carlsbad, New Mexico, and increase in prominence southwestward to Guadalupe Peak, the highest point in Texas (2667 msl). Here, on their west face, perpendicular cliffs stand in relief above the Salt Flats below. Along the length of the mountains, Capitan reef rock is exposed and cut by major canyons.

The Guadalupe Mountains are situated at the northern margin of the Chihuahuan Desert. The climate of the region is semiarid to arid, with an average winter temperature of 7°C, an average summer temperature of 27°C, and annual precipitation averaging between about 20-40 cm in the lower elevations and 50 cm in the higher elevations. More than half of the annual rainfall occurs during the summer months of July, August, and September. Vegetation includes cacti, succulents, and desert shrubs in the lower elevations, with transitional to montane coniferous forest on the ridge tops.

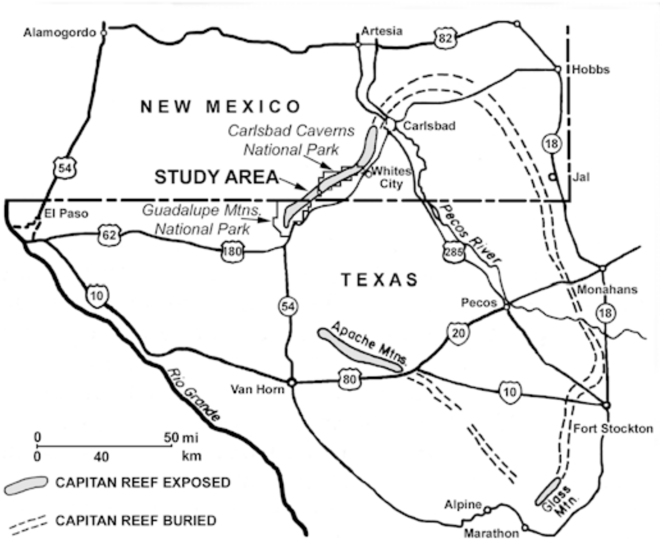

Figure 1. Location map of study area–the Guadalupe Mountains of southeastern New Mexico and west Texas.

The caves in the Guadalupe Mountains are developed within the Capitan Reef Complex, which includes the backreef, reef, and forereef facies of the Permian Capitan Formation. Cave development has been episodic since the Late Permian, but large horizontal cave passages date from about 12 Ma to the present.

Guadalupe caves have an unusual mode of speleogenesis – one involving sulfuric acid and the degassing of hydrogen sulfide from the hydrocarbon-rich Delaware Basin. This concept of basinal degassing relates to more than just the formation of unusual caves. It is also a key factor in understanding the migration of hydrocarbons, the formation of petroleum reservoirs, the deposition of uranium ore, and the origin of Mississippi Valley type (MVT) lead-zinc deposits. Thus, the sulfuric acid speleogenesis of Guadalupe caves, as discussed in this Symposium, is paramount to understanding a number of geologic processes that have heretofore remained enigmatic.

David H. Jagnow, Carol A. Hill, Donald G. Davis, Harvey R. DuChene, Kilmberly I. Cunningham, Diana E. Northup, and J. Michael Queen - History of sulfuric acid theory of speleogenesis in the Guadalupe Mountains, New Mexico. *Journal of Cave and Karst Studies 62*(2): 54-59.

HISTORY OF THE SULFURIC ACID THEORY OF SPELEOGENESIS IN THE GUADALUPE MOUNTAINS, NEW MEXICO

DAVID H. JAGNOW
P. O. Box 93398, Albuquerque, New Mexico 87119-3398 USA
CAROL A. HILL
17 El Arco Drive, Albuquerque, New Mexico 87123-9542 USA
DONALD G. DAVIS
441 S. Kearney St., Denver, Colorado 80224-1237 USA
HARVEY R. DUCHENE
7216 East Bentley Circle, Englewood, Colorado 80112-1197 USA
KIMBERLEY I. CUNNINGHAM
Geo-Microbial Technologies Inc., P.O. Box 132, Ochelata, Oklahoma 74051 USA
DIANA E. NORTHUP
Biology Department, University of New Mexico, Albuquerque, New Mexico 87131 USA
J. MICHAEL QUEEN
814 North Canal Street, Carlsbad, New Mexico 88220 USA

The history of events related to the sulfuric acid theory of cave development in the Guadalupe Mountains, New Mexico, USA, is traced from its earliest beginnings to the present. In the 1970s and early 1980s, when this hypothesis was first introduced, the reaction was one of skepticism. But as evidence mounted, it became more accepted by both the speleological and geological communities. Nearly 30 years after it was introduced, this theory is now almost universally accepted. In the last decade, the sulfuric acid theory of Guadalupe caves has been applied to other caves around the world. It has also impacted such diverse fields as microbiology, petroleum geology, and economic ore geology. This theory now stands as one of the key concepts in the field of speleology.

The caves of the Guadalupe Mountains are located in southeastern New Mexico, near the city of Carlsbad. More than 300 caves are known in the Guadalupes, the most famous being Carlsbad Cavern and Lechuguilla Cave. The caves are believed to have formed by an unusual mode of speleogenesis–one involving sulfuric acid. This theory, as currently understood, is that hydrogen sulfide leaked upward along fractures from hydrocarbon (oil and gas) deposits in the nearby Delaware Basin. Upon reaching oxygenated meteoric groundwater in the Capitan aquifer, sulfuric acid formed, dissolving large voids in the rocks of the Capitan Reef Complex at or below the water table. Cave deposits that are related to this mode of speleogenesis are gypsum blocks and rinds (Fig. 1), native sulfur (Fig. 2), and the minerals endellite (hydrated halloysite) (Fig. 3), alunite, natroalunite, aluminite, hydrobasaluminite, tyuyamunite, and metatyuyamunite.

The topic of this paper is how the theory of a sulfuric acid speleogenesis developed in the Guadalupes, and who the key people were in this process. Only those events or people directly related to the sulfuric acid aspects of cave development will be discussed, although many other important geologic, mineralogical, hydrologic, and biological studies have been done in these caves. This paper is an expanded version of previous presentations given by Jagnow (1986, 1996, 1998).

PRE-SULFURIC ACID THEORY: (1920-1969)

The first geologist to study any Guadalupe cave was Willis T. Lee (1924, 1925a,b), although his publications were primarily of a popular nature. The first technical geologic study was done by J Harlan Bretz, who throughout the summer of 1948 with his dog (R. Riley, Bretz's daughter, pers. comm. 1984), inspected the passages of Carlsbad Cavern and other caves in the Guadalupe Mountains (New, Cottonwood, Black, Hidden, Mudgetts, and McKittrick). Bretz published his now classic *Carlsbad Caverns and other caves of the Guadalupe Mountains, New Mexico* in 1949, wherein he proposed the theory of a phreatic origin for these caves. But Bretz was mystified by the gypsum blocks in Carlsbad and McKittrick, calling them "gypsum flowstone" and stating (p. 454): "It seems that the gypsum can only be the consequence of local pooling during the vadose history, recording temporary conditions when sulfate alone was precipitated. The local source may have been the Permian (Castile) gypsum both outcropping and known in wells close to the base of the near by scarp and higher than these cave chamber floors."

Other investigators, following Bretz's lead, attributed the massive gypsum in the caves to a late-stage back-up of water where the source of the cave gypsum was the Castile Formation of the Delaware Basin (Black 1954; Gale 1957;

Figure 1 (Top Left). Finely laminated (varved) structure in a gypsum block, Texas Trail, Big Room, Carlsbad Cavern. Photo by Dave Jagnow.
Figure 2 (Center Left). Massive sulfur deposits overlain by gypsum, then later penetrated by calcite stalactites, near Ghost Town (GDVB Survey), Lechuguilla Cave. Photo by Larry McLaughlin.

Figure 3 (Bottom Left). Blue-green endellite in Endless Cave. Largest piece of endellite is about 3 cm across. Photo by Peter and Ann Bosted.
Figure 4 (Top Right). Photo of Stephen Egemeier (left).
Figure 5 (Center Right). Speleologists Donald Davis, Michael Queen, Carol Hill, and Dave Jagnow at the Eighth International Congress post-convention field trip at Carlsbad Cavern in August 1981. Photo by Ronal Kerbo.
Figure 6 (Bottom Right). Diana Northup (left) and Penny Boston (right) collecting a sample of corrosion residue.

Good 1957; Sanchez 1964; Bullington 1968). Davies & Moore (1957) also reported the presence of the mineral endellite in Carlsbad Cavern.

SULFURIC ACID THEORY: FIRST DECADE (1970-1979)

Nearly 30 years elapsed before Bretz (1949) was challenged. Stephen Egemeier, in a 1971 report to Carlsbad Caverns National Park, briefly suggested that the large rooms of Carlsbad may have been dissolved by sulfuric acid. Egemeier (fig. 4) based his suggestion on the work he was doing for his PhD dissertation on the Kane Caves in Wyoming (Egemeier 1973).

In 1971-1973, David Jagnow undertook field work in the Guadalupes for his Masters thesis and, independent of Egemeier, also proposed a sulfuric acid origin for these caves. Jagnow (1977, 1978, 1979) attributed the source of sulfuric acid to the oxidation of pyrite in the Yates Formation, basing his model on the work he had done with David Morehouse in the Galena Limestone caves around Dubuque, Iowa (Morehouse 1968). Jagnow recognized that the massive gypsum deposits in Guadalupe caves were the end product of a sulfuric acid reaction.

Also at this time, Donald Davis–who had caved in the Guadalupe Mountains since 1960 and had seen Egemeier's 1971 report in the files of Carlsbad Caverns National Park while working there as a guide–began to consider the subject of sulfuric acid speleogenesis. The earliest published recognition of native sulfur in any Guadalupe cave (Cottonwood) proposed that sulfur was connected in origin to hydrocarbons. Davis (1973: 94) stated: "Petroleum and sulfate rocks, particularly gypsum and anhydrite, are plentiful (in the Guadalupe area)…I assume that the H_2S was mobile in the groundwater and that its hydrocarbon source may have been either near or remote…the dense Yates sandstone just above the cave may have had a capping effect (for H_2S)".

Also in 1973, J. Michael Queen produced the first strong evidence that gypsum had replaced calcite and dolomite over a scale of tens of meters in Guadalupe caves. Queen, along with Art and Peg Palmer (Queen *et al.* 1977), explained the origin of this gypsum replacement by a brine mixing mechanism, where replacement supposedly took place at the interface between fresh water and hypersaline phreatic water bodies. The "brines" were believed to be derived from gypsum and halite units of the Castile Formation in the nearby Delaware Basin. Later, Queen (1981, 1994) considered that the reduction of sulfates could have taken place in anoxic brines beneath the fresh-water zone, in the same way as in seacoast aquifers, and that the mixing between fresh and saline waters could aid in speleogenesis. Queen was also of the opinion that the large cave passages dated from the Late Cretaceous-Early Tertiary Laramide uplift.

Davis in 1979, seeing conflicts and apparent inadequacies in the mechanisms proposed by Jagnow and by Queen *et al.*, first published a critique of Jagnow's pyrite theory, suggesting (citing Egemeier's previously neglected work) that H_2S was a more significant source of sulfuric acid than pyrite. Davis (1980) then expanded this suggestion into a critical review of all the recent hypotheses of speleogenesis, and in this paper was the first to develop a coherent ascending-water model in which Guadalupe caves were viewed as having developed along rising limbs of deeply curving flow paths, where oxygenated meteoric water mixed with sulfidic brine which underwent additional oxidation at the air/water interface.

Concurrently, in the 1970s, Carol Hill was working on the mineralogy of Guadalupe caves. During the course of her mineralogical studies, Hill researched the endellite (hydrated halloysite) deposits in these caves (Fig. 3), and found from her readings that this mineral indicated the former presence of sulfuric acid. This origin corresponded to what Egemeier, Jagnow, and Davis had been hypothesizing, and, in late 1979, Hill had the first sulfur isotope determination performed on a sample of gypsum block collected from the Big Room, Carlsbad Cavern ($\delta^{34}S$ = -13.9‰). Hill immediately realized the importance of this analysis: the presence of isotopically light sulfur proved that the gypsum could not have been derived from the Castile Formation ($\delta^{34}S$ = +10.3‰, avg.), but had to have originated from hydrocarbons.

SULFURIC ACID THEORY: SECOND DECADE (1980-1989)

Hill reported additional sulfur isotope analyses on gypsum and native sulfur in a manuscript she sent to Carlsbad Caverns National Park in 1980. She also presented a condensed paper of her data at the Eighth International Congress of Speleology in Bowling Green, Kentucky (Hill 1981), after which a number of Guadalupe researchers gathered at Carlsbad Cavern for a post-Congress field trip (Fig. 5). A short time later, Douglas Kirkland (1982) performed additional sulfur isotope analyses on the gypsum blocks of the Big Room.

In 1985, Stephen Egemeier died after a long illness, and his *Theory for the origin of Carlsbad Caverns* was posthumously published in 1987 with the help of the Palmers. Also in 1987, Hill published a lengthy bulletin on the *Geology of Carlsbad Cavern and other caves of the Guadalupe Mountains, New Mexico and Texas*. In this tome, Hill detailed the possible connection between the presence of sulfuric acid in the caves, with hydrocarbon and economic sulfur deposits in the Delaware Basin, and with Mississippi Valley-type (MVT) sulfide ore deposits in the reef. She also attributed the chert deposits in the Big Room of Carlsbad to a sulfuric acid mechanism. The fact that the New Mexico Bureau of Mines and Mineral Resources published Hill's work shows that this controversial theory was becoming accepted by the geological community.

In May of 1986, a breakthrough dig was made into inner Lechuguilla Cave. Lechuguilla was a virgin cave (beyond the first hundred meters) where all of the speleogenetic features remained pristine. This new discovery provided a unique opportunity to test and expand the ideas of a sulfuric acid speleogenesis model, so the thrust of cave research in the

Guadalupes changed in the late 1980s from Carlsbad to Lechuguilla. From 1986 until the present, Davis published numerous reports in *Rocky Mountain Caving* and elsewhere, documenting the mineralogical and geologic features that characterize a large sulfuric acid cave like Lechuguilla. Two papers from this time period that condense some of these observations related to a sulfuric acid speleogenesis are Davis (1988) and Davis *et al.* (1990).

In 1988, the Palmers began a geologic survey of Lechuguilla and other Guadalupe caves in order to help define the connection between the geomorphic features of the caves and past hydrologic and geochemical dissolution regimes. They also offered insights into the cave patterns present in sulfuric acid caves (Palmer 1991), and were the first to identify alunite, natroalunite, and dickite in Lechuguilla Cave (Palmer & Palmer 1992). Their geochemical/hydrological work from 1988 to the present is summarized in Palmer & Palmer (2000).

In late 1989, Kimberley (Kim) Cunningham of the U.S. Geological Survey initiated an ambitious cave-wide research program in Lechuguilla, utilizing both private and federal funding. This research program was multi-disciplinary and designed to attract investigators in the subdisciplines of cave geology, geochemistry, biology/microbiology, climatology /microclimatology, and paleontology, among others. Cunningham's efforts crossed many of these project lines (e.g., Cunningham & LaRock 1991). Those specifically related to the sulfuric acid theory involved a systematic determination of whole-rock sulfur isotope ratios and the concentration of gases and fluids in two-phase inclusions (Spirakis & Cunningham 1992). The consistent light isotopic ratios and the ubiquitous presence of light-chain aliphatic hydrocarbons suggested that the massive sulfur deposits had formed inorganically beneath the water table, probably in zones of favorable oxygen content (Cunningham *et al.* 1994).

SULFURIC ACID THEORY: THIRD DECADE (1990-1999)

By the early 1990s the sulfuric acid theory had received wide recognition and acceptance among cavers and also by the geological community. This was, perhaps in part, due to Hill's (1990) paper in the *American Association of Petroleum Geologists Bulletin*, and to Palmer's (1991) paper in the *Geological Society of America Bulletin*, where he used Guadalupe Mountain caves as an example of a sulfuric acid-type hypogene speleogenesis.

In 1990, at the suggestion of Cunningham, Harvey DuChene submitted a proposal to Carlsbad Caverns National Park for a five-year inventory project on the mineralogy of Lechuguilla Cave. But, because of the desire of the National Park Service for a more comprehensive study, the scope of this project was expanded to include bedrock geology, paleontology, and speleogenetic features (DuChene 1996). Data on speleogenetic sulfur was published by DuChene in Cunningham *et al.* (1993, 1994), the mineralogical studies were summarized by DuChene (1997), and a description of bedrock features is included in this Symposium (DuChene 2000).

Late in 1992, shortly after the Palmers' find of alunite and natroalunite in Lechuguilla, Victor Polyak identified alunite and natroalunite in Carlsbad Cavern, and alunite in Virgin, Cottonwood, and Endless caves. Polyak, along with Cyndi Mosch (1995), then studied the uranium-vanadium minerals tyuyamunite and metatyuyamunite in Spider Cave, and Polyak, along with Paula Provencio (1998), discovered the minerals aluminite and hydrobasaluminite in Cottonwood Cave. All of these minerals are now considered to be speleogenetic in origin; i.e., related to a sulfuric acid mode of cave dissolution. Polyak *et al.* (1998) published $^{40}Ar/^{39}Ar$ dates on 10 samples of alunite in *Science*, establishing for the first time the approximate absolute ages of four elevation levels in five Guadalupe caves (12-4 Ma).

In the first half of the 1990s, Hill stopped working in the caves of the Guadalupe Mountains *per se*, choosing instead to try to understand how the caves fit into the overall regional geology. The results of Hill's regional geologic work were published in 1996 by the Society of Economic Paleontologists and Mineralogists (Permian Basin section): *Geology of the Delaware Basin–Guadalupe, Apache, and Glass Mountains, New Mexico and Texas*.

Because of the intriguing findings by Cunningham (1991a,b) of bacteria and fungi on mineral surfaces, Diana Northup began microbial studies in Lechuguilla in late 1989 and the early 1990s, utilizing techniques suggested by Clifford Dahm and Lauraine Hawkins (Northup *et al.* 1995; Cunningham *et al.* 1995). Northup's work, in turn, encouraged microbiologist Larry Mallory to begin studying cave bacterial communities that might be used to treat cancer and other diseases, and Penny Boston began studying caves as a parallel environment in the search for extraterrestrial life. Research findings in Lechuguilla eventually prompted Northup and coworkers to visit the Cueva de Villa Luz, Tabasco, Mexico to study microorganismal ecosystems operating in a sulfuric acid cave forming today (Hose & Pisarowicz 1999). In 1998, the team of Dahm, Boston, Northup and Laura Crossey was awarded a three-year, Life in Extreme Environments, National Science Foundation grant to study the geomicrobiological interactions within the caves corrosion residues (Fig. 6). The preliminary results of some aspects of this work are included in this Symposium (Northup *et al.* 2000). The fact that the National Science Foundation has supported their work in Lechuguilla Cave is confirmation that the sulfuric acid theory and related research has finally come of age.

CONCLUSIONS

It has taken almost 30 years for the sulfuric acid theory of cave development to be accepted by the speleological and geological communities. What began as a "far-out" hypothesis in the 1970s has turned into a theory supported by a number of different lines of evidence–geologic, geochemical, mineralogical, and microbial. Now, at least six other caves or cave systems besides those in the Guadalupe Mountains of New Mexico are known to be, or are suspected of being, sulfuric acid caves: (1) the Kane caves, Wyoming, (2) Fiume-Vento Cave, Italy, (3) La Cueva de Villa Luz, Mexico, and (4) Las Brujas Cave, Argentina (Hill 2000); and in addition (5) the Kugitangtou caves, Turkmenistan (Klimchouk *et al.* 1995) and (6) the Redwall caves, Grand Canyon, Arizona (Hill *et al.* 1999). Also, the concept of H_2S degassing of petroleum basins to produce sulfuric acid karst has been expanded to include the generation of hydrocarbon reservoirs (sulfuric acid oil-field karst; Hill 1995) and associated porosity (DuChene 2000); Mississippi Valley-type ore deposits (Hill 1994); and breccia pipe-type uranium deposits (Hill *et al.* 1999). It remains to be seen how this theory will affect other scientific disciplines in the future.

Acknowledgments

All of the authors thank Carlsbad Caverns National Park, Guadalupe Mountains National Park, Lincoln National Forest, and the Bureau of Land Management for their continued support over the last 30 years of research effort. We would especially like to thank Ronal Kerbo, Dale Pate, Jason Richards, Ransom Turner, Jim Goodbar, and Jerry Trout of these agencies for their cooperation and friendship over these many years. We also thank Art and Peg Palmer and Victor Polyak for reviewing this manuscript.

References

Black, T.H. (1954). The origin and development of the Carlsbad Caverns. *New Mexico Geological Society Guidebook 5*:136-142.

Bretz, JH. (1949). Carlsbad Caverns and other caves of the Guadalupe block, New Mexico. *Journal of Geology* 57(5): 447-463.

Bullington, N.R. (1968). Geology of the Carlsbad Caverns. *West Texas Geological Society Guidebook 68-55*: 20-23.

Cunningham, K.I. (1991a). Organic and inorganic composition of colored corrosion residues, Lechuguilla Cave: Preliminary report. *National Speleological Society News 49(8)*: 252, 254.

Cunningham, K.I. (1991b). News scrapbook. *National Speleological Society News 49(11)*: 325.

Cunningham, K.I. & LaRock, E.J. (1991). Recognition of microclimate zones through radon mapping, Lechuguilla Cave, Carlsbad Caverns National Park, New Mexico. *Journal of the Health Physics Society 61(4)*: 493-500.

Cunningham, K.I., DuChene, H.R. & Spirakis, C.S. (1993). Elemental sulfur in caves of the Guadalupe Mountains, New Mexico. *New Mexico Geological Society Guidebook 44th Field Conference, Carlsbad region, New Mexico and west Texas*: 129-136.

Cunningham, K.I., DuChene, H.R., Spirakis, C.S. & McLean, J.S. (1994). Elemental sulfur in caves of the Guadalupe Mountains, New Mexico (abs.). In Sasowsky, I.D. & Palmer, M.V. (eds.) *Breakthroughs in Karst Geomicrobiology and Redox Chemistry*. Karst Waters Institute Special Publication 1: 11-12.

Cunningham, K.I., Northup, D.E, Pollastro, R.M., Wright, W.G., & LaRock, E.J. (1995). Bacteria, fungi, and biokarst in Lechuguilla Cave, Carlsbad Caverns National Park, New Mexico. *Environmental Geology 25(1)*: 2-8.

Davies, W.E. & Moore, G.W. (1957). Endellite and hydromagnesite from Carlsbad Caverns. *Bulletin of the National Speleological Society 19*: 24-25.

Davis, D.G. (1973). Sulfur in Cottonwood Cave, Eddy County, New Mexico: *Bulletin of the National Speleological Society 35(3)*: 89-95.

Davis, D.G. (1979). Geology and speleogenesis of Ogle Cave: discussion. *NSS Bulletin 41(1)*:21-22.

Davis, D.G. (1980). Cave development in the Guadalupe Mountains: a critical review of recent hypotheses. *NSS Bulletin 42(3)*: 42-48.

Davis, D.G. (1988). The uniqueness of Lechuguilla Cave. *National Speleological Society News 46(11)*: 426-430.

Davis, D.G., Palmer, M.V. & Palmer, A.N. (1990). Extraordinary subaqueous speleothems in Lechuguilla Cave, New Mexico. *NSS Bulletin 52(2)*: 70-86.

DuChene, H.R. (1996). Interim report, April 1-September 30, 1996. Lechuguilla Cave Geological and Mineralogical Inventory Project report to Carlsbad Caverns National Park: 22 pp.

DuChene, H.R. (1997). Lechuguilla Cave, New Mexico, USA. In Hill, C.A. & Forti, P., *Cave minerals of the world, 2nd ed*. National Speleological Society, Huntsville, AL: 343-350.

DuChene, H.R. (2000). Bedrock features of Lechuguilla Cave, Guadalupe Mountains, New Mexico. *Journal of Cave and Karst Studies 62*(2): 109-119.

Egemeier, S.J. (1971). A comparison of two types of solution caves. Unpublished report to Carlsbad Caverns National Park, April 12: 7 pp.

Egemeier, S.J. (1973). Cavern development by thermal waters with a possible bearing on ore deposition. Unpublished PhD dissertation, Stanford University: 88 pp.

Egemeier, S.J. (1987). A theory for the origin of Carlsbad Cavern. *NSS Bulletin 49(2)*: 73-76.

Gale, B.T. (1957). Geologic development of the Carlsbad Caverns. In Hayes, P.T. (ed.). Geology of the Carlsbad Caverns East Quadrangle, New Mexico. *U.S. Geological Survey Geologic Quadrangle Map 98*, scale 1:62,500.

Good, J.M. (1957). Non-carbonate deposits of Carlsbad Caverns. *Bulletin of the National Speleological Society 19*: 11-23.

Hill, C.A. (1980). Speleogenesis of Carlsbad Caverns and other caves in the Guadalupe Mountains. Unpublished report to the National Park Service, Forest Service, and Bureau of Land Management: 201 pp.

Hill, C.A. (1981). Speleogenesis of Carlsbad Caverns and other caves in the Guadalupe Mountains. In Beck, B.F. (ed.), *Proceedings of Eighth International Congress of Speleology*, Bowling Green, Kentucky 1: 143-144.

Hill, C.A. (1987). Geology of Carlsbad Cavern and other caves in the Guadalupe Mountains, New Mexico and Texas. *New Mexico Bureau of Mines and Mineral Resources Bulletin 117*: 150 pp.

Hill, C.A. (1990). Sulfuric acid speleogenesis of Carlsbad Cavern and its relationship to hydrocarbons, Delaware Basin, New Mexico and Texas. *American Association of Petroleum Geologists Bulletin 74(11)*: 1685-1694.

Hill, C.A. (1994). Sulfur redox reactions–hydrocarbons, native sulfur, Mississippi Valley-type deposits, and sulfuric acid karst, Delaware Basin, New Mexico and Texas (abs.). In Sasowsky, I.D. & Palmer, M.V., *Breakthroughs in Karst Geomicrobiology and Redox Chemistry*. Karst Waters Institute, Special Publication 1: 25-28.

Hill, C.A. (1995). H_2S-related porosity and sulfuric acid oil-field karst. In Budd, D.A., Saller, A.H. & Harris, P.M. (eds.).*Unconformities in carbonate strata – Their recognition and the rignificance of associated porosity*. American Association of Petroleum Geologists Memoir 61, Ch. 15: 301-306.

Hill, C.A. (1996). Geology of the Delaware Basin – Guadalupe, Apache, and Glass Mountains, New Mexico and Texas. *Society of Economic Paleontologists and Mineralogists, Permian Basin Section, Publication 96-39*: 480 pp.

Hill, C.A. (2000). Sulfuric acid, hypogene karst in the Guadalupe Mountains of New Mexico and West Texas (U.S.A.). In Klimchouk, A.B., Ford, D.C., Palmer, A.N. & Dreybrodt, W. (eds.). *Speleogenesis: Evolution of karst aquifers*. Huntsville, AL, National Speleological Society: 309-316.

Hill, C.A, Polyak, V.J., Buecher, R.H., Buecher, D.C., Provencio, P., & Hill, A.E. (1999). Trip Report: Tsean-Bida Cave and Riverview mine, March 19-21, 1999, and Kaibab trail barite locality, November 18, 1998. Unpublished report to Grand Canyon National Park, September 17, 1999: 68 pp.

Hose, L.D. & Pisarowicz, J.A. (1999). Cueva de Villa Luz, Tabasco, Mexico: Reconnaissance study of an active sulfur spring cave and ecosystem. *Journal of Cave and Karst Studies 6(1)*: 13-21.

Jagnow, D.H. (1977). *Geologic factors influencing speleogenesis in the Capitan Reef Complex, New Mexico and Texas*. Unpublished MS thesis, University of New Mexico: 197 pp.

Jagnow, D.H. (1978). Geology and speleogenesis of Ogle Cave, New Mexico. *NSS Bulletin 40(1)*: 7-18.

Jagnow, D.H. (1979). *Cavern development in the Guadalupe Mountains*. Cave Research Foundation, Columbus, Ohio: 55 pp.

Jagnow, D.H. (1986). Current thoughts on cavern development in the Guadalupe Mountains, New Mexico. In Jagnow, D.H. & DuChene, H.R. (eds.). *Proceedings National Speleological Society Convention*, Tularosa, New Mexico: 85-102.

Jagnow, D.H. (1996). History of sulfuric acid theory of speleogenesis in the Guadalupe Mountains (abs.). *Journal of Cave and Karst Studies 58*(3): 209.

Jagnow, D.H. (1998). History of sulfuric acid theory of speleogenesis in the Guadalupe Mountains (abs.). *Guadalupe Mountains National Park Research and Resource Management Symposium, April 22-25, Carlsbad, New Mexico*: 1 p.

Kirkland, D.W. (1982). Origin of gypsum deposits in Carlsbad Caverns, New Mexico. *New Mexico Geology 4*: 20-21.

Klimchouk, A.B., Nasedkin, V.M. & Cunningham, K.I. (1995). Speleothems of aerosol origin. *NSS Bulletin 57(1)*: 31-42.

Lee, W.T. (1924). A visit to Carlsbad Cavern. *The National Geographic Magazine 45(1)*: 1-40.

Lee, W.T. (1925a). Carlsbad Cavern. *Scientific Monthly 21*:186-190.

Lee, W.T. (1925b). New discoveries in Carlsbad Cavern. *The National Geographic Magazine 48(3)*: 301-319.

Morehouse, D.F. (1968). Cave development via the sulfuric acid reaction. *Bulletin of the National Speleological Society 30(1)*: 1-10.

Northup, D.E., Carr, D.L., Crocker, M.T., Hawkins, L.K., Leonard, P. & Welbourn, W.C. (1995). Biological investigations in Lechuguilla Cave. *NSS Bulletin 56(2)*: 54-63.

Northup, D.E., Dahm, C.N., Melim, L.A., Spilde, M.N., Crossey, Lavoie, K.H., Mallory, L.M., Boston, P.J., Cunningham, K.I. & Barns, S.M. (2000). Evidence for geomicrobiological interactions in Guadalupe caves. *Journal of Cave and Karst Studies 62*(2): 80-90.

Palmer, A.N. (1991). Origin and morphology of limestone caves. *Geological Society of America Bulletin 103*: 1-21.

Palmer, A.N. & Palmer, M.V. (1992). Geochemical and petrologic observations on Lechuguilla Cave, New Mexico (abs.). *Friends of Karst Meeting, Tennessee Technological University, Cookeville, Tennessee*: 25-26.

Palmer, A.N & Palmer, M.V. (2000). Hydrochemical interpretation of cave patterns in the Guadalupe Mountains, New Mexico. *Journal of Cave and Karst Studies 62*(2): 91-108.

Polyak, V.J. & Mosch, C.J. (1995). Metatyuyamunite from Spider Cave, Carlsbad Caverns National Park, New Mexico. *NSS Bulletin 57(2)*: 85-90.

Polyak, V.J. & Provencio, P. (1998). Hydrobasaluminite and aluminite in caves of the Guadalupe Mountains, New Mexico. *Journal of Cave and Karst Studies 60(1)*: 51-57.

Polyak, V.J., McIntosh, W.C., Güven, N. & Provencio, P. (1998). Age and origin of Carlsbad Cavern and related caves from $^{40}Ar/^{39}Ar$ of alunite. *Science 279*: 1919-1922.

Queen, J.M. (1973). Large scale replacement of carbonate by gypsum in some New Mexico caves (abs.). *Proceedings National Speleological Society Convention*, Bloomington, Indiana: 12.

Queen, J.M. (1981). A discussion and field guide to the geology of Carlsbad Caverns. Preliminary report to the National Park Service for the 8th International Congress: 64 pp.

Queen, J.M. (1994). A conceptual model for mixing zone diagenesis based on the hydrogeology of Bermuda (abs). In Sasowsky, I.D. & Palmer, M.V. (eds). *Breakthroughs in Karst Geomicrobiology and Redox Chemistry*, Karst Waters Institute Special Publication 1: 65-66.

Queen, J.M., Palmer, A.N. & Palmer, M.V. (1977). Speleogenesis in the Guadalupe Mountains, New Mexico: Gypsum replacement of carbonate by brine mixing. *Proceedings of Seventh International Congress of Speleology*, Sheffield, England: 333-336.

Sanchez, P.G. (1964). *Geology of the Capitan Reef Complex of the Guadalupe Mountains, Culberson County, Texas and Eddy County, New Mexico*. Roswell Geological Society, Field Trip Guidebook for May 6-9: 65 pp.

Spirakis, C. & Cunningham, K.I. (1992). Genesis of sulfur deposits in Lechuguilla Cave, Carlsbad Caverns National Park, New Mexico. In Wessel, G. & Wimberley, B. (eds.). *Native Sulfur – Developments in Geology and Exploration.* American Institute of Mining, Metallurgical, and Petroleum Engineers (AIME): 139-145.

Watson, R.A., & White, W.B. (1985). The history of American theories of cave origin. In Drake, E.T. & Jordan, W.M. (eds.). *Geologists and ideas: A history of North American geology*. Geological Society of America, Centennial Special Volume 1, Boulder, CO: 109-123.

Carol A. Hill - Overview of the geologic history of cave development in the Guadalupe Mountains, New Mexico. *Journal of Cave and Karst Studies 62*(2): 60-71.

OVERVIEW OF THE GEOLOGIC HISTORY OF CAVE DEVELOPMENT IN THE GUADALUPE MOUNTAINS, NEW MEXICO

CAROL A. HILL
17 El Arco Drive, Albuquerque, NM 87123-9542 USA carolannhill@cs.com

The sequence of events relating to the geologic history of cave development in the Guadalupe Mountains, New Mexico, traces from the Permian to the present. In the Late Permian, the reef, forereef, and backreef units of the Capitan Reef Complex were deposited, and the arrangement, differential dolomitization, jointing, and folding of these stratigraphic units have influenced cave development since that time.

Four episodes of karsification occurred in the Guadalupe Mountains: Stage 1 fissure caves (Late Permian) developed primarily along zones of weakness at the reef/backreef contact; Stage 2 spongework caves (Mesozoic) developed as small interconnected dissolution cavities during limestone mesogenesis; Stage 3 thermal caves (Miocene?) formed by dissolution of hydrothermal water; Stage 4 sulfuric acid caves (Miocene-Pleistocene) formed by H_2S-sulfuric acid dissolution derived hypogenically from hydrocarbons. This last episode is reponsible for the large caves in the Guadalupe Mountains containing gypsum blocks/rinds, native sulfur, endellite, alunite, and other deposits related to a sulfuric acid speleogenetic mechanism.

This paper provides an overview of events affecting cave development in the Guadalupe Mountains of New Mexico. Table 1 outlines the sequence of karst events, integrated with the regional geology. This overview is also intended to provide a geologic framework for the other papers in this Symposium.

The Guadalupe Mountains are located in southeastern New Mexico and west Texas (Fig. 1). The caves in these mountains are developed in the Capitan Reef Complex—a horseshoe-shaped ring or belt of Permian-age limestone and dolomite rock ~8 km wide and ~650 km long that defines the perimeter of the Delaware Basin. The Capitan Formation in the Delaware Basin is exposed in the northwestern Guadalupe Mountains section, the southwestern Apache Mountains section, and the southeastern Glass Mountains section, but is located in the subsurface on the eastern and northern sides of the basin. Its whereabouts is unknown in the western, Salt Basin side of the Delaware Basin (Fig. 1). Caves exist in all parts of the Capitan reef, including the eastern and northern subsurface sections and Apache and Glass Mountain exposed sections (Hill 1996, 1999a), but the largest number of accessible and spectacular

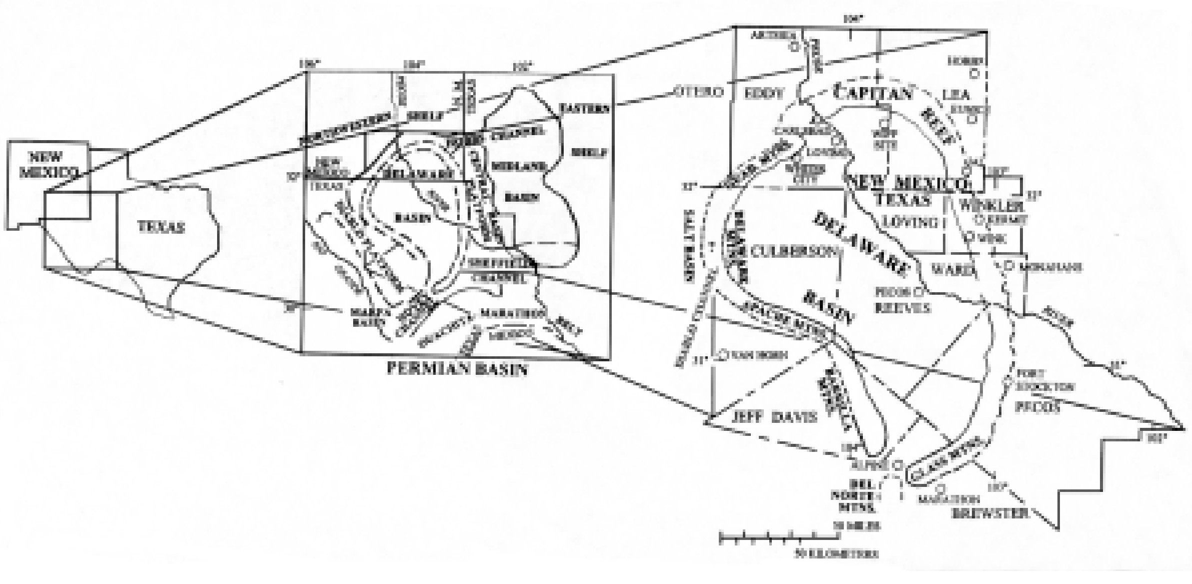

Figure 1. Location map of the Delaware Basin, southeastern New Mexico and west Texas. The caves are developed in the Capitan Reef Complex, which delineates the perimeter of the Delaware Basin (the western part of the Permian Basin). The Capitan reef is exposed in the Guadalupe Mountains, Apache Mountains, and Glass Mountains, but occurs in the subsurface on the eastern and northern sides of the basin. Its location is unknown on the western, Salt Basin, side of the Delaware Basin (marked ?).

Table 1. Sequence of events for development of caves in the Guadalupe Mountains. Regional geologic events are taken from Hill (1996).

Time Interval		Events in Guadalupe Mountains
Paleozoic		
Permian		
Guadalupian	~255-251 Ma	* Deposition of the Capitan reef, basinal Bell Canyon Formation, and backreef Seven Rivers, Yates, and Tansill Formations. * Dolomitization of backreef and forereef in Guadalupe Mountains and also parts of the Capitan reef in the Apache and Glass Mountains.
Ochoan	~251-250 Ma	* Deposition of the Castile Formation in the basin. * Delaware Basin is tilted eastward. Probable first uplift and exposure of Guadalupe Mountains. * Stage 1 fissure caves develop preferentially along a lithologic zone of instability between reef and backreef members.
Mesozoic		
Triassic-Jurassic	~250-135 Ma	* Guadalupe Mountains remain emerged above sea level; marine environment replaced by deltaic, lacustrine, and fluvial environment. * Stage 2 spongework caves form under slow-diffuse circulation during limestone mesogenesis. Some spongework cavities filled with montmorillonite clay (~188 ± 7 Ma).
Cretaceous		
Comanchean	~135-95 Ma	* Shallow sea advances over Delaware Basin and Guadalupe Mountains, leaving behind a veneer of siliceous (now-summit) gravels. * Stage 1 caves fill with gravel to form "Type 2" dikes.
Gulfian	~95-65 Ma	* Late Cretaceous Laramide Orogeny begins in western U.S.; Guadalupe Mountain area uplifted thousands of meters above sea level. * Stage 2 spongework caves reactivated; calcite spar lines some Laramide caves (~90 Ma).
Cenozoic		
Tertiary		
Paleocene	~65-58 Ma	* Laramide uplift continues into the Early Tertiary. * Stage 2 spongework caves become further enlarged and integrated.
Eocene	~58-40 Ma	* Time of quiescence in the Guadalupe Mountains. Laramide uplift stops and an elevated plain exists over much of western U.S. * Stage 2 caves probably become stagnant.
Oligocene	~40-25 Ma	* Time of Trans-Pecos magmatic province; Tertiary extrusives and intrusives form in southern part of Delaware Basin; intrusive dikes reach across the Delaware Basin almost to the Guadalupe Mountains. * Transition from volcanic phase to Basin and Range phase in Delaware Basin area. Delaware Basin area tilts eastward and heats up. * Maturation and migration of hydrocarbons; H_2S produced where hydrocarbons react with Castile anhydrite. * Time of emplacement of Mississippi Valley-type ore deposits (~40-20 Ma).
Miocene (Early)	~25-12 Ma	* Maximum uplift of Guadalulpe Mountain block begins (~20 Ma). * Geothermal gradient of Delaware Basin area reaches ~40-50°C/km; time of maturation and migration of hydrocarbons. H_2S produced when hydrocarbons react with evaporites. * Stage 3 thermal caves produced by hydrothermal circulating fluids; calcite spar fills Basin and Range fault zones and lines some cave passages (?).
Miocene (Late)	~12-5 Ma	* Stage 4 sulfuric acid caves form where H_2S ascends into Capitan reef. Gypsum blocks and rinds, native sulfur, endellite and alunite form as a result of a sulfuric acid speleogenesis. * Stage 4 cave passages develop from southwest to northeast along the Guadalupe Mountains; 11.3 Ma for Virgin Cave to 3.9 Ma for the Big Room level of Carlsbad Cavern. * Large Stage 4 sulfuric acid cave passages cut across earlier 3 stages of cave development.
Pliocene	~5-2 Ma	* Regional water table drops in response to base-level downcutting of the ancestral Pecos River. Caves develop along lowering water table levels. * Caves in higher, southeastern part of Guadalupe Mountains (e.g., Virgin) stop forming; caves in lower, northeastern parts (e.g., Carlsbad) continue forming at the water table. * As canyons downcut into the Guadalupe Mountain block, cave passages are intersected so that entrances form. * As the caves become air-filled, they become decorated with travertine.
Quaternary		
Pleistocene	~2 Ma-10 ka	* At ~600 ka the Capitan aquifer hydrologically connects with the Pecos River at Carlsbad. Possible time of water table draining out of Big Room-Lower Cave levels of Carlsbad and lower levels of Lechuguilla. * Air-filled caves continue to become decorated with travertine. Time of maximum decoration: ~600 ka and ~170-70 ka. * Animals inhabit air-filled caves.
Holocene	~10 ka-present	* Arid climate - travertine growth decreases. * Entrance air flow affects cave microclimates. * Pool chemistry evolves to present state.

caves are in the Guadalupe Mountain section. Over 300 caves are known in the Guadalupe Mountains. Carlsbad Cavern is perhaps the most famous of these caves, but it is neither the longest nor the deepest. Lechuguilla Cave is now the deepest (475 m) and longest (>170 km) cave in the Guadalupe Mountains, the deepest and third longest limestone cave in the United States, and the fifth longest cave in the world. Guadalupe caves are characterized by their unusual mode of speleogenesis, which is reflected in their large passage size, ramiform morphology, and enigmatic deposits of gypsum, native sulfur, endellite (hydrated halloysite), alunite, and uranium minerals.

The origin of Carlsbad Cavern and other caves in the Guadalupe Mountains has long been a subject of controversy. For more than 30 years, the prevailing theory had been that these caves formed like other caves; that is, by carbonic acid dissolution at or below the water table (Bretz 1949). But, since the late 1970s and early 1980s, this "normal" model of cave dissolution has been challenged by a new generation of speleologists (Jagnow *et al.* 2000). It is now nearly universally accepted that the caves of the Guadalupe Mountains are of "hypogene" origin, having developed where ascending H_2S, derived from hydrocarbons, became oxidized to sulfuric acid, which in turn dissolved out huge chambers at approximately the level (or levels) of the paleo-water table.

These large sulfuric acid caves, however, represent only the final chapter of cave development in a long history of periodic karstification in the Guadalupe Mountains. Porosity/karst development has occured in at least four stages throughout the diagenetic history of the Capitan Reef Complex, from Late Permian to the present. Thus, in order to understand the complete history of cave development in the Guadalupe Mountains, one must go back to the Permian, to a time when the great Capitan reef was growing upward around the intracratonic Delaware Basin.

This paper will only summarize the sequence of events in the Guadalupe Mountains from the Late Permian to the present; for a more detailed description, refer to Hill (1996).

PALEOZOIC

PERMIAN (GUADALUPIAN)

Guadalupian time (~255-251 Ma) in the Delaware Basin area was characterized by the growth of an extensive stratigraphic reef that separated the deep ocean basin from a shallow backreef shelf lagoon (Fig. 2). The classic model for the Delaware Basin in the Permian is that the basin was completely surrounded by the Capitan (and earlier reefs), and that sea water entered the basin through the Hovey Channel, located in the southern, Glass Mountains section of the basin (Fig. 1). However, Hill (1999b) challenged this classic paleogeographic map and placed the inlet (which she named the "Diablo Channel") to the basin on its western, Salt Basin side (Fig. 1, marked ?). Hill claimed that this channel position could account for the absence of the Capitan reef between Guadalupe Peak and the Apache Mountains. It might also account for the extensive growth of the Capitan reef along the Guadalupe Mountain section of the basin (near where "fresh" upwelling sea water from the deep ocean was entering the Delaware Basin), and for less dolomitization of the Capitan reef in the Guadalupe Mountains, as compared to the Glass Mountains which would have been farther from the source of "fresh" sea water if the Hovey Channel had been non-existent.

During Guadalupian time, when the Capitan reef was growing steadily upward and basinward in the Guadalupe Mountain area, a thick sequence of siliciclastics was deposited within the deep basin, and interbedded carbonates, siliciclastics and evaporites were deposited on the shallow lagoonal shelf behind the reef (Fig. 2). The Capitan Formation consists of two facies—a massive reef member composed of an organic framework and a thickly bedded forereef member. Both members grade laterally and vertically into each other and together reach thicknesses of 450-600 m in the Guadalupe Mountains. Time-correlative with the Capitan reef in the Guadalupe Mountains are the backreef Seven Rivers, Yates, and Tansill Formations of the Artesia Group and the basinal Bell Canyon Formation of the Delaware Mountain Group. These bedrock units deposited in the Late Permian were to influence all subsequent episodes of cave development in the Guadalupe Mountains (DuChene 2000).

CONTROLS ON CAVE DEVELOPMENT

Four properties of the Capitan in Late Permian time seem to have exerted control on later cavern development: (1) the arrangement of stratigraphic units; (2) differential dolomitization of these units; (3) joint patterns; and (4) positive structures (folds). All four controls first appeared in the Late Permian, although (3) and (4) have been modified by later tectonic and diagenetic events (Hill 1996).

Stratigraphy. As the Capitan reef was lithified in the Late Permian, the contacts between the reef-forereef and reef-backreef facies became zones of structural weakness that were to

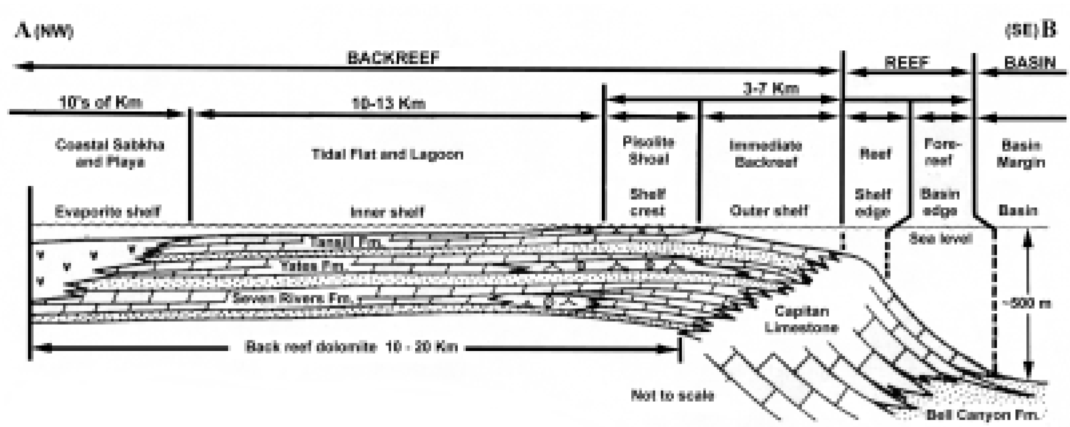

Figure 2. Facies patterns and depositional environments of the Capitan Reef Complex, Guadalupe Mountains, in Permian (Guadalupian) time, including the basin, forereef, reef, and backreef members. After Esteban & Pray (1983).

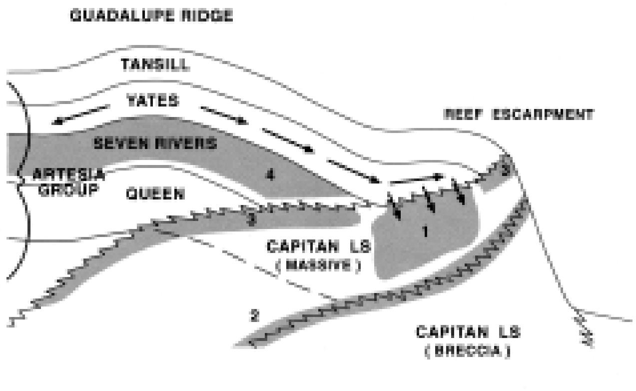

Figure 3. Four zones of preferential dissolution (shaded areas) in the Guadalupe Mountains: (1) below the Yates transition into the massive Capitan Limestone; (2) at the contact between the massive and forereef (breccia) members of the Capitan Limestone; (3) at the transition between the backreef Artesia Group members and Capitan Limestone; (4) immediately beneath the Yates Formation in the Seven Rivers. Arrows indicate movement of groundwater along impermeable siltstone in the Yates Formation. After Jagnow (1977).

become the focal point for later water movement and cave development. While some caves are developed within or beneath the Yates in the Seven Rivers Formation (Fig. 3), most of the major caves (e.g., Carlsbad, Lechuguilla) are developed at these reef-backreef and reef-forereef contacts (Jagnow 1977).

Dolomitization. Dolomitization (or the lack thereof) has also exerted control on cave development in the Guadalupe Mountains. The Capitan reef was not dolomitized equally in all parts of the basin in the Late Permian (Fig. 4). In the Apache Mountains the Capitan reef is, in large part, dolomitized but its younger parts grade into limestone (Wood 1968). In the Glass Mountains, the reef facies of the Capitan is also more dolomitized than in the Guadalupe Mountains (King 1930), with textures varying from somewhat dolomitized and with complete preservation of fossils (e.g., in the Old Blue Mountain area), to only matrix replacement, to total replacement (e.g., in Jail Canyon) (Haneef 1993). In the Guadalupe Mountains, the oldest part of the massive reef facies (the lower Capitan) is partially dolomitized, whereas the upper Capitan is predominantly limestone. This thin belt of limestone extends northeastward along the mountain front but gradually becomes dolomitized just southwest of Carlsbad (Fig. 4). Thus, a thin "island" of limestone exists *only* in the upper Capitan in the Guadalupe Mountains, and it is this "island" of rock that hosts the majority of caves. Since dolomitization of the Capitan occurred primarily in the Late Permian (Melim 1991), it has acted as a control on dissolution ever since.

Joints. Joints are a primary structural control on cavern development, and the major trunk passages are usually aligned along joints that are either parallel or perpendicular to the reef front. Brecciation and crude bedding planes in the forereef slope, however, seem to (at least partly) control the location of some passages (e.g., the eastern part of the Western Borehole, Lechuguilla Cave; DuChene 2000). The age and origin of joints in the Capitan are controversial (Hill 1996). However, it appears reasonably certain that the initiation of jointing

Figure 4. Idealized schematic diagram showing the distribution of dolomite in upper Permian units around the Delaware Basin. The upper Capitan in the Guadalupe Mountains is the only location where the Capitan is mostly undolomitized limestone. Diagonal lines show dolomitized rock, circles show rock with patchy dolomitization, white areas show limestone. The location of the Capitan and Goat Seep formations in the Salt Basin is unknown (?). After Hill (1996, 1999a).

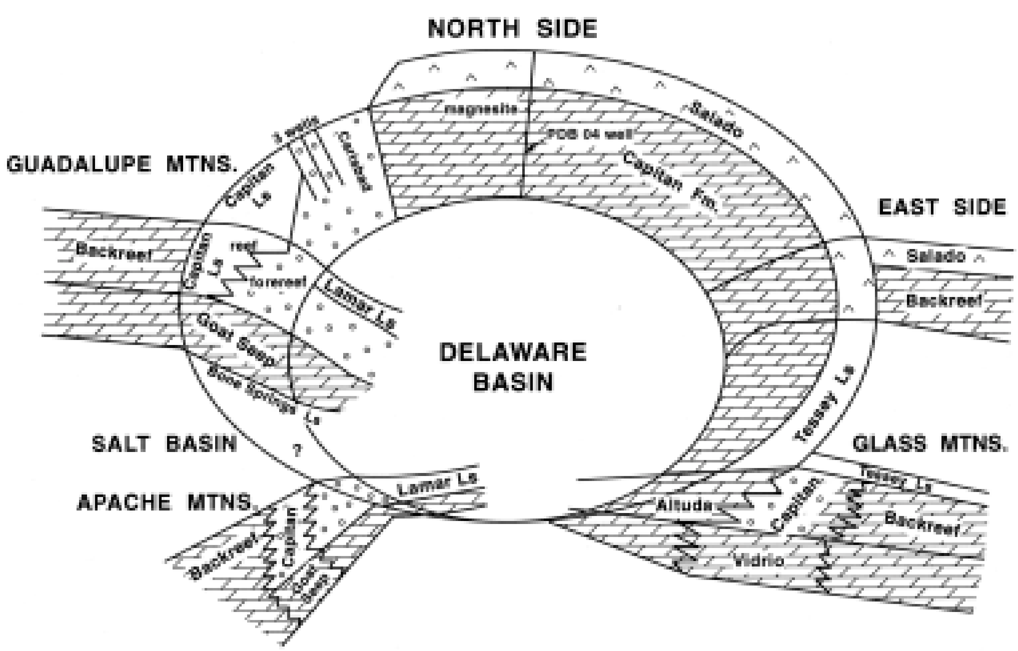

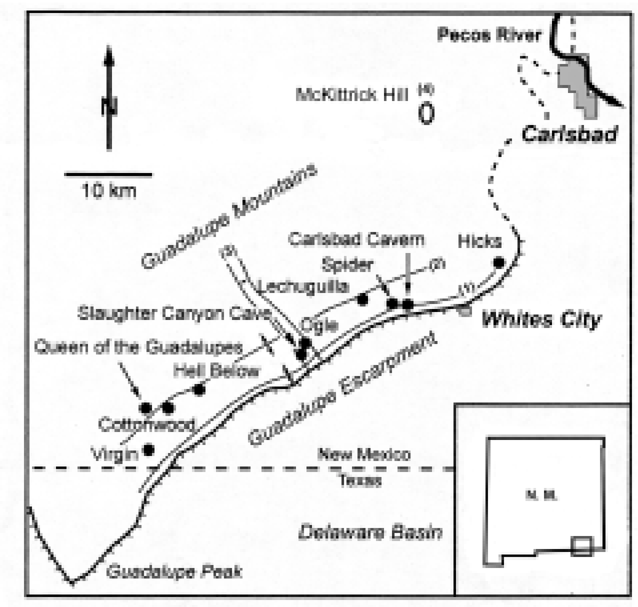

Figure 5. The relationship of major caves in the Guadalupe Mountains to positive structures (folds): (1) Reef anticline; (2) Guadalupe Ridge anticline; (3) Huapache monocline; (4) McKittrick Hill anticline (oval). Modified from Palmer & Palmer (2000).

occurred when the rock was being lithified in the Late Permian. Initial jointing probably occurred during the compaction phase of diagenesis in the Late Permian, and later jointing took place along these lines of weakness during tectonism—possibly during the Laramide and probably during Miocene Basin and Range block faulting. Similarly, initial cave development was along these Late Permian joints, with subsequent stages of karstification following along these same lines of weakness.

Positive Structures. Positive structures (e.g., anticlines) have been another control on cavern development. Carlsbad Cavern is located along the crest of the Reef anticline, Lechuguilla Cave and Cottonwood Cave are located along the Guadalupe Ridge anticline, the Slaughter Canyon caves are located along the Huapache monocline, and the McKittrick Hill caves are located along the flanks of the McKittrick Hill anticline (Fig. 5). The major large cave passages are concentrated along positive structures because these structures acted as avenues and traps for H_2S ascending into the reef. During the last (Stage 4) episode of cave development, sulfuric acid produced by oxidation of this H_2S dissolved out the large cave passages in the Guadalupe Mountains.

LATE PERMIAN (OCHOAN)

The Ochoan (~251-250 Ma) represents a time of dramatic change in sedimentation within the Delaware Basin. The inlet to the basin (whether the Hovey and/or Diablo Channels) became closed to marine waters so that the basin filled with thick sequences of evaporites and also with thinner sequences of red beds (i.e., the Castile, Salado, Rustler, and Dewey Lake Formations; refer to Hill 1996 for a description of these units). The first uplift of the Delaware Basin probably occurred in Ochoan time, as evidenced by a Late Permian unconformity between the Dewey Lake Red Beds and Triassic rocks. The western edge of the basin was tilted eastward, and at least the western part of the Guadalupe Mountains was probably uplifted above sea level. This brought about the first episode of karsting in the Guadalupe Mountains.

STAGE 1 FISSURE CAVES

Stage 1 fissure caves are characterized by small fissure-like cavities filled with breccia, limy mudstone, siliciclastics, and/or calcite spar. Most Stage 1 caves are located at or near the reef/backreef contact (Hill 1987), a location suggesting that they formed in a zone of structural instability between the Capitan reef core and backreef shelf members. Although Stage 1 fissure karst is commonly intersected by Stage 4 sulfuric acid cave passages, it has also been identified in outcrop. Melim & Scholle (1989) and Scholle *et al.* (1992) identified an exposure episode in the Guadalupe Mountains during which an initial stage of meteoric leaching of originally aragonitic material occurred with the development of a large-scale, dissolution-enlarged fracture system. These surface-exposed fractures are filled with clast-supported breccia and blocky calcite, and are oriented mainly parallel to the Capitan reef trend, with a secondary orientation perpendicular to the reef trend (Melim 1991). Individual fractures average 1 m wide but they also occur in anastomosing sets averaging 10-20 m wide. Melim (1991) found the breccia fragments in these fractures to be dolomitized and of local origin without evidence of significant transportation, and also identified a dolomite alteration front or halo extending around the fissures for a distance of 5-10 cm into the reef rock. From this evidence, Melim concluded that this dissolution episode probably occurred in the Late Permian (Ochoan?).

The following origin seems likely for the Stage 1 fissure karst episode. Subsequent to the deposition of the Capitan Limestone and equivalent backreef facies, probably in Ochoan time, tectonic activity caused the first uplift and tilting of the Capitan reef. Fractures (joints) that had initially formed in response to differential compaction between the rigid reef and less competent backreef became enlarged into fissures due to tectonism and/or dissolution. Locally derived clasts were then displaced downward and partially filled these voids. The anastomosing nature of these fracture sets, with extensive pinching and swelling of individual fractures, is easiest to explain by dissolution-enlargement of already-existing fractures or joint sets (Melim 1991). However, solutional activity does not appear to have been extensive. Dissolution-enlargement occurred prior to at least one dolomitization stage because the walls of Stage 1 fissure caves and breccia clasts within the fissures are dolomitized. Stage 1 fissure caves developed along the zone of weakness between the reef/backreef and then became avenues for water movement, porosity enhancement, and dissolutional enlargement during the subsequent three stages of karstification.

MESOZOIC

TRIASSIC-JURASSIC

During the entire Mesozoic, up until the Laramide Orogeny in the Late Cretaceous, the Guadalupe Mountains were emergent just above sea level, and a marine environment was replaced by a deltaic, lacustrine, and fluvial environment. Probably at this time, the Capitan reef experienced its first "flushing out" and next episode of karstification.

STAGE 2 SPONGEWORK CAVES

The second episode of porosity/karst development in the Guadalupe Mountains involved the enlargement of pores and joints in the massive Capitan Limestone into three-dimensional mazes. "Spongework" consists of interconnected dissolution cavities of varied size in a seemingly random, three-dimensional pattern like the pores of a sponge (Palmer 1991). Essentially, these cavities are freshwater lens voids, where phreatic water creates a spongework array of passages. Hill (1987) described Stage 2 spongework cavities in the Guadalupe Mountains as being small and randomly oriented, with some being partly filled with montmorillonite clay.

In the early stages of cave-system formation, a complex, three-dimensional array of pores and joints of minimal cross-sectional area can develop in the rock, but the pores and joints are not necessarily integrated so that flow under these conditions is diffuse. As dissolution continues over time, this array expands, and there is a progressive integration of conduits and enlargement of small portions of the array to create a cave system that eventually becomes continuous from input to output (Ford & Ewers 1978). In such a situation the limestone becomes honeycombed along joints, fractures, and bedding planes, and small caves up to a few meters in extent can form.

Stage 2 spongework caves represent this type of early karst development in the Guadalupe Mountains. These cavities/caves dissolved under phreatic conditions marked by the slow, diffuse circulation of aquifer water during limestone mesogenesis. Stage 2 spongework caves in the Capitan are exposed in the walls of the large cave passages as a three-dimensional array of "Swiss-cheese"-like holes or cavities; some holes are large enough to crawl through, although most are not. Stage 2 spongework porosity/karst may have formed over a long period of time, or more likely during several episodes from the Mesozoic to early Cretaceous. The Triassic-Jurassic was a time of emergence for the Delaware Basin area, and it was also probably a time of extensive dissolution. Montmorillonite clay filling a small percentage of Stage 2 spongework cavities has a speculative K-Ar date of 188±7 Ma (early Jurassic) (Hill 1987).

CRETACEOUS (COMANCHEAN)

The Delaware Basin region remained stable for most of the Mesozoic, but in the Early Cretaceous (Comanchean) a weak subsidence of the region permitted a shallow, epicontinental sea to transgress across the basin and over the top of the (then near sea level) Guadalupe Mountain area. Outcrops of Cretaceous rock can be found as lag gravels over the Tansill Formation near the edge of the reef escarpment, and these gravels also occur as remnants within Stage 1 fissure caves (the "Type 2" dikes of Hill 1996). This epicontinental sea withdrew from the area early in the Late Cretaceous in response to the Laramide Orogeny, and marked the last vestige of marine sedimentation in the Delaware Basin.

CENOZOIC (TERTIARY)

LARAMIDE PHASE, LATE CRETACEOUS - EOCENE

The long interval of relative quiescence in the Guadalupe Mountains during the Mesozoic was terminated by the Late Cretaceous-early Tertiary Laramide Orogeny. This tectonic event was responsible for the uplift of the entire western United States, and probably for more than 1.2 km of uplift in the Guadalupe Mountains area (Horak 1985). The Delaware Basin area was also subjected to broad arching during the Laramide, as can be seen in the Guadalupe and Delaware Mountains (King 1948). The steepest dip of this great Laramide arch is along its western flank; the crest of the arch was probably near the present summits of the southern Guadalupe Mountains because consequent streams radiate northeast, north, and northwest from this area.

The effect of Laramide uplift on cave development in the Guadalupe Mountains is not known, but it must have caused at least a partial reactivation of water moving through the Capitan reef and consequently a further enlargement and integration of Stage 2 spongework caves. A preliminary Late Cretaceous (~90 Ma) date on cave spar (Lundberg *et al* 2000) attests to at least some Laramide dissolution at this time. This activity probably slowed during the quiescent Eocene, at which time water in the Capitan reef may have been relatively stagnant.

VOLCANIC PHASE - OLIGOCENE

A phase of extrusive and intrusive volcanism occurred in the Trans-Pecos, Delaware Basin area during the early-middle Oligocene (~40-30 Ma). No known volcanic rocks are exposed in the Guadalupe Mountains, but a number of northeast-trending intrusive dikes (both on the surface and in the subsurface) exist in the basin just southeast of the Guadalupe Mountains escarpment. The Oligocene to early Miocene (~40-20 Ma) may have also been the time of Mississippi Valley-type (MVT) ore emplacement in the Guadalupe Mountains (e.g., Queen of the Guadalupes mine; Hill 1996). As H_2S began to ascend into the reef, it formed sulfide deposits in the reduced zone along structural (anticlinal) and stratigraphic (base of Yates Formation) traps where it mixed with metal-chloride complexes moving downdip from backreef evaporite facies (Figs. 2 & 6). Later, sulfuric acid caves formed along these same structural and stratigraphic traps in the oxidized zone.

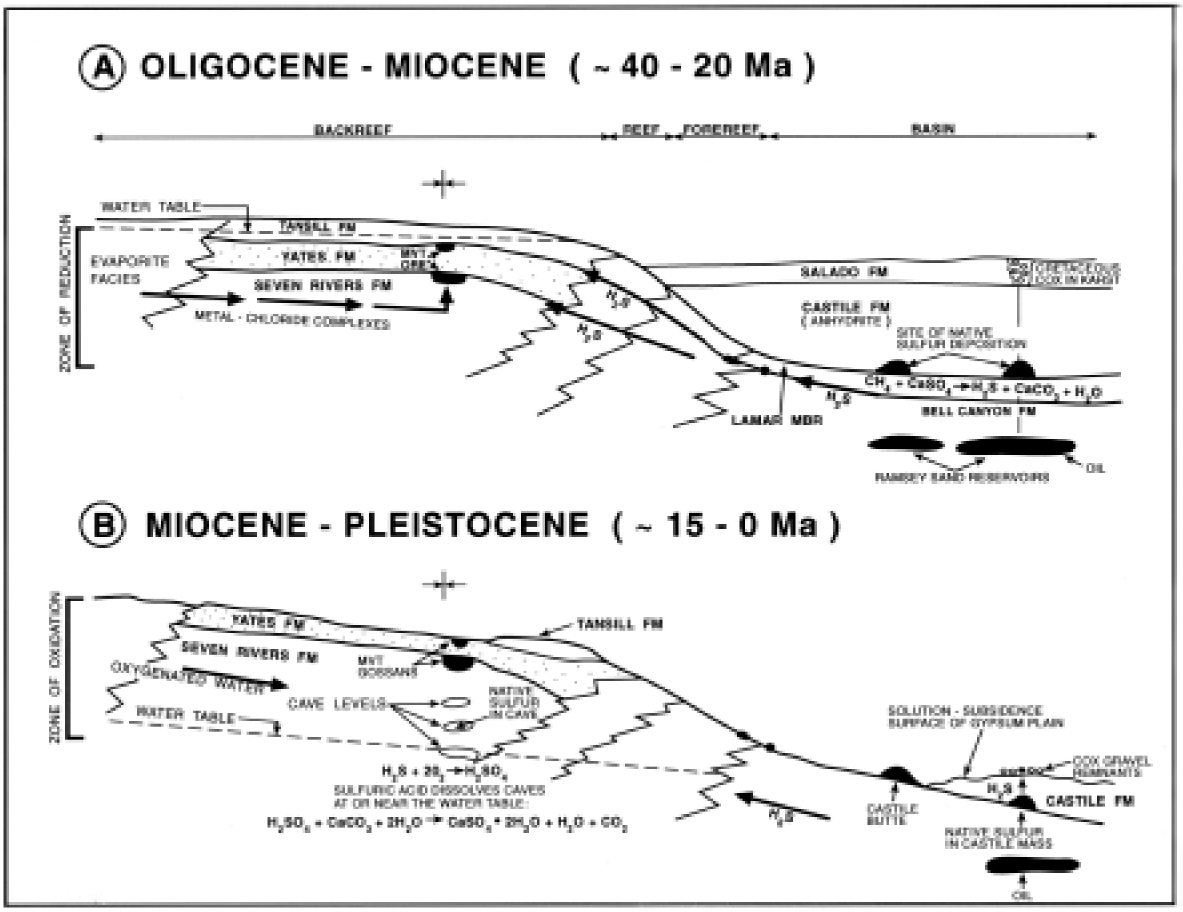

Figure 6. Idealized model for the origin of caves, and also for Mississippi Valley-type (MVT) sulfides, in the Guadalupe Mountains. This figure shows a genetic connection between hydrocarbons and native sulfur within the Delaware Basin, and MVT deposits and sulfuric acid caves in the carbonate-reef margin, although H_2S could have also come from other sources than the basin *per se*. (A) In the late Oligocene-early Miocene, during the Tertiary tilting of the Delaware Basin, H_2S was generated in the basin by reactions involving hydrocarbons and anhydrite. The H_2S oxidized to native sulfur in the basin, and also some migrated from basin to reef to accumulate there in structural (anticlinal) and stratigraphic (base of Yates) traps. Metals moved downdip as chloride complexes from backreef-evaporite facies, and where they encountered ascending H_2S below the water table in the zone of reduction, they formed MVT deposits. (B) Later in the Miocene and also in the Pliocene to Pleistocene, continued uplift and tilting of the Guadalupe Mountain block and Delaware Basin area caused increased H_2S generation and migration of gas from basin to reef. Cave dissolution occurred in the same structural and stratigraphic position as earlier MVT deposits, where H_2S oxidized to sulfuric acid at or near the water table in the zone of oxidation. Cave levels correspond to a descending base level caused by the regional lowering of the Pecos River. From Hill (1996).

The importance of the volcanic phase to the caves of the Guadalupe Mountains is that it initiated a general heating up of the Delaware Basin. This heating was responsible for: (1) the setting up of convectional circulation patterns within the porous, spongeworked Capitan reef; (2) the beginning of the maturation and migration of hydrocarbons in basinal rock; and (3) the production of H_2S from the interaction of these hydrocarbons with Castile Formation evaporite rock (Fig. 6). The volcanic phase in Oligocene time, thus, “sets the stage” for the last two episodes of karstification in the Guadalupe Mountains.

Basin and Range Phase - Miocene

The transition from the volcanic phase to the Basin and Range phase took place in the late Oligocene to early Miocene (~30-20 Ma) and represents a time of change from Laramide compression to Basin and Range regional extension. By ~20 Ma, the main uplift and tilting of the Guadalupe Mountain block had begun.

Stage 3 Thermal Caves

Stage 3 thermal caves are small caves characterized by crystalline dogtooth-spar linings (Fig. 7). Cavers call these “spar caves” or “geode caves” because of their spectacular spar crystals, which can be as large as footballs. Spar caves can be small individual caves exhibiting spar linings (e.g., Geode Cave, Crystal Ball Cave), or they can be small rooms or spar-lined passages which have been intersected by later sulfuric-acid dissolution (e.g., Diamond Chamber, Lechuguilla Cave).

Figure 7. A spar cave in the Guadalupe Mountains. Some of the dogtooth spar crystals lining the walls of this cave are as large as footballs. Photo by Alan Hill.

Stage 3 spar-lined caves exist in both the Guadalupe and Glass Mountains (Hill 1996).

From oxygen-isotope and fluid-inclusion studies, the dogtooth spar in these caves is known to have formed from ~30-65°C solutions. Thermal spar with similar isotopic values also permeates the Capitan reef filling pores and fault zones along the western escarpment of the Guadalupe Mountains (Hill 1996). Because the Miocene was a time when the geothermal gradient reached ~40-50°C/km (Barker & Pawlewicz 1987), Stage 3 thermal caves were thought by Hill (1996) to be most likely Miocene in age. However, the recent Laramide date of Lundberg *et al* (2000) challenges this assumption that all cave spar in the Guadalupe Mountains is Basin and Range age.

The following model can be invoked to explain the origin of Stage 3 thermal caves:

(1) Surface water input into the Capitan reef in Miocene time was meteoric. As this cold meteoric water descended along faults and joints, it heated in response to the 40-50°C/km geothermal gradient, and a convective circulation pattern was set up in the Capitan reef and also in stratigraphic units below the Capitan.

(2) As the convective water rose and cooled, the solubility of $CaCO_3$ gradually increased so that small (Stage 3) caves were dissolved in a deep "solutional zone" by the "cooling corrosion" mechanism of Bögli (1980).

(3) Although the solubility of $CaCO_3$ increased with the ascent of bathyphreatic fluid in the "solutional zone", it dropped sharply due to the loss of CO_2 in the shallower "depositional zone", so that solutions changed from aggressive to precipitative (Dublyansky 1995).

(4) As Stage 3 caves formed in the "solutional zone" were shifted into the "depositional zone" by tectonic uplift and/or descent of the water table, cave walls became lined with dogtooth spar. Conditions necessary for the growth of large spar crystals are: (a) solutions just barely saturated with respect to calcite; (b) a quiet, aqueous environment in which crystals can grow undisturbed; (c) enough time for crystals to grow large. All of these conditions must have been met in order for spar crystals to deposit in Stage 3 thermal caves from hydrothermal solutions.

STAGE 4 SULFURIC ACID CAVES

Later in the Miocene (12-5 Ma), and probably not long after the Stage 3 thermal cave episode, an entirely different mechanism created the last and most significant episode of karstification in the Guadalupe Mountains: Stage 4 sulfuric acid caves.

Description. The main caves/cave areas in the Guadalupe Mountains are: Carlsbad Cavern, Lechuguilla Cave, Cottonwood Cave, the Slaughter Canyon caves, and the McKittrick Hill caves (Fig. 5). These are located within 12 km of the reef escarpment (most are within 5 km); along the crests or flanks of anticlines or other positive structures (e.g., Reef anticline, Guadalupe Ridge anticline, Huapache monocline; Fig. 5); at the contact of major facies changes (Fig. 3); and between the limestone reef and more dolomitic backreef and forereef beds (Fig. 4).

The caves of the Guadalupe Mountains characteristically contain large rooms and passages (many are >15 m in height and width) along major elevation levels, with separate levels connected by steeply dipping passages (e.g., Main Corridor, Carlsbad Cavern), vertical tubular pits (e.g., Bottomless Pit, Carlsbad Cavern), or enlarged vertical fissures (e.g., Cable Slot, Carlsbad Cavern). In places, walls of large rooms and passages truncate Stage 1 fissure caves, are honeycombed with Stage 2 spongework caves, or truncate Stage 3 thermal caves lined with dogtooth spar crystals. Cave passages/rooms end abruptly without breakdown collapse or major passage extensions, and the caves lack a clear genetic relationship to surface topography. Intersections of caves with the land surface (entrances) are random and have no apparent relationship to recharge or resurgence points, either ancient or modern. Well-developed surface karst landforms (e.g., sinkholes) are not abundant.

Distinctive deposits in Guadalupe Mountain caves are thick floor blocks of massive gypsum ($CaSO_4•2H_2O$) and thinner wall rinds of gypsum; native sulfur (S) deposits; and colorful, waxy endellite [$Al_2Si_2O_5(OH)_4•2H_2O$] clay deposits. Alunite

[$K_2Al_6(SO_4)_4(OH)_{12}$], natroalunite [$Na_2Al_6(SO_4)_4(OH)_{12}$], tyuyamunite [$Ca(UO_2)_2(VO_4)_2 \bullet 5\text{-}8H_2O$], and metatyuyamunite [$Ca(UO_2)_2(VO_4)_2 \bullet 3\text{-}5H_2O$] are other speleogenesis-related cave minerals (Mosch & Polyak 1996; Polyak & Güven 1996, 2000).

Stage 4 caves are a result of combined bathyphreatic and water-table development (Hill 1987). Water table (shallow-water phreatic) conditions were responsible for the horizontal development of caves along certain levels (e.g., Big Room, Carlsbad Cavern), and bathyphreatic (deep-water phreatic) conditions were responsible for the strong vertical development of these caves (e.g., Main Corridor, Carlsbad). None of the caves are vadose in origin, with the possible exception of Queen of the Guadalupes, which might be a vadose domepit. Cave sediment, unlike that in vadose caves, is sparse and where it does occur it is usually (but not always) a coarse silt to fine-grained sand derived directly from the dissolution of siliciclastic facies in the bedrock (e.g., Sand Passage, Carlsbad Cavern).

Origin. Stage 4 caves are hypogenic, formed by acids of deep-seated origin (e.g., sulfuric acid), in contrast to epigenic caves, which form in the near surface where carbonic acid is derived from CO_2 in the atmospheric and soil zones (Palmer 1991). Hypogenic karst displays no relationship to recharge through the overlying surface, and cave passages are typically ramiform, network, or spongework patterns (Palmer & Palmer 2000).

Stage 4 caves in the Guadalupe Mountains were dissolved primarily by sulfuric acid. The source of the sulfuric acid was H_2S derived from hydrocarbons within the Delaware Basin (Fig. 6). Alternatively, it could have come from oil fields in the north part of the basin, from the backreef, or from deep source rocks below the Capitan reef (DuChene 1986; Hill 1990). A number of different lines of evidence point to a sulfuric acid/hydrocarbon origin for Stage 4 caves (Hill 1987, 1990):

(1) Massive gypsum blocks (up to 10 m high) and native sulfur deposits (up to thousands of kilograms) in these caves formed as by-products of a sulfuric acid mode of dissolution. Epigenic, carbonic-acid caves do *not* contain these types of deposits.

(2) The low-pH, sulfuric-acid indicator minerals endellite (hydrated halloysite), alunite and natroalunite occur in these caves.

(3) High uranium, radon, and the minerals tyuyamunite/metatyuyamunite in these caves are all indicative of a H_2S system where uranium (and vanadium) have precipitated along a redox boundary interface (Hill 1995).

(4) Other sulfuric acid caves are known worldwide, and these are also associated with hydrocarbons. Some of these caves are actively forming today by a sulfuric acid mechanism; e.g., Cueva de Villa Luz, Tabasco, Mexico, is a sulfuric acid cave related to hydrocarbons in the Gulf of Campeche. A milky-white river, with dissolved gypsum and sulfur, flows from the cave, and sulfur crystals are growing in areas where drip water has a measured pH of 0-3 (Palmer & Palmer 1998; Hose & Pisarowicz 1999). Sulfur isotope values for sulfur and gypsum in Cueva de Villa Luz ($\delta^{34}S$ = -26 to -22‰; CDT) are within the same range as the sulfur and gypsum in Guadalupe Mountain caves (Fig. 8).

(5) The isotopically light composition of the massive gypsum, sulfur, alunite and natroalunite deposits in Stage 4 caves (Fig. 8) is the most convincing evidence for a sulfuric acid origin related to hydrocarbons. Only biologically aided reactions such as occur with hydrocarbons could have produced the large isotopic fractionations found in these deposits. Gypsum and native sulfur deposits in Guadalupe Mountain caves are significantly enriched in ^{32}S, and depletions in $\delta^{34}S$ as great as -25.6‰ for gypsum and -25.8‰ for sulfur have been measured (Fig. 8). The same isotopically light signatures also characterize alunite and natroalunite (Polyak & Güven 1996; Fig. 8).

The sulfur isotope results are crucial to understanding the hypogenic process of speleogenesis that produced the large Stage 4 cave passages in the Guadalupe Mountains. The evidence provided by the isotopic data demonstrates that the cave gypsum could not have been derived from Castile anhydrite beds by the local pooling model of Bretz (1949) or by the mixing model of Queen *et al.* (1977). The average isotopic composition of Castile gypsum and anhydrite is +10.3‰ (Fig. 8). If the cave gypsum had precipitated amicrobially from Castile brines, as modeled by these authors, then the cave gypsum and Castile Formation gypsum and anhydrite should have virtually identical isotopic compositions. The sulfur isotope data also discount an origin from pyrite as proposed by Jagnow (1977). Sulfide minerals (mostly pyrite) in the Guadalupe Mountains range from $\delta^{34}S$ = -9.3 to +12.6‰ (mean = -2.2‰ for 20 samples; Fig. 8). Since there is no significant isotopic fractionation involved in the leaching of sulfides (less than 1‰), it is logical to conclude that the isotopically lighter cave gypsum and sulfur (mean = -16.8‰ for 22 samples) could not have derived from this source. Instead, the isotopically light deposits implicate a hydrocarbon connection for these caves (Hill 1990).

Cave dissolution by sulfuric acid. Hydrogen sulfide, generated from hydrocarbon reactions in the basin or elsewhere, migrated into the surrounding Capitan reef and accumulated in structural and stratigraphic traps (Fig. 6). Where it met with oxygenated meteoric groundwater descending to or below the water table along dipping backreef beds or joints in the overlying land surface it formed sulfuric acid (Palmer & Palmer 2000):

$$H_2S + 2O_2 = 2H^+ + SO_4^{2-} \tag{1}$$

$$2H^+ + SO_4^{-} + CaCO_3 = Ca^{2+} + SO_4^{2-} + H_2O + CO_2 \tag{2}$$

The sulfuric acid produced in (1) dissolved the Capitan reef limestone to produce the cave void, caused gypsum to precipitate or replace the limestone as blocks or rinds, and generated CO_2 (2). According to this model, vertical tubes, fissures and pits in Guadalupe caves are interpreted as having formed along injection points for H_2S (bathyphreatic dissolution), and hori-

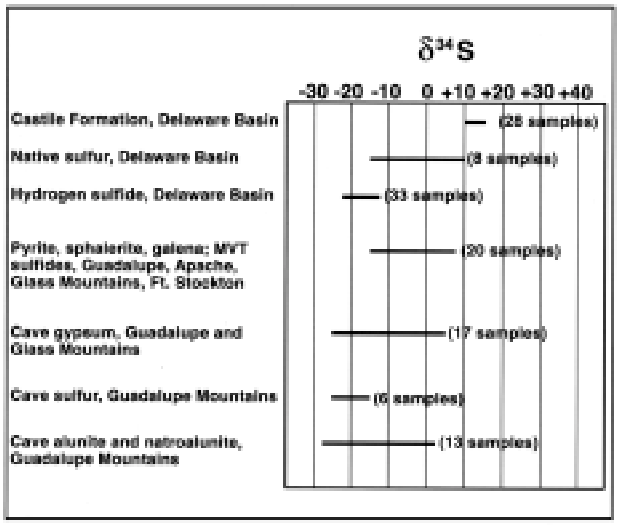

Figure 8. Range of sulfur isotope values for various types of deposits, Delaware Basin. Note that the cave gypsum and sulfur are significantly enriched in the light isotope of sulfur compared to the Castile Formation. The isotopically light composition of sulfur deposits in the basin (H_2S gas, native sulfur) and reef (sulfides and sulfur/gypsum cave deposits) resulted from bacterial sulfate reduction (BSR) reactions where sulfate solutions mixed with hydrocarbons to produce isotopically light hydrogen sulfide. Cave alunite and natroalunite values are from Polyak & Güven (1996). After Hill (1995).

zontal levels are interpreted as forming at the water table where dissolved oxygen was the most concentrated (water-table dissolution). This H_2S was also responsible for native sulfur deposits, which have been slowly oxidizing to gypsum when in the presence of meteoric water (Spirakis & Cunningham 1992; Hill 1995). A low-pH, sulfuric acid environment also caused clay minerals to reconstitute to endellite, alunite and natroalunite, and (ultimately) caused the precipitation of the secondary, later-stage, uranium-vanadium minerals tyuyamunite and metatyuyamunite. The above reactions (1) and (2) were most likely facilitated by microbial action. Microbes, from the time of speleogenesis until the present, have altered the geology of Guadalupe caves in ways that are just beginning to be discovered (Northup *et al.* 2000).

Age. The age of the Stage 4 sulfuric acid karst event is still somewhat controversial, but it appears that the beginning of Stage 4 dissolution may be somewhat older than the Pliocene-Pleistocene age ascribed by Hill (1987). Maximum uplift and tilting of the Guadalupe block is now believed to have occurred in the Miocene (20-5 Ma), which means that H_2S could have been migrating throughout the middle to late Tertiary with the potential for cave formation (K. Cunningham, pers. comm. 1995; Hill 1996).

Polyak *et al.* (1998) $^{40}Ar/^{39}Ar$-dated the mineral alunite in four Guadalupe caves, and established that these Stage 4 cave passages formed from about 12 Ma in the southwestern part of the reef (e.g., Virgin Cave) to about 4 Ma in the northeastern part of the reef (e.g., Carlsbad Cavern and Lechuguilla Cave). These absolute dates are very important because they correlate with the time of major uplift of the Guadalupe Mountains and the proposed time of migration of H_2S from the basin into the Capitan reef (Polyak & Provencio 2000). Since supergene alunite is known to form at or near the water table (Rye *et al.* 1992), the dates of Polyak *et al.* (1998) represent water-table development of the caves: bathyphreatic development would have been earlier or concurrent (but at a lower level).

BASIN AND RANGE PHASE - PLIOCENE

The large cave passages in the Guadalupe Mountains continued to form throughout the Pliocene (~5-2 Ma). During this time the discharge point for the Capitan aquifer was at Hobbs, New Mexico, ~110 km east of Carlsbad, rather than at Carlsbad as it is today (Hiss 1980). Therefore, water levels in Guadalupe caves during this time must have been at least partially controlled by the Hobbs discharge point. As canyons downcut into the uplifting Guadalupe Mountain block, cave passages were intersected and entrances formed (DuChene & Martinez 2000). Entrances allowed these caves to be inhabited by bats and other animals.

CENOZOIC (QUATERNARY)

PLEISTOCENE

By the Quaternary (~2-0 Ma), Basin and Range extension and uplift had decreased in the Guadalupe Mountain area, as had the geothermal gradient. The present-day geothermal gradient in the Delaware Basin is ~20°C/km as compared to ~40-50°C/km in the Miocene. The decrease in uplift and tilting in the Pleistocene was an important factor that could have halted the processes by which Stage 4 sulfuric acid caves formed.

Another late-stage impact on development of Guadalupe caves near the northeast end of the reef (e.g., Carlsbad and Lechuguilla) may have been a change in the hydrologic regime at ~600 ka when the Capitan aquifer began to discharge at Carlsbad Springs instead of at Hobbs (Bachman 1984). The relationship of cave development in the Guadalupe Mountains with respect to regional hydrologic events is still poorly understood, but it is known that Guadalupe caves must somehow have been related to past positions and levels of the ancestral Pecos River, and that the major cave levels are attributable to long periods of stability as defined by these former base levels. Dates on the cloud and folia linings in the lowest levels of Carlsbad Cavern (Lake of the Clouds) and Lechuguilla Cave (Lake of the White Roses) are >350 ka (uranium-series method; D. Ford, pers. comm.), and ~600 ka (electron spin resonance method; K. Cunningham, pers. comm.). Since cave clouds are believed to form in the shallow phreatic zone (Hill & Forti 1997), these dates could signify a time just before the water table dropped below the lowest cave level in response to the Hobbs-Carlsbad change in regional hydrologic regime (Hill 1996, 2000).

Sometime after Stage 4 cave passages became air-filled, they began to be decorated with travertine. The different speleothems and speleogens in Guadalupe caves are both diverse and noteworthy, and have been described by Hill (1987), DuChene (1997), Hill & Forti (1997), and Davis (2000). Pleistocene travertine deposition in Guadalupe caves appears to have occurred in two main episodes: around 600 ka and around the time of the Sangamon Interglacial (~170-70ka) (Hill 1987).

HOLOCENE

The Guadalupe Mountains area turned more arid in the Holocene (10 ka to present). This change in climate affected water percolation patterns and, thus, the deposition of travertine. Water percolation and entrance air-flow patterns, in turn, affected cave microclimates and the geochemistry of cave pools (Forbes 2000; Turin & Plummer 2000). Today, travertine is still actively forming in some caves (e.g., Lechuguilla), but is almost inactive in others (e.g., Carlsbad).

CONCLUSIONS

This paper is a synthesis of information that relates to the history of geologic events and cave development in the Guadalupe Mountains. In summary, these events are:

(1) Late Permian. The Capitan reef and forereef facies and corresponding backreef and basinal facies were deposited in the Guadalupe Mountain area. The Guadalupe Mountains experienced their first uplift and exposure, and Stage 1 fissure caves formed along zones of weakness at the reef/backreef contact.

(2) Mesozoic. The Guadalupe Mountain area remained stable and emergent just above sea level. The first "flushing out" of the Capitan reef produced Stage 2 spongework caves during limestone mesogenesis.

(3) Late Cretaceous-Early Tertiary. The Laramide Orogeny uplifted the Guadalupe Mountain area at least 1.2 km above sea level. Stage 2 spongework caves probably enlarged, some may have been lined with calcite spar.

(4) Oligocene-Miocene. Trans-Pecos volcanism caused the Delaware Basin-Guadalupe Mountain area to heat up. This initiated the maturation and migration of hydrocarbons, and created a pattern of convective hydrothermal water circulation in the Capitan reef. Stage 3 thermal caves formed; some may have been lined with calcite spar.

(5) Miocene-Pleistocene. Tilting of the Delaware Basin eastward caused hydrocarbons to react with anhydrites in basinal rock to form H_2S. The main uplift of the Guadalupe Mountain block further caused this H_2S to migrate into the Capitan reef and there to become oxidized to sulfuric acid. This acid dissolved out the large cave passages and produced, as speleogenetic by-products, the gypsum blocks/rinds, native sulfur, endellite, and alunite found in these caves. Air-filled parts of the caves became decorated with travertine and inhabited by animals.

(6) Holocene. The arid climate caused a decline in the amount of travertine deposition in Guadalupe caves. Cave microclimate and pool chemistry was affected by entrance air flow and water percolation patterns in the vadose zone.

ACKNOWLEDGMENTS

I thank Art Palmer, Peg Palmer, and Donald Davis for reviewing the manuscript. I also acknowledge Unocal Corporation for redrafting some of the figures of Hill (1996).

REFERENCES

Bachman, G.O. (1984). Regional geology of Ochoan evaporites, northern part of Delaware Basin. *New Mexico Bureau of Mines and Mineral Resources Circular 184*: 22 pp.

Bretz, J H. (1949). Carlsbad Caverns and other caves of the Guadalupe block, New Mexico. *Journal of Geology 57 (5)*: 447-463.

Barker, C.E. & Pawlewicz, M.J. (1987). The effects of igneous intrusions and higher heat flow on the thermal maturity of Leonardian and younger rocks, western Delaware Basin, Texas. In Cromwell, D.W. & Mazzullo, L. (eds.). *Glass Mountains*. Society of Economic Paleontologists and Mineralogists Guidebook: 69-83.

Bögli, A. (1980). *Karst hydrology and physical speleology*: New York, Springer-Verlag: 284 pp.

Davis, D.G. (2000). Extraordinary features of Lechuguilla Cave, Guadalupe Mountains, New Mexico. *Journal of Cave and Karst Studies 62*(2): 147-157.

Dublyansky, Y.V. (1995). Speleogenetic history of Hungarian thermal karst. *Environmental Geology 25*: 24-35.

DuChene, H.R. (1986). Observations on previous hypotheses and some new ideas on cavern formation in the Guadalupe Mountains. In Jagnow, D.H. (ed.). *National Speleological Society Convention Guidebook, Tularosa, NM*: 96-100.

DuChene, H.R. (1997). Lechuguilla Cave, New Mexico, U.S.A. In Hill, C.A. & Forti, P. *Cave minerals of the world*, 2nd ed., Huntsville, AL, National Speleological Society:343-350.

DuChene, H.R. (2000). Bedrock features of Lechuguilla Cave, Guadalupe Mountains, New Mexico. *Journal of Cave and Karst Studies 62*(2): 109-119.

DuChene, H.R. & Martinez, R. (2000). Post-speleogenetic erosion and its effect on cave development in the Guadalupe Mountains, New Mexico and west Texas. *Journal of Cave and Karst Studies 62*(2): 75-79.

Esteban, M. & Pray, L.C. (1983). Pisoids and pisolite facies (Permian), Guadalupe Mountains, New Mexico and West Texas. In Peryt, T.M. (ed.). *Coated grains*. Berlin, Springer-Verlag: 503-537.

Forbes, J.R. (2000). Geochemistry of Carlsbad Cavern pool waters, Guadalupe Mountains, New Mexico. *Journal of Cave and Karst Studies 62*(2): 127-134.

Ford, D.D. & Ewers, R.O. (1978). The development of limestone cave systems in the dimensions of length and depth. *Canadian Journal of Earth Sciences 15 (11)*: 1783-1798.

Haneef, M. (1993). *Lithofacies and depositional environment of Altuda, Capitan and Tessey Formations (Permian), Glass*

Mountains, West Texas. Unpublished MS Thesis, Sul Ross State University, Alpine, Texas: 208 pp.

Hill, C.A. (1987). *Geology of Carlsbad Cavern and other caves in the Guadalupe Mountains, New Mexico and Texas*. New Mexico Bureau of Mines and Mineral Resources Bulletin 117: 150 pp.

Hill, C.A. (1990). Sulfuric acid speleogenesis of Carlsbad Cavern and its relationship to hydrocarbons, Delaware Basin, New Mexico and Texas: *American Association of Petroleum Geologists Bulletin 74(11)*: 1685-1694.

Hill C.A. (1995). Sulfur redox reactions, native sulfur, Mississippi Valley-type deposits and sulfuric acid karst, Delaware Basin, New Mexico and Texas. *Environmental Geology 25*: 16-23.

Hill, C.A. (1996). *Geology of the Delaware Basin: Guadalupe, Apache and Glass Mountains, New Mexico and West Texas.* Society of Economic Paleontologists and Mineralogists, Permian Basin section, Publication no. 96-39: 480 pp.

Hill, C.A. (1999a). Origin of caves in the Capitan. In Saller, A.H., Harris, P.M., Kirkland, B.L., & Mazzullo, S.J. (eds.), *Concepts in sedimentology and paleontology: Geologic framework of the Capitan Reef*: Society of Economic Paleontologists and Mineralogists, Special Publication no. 65: 211-222.

Hill, C.A. (1999b). Reevaluation of the Hovey Channel in the Delaware Basin, West Texas. *American Association of Petroleum Geologists Bulletin 83(2)*: 277-294.

Hill, C.A. (2000). Sulfuric acid, hypogene karst in the Guadalupe Mountains of New Mexico and west Texas, U.S.A. In Klimchouk, A., Ford, D.C., Palmer, A.N., & Dreybrodt, W. (eds.). *Speleogenesis: Evolution of karst aquifers*: Huntsville, AL, National Speleological Society: 309-316.

Hill, C.A. & Forti, P. (1997). *Cave minerals of the world*. 2nd ed.. Huntsville, AL, National Speleological Society: 463 pp.

Hiss, W.L. (1980). Movement of ground water in Permian Guadalupian aquifer systems, southeastern New Mexico and western Texas. In Dickerson, P.W. & Hoffer, J.M. (eds). *Trans-Pecos Region*: New Mexico Geological Society Guidebook, 31st Field Conference: 289-294.

Horak, R.L. (1985). Tectonic and hydrocarbon maturation history in the Permian Basin. *Oil and Gas Journal 83 (21)*: 124-125.

Hose, L.D. & Pisarowicz, J.A. (1999). Cueva de Villa Luz, Tabasco, Mexico: Reconnaisance study of an active sulfur spring cave and ecosystem: *Journal of Cave and Karst Studies 6 (1)*: 13-21.

Jagnow, D.H. (1977). *Geologic factors influencing speleogenesis in the Capitan Reef Complex, New Mexico and Texas*. Unpublished M.S. Thesis, University of New Mexico, Albuquerque: 197 pp.

Jagnow, D.H., Hill, C.A., Davis, D.G., DuChene, H.R., Cunningham, K.I., Northup, D.E. & Queen, J.M. (2000). History of sulfuric acid theory of speleogenesis in the Guadalupe Mountains, New Mexico and west Texas. *Journal of Cave and Karst Studies 62(*2): 54-59.

King, P.B. (1930). *The Geology of the Glass Mountains*. Bureau of Economic Geology, University of Texas at Austin, pt. 1, no. 3038: 167 pp.

King, P.B. (1948). *Geology of the southern Guadalupe Mountains, Texas*: U.S. Geological Survey Professional Paper 215: 183 pp.

Lundberg, J., Ford, D.C. & Hill, C.A. (2000). A preliminary U-Pb date on cave spar, Big Canyon, Guadalupe Mountains, New Mexico, USA. *Journal of Cave and Karst Studies 62*(2): 144-146.

Melim, L.A. (1991). *The origin of dolomite in the Permian (Guadalupian) Capitan Formation, Delaware Basin, west Texas and New Mexico—Implications for dolomitization models*: Unpublished PhD dissertation, Southern Methodist University, Dallas, Texas: 200 pp.

Melim, L.A. & Scholle, P.A. (1989). Dolomitization model for the forereef facies of the Permian Capitan Formation, Guadalupe Mountains, Texas-New Mexico. In Harris, P.M. & Grover, G.A. (eds.). *Subsurface and outcrop examination of the Capitan shelf margin, northern Delaware Basin*. Society of Economic Paleontologists and Mineralogists, Workshop no. 13, San Antonio, Texas: 407-413.

Mosch, C.J. & Polyak, V.J. (1996). Canary-yellow cave precipitates: Late-stage hydrated uranyl vanadate, uranyl silicate, and iron sulfate cave minerals (abs.). *Journal of Cave and Karst Studies 58*(3): 209.

Northup, D.E., Dahm,C.N., Melim, L.A., Spilde, M.N., Crossey, Lavoie, K.H., Mallory, L.M., Boston, P.J., Cunningham, K.I. & Barns, S.M. (2000). Evidence for geomicrobiological interactions in Guadalupe caves. *Journal of Cave and Karst Studies 62*(2): 80-90.

Palmer, A.N. (1991). Origin and morphology of limestone caves. *Geological Society of America Bulletin 103*: 1-21.

Palmer, A.N., & Palmer, M.V. (1998). Geochemistry of Cueva de Villa Luz, Mexico, an active H_2S cave (abs): *Journal of Cave and Karst Studies 60(3)*: 188.

Palmer, A.N & Palmer, M.V. (2000). Hydrochemical interpretation of cave patterns in the Guadalupe Mountains, New Mexico. *Journal of Cave and Karst Studies 62*(2): 91-108.

Polyak, V.J. & Güven, N. (1996). Mineralization of alunite, natroalunite, and hydrated halloysite in Carlsbad Cavern and Lechuguilla Cave, New Mexico. *Clays and Clay Minerals 44 (6)*: 843-850.

Polyak, V.J. & Güven, N. (2000). Clays in caves of the Guadalupe Mountains, New Mexico. *Journal of Cave and Karst Studies 62*(2): 120-126.

Polyak, V.J., McIntosh, W.C., Güven, N. & Provencio, P. (1998). Age and origin of Carlsbad Cavern and related caves from $^{40}Ar/^{39}Ar$ of alunite. *Science 279*: 1919-1922.

Polyak, V.J. & Provencio, P.P. (2000). Summary of the timing of sulfuric acid speleogenesis for the Guadalupe caves based on ages of alunite. *Journal of Cave and Karst Studies 62*(2): 72-74.

Queen, J.M., Palmer, A.N. & Palmer, M.V. (1977). Speleogenesis in the Guadalupe Mountains, New Mexico—gypsum replacement of carbonate by brine mixing. Proceedings, 7th International Congress of Speleology, Sheffield, United Kingdom: 332-336.

Rye, R.O., Bethke, D.M. & Wasserman, M.O. (1992). The stable isotope geochemistry of acid sulfate alteration. *Economic Geology 87*(2): 225-262.

Scholle, P.A., Ulmer, D.S. & Melim, L.A. (1992). Late-stage calcites in the Permian Capitan Formation and its equivalents, Delaware Basin margin, west Texas and New Mexico—Evidence for replacement of precursor evaporites. *Sedimentology 39*: 207-234.

Spirakis, C.S. & Cunningham, K.I. (1992). Genesis of sulfur deposits in Lechuguilla Cave, Carlsbad Caverns National Park, New Mexico. In Wessel, G. & Wimberley, B. (eds.). *Native sulfur development in geology and exploration*. Proceedings of Society for Mining, Metallurgy and Exploration, American Institute of Mining, Metallurgical, and Petroleum Engineers, Phoenix, AZ: 139-154.

Turin, H.J. & Plummer, M.A. (2000). Lechuguilla Cave pool chemistry, 1986-1999. *Journal of Cave and Karst Studies 62*(2): 135-143.

Wood, J.W. (1968). *Geology of Apache Mountains, Trans-Pecos Texas*. Bureau of Economic Geology, University of Texas at Austin: 32 pp., Text accompanying Geologic Quadrangle map no. 35.

Victor J. Polyak and Paula P. Provencio - Summary of the timing of sulfuric acid speleogenesis for the Guadalupe caves based on ages of alunite. *Journal of Cave and Karst Studies* *62*(2): 72-74.

SUMMARY OF THE TIMING OF SULFURIC-ACID SPELEOGENESIS FOR GUADALUPE CAVES BASED ON AGES OF ALUNITE

VICTOR J. POLYAK
Department of Earth and Planetary Sciences, University of New Mexico, Northrop Hall, 200 Yale Blvd., Albuquerque, New Mexico 87131 USA
PAULA P. PROVENCIO
Sandia National Laboratories, Albuquerque, New Mexico 87185 USA

The H_2SO_4 caves in the Guadalupe Mountains, New Mexico, USA, such as Carlsbad, Cottonwood, Endless, Lechuguilla, and Virgin caves, formed during the late Miocene and early Pliocene (12-4 Ma). It has been demonstrated that the caves at the higher elevations are the oldest. The timing of speleogenesis was determined by the $^{40}Ar/^{39}Ar$ dating of the mineral alunite, which is a direct by-product of H_2SO_4 speleogenesis.

Five caves (Carlsbad, Cottonwood, Endless, Lechuguilla, and Virgin) in the Guadalupe Mountains of southeastern New Mexico, U.S.A., contain by-products of their H_2SO_4-related origin (Fig. 1). See Hill (2000) for an overview of the geology of these caves, and Jagnow *et al.* (2000) for a history of how this theory of speleogenesis developed for Guadalupe caves.

Caves formed by carbonic acid dissolution of limestone or dolostone usually leave no material trace of their origin. As Sasowsky (1998) noted, determining the age of what is not there has been a difficult task. However, caves formed by sulfuric acid-bearing water (H_2SO_4-speleogenesis) contain direct by-products of their origin. In the Guadalupe caves, Egemeier (1973) and Jagnow (1977) reported gypsum as a by-product of H_2SO_4-speleogenesis, and Hill (1987) reported gypsum and endellite (hydrated halloysite). More recently, Palmer & Palmer (1992), Polyak & Güven (1996), and Polyak & Provencio (1998) have reported that alunite, and other by-products such as hydrobasaluminite, also occur in these caves. Of these, alunite, $KAl_3(SO_4)_2(OH)_6$, is unique because it contains potassium which gives it the potential to be dated by the K-Ar or $^{40}Ar/^{39}Ar$ dating methods.

Alunite was sampled from Carlsbad, Cottonwood, Endless, Lechuguilla, and Virgin caves. William C. McIntosh at New Mexico Tech in Socorro, New Mexico used $^{40}Ar/^{39}Ar$ to date the fine-grained alunite from the Guadalupe caves (methods are found in Polyak *et al*. 1998). The deposits suitable for dating contained alunite (1-10 µm-sized crystals) mixed with hydrated halloysite (endellite). Purified samples (where the halloysite was removed) contained only tightly packed alunite.

Alunite can form by the alteration of aluminum- and potassium-bearing materials such as aluminosilicates (clays) in an environment of sulfide oxidation; i.e., high Eh, low pH (Kelepertsis 1989; Long *et al.* 1992; Rye *et al.* 1992). Similarly, during H_2SO_4-speleogenesis of the Guadalupe caves, alunite formed by sulfuric acid interaction with clays that contain potassium–clays such as illite and montmorillonite (Polyak & Güven 1996). For instance, in the Green Clay Room of Carlsbad Cavern, alunite was produced by the alteration of montmorillonite-rich clay. An alteration reaction for this situation may be expressed as follows:

$$\begin{aligned} &2\,H_2SO_4 + 3[(K,Na)(Al_{1.24}Mg_{0.47}Fe_{0.29})(Si_{3.56}Al_{0.44})O_{10}(OH)_2\cdot nH_2O] \\ \Leftrightarrow\quad &1\,[(K,Na)Al_3(SO_4)_2(OH)_6] + 1\,[Al_2Si_2O_5(OH)_4)\cdot 2(H_2O)] \\ &+ 9\,SiO_2 + \text{residual } (Na^+, K^+, Fe^{2+}, Mg^{2+}) \end{aligned}$$

where the formula for the clay was determined from energy dispersive X-ray microanalysis of montmorillonite containing small amounts of illite and kaolinite. In these caves, the alteration reaction ceased when the supply of H_2SO_4 was terminated.

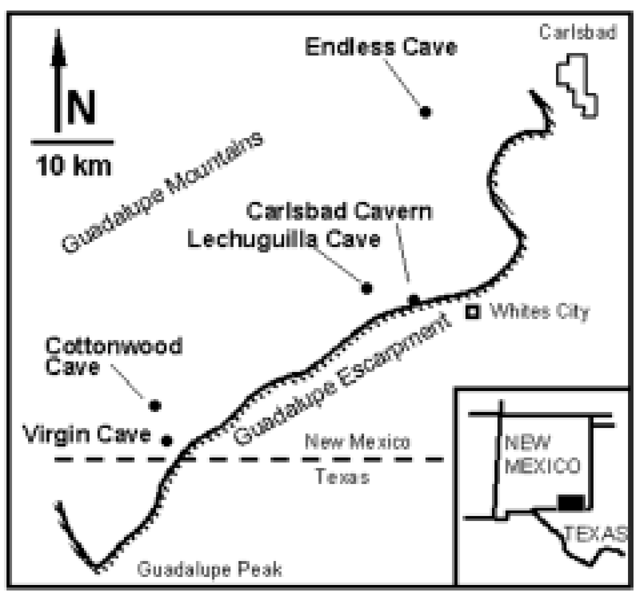

Figure 1. Study area map showing general location of five caves where the mineral alunite was collected.

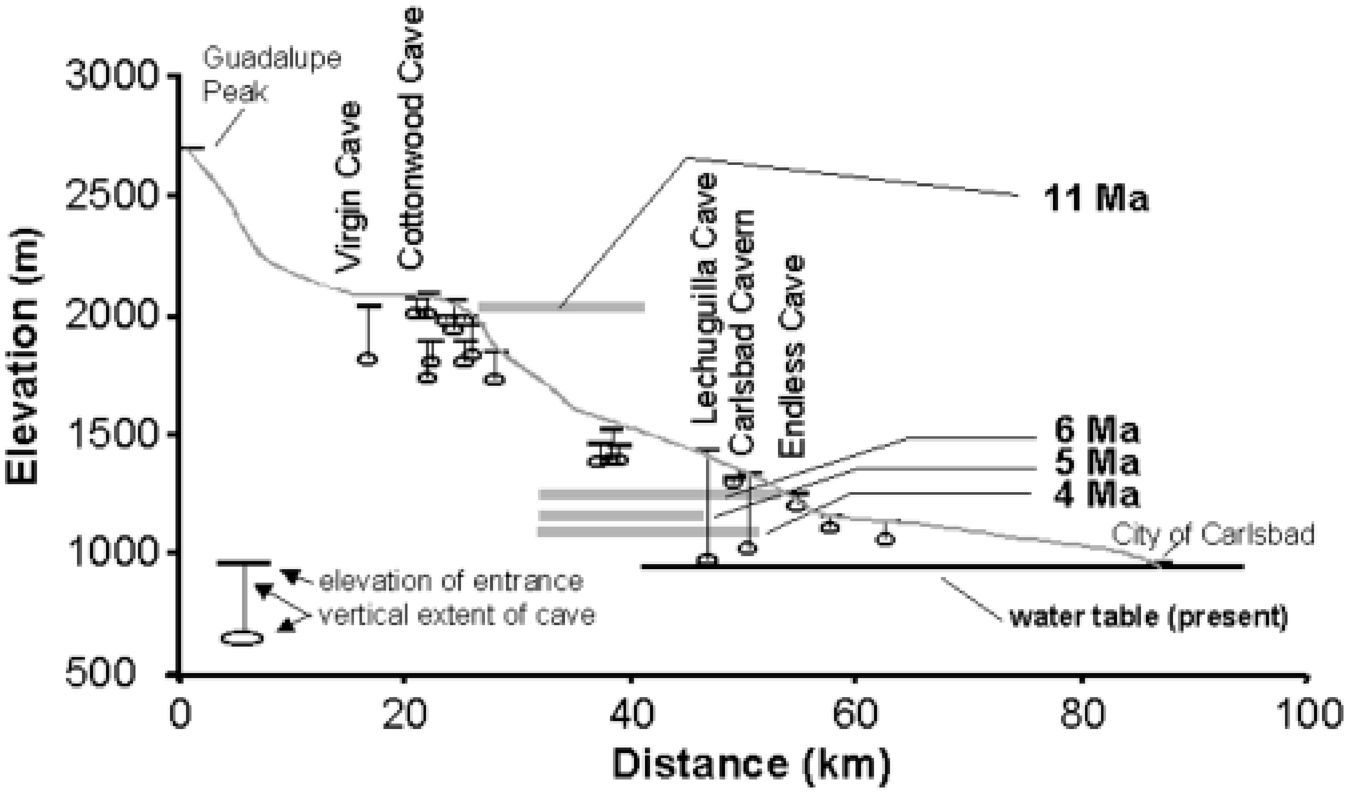

Figure 2. Profile of the Guadalupe Mountains from Guadalupe Peak to the city of Carlsbad. Locations of major caves are plotted on the profile according to their elevation. The gray line from Guadalupe Peak to the city of Carlsbad represents the surface elevation in the Guadalupe Mountains along the Guadalupe Ridge and the Capitan reef escarpment. Note the four elevation intervals where the timing of H_2SO_4-influenced speleogenesis has been established.

TIMING OF H_2SO_4-INFLUENCED SPELEOGENESIS

$^{40}Ar/^{39}Ar$ ages of alunite from Carlsbad, Cottonwood, Endless, Lechuguilla, and Virgin caves indicate that H_2SO_4-speleogenesis took place from the late Miocene to early Pliocene (12-4 Ma). These data represent four elevation intervals of speleogenesis (Fig. 2). Alunite in Cottonwood and Virgin caves at the higher elevations, 2000-2040 m, dates from 12.3 to 11.3 Ma (oldest dates). Two levels of Lechuguilla Cave are represented by alunite ages of 6.0 (Glacier Bay at an elevation of 1230 m) and 5.2 Ma (Lake Lebarge at an elevation of 1150 m). Glacier Bay in Lechuguilla Cave and Endless Cave, both at the same elevation of 1230 m, provided the same alunite age, ~6 Ma, even though they are located >20 km apart. Alunite from the Big, Green Clay, and New Mexico rooms of Carlsbad Cavern, at the elevation interval of 1090-1120 m, all have ages of 4.0-3.9 Ma. See Polyak *et al*. (1998) for a complete table and description of the age data.

CONCLUSION

H_2SO_4-speleogenesis took place at or near the water table (Hill 1987; Palmer & Palmer 2000). The relationship of the alunite ages with respect to elevation of the caves suggests an 1100-m apparent decline in the water table from 12 Ma to the present (Polyak *et al*. 1998). These correlations suggest that the Capitan aquifer water table was relatively flat during the late Miocene and Pliocene in areas of speleogenesis. Caves formed by the H_2SO_4-speleogenesis at any given period are located along the same elevation, as depicted by Jagnow & Jagnow (1992). Knowing the absolute timing of H_2SO_4 speleogenesis for the Guadalupe caves provides a framework for resolving long-sought questions regarding the caves and the mountains.

ACKNOWLEDGMENTS

We are grateful to Necip Güven for his earlier contribution related to clay analyses, and to William C. McIntosh for the $^{40}Ar/^{39}Ar$ analyses of the alunite samples. Both were authors on the *Science* paper. We thank Carol A. Hill for reviewing our paper. We also thank Ransom Turner of the Lincoln National Forest Service, Dale Pate and Jason Richards of the Carlsbad Caverns National Park, and Jim Goodbar of the Carlsbad District Bureau of Land Management for field assistance and for permission to collect samples.

REFERENCES

Egemeier, S.J. (1973). *Cavern development by thermal waters with a possible bearing on ore deposition*. Unpublished PhD dissertation. Stanford University, Stanford, CA: 88 pp.

Hill, C.A. (1987). Geology of Carlsbad Cavern and other caves in the Guadalupe Mountains, New Mexico and Texas. *New Mexico Bureau of Mines and Mineral Resources Bulletin 117*: 150 pp.

Hill, C.A. (2000). Overview of geologic history of cave development in the Guadalupe Mountains, New Mexico and west Texas. *Journal of Cave and Karst Studies 62*(2): 60-71.

Jagnow, D.H. (1977). Geologic factors influencing speleogenesis in the Capitan Reef Complex, New Mexico and Texas. Unpublished MS thesis, University of New Mexico, Albuquerque: 203 pp.

Jagnow, D.H. & Jagnow, R.R. (1992). *Stories from stones – The geology of the Guadalupe Mountains*. Carlsbad Caverns Guadalupe Mountains Association, Carlsbad, NM: 40 pp.

Jagnow, D.H., Hill, C.A., Davis, D.G., DuChene, H.R., Cunningham, K.I., Northup, D.E. & Queen, J.M. (2000). History of sulfuric acid theory of speleogenesis in the Guadalupe Mountains, New Mexico and west Texas. *Journal of Cave and Karst Studies 62*(2): 54-59.

Kelepertsis, A.E. (1989). Formation of sulfates at the Thiaphes area of Milos Island: Possible precursors of kaolinite mineralization. *Canadian Mineralogist 27*: 241-245.

Long, D.T., Fegan, N.E., McKee, J.D., Lyons, W.B., Hines, M.E., & Macumber, P.G. (1992). Formation of alunite, jarosite and hydrous iron oxides in a hypersaline system: Lake Tyrrell, Victoria, Australia. *Chemical Geology 96*: 183-202.

Palmer, A.N. & Palmer, M.V. (1992). Geochemical and petrologic observations in Lechuguilla Cave, New Mexico (abs.). In Ogden, A.E. (ed.), *Friends of Karst Meeting: Proceedings*. Tennessee Tech University, Cookesville, Tennessee: 25-26.

Palmer, A.N & Palmer, M.V. (2000). Hydrochemical interpretation of cave patterns in the Guadalupe Mountains, New Mexico. *Journal of Cave and Karst Studies 62*(2): 91-108.

Polyak, V.J. & Güven, N. (1996). Alunite, natroalunite and hydrated halloysite in Carlsbad Cavern and Lechuguilla Cave, New Mexico. *Clays and Clay Minerals 44*: 843-850.

Polyak, V.J., McIntosh, W.C., Güven, N., & Provencio, P. (1998). Age and origin of Carlsbad Cavern and related caves from $^{40}Ar/^{39}Ar$ of alunite. *Science 279*: 1919-1922.

Polyak, V.J. & Provencio, P. (1998). Hydrobasaluminite and aluminite in caves of the Guadalupe Mountains, New Mexico. *Journal of Cave and Karst Studies 60(1)*: 51-57.

Rye, R.O., Bethke, P.M., & Wasserman, M.D. (1992). The stable isotope geochemistry of acid sulfate alteration. *Economic Geology 87*: 225-262.

Sasowsky, I.D. (1998). Determining the age of what is not there. *Science 279*: 1874.

Harvey R. DuChene and Ruben Martinez - Post-speleogenetic erosion and its effect on cave development in the Guadalupe Mountains, New Mexico and west Texas. *Journal of Cave and Karst Studies 62*(2): 75-79.

POST-SPELEOGENETIC EROSION AND ITS EFFECT ON CAVES IN THE GUADALUPE MOUNTAINS, NEW MEXICO AND WEST TEXAS

HARVEY R. DUCHENE
7216 E. Bentley Circle, Englewood, Colorado 80112-1197 USA hduchene@compuserve.com
RUBEN MARTINEZ
Cody Energy LLC, 7555 E. Hampden Ave, Suite 600, Denver, Colorado 80231 USA

The Guadalupe Mountains of New Mexico and west Texas are a northeast-tilted fault block cut by canyons that increase in frequency and topographic relief from east to west. The processes of erosion and mass wasting have exposed more than 300 known caves, which range from systems like Lechuguilla Cave (>170 km) and Carlsbad Cavern (>49 km) in the east, to caves with less than 10 m of passage in the west. Erosion of the Capitan, Yates and Seven Rivers formations progressively removed more cave-bearing strata and destroyed more caves from east to west. It is likely that modern-day canyons in the central and western Guadalupe Mountains were once sites of long cave systems that have been truncated or destroyed by erosion and mass wasting.

The Guadalupe Mountains of New Mexico and west Texas are a northeast tilted fault block ranging in elevation from 2667 m at Guadalupe Peak to 960 m near the city of Carlsbad (Fig. 1). The mountains are an exhumed portion of the Capitan Reef Complex, a Permian (Guadalupian) shelf margin that nearly rings the Delaware Basin (DuChene & Hill 2000). Formations that crop out throughout the mountains are the Capitan, Seven Rivers, Yates and Tansill, with older rocks of the Goat Seep and Queen exposed to the west in deep canyons and along the Western Escarpment (King 1948; Hayes & Gale 1957; Hayes & Koogle 1958; Motts 1962; Hayes 1964; DuChene 2000). The Guadalupe Mountains contain an estimated 300 known caves (Jagnow 1979), some of which were formed by sulfuric acid derived from hydrocarbons in the Delaware Basin (Davis 1980; Hill 1987, 1990; Palmer & Palmer 2000). The two largest and longest caves, Lechuguilla (>170 km) and Carlsbad (>49 km), are in the relatively undissected area east of Rattlesnake Canyon, whereas smaller and shorter caves are concentrated in the more-deeply dissected area to the west. Ages of sulfuric acid caves range from 12.3 Ma in the higher elevations of the western Guadalupes to 3.9 Ma in the east at Carlsbad Cavern (Polyak *et al.* 1998; Polyak & Provencio 2000).

One of the great puzzles of the Guadalupes is why no long cave systems have been found in the western part of the mountains. It may be that none were formed, but it is also possible that they were once present but have been destroyed by erosion. In this paper, we investigate the rate and amount of erosion that has probably occurred in the Guadalupe Mountains since the horizontal cave passages formed about 12 - 4 Ma, and consider factors that may have controlled the locations of caves and canyons.

For this paper, we define a *long* cave as one with more than 8 km of passage, and a *short* cave as one with less than 8 km of passage. A *large* cave has great volume compared to its length and typically has passages or rooms more than 15 m wide and 10 m high. A *truncated* cave passage is one that was once part of a larger cave system that has been mostly destroyed by erosion.

The purposes of this paper are to show how much material has been eroded from the Guadalupe Mountains during the last 12 Ma, and to consider how erosion has impacted the caves. Subjects such as the possible causes for lowering of the water table, the timing of uplift, and the causes of faulting in and near the Guadalupe Mountains are not discussed. These controversial topics are beyond the scope of this paper and have been addressed elsewhere (e.g. Chapin & Cather 1994; Eaton 1987; Hill 1996; Lindsay 1998).

METHODS

The study area extends from the Western Escarpment of the mountains near Guadalupe Peak to a point 65 km east near the city of Carlsbad (Fig. 1). The southern boundary is the Capitan Reef Escarpment, which marks the basinward limit of the Capitan Reef Complex. The width of the area is approximately 7.5 km and includes the Capitan Formation as well as most of the cave-bearing carbonate beds of the Seven Rivers, Yates, and Tansill formations (DuChene 2000: his Fig. 3). The estimated aggregate thickness of the Capitan reef, backreef and forereef is 600 m.

The study area is divided into three segments based on geomorphic characteristics and topographic slope (Fig. 1 & Table 1). The western segment extends from the Western Escarpment to Double Canyon and has an area of 296 km². It has an average slope of 21 m/km to the northeast, is characterized by deep, steep-walled, mostly northwest-trending canyons, and contains numerous short, truncated caves. There are a number of large passages in caves such as Cottonwood, Virgin and

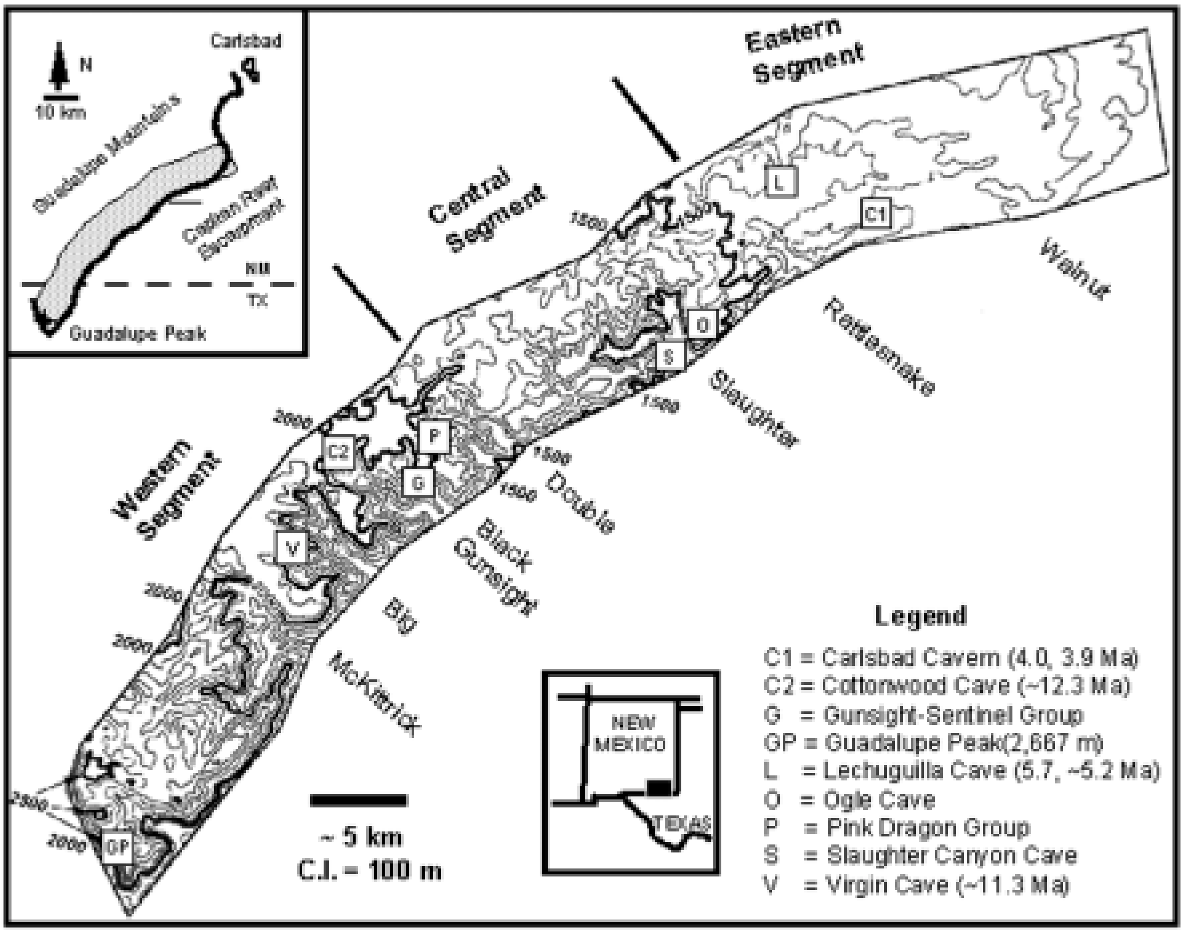

Figure 1. Topographic map of the Guadalupe Mountains showing the locations of caves and canyons discussed in the text. The key to symbols and the ages of significant caves (Polyak *et al.* 1998) are listed in the legend.

Gunsight, but no known long caves. The central segment extends from Double Canyon to Rattlesnake Canyon and has an area of 127 km². It has an average slope of 38.4 m/km and has steep-walled, northwest- and northeast-trending canyons. Caves in this segment are also short, but a few, such as Ogle and Slaughter Canyon (formerly called New Cave), are large.

The eastern segment covers 159 km² and extends from Rattlesnake Canyon to the eastern limit of the study area near Carlsbad. It has an east-northeast slope averaging 18 m/km and low relief compared to the other two segments. This segment has fewer entrances, but contains Carlsbad Cavern and Lechuguilla Cave, the two longest and largest caves in the Guadalupe Mountains.

Table 1. Summary of volume calculations and statistics for Guadalupe Mountains.

Table 1

Calculation of volume of material eroded from Guadalupe Mountains during last 12.3 Ma						East-northeast plunge		Vertical relief (ridge top to canyon bottom) in m			Downcutting in m/Ma		
Segments	Maximum age of caves in block in Ma (from Polyak et al, 1998)	Area in km2	Original volume (pre-erosion) in km3	Volume removed by erosion in km3	% of volume removed by erosion	m/km	degrees	minimum	maximum	median	minimum	maximum	median
1 (West)	12.3	296.15	177.7	40.9	32.0%	21	1.2	650	1140	895	53	93	73
2 (Central)	9 (est)	127.43	76.5	16.1	21.1%	38	2.2	200	650	425	22	72	47
3 (East)	5.7	159.42	95.7	7.2	7.5%	19	1.1	0	200	100	0	35	18
Totals		583.00	349.8	64.2	18.3%								

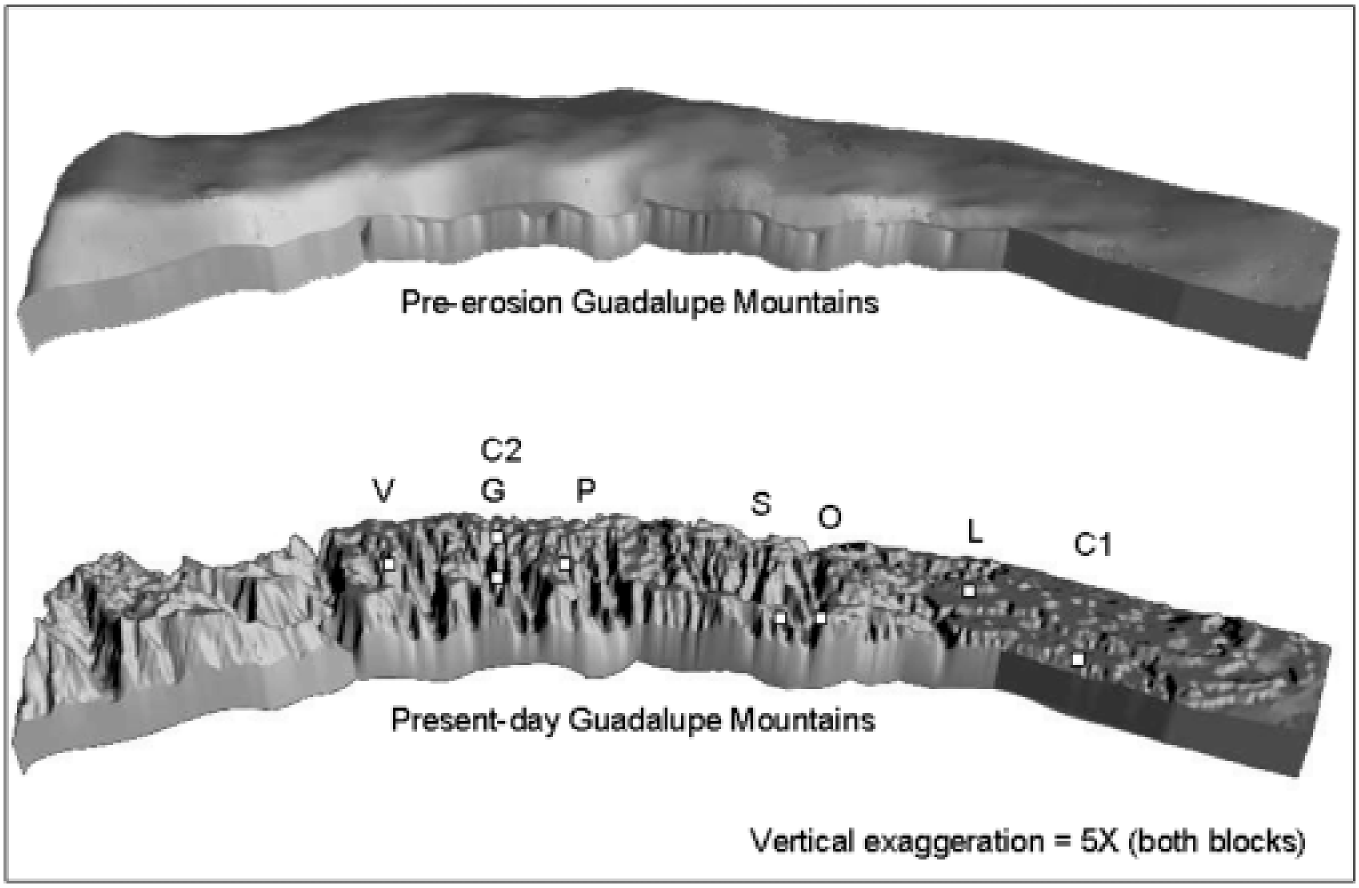

Figure 2. Block diagrams showing the pre-erosion and post-erosion topography of the Guadalupe Mountains. Symbols are the same as in figure 1.

Volume calculations for the Guadalupe Mountains were derived from U.S. Geological Survey digital topographic data for the Carlsbad East and Van Horn East 1° quadrangles and are computer-generated. The 3 arc-second Digital Elevation Model data depicting the present topography of the Guadalupe Mountains was imported into AutoCad and converted into a UTM Zone 13 projection, with a grid density of 100 m. Two surfaces were created to calculate the eroded and original volumes of the mountains. The pre-erosion surface was hand contoured and electronically converted to a grid that matches the present-day topographic surface. The surface representing the base of the Capitan Reef Complex was determined by subtracting 600 m from the top of the pre-erosion surface. The volume of eroded material was calculated by subtracting the present topographic surface from the pre-erosion surface, and the total volume was calculated by subtracting the bottom surface from the top of the pre-erosion surface (i.e., the pre-erosion volume of the study area is the area multiplied by the thickness). To simplify the calculations, it was assumed that the Guadalupe Mountain block had no significant erosion prior to the onset of sulfuric acid speleogenesis in the Middle to Late Miocene, although it is likely that some erosion of the block occurred earlier (Hill 1996, 2000). Pre- and post-erosion volumes and rates of downcutting were calculated for the eastern, central and western segments; the results are summarized in table 1. Downcutting is reported as maximum, minimum and median rates for each segment.

RESULTS

The western segment has pre- and post-erosion volumes of 127.7 km³ and 86.8 km³, respectively. Canyons range in depth from 1,140-650 m from west to east, and ~32% of the original volume has been removed by erosion. The rate of downcutting ranges from 93 m/Ma in the west to 53 m/Ma on the east with a median rate of 73 m/Ma. The central segment has pre- and post-erosion volumes of 76.5 km³ and 60.4 km³, respectively. Depth of erosion ranges from 650-200 m from west to east and ~21% of the original volume has been removed. The rate of downcutting is based on an estimated cave age of 9 Ma because no alunite age dates have been determined for this segment (Polyak *et al.* 1998; Polyak & Provencio 2000). The rate of downcutting ranges from ~72 m/Ma on the west to 22 m/Ma on the east, with a median rate of 47 m/Ma. The eastern segment has pre- and post-erosion volumes of 95.7 km³ and 88.5 km³, respectively, and topographic relief is a maximum of 200 m, decreasing to the east. The amount of material removed by erosion is about 7.5% of the original volume. The rate of downcutting in this segment ranges from 0-35 m/Ma, with a median rate of 18 m/Ma.

The rate of downcutting and volume of eroded material reported for each segment of the Guadalupe Mountains assumes that erosion occurred at a constant rate during the last 12 Ma. Certainly, the rates have varied in response to changes in the amount of precipitation and recharge over time. However, since these variables are unknown, and for simplicity, we have assumed a constant rate.

DISCUSSION

Most of the major cave passages in the Guadalupe Mountains are developed along joints that are either parallel or perpendicular to the Reef Escarpment. Most of these caves are developed near the reef-forereef contact in the Capitan Formation, or the reef-backreef contact between the Capitan and Seven Rivers and Yates formations (Jagnow 1979; Hill 1996, 1999, 2000; DuChene 2000). Guadalupe Mountain canyons also either parallel the Reef Escarpment or are perpendicular to it (Fig. 1). These canyons, especially those that parallel the Reef Escarpment, are excavated into those parts of the Capitan, Seven Rivers and Yates formations that are most likely to contain caves. The processes of erosion and mass wasting that are excavating the canyons are also destroying many of the caves.

In the eastern segment of the Guadalupe Mountains, erosion has not reached the parts of the Seven Rivers and Capitan where most known cave passages occur (DuChene 2000). Since only ~7.5% of the rock has been removed, this segment has the highest chance of containing long, undissected cave systems, and the smallest chance of having cave entrances.

In the central segment, ~21% of the bedrock has been removed. Topographic relief ranges from 200-650 m and erosion has cut deeply into the cave-bearing rocks of the Seven Rivers and Capitan, especially in West Slaughter Canyon. Canyons in this area have many entrances in their walls including those for Ogle and Slaughter Canyon caves, which are located on opposite sides of Slaughter Canyon and horizontally separated by only 1125 m (Figs. 1 & 2). It is possible that these two caves were once part of a longer system, but downcutting of Slaughter Canyon has destroyed most of the original cave. This hypothetical cave system is located approximately at the same stratigraphic position as Carlsbad Cavern and would have been comparable in size. A prominent set of northwest-trending joints probably controlled both speleogenesis and erosion near the mouth of Slaughter Canyon. Surface erosion and mass wasting deepened and widened the canyon, eventually destroying most of this cave system, but with Ogle, Slaughter Canyon and a few smaller remnant cave passages remaining "stranded" high on the walls of the canyon.

In the western segment, ~32% of the original bedrock has been removed, and topographic relief ranges from 650-1140 m. Erosion has cut completely through the prime cave-bearing parts of the Yates, Seven Rivers and Capitan formations, and many truncated caves are exposed, especially in Double, Black and Gunsight canyons. If surface erosion and mass wasting followed the joint systems that controlled speleogenesis, then the largest parts of many of these caves have been destroyed. Two examples of areas where there are clusters of truncated caves are Black Canyon near Gunsight and Sentinel caves, and Double Canyon at the Pink Dragon group of caves (Figs. 1 & 2). The caves in both of these areas were probably once parts of larger systems, but erosion has destroyed all but these remnant passages.

CONCLUSIONS

The Guadalupe Mountains can be divided into western, central and eastern segments based on their elevation, slope and topography. From east to west, the depth and magnitude of erosion increases, and the number of exposed caves increases. The longest known caves are in the eastern segment of the mountains where erosion has not cut deeply enough to expose cave-bearing strata of the Capitan and Seven Rivers formations.

Downcutting progressed at an average rate of 73 m/Ma in the western segment of the Guadalupe Mountains. In the central segment, the average rate is 47 m/Ma, and in the eastern segment, it is 18 m/Ma. Erosion has removed ~7.5% of the original volume of rock from the eastern segment, ~21% from the central segment, and ~32% from western segment of the mountains.

Most caves in the Guadalupe Mountains are located near the reef-backreef contact between the Capitan formation and the Seven Rivers and Yates formations. In the central and western segments, canyons are deeply incised into cave-bearing strata and a large amount of the limestone most likely to contain caves has been removed by erosion. Long cave systems probably once existed throughout the Guadalupe Mountains, but west of Rattlesnake Canyon erosion has mostly destroyed them, leaving only truncated remnants stranded high on canyon walls.

ACKNOWLEDGMENTS

We are grateful to Carol Hill, Darryl Granger, and Donald Davis for suggestions that resulted in significant improvement to this paper, and to Kim Cunningham and Victor Polyak who provided the inspiration.

REFERENCES

Chapin, C.E. & Cather, S.M. (1994). Tectonic setting of the axial basins of the northern and central Rio Grande Rift. In Keller, G.R. & Cather, S.M. (eds.). *Basins of the Rio Grande Rift.* Geological Society of America Special Paper 291: 5-25.

Davis, D.G. (1980). Cave development in the Guadalupe Mountains: A critical review of recent hypotheses. *NSS Bulletin 42(3)*: 42-48.

DuChene, H.R. (2000). Bedrock features of Lechuguilla Cave, Guadalupe Mountains, New Mexico. *Journal of Cave and Karst Studies 62*(2): 109-119.

DuChene, H.R. & Hill, C.A. (2000). Introduction to the Guadalupe Mountains Symposium. *Journal of Cave and Karst Studies 62*(2): 53.

Eaton, G.P. (1987). Topography and origin of the southern Rocky Mountains and Alvarado Ridge. In Coward, M.P., Dewey, J.F., & Hancock, P.L. (eds.). *Continental extension tectonics.* Geological Society of America Special Publication No. 28: 355-369.

Hayes, P.T. (1964). Geology of the Guadalupe Mountains: *U.S. Geological Survey Professional Paper 446*: 69 pp.

Hayes, P.T. & Gale, B.T. (1957). Geology of the Carlsbad Caverns East Quadrangle, New Mexico. *U.S. Geological Survey Geologic Quadrangle Map 98*, scale 1:62,500.

Hayes, P.T., & Koogle, R.L. (1958). Geology of the Carlsbad Caverns West Quadrangle, New Mexico-Texas: *U. S. Geological Survey Geological Quadrangle Map GQ-112,* scale 1:62,500.

Hill, C.A. (1987). Geology of Carlsbad Cavern and other caves in the Guadalupe Mountains, New Mexico and Texas. *New Mexico Bureau of Mines and Mineral Resources Bulletin 117*: 150 pp.

Hill, C.A. (1990). Sulfuric acid speleogenesis of Carlsbad Cavern and its relationship to hydrocarbons, Delaware Basin, New Mexico and Texas. *American Association of Petroleum Geologists Bulletin 74(11)*: 1685-1694.

Hill, C.A. (1996). Geology of the Delaware Basin–Guadalupe, Apache and Glass Mountains, New Mexico and West Texas. *Society of Economic Paleontologists and Mineralogists, Permian Basin Section Publication No. 96-39*: 480 pp.

Hill, C.A. (1999). Origin of caves in the Capitan. In Saller, A.H., Harris, P.M., Kirkland, B.L., & Mazzulo, S.J. (eds.), *Geologic framework of the Capitan Reef.* Society of Economic Paleontologists and Mineralogists Special Publication No. 65: 211-222.

Hill, C.A. (2000). Overview of geologic history of cave development in the Guadalupe Mountains, New Mexico and west Texas. *Journal of Cave and Karst Studies 62*(2): 60-71.

Jagnow, D.H. (1979). *Cavern development in the Guadalupe Mountains*. Cave Research Foundation, Columbus, Ohio: 55 pp.

King, P.B. (1948). Geology of the southern Guadalupe Mountains, Texas: *U. S. Geological Survey Professional Paper 215*: 183 pp.

Lindsay, R.F. (1998). Meteoric recharge, displacement of oil columns and the development of residual oil intervals in the Permian Basin. In DeMis, W.D. & Nelis, M.K. (eds.). *The search continues into the 21st Century.* West Texas Geological Society Publication No. 98-105: 271-273.

Motts, W.S. (1962). Geology of the West Carlsbad Quadrangle, New Mexico*: U. S. Geological Survey Geological Quadrangle Map GQ-167*. Scale, 1:62,500.

Palmer, A.N. & Palmer, M.V. (2000). Hydrochemical interpretation of cave patterns in the Guadalupe Mountains, New Mexico. *Journal of Cave and Karst Studies 62*(2): 91-108.

Polyak, V.J. & Provencio, P.P. (2000). Summary of the timing of sulfuric acid speleogenesis for the Guadalupe caves based on ages of alunite. *Journal of Cave and Karst Studies 62*(2): 72-74.

Polyak, V.J., McIntosh, W.C., Güven, N. & Provencio, P. (1998). Age and origin of Carlsbad Cavern and related caves from $^{40}Ar/^{39}Ar$ of alunite. *Science 279*: 1919-1922.

Diana E. Northup, Clifford N. Dahm, Leslie A. Melim, Michael N. Spilde, Laura J. Crossey, Kathy H. Lavoie, Lawrence M. Mallory, Penelope J. Boston, Kimberley I. Cunningham and Susan M. Barns - Evidence for geomicrobiological interactions in Guadalupe caves. *Journal of Cave and Karst Studies 62*(2): 80-90.

EVIDENCE FOR GEOMICROBIOLOGICAL INTERACTIONS IN GUADALUPE CAVES

DIANA E. NORTHUP
Biology Department, University of New Mexico, Albuquerque, NM 87131 USA dnorthup@unm.edu
CLIFFORD N. DAHM
Biology Department, University of New Mexico, Albuquerque, NM 87131 USA
LESLIE A. MELIM
Department of Geology, Western Illinois University, Macomb, IL 61455 USA
MICHAEL N. SPILDE
Institute of Meteoritics, University of New Mexico, Albuquerque, NM 87131 USA
LAURA J. CROSSEY
Earth and Planetary Sciences, University of New Mexico, Albuquerque, NM 87131 USA
KATHLEEN H. LAVOIE
College of Arts and Sciences, SUNY-Plattsburgh, Plattsburgh, NY 12901 USA
LAWRENCE M. MALLORY
Biomes, Inc., Olney, MD 20832 USA
PENELOPE J. BOSTON
Complex Systems Research, Inc., Boulder CO 80503 USA
KIMBERLEY I. CUNNINGHAM
Geo-Microbial Technologies Inc., P.O. Box 132, Ochelata, OK 74051 USA
SUSAN M. BARNS
Environmental Molecular Biology, Los Alamos National Laboratory, Los Alamos, NM 87545 USA

Caves in the Guadalupe Mountains offer intriguing examples of possible past or present geomicrobiological interactions within features such as corrosion residues, pool fingers, webulites, u-loops, and moonmilk. Scanning electron microscopy, transmission electron microscopy, molecular biology techniques, enrichment cultures, bulk chemistry, and X-ray diffraction techniques have revealed the presence of iron- and manganese-oxidizing bacteria in corrosion residues, which supports the hypothesis that these organisms utilize reduced iron and manganese from the limestone, leaving behind oxidized iron and manganese. Metabolically active populations of bacteria are also found in "punk rock" beneath the corrosion residues. Microscopic examination of pool fingers demonstrates that microorganisms can be inadvertently caught and buried in pool fingers, or can be more active participants in their formation. Enrichment cultures of moonmilk demonstrate the presence of a variety of microorganisms. Humans can have a deleterious impact on microbial communities in Guadalupe caves.

The caves of the Guadalupe Mountains are located in southeastern New Mexico, U.S.A., near the city of Carlsbad (Fig. 1). Over 300 known caves exist in these mountains, the most famous being Carlsbad Cavern and Lechuguilla Cave. These caves are filled with secondary mineral deposits (speleothems), which have been described and classified by Hill (1987) and Hill & Forti (1997).

Microorganisms have been found in association with carbonate and silicate speleothems, sulfur compounds, iron and manganese oxides, and saltpeter (Northup *et al.* 1997). As in surface environments, cave microorganisms participate in precipitation of minerals either passively by acting as nucleation sites (Went 1969), or actively through the production of enzymes or substances that lead to precipitation by changing the microenvironment (Danielli & Edington 1983). Microorganisms can also cause the dissolution of cave features through acidic metabolic by-products. While geomicrobiological interaction studies in the outside world are rather common (Ehrlich 1996), such studies in caves are just beginning. Studies of geomicrobiological interactions in caves can shed light on basic mechanisms of dissolution and precipitation by microorganisms, and, thus on the origin of specific types of speleothems.

Guadalupe Mountain caves contain a number of examples of possible interactions between microorganisms and speleothems. In particular, Lechuguilla and Cottonwood caves contain speleothems that have been referred to as "biothems" by Cunningham *et al.* (1995)–features such as webulites and u-loops that appear to be calcified filamentous microorganisms. The discovery of "snottites" in Cueva de Villa Luz (Hose & Pisarowicz 1999; Hose *et al.* 2000), a cave with active hydrogen sulfide vents, allows researchers to speculate that such

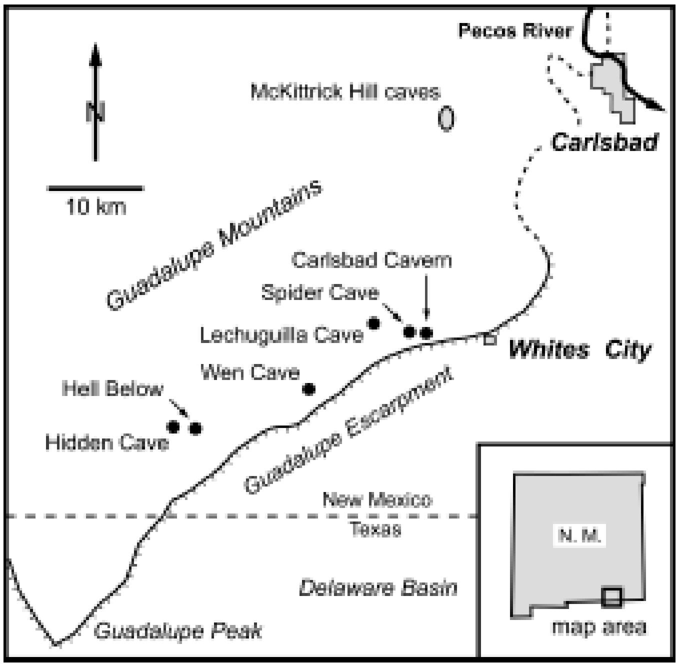

Figure 1. Location map of caves mentioned in the text. Modified from Palmer & Palmer (2000).

bacterial structures could become lithified later in the evolution of the cave, producing the u-loops that we see in Lechuguilla Cave today.

Other speleothems in Guadalupe caves also show microscopic or macroscopic evidence of possible bacterial interaction in their formation. Lechuguilla and Hidden caves contain pool fingers that show evidence of bacterial presence (Fig. 2). Also, a pool basin in Hell Below Cave contains unusual growths that resemble stiff meringue peaks. Manganese and iron oxide material in the form of "corrosion residues" from

Figure 2. Pool fingers in Hidden Cave. Note their "robust" nature and covering of popcorn-like crust. Photo by Kenneth Ingham.

Figure 3. Corrosion residues in EA survey in Lechuguilla Cave. Corrosion residues remain on the cave walls and ceiling after the carbonate fraction of the wall rock has been dissolved away. Field of view is ~5 cm. Photo by Robert Buecher.

Lechuguilla and Spider caves contain bacteria whose closest relatives are iron-oxidizing bacteria, a group of organisms that can contribute to corrosion (Fig. 3). Davis *et al.* (1990) demonstrated the presence of filaments in the cores of the "rusticles", an iron oxide speleothem in Lechuguilla Cave.

In this paper we investigate the nature of the relationship between the presence of bacteria in speleothems and bedrock residues, and the dissolution and precipitation of these deposits. We do this by presenting three case studies: corrosion residues, pool fingers, and moonmilk. We then discuss the impact that humans can have on microbiological and geologic interactions.

METHODS

FIELD TECHNIQUES

Samples of corrosion residues were collected from the EA survey, Sanctuary, PHD Room, Ghostbusters Hall, Apricot Pit, Rainbow Room, the FN survey, and the Snowing Passage (FN27) in Lechuguilla Cave (Fig. 4) and from the Grand Canyon, H1X, and the Decision Room in Spider Cave (Fig. 5). Enrichments for iron- and manganese-oxidizing bacteria were inoculated using aseptic techniques on site in the PHD Room and Sanctuary in Lechuguilla Cave (Fig. 4), and at TM12 off the Decision Room and at H1X in Spider Cave (Fig. 5). Samples for DNA extraction were immediately placed on dry ice for transport to the lab and then stored in an ultra-cold freezer. Pool finger specimens were collected from Lechuguilla and Hidden caves (Fig. 1). Samples of moonmilk were collected from the Deep Point in Spider Cave (Fig. 5).

Corrosion residues and punk rock for metabolic activity studies were aseptically sampled using a flame-sterilized spat-

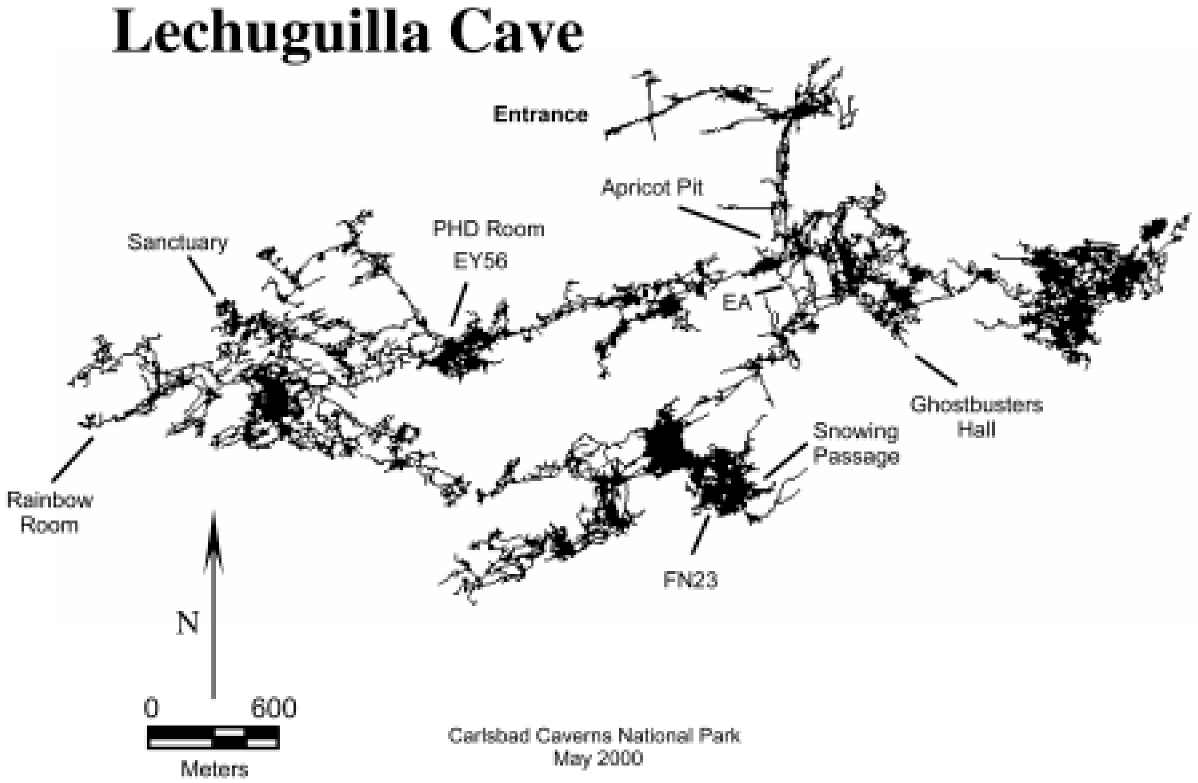

Figure 4. Sample sites in Lechuguila Cave. Map by Stan Allison and Paul Burger, U.S. National Park Service.

ula. Punk rock was sampled by carefully removing the surface corrosion material before sampling. Sample material was placed directly into sterile microcentrifuge tubes and controls were killed using formalin. A respiratory dye solution, [2-(p-iodophenyl)-3-(p-nitrophenyl)-5-phenyltetrazolium chloride]: INT, was added to all tubes and incubated for 4 hours, then formalin was added to the live tubes.

LABORATORY TECHNIQUES

Scanning electron microscopy (SEM), transmission electron microscopy (TEM), energy dispersive X-ray spectrometry (EDX), and light microscopy. SEM, coupled with an EDX analyzer, was used to study the surfaces of samples for evidence of bacteria and their by-products. All samples were coated with gold-palladium. Freshly broken pool fingers were acid-etched before SEM examination. Samples for transmission electron microscopy (TEM) were ground in acetone, mounted in a liquid suspension on a porous carbon grid, and mounted in the microscope. This method is useful on crystalline material for imaging crystal lattice fringes and diffraction patterns. Amorphous and microcrystalline Fe and Mn oxyhydroxides, present in many of the corrosion residues, were also identified by transmission electron microscopy (TEM). Microbial populations were viewed with light microscopy using methylene blue, gram, acid fast, and sudan black stains (Clark 1973).

Chemical analyses. Chemical analyses were performed on whole rock samples of wall rock, punk rock, and corrosion residue. For major and most trace elements, samples were analyzed using X-ray fluorescence (XRF). Selected trace elements were also analyzed by atomic adsorption. Other analytical determinations included insoluble residue analysis by dissolution of bedrock samples, water content, and Fe^{+2}/Fe^{+3} (Husler & Connolly 1991; Kolthoff & Sandell 1952). Mineralogical compositions were determined by X-ray diffraction (XRD) and scanning electron microscopy.

Enrichments. Enrichment and isolation media for manganese- and iron-oxidizing bacteria were prepared such that reduced iron (Fe^{+2}) or manganese (Mn^{+2}) was suspended in a stable gel to allow O_2 to diffuse towards the reduced material.

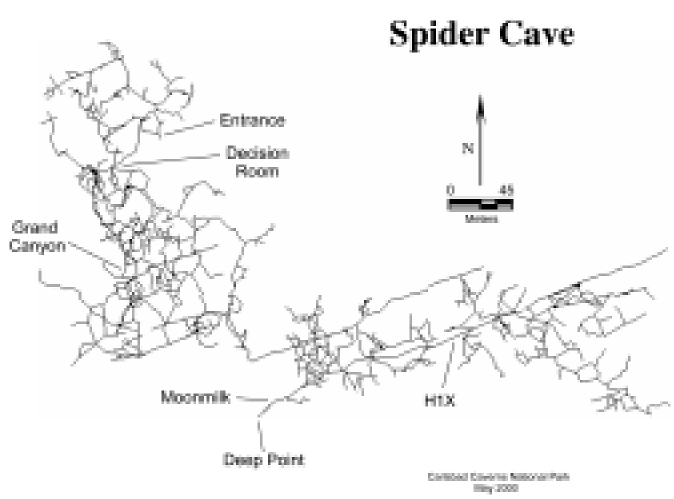

Figure 5. Sample sites in Spider Cave. Map by Stan Allison, U.S. National Park Service.

Hanert's modification of Wolfe's FeS medium was used for iron-oxidizing strains, and steel carpet tacks were added to the bottom of the media as a source of iron (Hanert 1992). Samples of moonmilk from Spider were inoculated on site into a very low nutrient medium developed for microbes using low molecular weight organic carbon sources (C_1-C_3) compounds and into an organic-rich medium suitable for various actinomycetes and fungi (Hose *et al*. 2000).

Molecular phylogeny. To avoid the limitations of culture-based techniques (Amann *et al*. 1995; Ward *et al*. 1992), molecular phylogenetic methodology that uses genetic sequence data from the small subunit ribosomal RNA (SSU rRNA) was utilized (Barns *et al*. 1994; Reysenbach *et al*. 1994).

Using techniques developed at Los Alamos National Laboratory for soil, we extracted DNA from Lechuguilla Cave corrosion residue samples using bead mill homogenization, followed by nucleic acid purification (Kuske *et al.* 1997). We then performed the polymerase chain reaction (PCR) employing primers specific for rRNA genes (rDNAs) to produce copies of the rDNAs in the extracted DNA. Amplification products were sorted by cloning into plasmid vectors. PCR products from eighty-two clones with the correct size insert were purified with a QIAprep plasmid miniprep kit (Qiagen, Inc., Chatsworth, Calif.). Purified DNA was used as a template in cycle sequencing. Sequences were tested for the presence of PCR-produced chimeric artifacts known to occur during this type of natural population analysis (Liesack *et al.* 1991; Kopczynski *et al.* 1994).

Bacterial metabolic activity. Direct estimates of total and respiring cells in both corrosion material and "punk rock" were made using microscopic techniques (Rusterholtz & Mallory 1994). Total cells were determined by counting cells stained with acridine orange, a dye that intercalates into DNA and is detected using epifluorescence microscopy. Acridine orange-stained cells fluoresce a bright green. Respiring cells are detected by staining cells with a respiratory dye ([2-(p-iodophenyl)-3-(p-nitrophenyl)-5-phenyltetrazolium chloride]: INT), added on site in the cave. This chemical is taken up and reduced by actively respiring cells. The reduced dye is seen as a distinct red crystal using bright-field microscopy. Killed controls and previously live samples were stained with a 0.1% acridine orange solution in the laboratory.

CASE STUDIES

CASE STUDY I: CORROSION RESIDUES

One cave environment having a high potential for geomicrobiological interactions is that of the "corrosion residues" (Fig. 3). Lechuguilla Cave is notably rich in this material, while lesser amounts exist in Spider Cave, Carlsbad Cavern, other Guadalupe caves, and also in caves in other parts of the world. Researchers have often assumed that corrosion residues are essentially insoluble components remaining after acid dissolution of cave bedrock that formed by abiological, dominantly inorganic, processes. For example, Queen (1994) hypothesized that corrosion residues are the long-term result of upwelling corrosive air where Rayleigh-Benard convection may induce air circulation that cools upon reaching the ceiling of the cave, resulting in the condensation of water droplets that absorb CO_2, forming carbonic acid that corrodes the bedrock.

Discovery of bacterial and fungal communities in the corrosion residues (Cunningham 1991a,b; Cunningham *et al*. 1995; Northup *et al*. 1995) has led to another explanation: that microbes could be active participants in the production of corrosion residues, in conjunction with abiological processes. Potentially, microorganisms could oxidize reduced compounds from the atmosphere or wall rock, producing acidity as a by-product. Extracellular polymers from bacteria are usually acidic and contain functional groups that readily bind metal ions and contribute to corrosion of metals and the breakdown of carbonates and silicates (Ford & Mitchell 1990; Little *et al.* 1986ab). Seminal studies by Costerton *et al.* (1987) have shown that microbial biofilms can greatly affect the substrates on which they grow by altering the microenvironments under the films to enhance corrosion and degradation of many materials.

Energy sources in corrosion residues, "punk rock", and wall rock. Bulk chemical and XRD analyses of host carbonates, punk rock, and corrosion residues have allowed us to track the mineral transformation from the interior of the rock out to the corrosion residues and identify potential energy sources for microorganisms. Corrosion residue in Guadalupe caves occurs as coatings up to 2 cm thick, overlying a layer of altered carbonate host rock on cave walls, floors and ceilings and even on loose boulders (Fig. 3). The host rock can be altered to a depth of up to 10 cm or more, an occurrence that was first termed "punk rock" by Hill (1987). Our studies indicate that host carbonates (dolomite/limestone) of the Permian Capitan Reef Complex contain up to 2.3% insoluble residue of quartz and clays (illite, kaolinite, dickite, and smectite) (see also Polyak & Güven 2000).

Cunningham's (1991a,b) analysis of corrosion residues from Lechuguilla Cave using SEM and EDX techniques identified several iron and manganese phases: todorokite $[(Mn^{2+},Ca,Mg)\ Mn_3^{4+}O_7 \cdot H_2O]$ and poorly ordered iron oxides and hydroxides (mainly hematite and goethite), which are potential end products of bacterial metabolism. Mineral analyses of corrosion residues show a very high (50-80% by weight) manganese mineral component (Cunningham *et al.* 1995). DuChene's (1997) mineralogical inventory of corrosion residues in Lechuguilla Cave also showed the presence of ankerite, endellite, gibbsite, hydrated halloysite (endellite), hematite, goethite, griegite, nordstrandite, rancieite, and todorokite.

Our study of corrosion residues in Lechuguilla and Spider caves supports the variability of their mineralogical composition. Carbonates and quartz are either absent or limited. Kaolinite, dickite, and endellite (10-Angstrom hydrated halloysite $[Al_2Si_2O_5(OH)_4 \cdot 2H_2O]$) clays may be present, along with well-ordered aluminum hydroxide (mainly gibbsite).

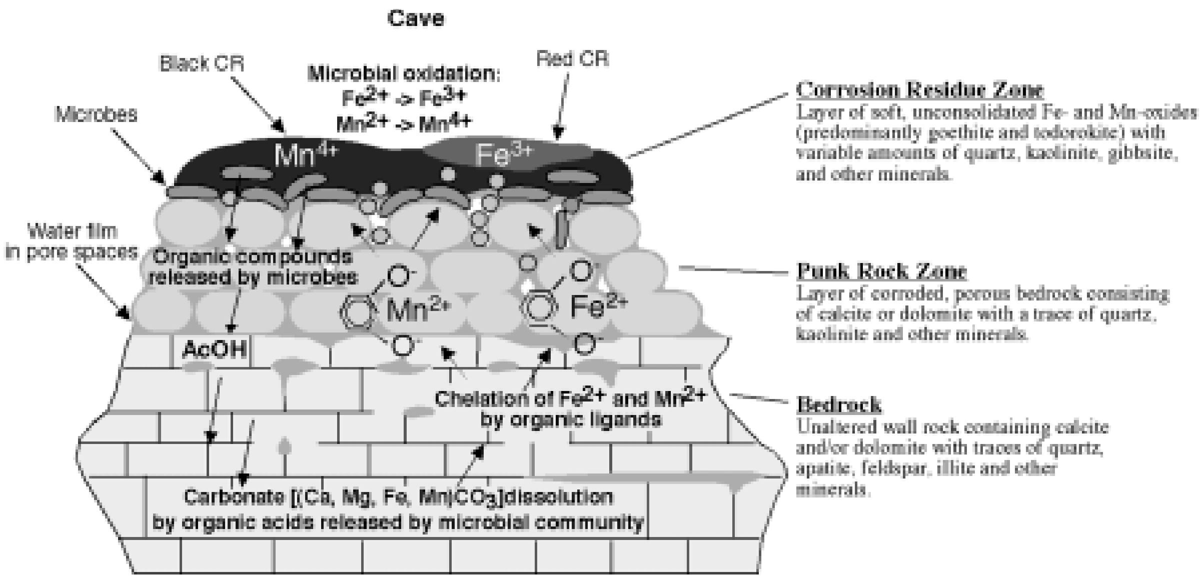

Figure 6.

Schematic depiction of a cross-section from the aerobic cave environment to more reducing conditions encountered within the wall. Modified from L. Mallory (unpublished). CR = corrosion residue.

Todorokite, goethite and hematite most likely represent oxidized by-products of reduced Mn and Fe present in trace or minor amounts in the original carbonate minerals.

Chemical analyses confirm that high concentrations of manganese and iron exist in corrosion residues, with a good correlation between color and chemical composition. Iron is associated with red, red-brown, brown and black (40, 50, 80, and 25 wt% oxide, respectively), and manganese is strongly associated with the black residues, which have yielded as high as 21.6 wt% Mn-oxide. Therefore, the corrosion residue shows a strong enrichment of manganese and iron relative to whole rock composition.

The corrosion residues do not form simply through dissolution of the host carbonate. They are mineralogically and chemically distinct from whole rock insoluble residue as shown by comparison of elemental ratios. Using the insoluble constituent aluminum for normalization, the ratio of SiO_2 /Al_2O_3 is about 5.5 in the insoluble residue, but is closer to 1 in most corrosion residue analyses. Iron and manganese are highly enriched in almost all corrosion residues. Melim (1991) found that Mn^{+2} ranged from 30-220 ppm in the bedrock of Capitan Formation (reef and forereef) and from 20-200 ppm in the bedrock of backreef (Tansill and Yates formations), while Fe^{+2} ranged from 50-2863 ppm in the reef and forereef and from 64-2428 ppm in the backreef. Utilizing both these published ranges for manganese concentrations of 20-200 ppm in host rock Mn (our unpublished SIMS analyses for selected host carbonates yield concentrations from 18-50 ppm), and ~11% MnO in corrosion residues, mass balance calculations indicate a concentration factor of about 50 times by weight for Mn. However, the low density of corrosion residue translates to a thickness of 2.2 cm of host rock required to generate 1 cm of residue. Other elements, including Al, Fe, Si, and Mg, have been leached from punk rock. Ca, Mg, and Si have also probably been partially removed through aqueous leaching, although only trace amounts of liquid water are present.

Figure 6 schematically depicts a hypothesized cross-section from the aerobic cave environment to more reducing conditions encountered within the wall rock itself. Carbonate removal is proposed to be accomplished through microbially assisted dissolution of dolomite and limestone within the punk-rock zone. The presence in corrosion residues of bacteria whose closest identified relatives are bacteria known to utilize Fe or Mn oxidation as a metabolic pathway (*Leptothrix*, *Pedomicrobium manganicum*, and unidentified iron-oxidizing bacteria) lends support to this hypothesis. Quartz and illite in the wall rock react to form more acid-stable clays such as kaolinite; excess aluminum is incorporated into gibbsite in corrosion residues. As iron and manganese are oxidized, todorokite and amorphous/poorly crystalline ferric phases form, later aging to goethite and hematite.

Microscopic evidence of bacteria associated with corrosion residues. The morphology of putative bacteria in corrosion residues, punk rock, and wall rock includes coccoids, filaments, rods, stalked bacteria and more unusually shaped forms (Fig. 7a&b). Interwoven fabrics of filaments found in corrosion residues hanging and falling from the ceiling of Snowing Passage in Lechuguilla Cave (Fig. 8a&b) appear to be mineral. EDX studies show these filaments to be manganese oxides (todorokite), which knit together to form a mineral surface. Studies underway will establish whether there is any microbial involvement in their initial formation.

Enrichments for manganese- and iron-oxidizing bacteria. Enrichment cultures targeting iron-oxidizing bacteria, which utilize reduced iron in the media, produced visible growth in 72% (26/36) of tubes. Those targeting manganese-oxidizing bacteria produced growth in 90% (28/31) of tubes. In most instances, growth occurred as a band between 2-9 mm below the surface of the medium; occasionally growth at greater depths was observed. Visible growth ranged in color from white to yellow/orange (sometimes with black speckles) to black/brown. More black/brown growth was observed in the

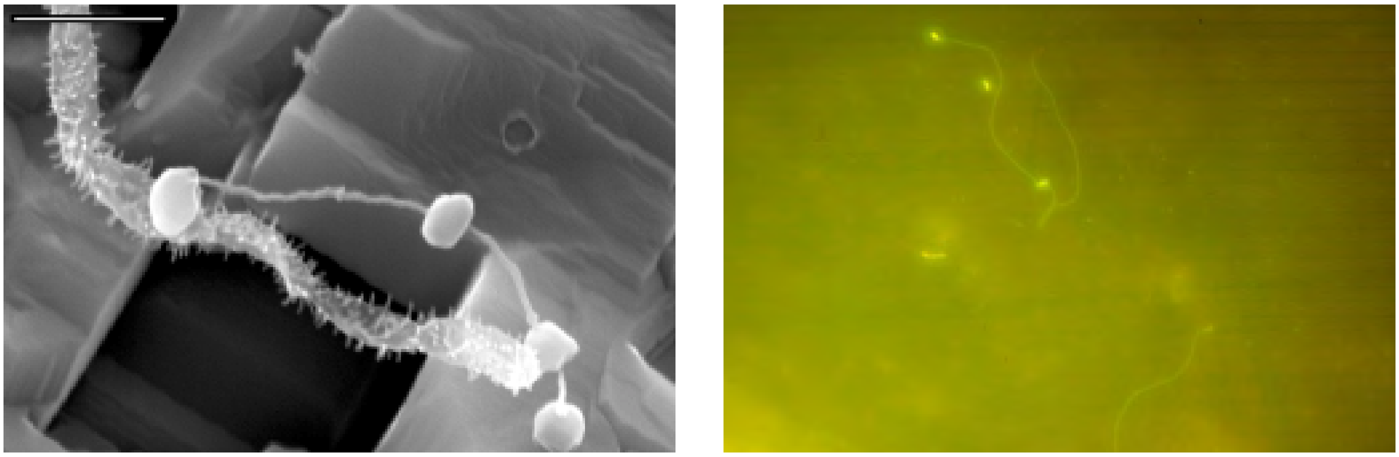

Figure 7. (a - Left) Bacteria found on corroded speleothem in Spider Cave. Note probable attachment structures. Scale bar = 2 µm. (b - Right) Stalked bacteria and rods stained with acridine orange. Field of view is ~200 µm. Photo by Rachel Schelble.

manganese enrichments. Examination of culture material with SEM/EDX revealed the presence of iron and manganese, presumably in the form of oxy-hydroxides. Such deposits were not part of the original media and demonstrate the ability of the cultured organisms to produce iron and manganese oxides. Molecular phylogenetic analysis of one culture showed the closest relatives to be actinomycetes. Some iron and manganese bacteria produce acidity as a product of their metabolic reactions (Ehrlich 1996). Therefore, these organisms are possible candidates for promoting dissolution of the wall rock and formation of corrosion residue.

Molecular evidence of manganese- and iron oxidizing bacteria from corrosion residues. Red-brown corrosion residues at the EA site have yielded diverse groups of organisms using molecular phylogenetic techniques from analysis of 46 clones. The closest known relatives of these microbes include low temperature archaea (the dominant clones at 56.5%), actinomycetes, nitrite-oxidizing bacteria, gram-positive bacteria, and Proteobacteria in the beta, gamma, and alpha subdivisions. Of particular interest for geomicrobiological studies is the presence of clones whose closest relatives are unidentified iron-oxidizing bacteria, *Leptothrix*, and *Variovorax paradoxus* in the beta subdivision of the Proteobacteria. *Leptothrix* is a manganese-oxidizing bacterium and *Variovorax paradoxus* is capable of lithoautotrophic growth using H_2 as an energy source. One clone's closest relative in the alpha subdivision is *Pedomicrobium manganicum*, a budding bacterium that accumulates iron and manganese oxides (Bergey 1989). Several sequences show less than 0.5 similarity to any other known 16S rDNA sequence, indicating they are novel organisms.

Studies of bacterial metabolic activity. Preliminary results show moderately large and active populations of bacteria in both corrosion material and punk rock. Respiring cell counts for corrosion residues examined in the EA survey indicate 1.6 x 10^7 cells per cm^3 of material representing 30% of total cells. Cell densities in punk rock were more varied. Respiring cell counts for punk rock examined in the EA survey ranged from 1 x 10^6 to 8.6 x 10^6 cells per cm^3 of material, representing 15-29% of total cells. The highest counts to date were found in the Sanctuary where 2 x 10^7 actively respiring cells per cm^3 of corrosion material were detected. These cells represent 37% of the total cells detected.

Summary. The presence of reduced iron and manganese compounds in wall rock, the existence of bacterial morphologies in corrosion residues and wall rock, culturing of putative iron- and manganese-oxidizing bacteria from corrosion residues, identification of organisms whose close relatives are iron- and manganese-oxidizing bacteria using molecular phylogenetic techniques, and bacterial metabolic activity in the punk rock region provide preliminary support for the hypothesis that microorganisms participate in the dissolution of the wall rock to form corrosion residues. We propose that the corrosion residues have built up over long time periods through microbially assisted dissolution and leaching of underlying host carbonate rock.

CASE STUDY II: POOL FINGERS

Davis *et al.* (1990: 80) described pool fingers as "slightly wiggly, slender calcite fingers up to 30 cm long and about 1.5-6 mm in diameter". Pool fingers are found in many dry and some active pools in Lechuguilla Cave, and also in Carlsbad Cavern and Hidden Cave. Pool fingers show evidence of bacterial presence, although the degree to which bacteria are involved in their formation has not been established.

Hidden Cave pool fingers. These pool fingers occur in a dry cave pool below the former water level and range from 1 to 5 cm in diameter and up to 20 cm long. They are more "robust" than those in Lechuguilla, having a rough outer surface with knobby protrusions up to 1 cm in diameter that extend up to 5 mm out from the side of each finger.

The core of each sampled pool finger consists of micritic

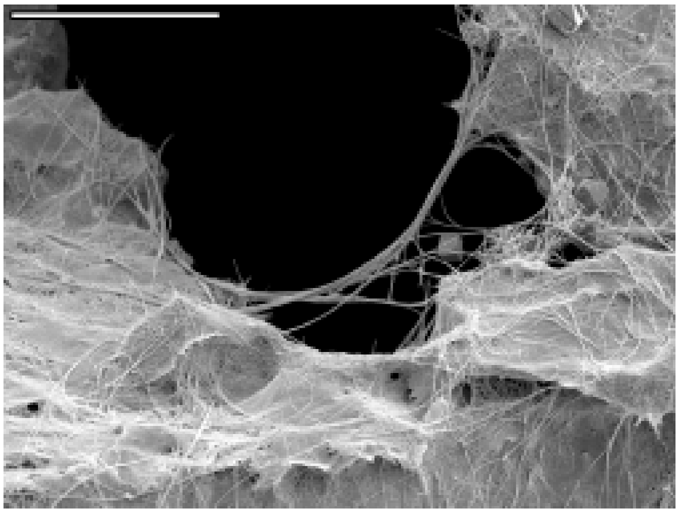

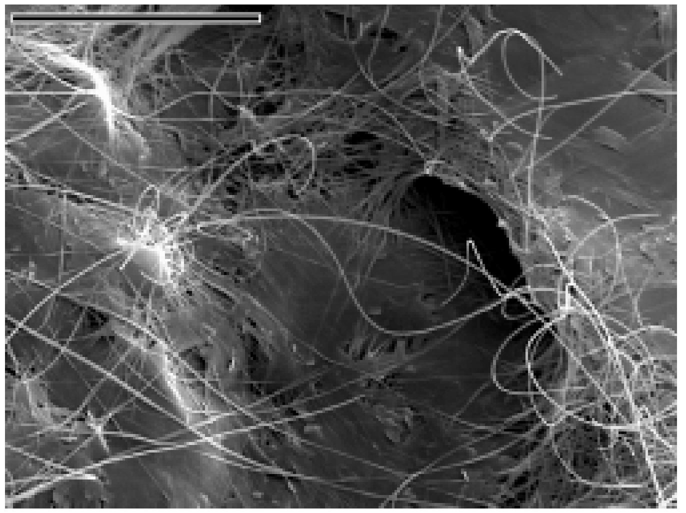

Figure 8. (a - Left) Interwoven fabric of filaments found hanging and falling from the ceiling of Snowing Passage in Lechuguilla Cave. The material may be mineralized microbial filaments. Scale bar = 20 µm. (b - Right) Higher magnification image of possible mineralized microbial filaments. Scale bar = 10 µm.

calcite, usually with dark-brown, 30-50 µm spherical lumps (Fig. 9). The thickness of the core ranges from 1-3 mm and varies within and between pool fingers. The core is not solid but rather has irregular, rounded pores up to 500 µm in diameter that are either open or filled later with brown clay and, rarely, hydromagnesite. These pores are much larger than the micritic material and are similar in appearance to fenestral pores found in marine limestones.

The outer part of each pool finger is composed of alternating layers of dark micritic calcite and bladed to dogtooth calcite spar (Fig. 9). The ratio of micrite to spar is highly variable, both between samples and within individual samples. For example, HC-3 is almost 50% micrite while HC-4 is only about 20% micrite. Micritic layers are usually <1 mm thick but reach up to 3 mm in thickness. The micrite varies from vaguely laminated to clotted with dark-brown, 30-100 µm blebs. Individual laminae thicken and thin dramatically along the length of each pool finger, often expanding into distinct clotted lumps up to 1 mm high made up of coalescing micrite. The protrusions seen on the macroscopic scale are underlain by clotted lumps of micrite on the microscopic scale that have been later coated and expanded by layers of calcite spar.

Spar layers are irregular and composed of crystals 50-100 µm wide and up to 2 mm long, often radiating out from dense micritic cores (Fig. 9). The distinction between spar and micrite is often gradational over ~1 mm, from micrite to microspar to coarse bladed calcite. Inclusions elongate and parallel to the long axis of the crystal are common. Some of these appear empty; others appear to be filled with micrite.

Preliminary SEM results document evidence of bacteria within the "robust" pool fingers of Hidden Cave. Rods, filaments, and more complex diamond, cross-hatched forms were observed on both freshly broken and etched samples (10% HCl after polishing). Some of these rods are hollow (Fig. 10). The dark, micritic cores of the Hidden Cave pool fingers are very similar to pelmicritic fabrics from marine environments that have been shown by Chafetz (1986) to be bacterial in origin. The laminated to clotted fabrics look like microbialites described from modern lacustrine (e.g., Braithwaite & Zedef 1996), hot spring (e.g., Chafetz & Folk 1984), and marine (e.g., Burne & Moore 1987; Chafetz & Buczynski 1992) environments. Based on the similarity of fabrics and the SEM documented occurrence of fossil bacteria, it is possible that bacteria contributed to the precipitation of the "robust" pool fingers.

Lechuguilla Cave pool fingers. The Lechuguilla Cave pool fingers sampled (1-1.5 cm across) are only slightly larger than those described by Davis *et al.* (1990). They are composed of radiating crystals of bladed calcite exhibiting a sweeping

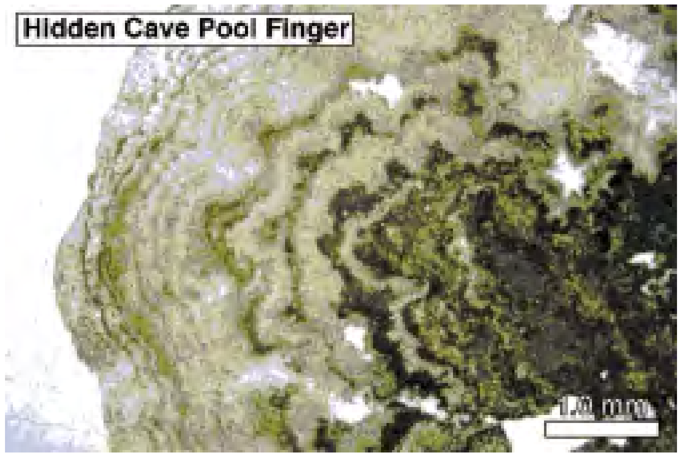

Figure 9. Photomicrograph of a cross-sectioned Hidden Cave pool finger showing alternating layers of dense micrite and light-colored spar. Note the distinct clumping of micrite in some layers.

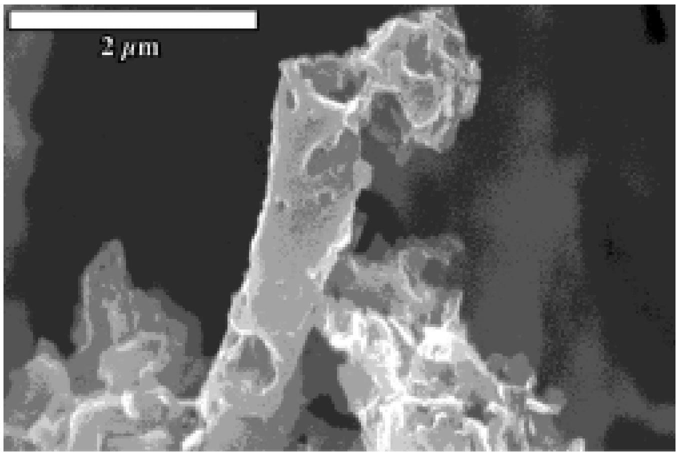

Figure 10. Scanning electron photomicrograph of hollow tube interpreted as bacterial filament found in Hidden Cave pool finger, etched sample.

extinction pattern and dogtooth terminations. The pool fingers do not have a distinct core. Individual crystals usually extend from the center of the finger all the way to the outer edge (5-7 mm), with the width increasing as the diameter of the finger increases. The crystals are limpid for the first 2-3 mm and then show faint-yellow, inclusion-rich banding. The bands are 100-200 μm thick inclusion-rich layers that form ghost outlines of dogtooth crystal terminations.

Like the spar in the Hidden Cave pool fingers, elongate inclusions are common in the Lechuguilla samples; however, micritic layers are absent. Filamentous inclusions occur irregularly, usually associated with patches of elongate or equant inclusions (Fig. 11a). The filaments are 1 μm in width and 50-100 μm long and intertwine like tangled hairs (Fig. 11b). The filaments do not appear to branch, but the way they intertwine makes it difficult to be sure. The filaments are most common in the clear portions and are nearly absent in the yellow, inclusion-rich bands of ghost crystals. These filaments are probably bacteria, but they do not appear to have been responsible for mineral precipitation because of their irregular distribution. Chafetz & Folk (1984) documented similar fabrics and considered them passive colonies engulfed by growing crystals.

Summary. Pool fingers are elongate, pendant speleothems that form underwater. They have an irregular, knobby external appearance underlain by laminations of dark, clotted micrite and/or clear, inclusion-rich calcite spar. In some samples, the inclusions are obviously bacterial. The external and internal fabrics of Hidden Cave pool fingers strongly resemble well-described microbialites from surface environments. This similarity, combined with SEM identification of fossil bacteria in etched samples, suggests bacterial involvement in the formation of the pool fingers.

CASE STUDY III: MOONMILK

Moonmilk is a generic term for a pasty, semi-fluid material consisting of a suspension of micrometer-sized crystals of calcite, hydromagnesite, gypsum, or other minerals (Hill & Forti 1997). Some moonmilk is thought to be the result of chemical precipitation, particularly in the case of gypsum paste residue from the reaction of limestone with sulfuric acid. However, other types of moonmilk may have a microbial origin, either by direct precipitation of calcite by microorganisms (Northup *et al.* 1997; Castanier *et al*. 1999), or by forming a nucleation surface on which minerals precipitate (Pentecost & Bauld 1988; Jones & Kahle 1993).

Although moonmilk is present in many caves in the Guadalupe Mountains, it rarely occurs as extensive deposits. In Spider Cave, however, a spectacular type of moonmilk coats the walls and ceilings of the lowest portions of the cave. This moonmilk resembles curds of cottage cheese with a greasy texture and is slippery under foot. When examined by SEM, this material exhibits a filamentous habit (Fig. 12), and resembles a felted mat of fibers. The individual fibers have a curved morphology unlike most crystalline minerals. EDX analysis in the

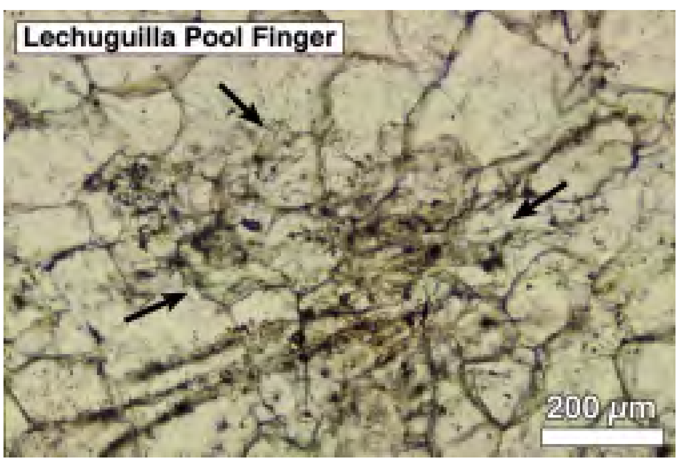

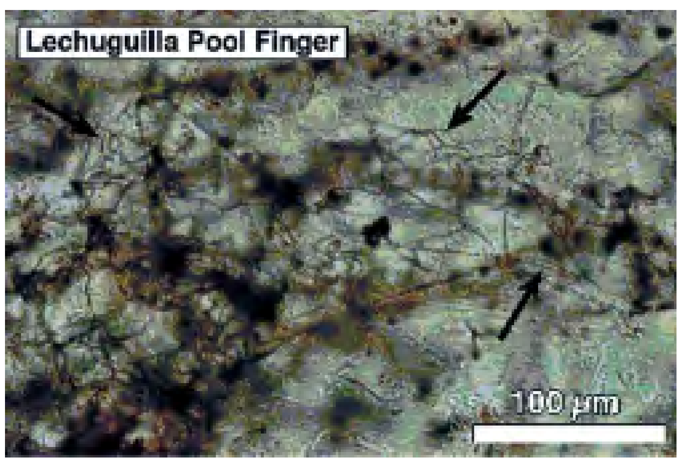

Figure 11. (a - Left) Lechuguilla Cave pool finger showing fine filaments (arrows) in clear spar associated with inclusions (dark areas). (b - Right) Higher magnification image of filaments (arrows).

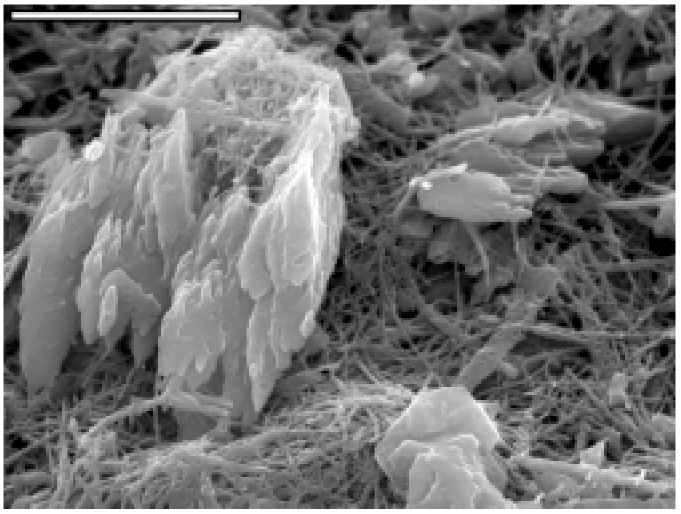

Figure 12. Fibrous calcite from Spider Cave. SEM micrograph of filamentous calcite moonmilk. Both fibers and corroded calcite crystals are present. Scale bar = 5 µm.

SEM shows the presence of Ca, O and C peaks; X-ray diffraction patterns indicate that only calcite makes up the bulk material. When the curds are dissolved in dilute hydrochloric acid, a gelatinous mass remains. This fact, coupled with its unusual filamentous fabric, suggests that the material may consist of microbial filaments coated or mineralized with calcite. However, when samples are viewed under TEM the resulting images show straight, needle-like fibers of crystalline calcite. Since mineral texture alone did not seem sufficient to determine origin, biological culturing experiments were also conducted on this moonmilk.

Viable cultures of mixed cellular types were obtained on three different versions of low nutrient media. Coccoid, ovoid, and stubby rod-shaped cells (~1-2 µm) were present upon inspection with a number of standard light microscopy techniques. In addition, fibers of a bimodal size distribution were present. Large fibers ranged from 1-2 µm in diameter and ranged from 10-50 µm in length; small fibers range from 0.05-0.1 µm in diameter and <2 µm long.

Only a few of the coccoid cells stained with simple methylene blue stain. Interestingly, and surprisingly, some of the fibers also stained with methylene blue. There were mixed gram negative and gram positive cells of all shapes. There were no acid-fast cells, but some of the small fibers did show positive acid-fast staining. No cells or fibers took up the sudan black into their interiors. Acridine orange (AO) stained many of the cellular bodies and also many of the fibers, especially the large fibers. Different concentrations of AO were used, and the length of time the samples took to be stained varied. In culture, the number of visually distinguishable cell types diminished, although cellular densities remained high over 3 to 6 months. Fibers grew in the initial cultures, but after the third transfer few were left.

The nature of the fibers (mineral, biological or both) is unclear. Some of the fibers may be composed of exterior mineral coatings overlying living interiors. Such a possibility would explain why some fibers took up biological dyes. The fibers also may be non-living mineral by-products of cell metabolism. Alternatively, the fibers may be unrelated mineral phases that occur by means of purely mineralogical processes, with the resulting material simply being a suitable habitat for microbial colonization. Future experiments will include the extraction of DNA directly from moonmilk for molecular phylogenetic studies, *in situ* experiments looking for metabolic and enzymatic activity in the moonmilk, and further SEM studies to view the matrix of the material.

Summary. SEM studies of the extensive moonmilk deposits in Spider Cave revealed a felted mat of fibers composed of calcite. The images of the filaments suggest a microbial origin, but TEM studies suggest they are crystalline calcite. Enrichment cultures reveal a diverse microbial community, including filamentous bacteria, associated with the moonmilk. These conflicting results support the need for additional studies.

HUMAN IMPACT ON MICROBIOLOGICAL/GEOLOGIC INTERACTIONS

Rich and unique microbial communities in caves can be harmed by human visitation. Humans are great reservoirs of organic matter that can be shed in the form of hair, skin fragments, and clothing lint. Many microorganisms important in geomicrobiological interactions do not thrive in environments rich in organic matter, such as those created by the dumping of urine or feces. Dumped urine represents a very rich source of nitrogen-rich organic compounds that can support the growth of both bacteria and fungi alien to low-nutrient cave environments, eliminating native species and reducing biodiversity.

To assess the extent of harm of urine dumping cases, we studied total heterotrophic bacteria and fungi population changes through time in response to additions of urine or water to soil samples collected from Lechuguilla Cave. The loss of urea was measured as an indication of recovery time. Overall, population levels in all samples started out relatively low ($<10^4$ colony forming units/g) and stayed low when water was added to soils. Bacteria and fungi responded to the addition of large or small amounts of urine with an increase in the number of colonies by a factor of 100-1000 times. Concentrations of urea in the samples gradually decreased over the course of a month. When urine was re-added to the soils, the response of the microbes was much quicker, showing an accumulation and persistence of urine-utilizing bacteria in the soil. The build-up of microbes caused changes in the texture and structure of the soils. The addition of water to the soils that had first been treated with urine showed only minor changes in populations, demonstrating the importance of the added nutrients in urine to support microbial growth. These results show that urination in caves can cause drastic changes on population levels of microbes in soils, and that these changes persist after urine-derived organic compounds have been removed by biological action. The effects appear to be additive, and responses of the microbial community to multiple applications are rapid.

Poor sanitation conditions while camping underground can lead to fecal contamination of drinking sources and cave soils (Boston 1999). Red Lake, in Lechuguilla Cave, has been used as an in-cave water source for many years, but fecal contamination was suspected after an expedition using the lake developed gastro-intestinal problems. Upon analysis, coliform bacteria were found in puddles and on surfaces near Red Lake, but not in the main pool itself. In an emergency response, the water from puddles was collected and hauled off to urine dump sites, and the Red Lake area closed to human traffic. Follow-up sampling showed the persistence of coliforms in all contaminated sites after 6 and 14 months.

Summary. Input of organic material can have a detrimental effect on oligotrophic microbial communities, resulting in changes in population and community structure. Bacteria that utilize inorganic energy sources, such as those reported in corrosion residues and sulfur deposits, also are negatively impacted by organic enrichment. Urine deposition and other sources of organic carbon enrichment can seriously impact indigenous populations of microbes, and must be minimized if indigenous microbial communities are to be preserved. We strongly recommend that to reduce human impact in Guadalupe caves, a filtration system be devised or that urine be removed from the cave.

CONCLUSIONS

Metabolically active microorganisms are present on corroded formations in Spider Cave, and within punk rock and corrosion residues in Lechuguilla and Spider caves. Targeted enrichments and molecular phylogenetic studies confirm that at least some of these bacteria are iron- or manganese-oxidizing bacteria that may contribute to carbonate dissolution. Bulk chemistry and XRD studies have shown that the corrosion residues are not merely the product of dissolution. These results begin to build a case for microbially assisted dissolution and leaching of underlying host carbonate rock. Hidden Cave pool fingers show a dense micritic core, resembling pelmicritic fabrics of probable bacterial origin and laminated fabrics resembling microbialites. Lechuguilla Cave pool fingers show none of these features; filaments do occur, but are irregularly distributed. Thus, pool fingers show differing degrees of microbial involvement. Spider Cave moonmilk shows extensive filamentous deposits upon SEM examination, but TEM studies could not confirm a microbial component. Microbial enrichments of these deposits demonstrate the presence of a diverse microbial community, including filamentous bacteria. Thus, the evidence is equivocal.

Studies of the impact of urine dumping in low nutrient caves demonstrate that the addition of organic carbon can be highly detrimental to indigenous microbial populations. Therefore, limiting organic carbon addition is critical.

Ongoing studies of pool fingers, corrosion residues, and moonmilk will further elucidate the extent of bacterial-rock interactions. Other speleothems, such as cave pearls, show great promise of microbial involvement in their formation and await investigation. The study of geomicrobiological interactions in Guadalupe Mountain caves is only beginning.

ACKNOWLEDGMENTS

The authors wish to express their gratitude to Dale Pate, Stan Allison, Jason Richards, and Paul Burger of the National Park Service and Ransom Turner, Kevin Glover, and Susan Herpin of the U.S. Forest Service for their support of our field studies. Collection of all samples was by permit from Carlsbad Caverns National Park and the U.S. Forest Service. This work was supported by National Science Foundation grant number DEB-9809096, the National Speleological Society, and the Biology Department and the Institute of Meteoritics, University of New Mexico. Laura Bean, Rachel Schelble, Kathy Dotson, Andi Hunter, Cynthia Connolly, Marian Skupski, Don Natvig, Megan Armstrong, and Kristen Shinglman provided valuable lab assistance. Anna-Louise Reysenbach and Norm Pace provided critical technical guidance and lab support for the molecular work. We thank Gregor Eberli and Peter Swart for their support during the project. J. Michael Queen provided seminal discussions and field assistance. The manuscript benefited greatly from careful review by Carol Hill and Norman Pace.

REFERENCES

Amann, R.I., Ludwig, W. & Schleifer, K.-H. (1995). Phylogenetic identification and *in situ* detection of individual microbial cells without cultivation. *Microbiological Reviews 59*: 143-169.

Barns, S.M., Fundyga, R.E., Jeffries, M.W. & Pace, N.R. (1994). Remarkable archaeal diversity detected in a Yellowstone National Park hot spring environment. *Proceedings of the National Academy of Sciences USA 91*: 1609-1613.

Bergey, D. H. (1989). *Bergey's manual of systematic bacteriology*, v. 3. Williams and Wilkins, Baltimore, MD: 1601-2298.

Boston, P.J. (1999). Red Lake contamination. Unpublished technical report to Carlsbad Caverns National Park: 6 pp.

Braithwaite, C.J.R. & Zedef, V. (1996). Hydromagnesite stromatolites and sediments in an alkaline lake, Salda Gölü, Turkey. *Journal of Sedimentary Research 66*: 991-1002.

Burne, R.V. & Moore, L.S. (1987). Microbialites: Organosedimentary deposits of benthic microbial communities. *Palaios 2*: 241-255.

Castanier, S., Metayer-Levrel, G.L. & Pertuisot, J.P. (1999). Ca-carbonate precipitation and limestone genesis-The microbiogeologist point of view. *Sedimentary Geology 126*: 9-23.

Chafetz, H.S. (1986). Marine peloids: A product of bacterially induced precipitation of calcite. *Journal of Sedimentary Petrology 56*: 812-817.

Chafetz, H.S. & Buczynski, C. (1992). Bacterially induced lithification of microbial mats. *Palaios 7*: 277-293.

Chafetz, H.S. & Folk, R.L. (1984). Travertines: Depositional morphology and the bacterially constructed constituents. *Journal of Sedimentary Petrology 54*: 289-316.

Clark, G. (1973). *Staining procedures used by the biological stain commission. 3rd ed*. The Williams & Wilkins Co., Baltimore, Maryland: 418 pp.

Costerton, J.W., Cheng, K.-J., Geesey, G.G., Ladd, T.I., Nickel, J.C., Dasgupta, M. & Marrie, T.J. (1987). Bacterial biofilms in nature and disease. *Annual Review of Microbiology 41*: 435-464.

Cunningham, K.I. (1991a). Organic and inorganic composition of colored corrosion residues: Lechuguilla Cave: Preliminary report. *NSS News 49*: 252,254.

Cunningham, K.I. (1991b). News scrapbook. *NSS News 49*: 325.

Cunningham, K.I., Northup, D.E., Pollastro, R.M., Wright, W.G. & La Rock, E.J. (1995). Bacteria, fungi and biokarst in Lechuguilla Cave, Carlsbad Caverns National Park, New Mexico. *Environmental Geology 25*: 2-8.

Danielli, H.M.C. & Edington, M.A. (1983). Bacterial calcification in limestone caves. *Geomicrobiology Journal 3*: 1-16.

Davis, D.G., Palmer, M.V. & Palmer, A.N. (1990). Extraordinary subaqueous speleothems in Lechuguilla Cave, New Mexico. *NSS Bulletin 52*: 70-86.

DuChene, H.R. (1997). Lechuguilla Cave, New Mexico, U.S.A. In Hill, C.A. & Forti, P. (eds.) *Cave minerals of the world*. *2nd ed*. Huntsville, AL. National Speleological Society: 343-350.

Ehrlich, H.L. (1996). *Geomicrobiology*. New York, Marcel Dekker: 719 pp.

Ford, T. & Mitchell, R. (1990). The ecology of microbial corrosion. In Marshall, K.C. (ed.). *Advances in microbial ecology II*. Plenum Press, New York, NY: 231-262.

Hanert, H.H. (1992). The genus *Gallionella*. In Balows, A. (ed.) *The prokaryotes: A handbook on the biology of bacteria: Ecophysiology, isolation, identification, applications*. Springer-Verlag, New York, NY: 509-515.

Hill, C.A. (1987). *Geology of Carlsbad Cavern and other caves in the Guadalupe Mountains, New Mexico and Texas*. New Mexico Bureau of Mines and Mineral Resources Bulletin 117: 150 pp.

Hill, C.A. & Forti, P (1997). *Cave Minerals of the World*, *2nd ed*. Huntsville, Alabama. National Speleological Society: 463 pp.

Hose, L.D., Palmer, A.N., Palmer, M.V., Northup, D.E., Boston, P.J. & DuChene, H.R. (2000). Effects of geomicrobiological processes in a hydrogen sulphide-rich karst environment. *Chemical Geology 169*: 399-423.

Hose, L.D. & Pisarowicz, J.A. (1999). Cueva de Villa Luz, Tabasco, Mexico: Reconnaissance study of an active sulfur spring cave and ecosystem. *Journal of Cave and Karst Studies 61*: 13-21.

Husler, J. & Connolly, J. (1991*). Procedures for laboratory sample bulk chemical determination*. Sandia National Laboratory Technical Procedures 61: 72 pp.

Jones, B. & Kahle, C.F. (1993). Morphology, relationship, and origin of fiber and dendrite calcite crystals. *Journal of Sedimentary Petrology 63*: 1018-1031.

Kolthoff, I.M. & Sandell, E.B. (1952). *Textbook of quantitative inorganic analysis*. *3rd ed*. New York. Macmillan: 759 pp.

Kopczynski, E.D., Bateson, M.M. & Ward, D.M. (1994). Recognition of chimeric all-subunit ribosomal DNAs composed of genes from uncultivated microorganisms. *Applied and Environmental Microbiology 60*: 746-748.

Kuske, C. R., Barns, S.M. & Busch, J.D. (1997). Diverse uncultivated bacterial groups from soils of the arid southwestern United States that are present in many geographic regions. *Applied and Environmental Microbiology 63*: 3614-3621.

Liesack, W., Weyland, H. & Stackebrandt, E. (1991). Potential risks of gene amplification by PCR as determined by 16S rDNA analysis of a mixed-culture of strict barophilic bacteria. *Microbial Ecology 21*: 191-198.

Little, B.J., Wagner, P. & Gerchakov, S.M. (1986a). A quantitative investigation of mechanisms for microbial corrosion. In Dexter, S.C. (ed.) *Biologically induced corrosion*. National Association of Corrosion Engineers: 209-214.

Little, B.J., Wagner, P. Gerchakov, S.M., Walch, M. & Mitchell, R. (1986b). The involvement of a thermophilic bacterium in corrosion processes. *Corrosion 42*: 533-536.

Melim, L.A. (1991). *The origin of dolomite in the Permian (Guadalupian) Capitan Formation, Delaware Basin, west Texas and New Mexico: Implications for dolomitization models*. Unpublished PhD dissertation, Southern Methodist University, Dallas, TX: 215 pp.

Northup, D.E., Carr, D.L., Crocker, M.T., Hawkins, L.K., Leonard, P. & Welbourn, W.C. (1995). Biological investigations in Lechuguilla Cave. *NSS Bulletin 56*: 54-63.

Northup, D.E., Reysenbach, A.L. & Pace, N.R. (1997). Microorganisms and speleothems. In Hill, C.A. & Forti, P. (eds.) *Cave Minerals of the World 2nd ed*. National Speleological Society, Huntsville, Alabama: 261-266.

Palmer, A.N & Palmer, M.V. (2000). Hydrochemical interpretation of cave patterns in the Guadalupe Mountains, New Mexico. *Journal of Cave and Karst Studies 62*(2): 91-108.

Pentecost, A. & Bauld, J . (1988). Nucleation of calcite on the sheaths of cyanobacteria using a simple diffusion cell. *Geomicrobiology Journal 6*: 129-135.

Polyak, V.J. & Güven, N. (2000). Clays in caves of the Guadalupe Mountains, New Mexico. *Journal of Cave and Karst Studies 62*(2): 120-126.

Queen, J.M. (1994). Influence of thermal atmospheric convection on the nature and distribution of microbiota in cave environments. In Sasowsky, I.D. & Palmer, M.V. (eds.) *Breakthroughs in karst geomicrobiology and redox chemistry*, Karst Waters Institute Special Publication 1: 62-64.

Reysenbach, A.-L., Wickham, G.S. & Pace, N.R. (1994). Phylogenetic analysis of the hyperthermophilic pink filament community in Octopus Spring, Yellowstone National Park. *Applied and Environmental Microbiology 60*: 2113-2119.

Rusterholtz, K. & Mallory, L.M. (1994). Density, activity and diversity of bacteria indigenous to a karstic aquifer. *Microbial Ecology 28*: 79-99.

Ward, D.M., Bateson, M.M., Weller, R. & Ruff-Roberts, A.L. (1992). Ribosomal RNA analysis of microorganisms as they occur in nature . *Advances in Microbial Ecology 12*: 219-286.

Went, F.W. (1969). Fungi associated with stalactite growth. *Science 166*: 385-386.

HYDROCHEMICAL INTERPRETATION OF CAVE PATTERNS IN THE GUADALUPE MOUNTAINS, NEW MEXICO

ARTHUR N. PALMER
Department of Earth Sciences, State University of New York, Oneonta, NY 13820 USA
MARGARET V. PALMER
619 Winney Hill Road, Oneonta, NY 13820 USA

Most caves in the Guadalupe Mountains have ramifying patterns consisting of large rooms with narrow rifts extending downward, and with successive outlet passages arranged in crude levels. They were formed by sulfuric acid from the oxidation of hydrogen sulfide, a process that is now dormant. Episodic escape of H_2S-rich water from the adjacent Delaware Basin, and perhaps also from strata beneath the Guadalupes, followed different routes at different times. For this reason, major rooms and passages correlate poorly between caves, and within large individual caves. The largest cave volumes formed where H_2S emerged at the contemporary water table, where oxidation was most rapid. Steeply ascending passages formed where oxygenated meteoric water converged with deep-seated H_2S-rich water at depths as much as 200 m below the water table. Spongework and network mazes were formed by highly aggressive water in mixing zones, and they commonly rim, underlie, or connect rooms. Transport of H_2S in aqueous solution was the main mode of H_2S influx. Neither upwelling of gas bubbles nor molecular diffusion appears to have played a major role in cave development, although some H_2S could have been carried by less-soluble methane bubbles. Most cave origin was phreatic, although subaerial dissolution and gypsum-replacement of carbonate rock in acidic water films and drips account for considerable cave enlargement above the water table. Estimates of enlargement rates are complicated by gypsum replacement of carbonate rock because the gypsum continues to be dissolved by fresh vadose water long after the major carbonate dissolution has ceased. Volume-for-volume replacement of calcite by gypsum can take place at the moderate pH values typical of phreatic water in carbonates, preserving the original bedrock textures. At pHs less than about 6.4, this replacement usually takes place on a molar basis, with an approximately two-fold volume increase, forming blistered crusts.

Caves in the Guadalupe Mountains of southeastern New Mexico include some of the world's best-documented examples of sulfuric acid speleogenesis (Davis 1980; DuChene 1986; Hill 1987; Egemeier 1987; Jagnow 1989; Cunningham *et al*. 1995; Palmer *et al*. 1998; Polyak *et al*. 1998). Although the cave-forming process is now dormant, its overall picture seems clear: water rich in hydrogen sulfide (H_2S) rose from depth and, as it approached the water table, the H_2S reacted with oxygen to produce sulfuric acid, the main cave-forming agent. It is fortunate that the caves are now inactive, because the toxicity of H_2S would probably make them impossible to explore. Interpretations of cave origin must rely on indirect evidence.

This paper summarizes the geometry of these caves and examines the hydrologic and chemical conditions that formed them. Interpretations are based on geologic leveling surveys in about 10 km of cave passages, calculation of relevant geochemical equilibria, and comparison with caves elsewhere that are still forming by similar processes. Leveling surveys were conducted with a hand level or tripod-mounted Brunton compass, with mean closure errors of 0.05%. Chemical relationships were derived from free-energy data tabulated by Woods & Garrels (1987) and from calculations with the geochemical software program **SI** (Palmer 1996).

GEOLOGIC SETTING

The geologic setting for the Guadalupe caves is shown in figure 1. For more details see Jagnow (1979), Hill (1987, 1996), Harris & Grover (1989), and Jagnow & Jagnow (1992). The Guadalupe Mountains consist of an uplifted block of Permian limestones and dolomites. The southeastern border of the mountains, which drops off steeply as the Guadalupe Escarpment, consists of the massive Capitan Limestone, a reef that built upward and southeastward as the Permian sea level rose. It contains a loose framework of bryozoan, sponge, and algae fossils in a matrix of fine-grained limestone (DuChene 2000). The Capitan grades downward and laterally into the dolomitized reef rock of the Goat Seep Formation. To the northwest are prominently bedded back-reef dolomites and limestones. Of these, the Yates Formation is the only one with a large insoluble content, mainly quartz silt. To the southeast, the reef is bordered by an apron of talus formed by blocks broken off the steep reef front as it built upward. The talus, now dolomitic, merges diagonally downward with limestones and other strata deposited in deeper water within the Delaware Basin. The basinal rocks are overlain by Permian gypsum and other evaporites, mainly of the Castile Formation. These and other sediments once filled the entire Delaware Basin at least as high as the top of the Capitan reef, but much of this thickness has been removed by post-Permian erosion.

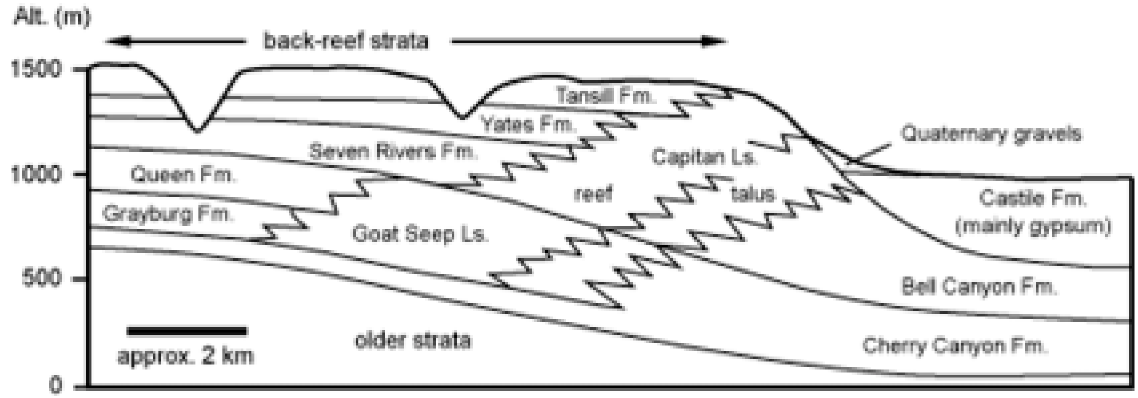

Figure 1. Geologic cross section through the Guadalupe Mountains, adapted from King (1948) and Hayes (1964). See text for brief description of rock types.

The Guadalupe Mountains owe their height to Late Permian, Mesozoic, and Cenozoic uplift, accompanied by faulting, minor folding, and broad southeastward tilting (Hill 2000). The main phase of uplift and cave development took place within the past 12-15 Ma (Hill 1996, 2000; Polyak *et al*. 1998). The carbonate rocks, which are considerably more resistant than the neighboring evaporites, now stand in high relief. The overall southeasterly dip of the back-reef beds is disrupted by broad folds parallel to the reef front (Hayes 1964; Jagnow 1979). The dip varies from bed to bed, even in the same vertical section, because of differences in formation thickness. In the cave area, the mean dip of the back-reef beds is <10° over large areas, but local dips can exceed 15°.

Normal faults along the western edge of the mountains have displacements as much as several hundred meters. Other faults within the mountains have only minor displacements. Prominent joints are oriented in at least two major sets roughly parallel and perpendicular to the reef front. Bedding-plane partings are conspicuous only in the back-reef strata. Paleokarst features include Permian breccias, breccia dikes, and solutional voids and small caves now lined with calcite spar, as well as clay-filled spongework representing Mesozoic enlargement of primary pores (Hill 2000). All of these structures and openings have helped to guide later cave development.

Most groundwater in the Guadalupe Mountains now flows parallel to the reef front and emerges in the Pecos River valley at Carlsbad Springs in the city of Carlsbad (Fig. 2). See Hiss (1980) for information on the regional hydrology.

CAVE PATTERNS

Cave patterns in the Guadalupe Mountains are of concern not only to geologists, but also to explorers and mappers who use their intuitive feel for the caves' layout to make new discoveries. Individual caves are scattered unevenly and it is difficult to verify their overall distribution. Most known caves have only a single entrance, and it is likely that many have no accessible entrance at all. Locations of caves used as examples in this paper are shown on figure 2, which includes most of the large Guadalupe caves.

The typical Guadalupe cave has a ramifying pattern consisting of irregular rooms and mazes with passages branching outward from them (Fig. 3). The map of a typical large Guadalupe cave resembles an ink blot, with many overlapping tiers. Branches do not converge as tributaries, but instead serve as distributary outlets at successively lower elevations. Many caves, or parts of caves, have a network or spongework pattern. Some involve simple widening of one or more fractures. Typical Guadalupe cave patterns are illustrated by the maps and profiles of Carlsbad Cavern and Hicks Cave (Figs. 4 & 5).

The overall layout of the caves is governed by the pattern of groundwater flow and sulfuric acid production. However, individual passages are guided in part by local geologic structures (Figs. 6 & &). Although caves tend to concentrate in the least dolomitized rocks, the main geologic control of individual cave patterns is evidently not lithologic, because many of

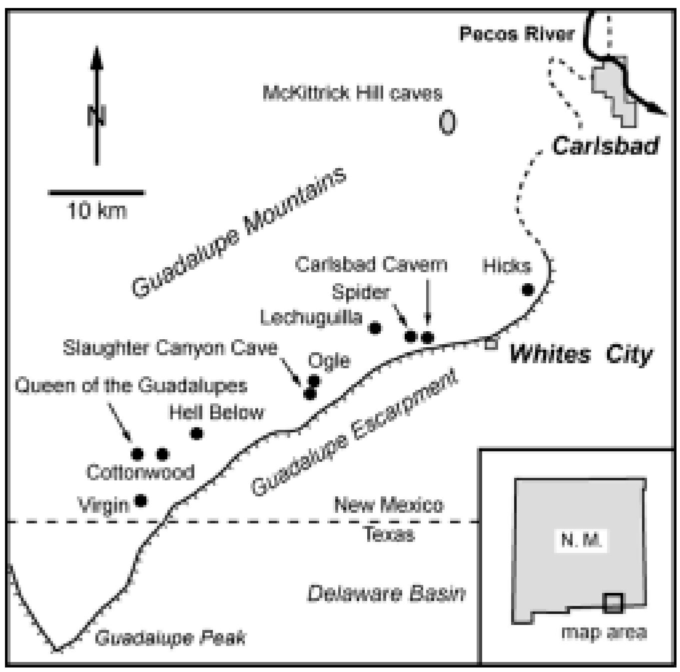

Figure 2. Location of caves and other features described in this paper.

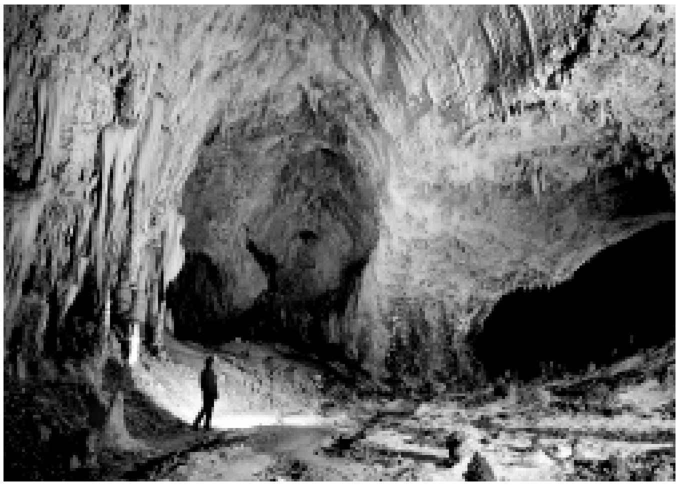

Figure 3. Lower Cave of Carlsbad Cavern, formed by dissolution at a former water table, with arched ceilings formed by gypsum replacement and condensation-corrosion. All photos by A.N. Palmer.

them cut discordantly across different rock types with only minor effects on passage morphology. The massive Capitan reef is structurally most competent, least dolomitized, and contains the largest cave rooms and passages. Many of these are guided by large fractures. Primary porosity fosters fine-textured spongework. The reef talus behaves similarly because the talus blocks are cemented into a single coherent unit. Backreef strata produce passage cross sections that are elongate along the bedding, but discordant joints produce many fissures as well. Impure beds (e.g., the siltyYates Formation) can serve as confining units that limit the vertical range of passages.

The purely geologic factors described here cannot account for the great variety and unusual characteristics of Guadalupe caves. Flow patterns and water chemistry are the keys to understanding them.

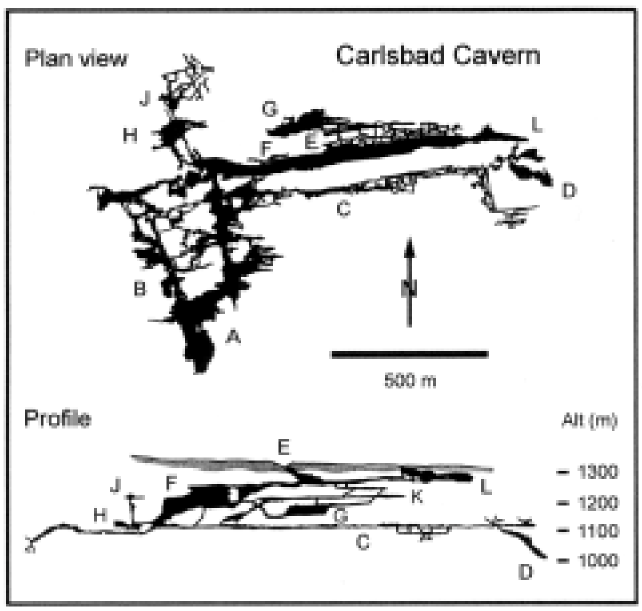

Figure 4. Map and profile of Carlsbad Cavern, based on surveys by the Cave Research Foundation (1992). A = Big Room; B = Lower Cave; C = Left Hand Tunnel; D = Lake of the Clouds; E = entrance; F = Main Corridor; G = Guadalupe Room; H = New Mexico Room; J = Chocolate High; K = New Section; L = Bat Cave.

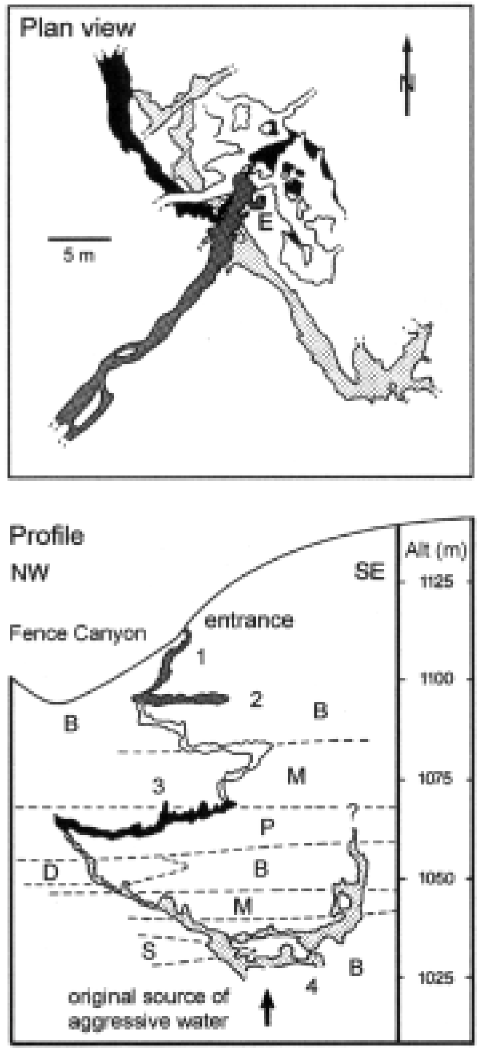

Figure 5. Partial map and geologic profile through Hicks Cave, based on geologic leveling survey. 1 = irregular tube ascending into surface canyon; 2 = major room level, apparently formed at a former water table, with a horizontal passage leading to a former outlet; 3 = intermediate levels of complex rooms, with former outlets in uncertain directions; 4 = low-level fissures, partly sediment-choked, apparently the original paths for incoming aggressive water. E = entrance; B = carbonate breccia; M = microcrystalline limestone and dolomite; P = pisolitic limestone; S = silty limestone and dolomite. Patterns show the relation between passages on map and on profile.

CAVE-FORMING PROCESSES IN THE GUADALUPE MOUNTAINS

The following sequence of steps is well accepted for the origin of Guadalupe caves (see Hill 1987): (1) reduction of sulfates (gypsum and anhydrite) at depth within the Delaware Basin to produce hydrogen sulfide (H_2S); (2) ascent of H_2S, either in solution or as a gas, into the carbonate rocks of the Guadalupe Mountains; (3) oxidation of H_2S to sulfuric acid, either where oxygen-rich groundwater mixes with the H_2S or at the water table; (4) dissolution of carbonate rock by sulfuric acid; and (5) removal of the dissolved solids to springs by groundwater flow. An idealized view of the geologic setting and flow patterns during cave origin is shown in figure 8. The chemical reactions involved are:

$$H_2S + 2O_2 \Leftrightarrow H^+ + HSO_4^- \Leftrightarrow 2H^+ + SO_4^{2-} \quad (1)$$

Reaction (1) often involves an intermediate sulfur phase, which is in turn oxidized. HSO_4^- is the dominant sulfate species only at pH less than about 2. Dissolution of limestone (calcite) and dolomite proceeds as follows:

$$2H^+ + SO_4^{2-} + CaCO_3 \Leftrightarrow Ca^{2+} + SO_4^{2-} + CO_2 + H_2O \quad (2)$$

$$4H^+ + 2SO_4^{2-} + CaMg(CO_3)_2 \Leftrightarrow Ca^{2+} + Mg^{2+} + 2SO_4^{2-} + 2CO_2 + 2H_2O \quad (3)$$

To explain specific cave patterns these processes must be examined in detail.

NATURE OF HYDROGEN SULFIDE SOURCE

Organic carbon compounds, such as those in oil fields, react readily with oxygen. Deep below the surface most groundwater has limited oxygen content, and where organic carbon is present nearly all oxygen is quickly consumed. In the absence of "free" oxygen, the most accessible remaining source is sulfate in zones of gypsum and anhydrite. Oxidation of organics, with simultaneous reduction of sulfate, produces H_2S and HCO_3^-, among other things. The most likely source for the H_2S-rich water is the Delaware Basin, which contains sulfate rocks as well as abundant hydrocarbons (Hill 1987, 1990). Water analyses from oil wells in the basin also show abundant hydrogen sulfide (Wiggins *et al*. 1993). The patterns of the largest Guadalupe caves are most compatible with this source.

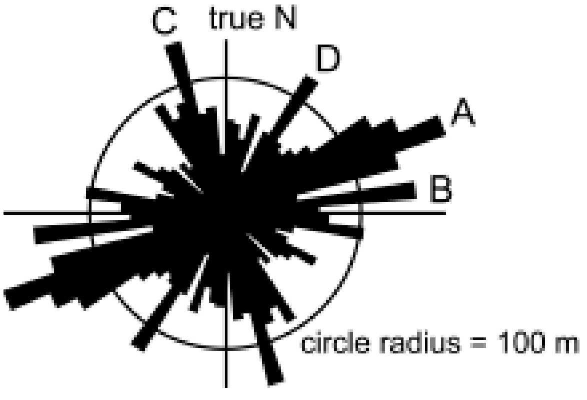

Figure 6. Rose diagram of compass azimuths from the geologic survey of Lechuguilla Cave (including Entrance series, Rift area, Southeastern Branch). A - D = major trends of fissure passages.

Figure 7. Main passage of Ogle Cave, oriented along trend C shown in figure 6.

However, several alternative H_2S sources may have contributed to cave origin, and their relative importance has yet to be determined. As in seacoast aquifers, H_2S may have been generated in sulfate-rich brines beneath a fresh-water lens, and speleogenesis could have been augmented by mixing between the fresh and saline water (Queen 1994). In the McKittrick Hill caves, some gypsum reduction may have taken place right in the cave-forming zone in the presence of hydrocarbons, which still impart an oily smell to the bedrock and calcite spar (M. J. Buck, pers. comm., 2000). H_2S could also have been carried by groundwater flow from the northwest, up the dip of the Capitan Formation, from low areas near the present city of

Carlsbad (DuChene & McLean 1989).

Hydrogen sulfide in solution forms a mild acid as the result of its dissociation to H^+ and HS^-, especially at pH values above 7, but the build-up of HCO_3^-, in combination with Ca^{++} from the sulfate rocks, causes calcite supersaturation at the sites of sulfate reduction. The resulting solution is unable to dissolve further calcite, and in fact often precipitates it. Thus, the H_2S-rich water that rose into the Guadalupes during cave development was almost certainly near saturation with respect to calcite, and probably also dolomite.

The water also contained much sulfate that escaped reduction. When this water emerged into the cave-forming area, it was already well on its way toward gypsum saturation, which gave the water a head start in depositing subaqueous gypsum in the caves. The water also contained much carbon dioxide, but although it allowed high saturation concentrations of carbonate minerals, saturation had already been achieved, and so the CO_2 did not take an active role in cave development. These characteristics are typical of similar waters in other karst areas. For example, water rising into limestone from oil fields in Tabasco, Mexico, has been measured to be almost exactly at calcite saturation, only slightly undersaturated with dolomite, more than 60% saturated with gypsum, and having a P_{CO_2} of 0.1 atm (Palmer & Palmer 1998). A literature review shows that most sulfur springs throughout the world have similar chemistry.

Gases can rise through water as buoyant bubbles, following continuous fractures in an ever-ascending pattern. In contrast,

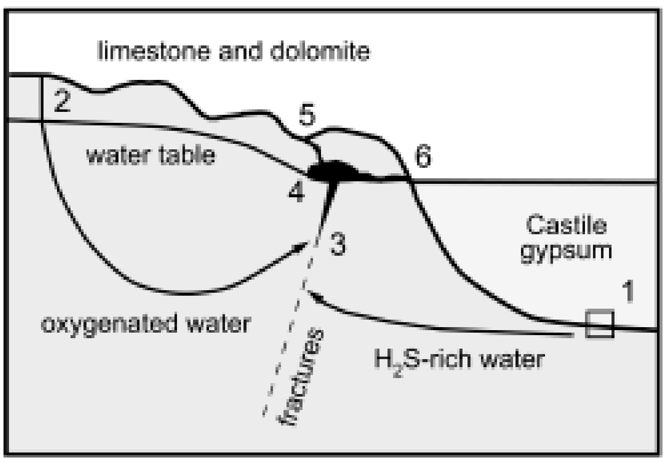

Figure 8. Idealized diagram of flow patterns and processes during cave origin. 1 = possible sites of gypsum reduction (after Hill 1987); 2 = infiltration of fresh water from high mountains; 3 = rifts formed by mixing of the two water sources below the water table; 4 = large rooms and passages formed at sites of rapid H_2S oxidation at the water table; 5 = passages ascending to former spring outlets, later enlarged by corrosion where H_2S was absorbed by vadose moisture; 6 = passages to progressively lower spring outlets. The level of water-table cave development was not necessarily at the elevation of the top of the Castile gypsum.

gases in solution must be conveyed by water flow or molecular diffusion. The distinction between gaseous and aqueous transport is important, because it determines the paths by which H_2S entered and moved through the cave-forming zone. A dissolved gas forms bubbles only where its equilibrium partial pressure exceeds the static groundwater pressure. The partial pressure of H_2S in atmospheres is about 10 times its molar concentration. The relationship between H_2S concentration and maximum depth at which degassing can take place is shown in figure 9. At lesser depths, some H_2S forms bubbles, while the remainder stays in solution.

Wiggins *et al.* (1993) reported an H_2S concentration of 600 mg/L in the Henderson oil field in the Delaware Basin, 120 km east of the Guadalupe Escarpment. A maximum of 394 mg/L was measured in sulfur springs in Tabasco, Mexico, and 103 mg/L in the well-known sulfur spa at Sharon Springs, New York (Palmer & Palmer 1998). Egemeier (1981) measured 6 mg/L in Lower Kane Cave, Wyoming, and 15 mg/L at nearby Hellespont Cave. Movile Cave in Romania contains 10 mg/L (Sarbu *et al*. 1996). Even in these well-known examples of active H_2S systems, the concentrations are not enough to form gas bubbles more than a couple of meters below the water surface (Fig. 9). Thus, the vast majority of H_2S involved in Guadalupe cave development probably arrived in aqueous form.

On a molar basis, methane (CH_4), the most common natural gas, is only ~1.3% as soluble in water as H_2S. Carbon dioxide (CO_2) is ~35% as soluble as H_2S. It is possible that some H_2S was carried by bubbles of these gases, although the depth of degassing is still rather limited (Fig. 9), and the process is not often observed at H_2S springs.

H_2S can also migrate toward oxidizing zones by molecular diffusion. As H_2S is consumed by oxidation, a concentration gradient develops in that direction and H_2S diffuses toward lower concentrations. Fissures extending downward to deep

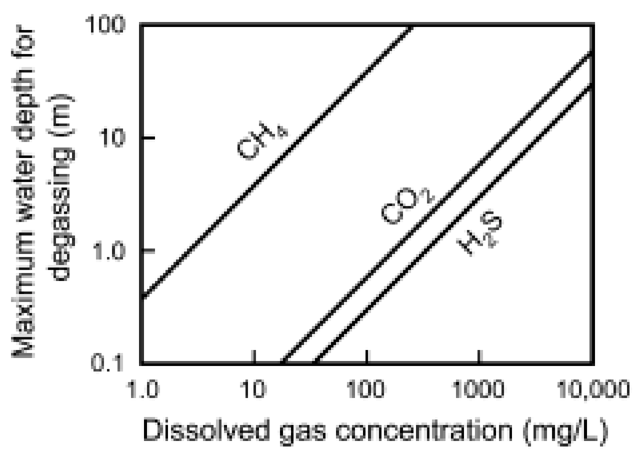

Figure 9. Maximum depth at which degassing of H_2S, CO_2, and CH_4 can take place below the water table. Partial degassing of a gas takes place at depths below its respective line, but no degassing can take place above the line.

anoxic water could potentially serve as paths for diffusion. The steady-state diffusion equation is

$$q = -D \frac{dC}{dx} A \quad (4)$$

where q = transfer rate of dissolved components (g/sec), D = diffusion coefficient (cm²/sec), dC/dx = local concentration gradient (g/cm³ per cm), and A = cross-sectional area across which the diffusion takes place (cm²). The minus sign adjusts for the negative gradient. D varies with temperature, chemical species, porosity pattern, and very slightly with concentration; a typical value is 1.5×10^{-5} cm²/sec. Eddies or convection, if present, can greatly increase the transfer rate but are not covered by Eq. (4).

As a feasible example, consider a vertical fissure 100 m deep, with a horizontal cross section 10 cm x 10 m, and with constant H_2S concentrations of 500 mg/L at its base and 10 mg/L at its top. Eq. (4) shows that diffusion alone could deliver only 0.23 gram of H_2S per year. If the entire amount is converted to sulfuric acid (rarely true), and all the acid is expended in dissolving limestone, the dissolved calcite would total only about 0.25 cm³/yr. Apparently H_2S diffusion alone cannot produce caves unless unusually steep concentration gradients persist through large openings for very long times.

NATURE OF THE OXYGEN SOURCE

To produce the Guadalupe caves, the rising H_2S-rich water had to mix with oxygen. This is abundant at the water table, and much sulfuric-acid production appears to have taken place there. However, long ascending passages (discussed later) show that some mixing must have taken place as much as hundreds of meters below the water table.

The only feasible source for oxygen at such depth was fresh water that infiltrated at higher elevations in the Guadalupes and followed deep flow paths on its way to springs (Fig. 8). Guadalupe caves enlarge upward toward former water tables, indicating that the oxygen was not generated at depth. Oxygen levels are low in most groundwater, but less so in mountainous areas because the soil is thin and poor in organics, which easily consume oxygen. Measurements of dissolved oxygen in well water in the Basin and Range province in Nevada and Arizona show rather consistent oxygen levels of 2-8 mg/L (Winograd & Robertson 1982). The Guadalupe Mountains are part of this geomorphic province, and although today's measurements tell nothing of the conditions that may have prevailed while the caves originated in the late Tertiary Period, the presence of oxygen in groundwater today is a promising indicator of past conditions under similar climates.

Water wells are scarce in the Guadalupes, since the area is mainly federal land. The chemistry of the water supply at the Dark Canyon Lookout (near Cottonwood Cave) has been measured by state agencies (reported by Hill 1987: 20). From this information, equilibrium calculations show that the water is essentially at saturation with calcite and dolomite and highly undersaturated with gypsum. By itself, this water is not capable of producing deep caves in limestone or dolomite.

GROUNDWATER FLOW PATTERNS DURING SPELEOGENESIS

Guadalupe caves extend into some of the highest topography of the region. For example, the entrance passages of Carlsbad Cavern and Lechuguilla Cave are nearly at the tops of their local ridges. Yet the cave morphology indicates that these passages were originally outlets for rising groundwater. Only those parts of the Guadalupe Mountains to the southwest of the main cave areas rise to substantially higher elevations, and they were the likely sources for oxygenated groundwater (Fig. 8). At that time (probably in the Miocene; see Hill 2000), sediments in the Delaware Basin extended nearly to the top of the Guadalupe Escarpment, and nearby surface rivers were essentially at the same elevation.

The great vertical range of passages in many of the caves shows that rising water must have been chemically aggressive to depths as much as 200 m below the surface. H_2S-rich water could easily have come from still deeper sources, but oxygenated water was an equally important part of the aggressive mixture and probably its major flow component. Considerable meteoric groundwater must have followed deep flow paths along joints and faults, which are especially prominent in the vicinity of the Guadalupe Escarpment, where the majority of cave development has taken place. A depth of several hundred meters is only a small percentage of the maximum possible horizontal distance between infiltration sources and springs.

Hill (1987, 2000) considered that the H_2S was generated at or near the base of the Castile gypsum and migrated upward through underlying non-evaporite strata, since the plastic nature of the gypsum gives it a very low permeability by sealing joints. She concluded that the sandstone beds of the directly underlying Bell Canyon Formation were among the favored paths. But how did the H_2S-rich water rise from reducing zones at lower elevations? This is no problem if the water table above the source was higher than at the outlet. Even today, the water table in parts of the Gypsum Plain at the foot of the mountains lies as much as 100 m higher than that in the cavernous Capitan reef (Sares & Wells 1987). The high permeability of the cavernous carbonate rock allows efficient groundwater drainage toward the northeast.

Another mechanism may have helped move the H_2S water. It is common in sedimentary basins for accumulation of sediments and tectonic forces to raise the hydrostatic pressure to values greater than could be achieved by water depth alone. Such "overpressured" water is able to escape along paths of weakness, typically around the margins of the basin, and can rise to elevations higher than that of the water table above its source area. Such flow tends to be episodic, driven by occasional tectonic stresses and released to the surface by fracturing. It alternates with lengthy dormant periods. This scenario fits the Guadalupes better than steady-state flow in the direction of a sloping water table, as shown later. Yet it is not certain that overpressuring was the only mode of H_2S expulsion, or even the dominant one.

Mylroie *et al*. (1995) noted that the morphology of Guadalupe caves and their origin by mixing of oxygenated and

H_2S-rich water resembles the morphology of seacoast caves in porous limestone and their origin by mixing between fresh water and saltwater. Diffuse flow through a seacoast aquifer produces caves in mixing zones and exits as diffuse flow once again, producing isolated chambers. This is a reasonable comparison, although most flow in the Guadalupes is focused along major fissures, and the exiting water usually follows discrete passages. This model may help to explain the origin of rooms that seem to lack outflow passages at the level of maximum cave development.

The temperature of the cave-forming water was probably not much above the ambient groundwater temperature of today (16-20°C). In aqueous solutions warmer than about 35°C at atmospheric pressure, anhydrite is the stable calcium sulfate, rather than gypsum. The equilibrium temperature drops with increasing pressure. Microscopic examination by M.V. Palmer has so far shown no evidence for anhydrite or pseudomorphs of former anhydrite in the gypsum wall crusts in Guadalupe caves, including replacement crusts of phreatic origin.

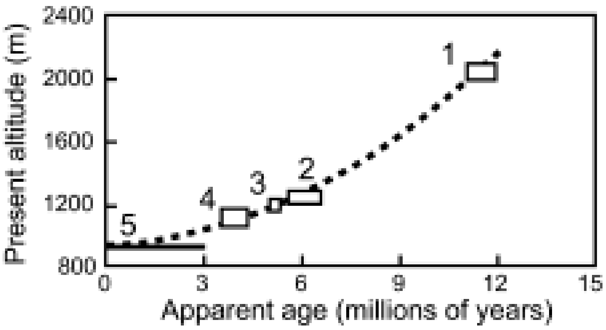

Figure 10. Age vs. elevation for several cave levels in the Guadalupe Mountains (from Polyak *et al.* 1998). 1 = Cottonwood Cave and Virgin Cave; 2 = Endless Cave and Glacier Bay (Lechuguilla Cave); 3 = Lake Lebarge (Lechuguilla Cave); 4 = New Mexico Room, Big Room, and Green Clay Room (Carlsbad Cavern); 5 = present water table.

CONSTRAINTS ON CAVE-FORMING PROCESSES

Although it is difficult to reconstruct the exact conditions during cave development, it is still possible to establish some limits on the processes and their rates. The ultimate time limit for cave origin in the Guadalupes is given by radiometric dating of the clay mineral alunite, which is a by-product of sulfuric acid speleogenesis (Polyak *et al*. 1998; Polyak & Provencio 2000). The highest sampled sites appear to be about 12 Ma old (Fig. 10). The age decreases downward at a decelerating rate, which indicates a slowing of tectonic uplift and water-table decline with time. The size of the sampled rooms and passages, plus the presence of massive gypsum (or clues of its former presence), show that these sites were probably produced by high dissolution rates at former water tables. Figure 10 suggests at least half a million years for any of the sampled levels to form.

During large H_2S influxes, the delivery rate of oxygen was the limiting factor in cave development, and enlargement rates varied with the production rate of sulfuric acid. Whenever H_2S was absent, as it is today, phreatic dissolution of carbonate rock virtually ceased, although vadose condensation-corrosion may have continued. On a molar basis, the production of sulfuric acid requires twice as much O_2 as H_2S (reaction 1), and at the low oxygen concentrations in groundwater, the optimum rate of phreatic cave enlargement would be achieved by a flow of meteoric water considerably larger than that of H_2S-rich water. Bacterial mediation can greatly speed the oxidation rate, and conversion of H_2S to sulfuric acid in a single step (reaction 1) may require the intervention of certain species of sulfur-oxidizing bacteria (Ehrlich 1996: 514).

In most sulfur springs, contact with oxygen is very limited until the water emerges at the surface. The Guadalupe caves owe their unusual character to the abundance of oxygenated groundwater, which allowed cave development to begin far upflow from the springs. As the caves enlarged, air exchange with the surface allowed still greater enlargement rates. Where dissolved H_2S or O_2 concentrations were small, the cave enlargement rate could be kept high by a large discharge, although oxidation would have been spread over longer distances, causing more H_2S to escape at the springs.

It is difficult to separate the effect of sulfuric acid from that of carbonic acid, because not only does most groundwater have a fairly high CO_2 content, but CO_2 is also generated by dissolution of carbonate rocks by sulfuric acid. If some of the generated CO_2 is retained within the caves, dissolution is greatly enhanced (Fig. 11). Very high CO_2 concentrations can retard dissolution of carbonate rocks by sulfuric acid, since CO_2 is a by-product (reactions 2 and 3), but sufficiently high CO_2 levels are rarely, if ever, achieved in carbonate aquifers.

It is logical to think of sulfuric acid as a far more potent cave-former than carbonic acid. This is not necessarily so. Although sulfuric acid is diprotic (supplying two H^+ ions), in general only one reacts with limestone, while the other combines with HCO_3^- to produce CO_2. In a moderately closed environment the CO_2 builds up, increasing the amount of dissolved limestone that can be held in solution. However, under totally closed conditions oxygen is unable to enter the system to produce sulfuric acid. Under typical field conditions, sulfuric acid generated from H_2S can increase the amount of dissolved limestone by only about 30-50% (see Fig. 11). But if oxygen is available deep within an aquifer, as in the Guadalupes, most of the solvent capacity of sulfuric acid is expended on cave development. In contrast, the carbonic acid dissolution typical of most karst areas is dispersed over long flow distances, and most of it is consumed at and near the bedrock surface, leaving relatively little for cave enlargement at depth.

With a few assumptions, it is not difficult to estimate the mass of H_2S needed to produce the Guadalupe caves, or at least a representative volume of cave. If all the H_2S is consumed in reactions (1) and (2), one mole of H_2S (34 g/mole) would dissolve one mole of calcite (100 g/mole), regardless of whether an intermediate sulfur phase is involved, or whether gypsum is a temporary by-product. If the limestone is nearly pure calcite (density = 2.7 g/cm³), the dissolution of 1 m³ of calcite would require 9.18 x 10^5 grams of H_2S. Conversion to volume of H_2S-bearing water within the source area could be misleading, because H_2S continued to be generated over a long time within the source area while it migrated out elsewhere, and was not simply depleted from static storage. To produce this amount of H_2S by reduction of sulfate (a 1:1 molar conversion) would require 2.0 m³ of gypsum or 1.2 m³ of anhydrite. In the simple model assumed here, the required volume of gypsum would be twice as great as the volume of cave dissolution.

To maintain the mass balance, the rate of cave enlargement (volume/time) must equate to $Q\Delta C/\rho$, where Q = groundwater discharge, ΔC = increase in dissolved solids between the incoming and outflowing water, and ρ = density of the soluble bedrock. Consider that the discharge through a given cave passage is 10 L/sec, and that H_2S is carried in at 100 mg/L (0.003 mole/L) in a solution saturated with calcite and containing 0.001 mole/L CO_2. These conditions fall within the range of observed H_2S systems elsewhere. If the ambient CO_2 in the cave air is 0.01 atm and there is sufficient oxygen to convert all the H_2S to sulfuric acid, figure 11 shows that ~200 mg/L of additional $CaCO_3$ could be dissolved. At a discharge of 10 L/sec, this amounts to ~23 m³ of limestone per year. At that rate, even the largest cave rooms in the Guadalupes could form

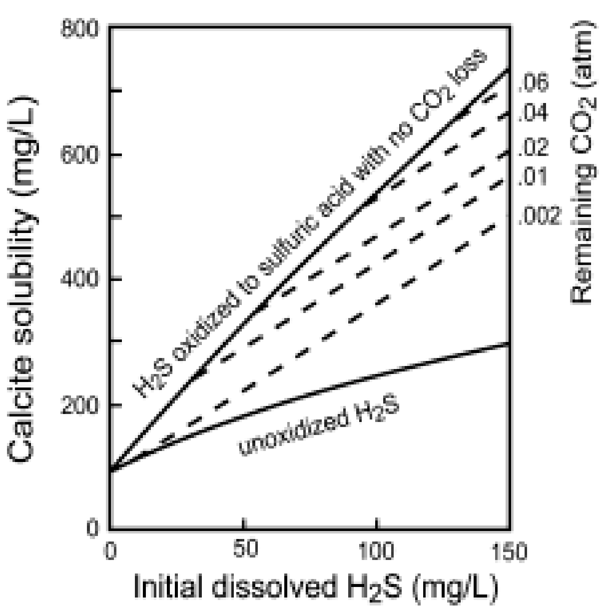

Figure 11. Increase in calcite dissolution caused by oxidation of H_2S to sulfuric acid. Initial CO_2 concentration is 0.001 mole/liter. Lower line = calcite saturation in the initial H_2S–CO_2 solution. Upper line = calcite saturation after complete oxidation of H_2S to sulfuric acid, with no degassing of CO_2. Dashed lines show diminished dissolution if CO_2 degassing takes place. After Palmer (1991).

in less than 100,000 years. Not all of this potential is achieved, because some H_2S may not convert to sulfuric acid. Much of the reaction with limestone produces gypsum, which complicates the volume estimate. Despite the many uncertain variables, this plausible example shows how potent this mode of speleogenesis can be.

GYPSUM DEPOSITION AND BEDROCK REPLACEMENT

Sulfuric acid cave origin is not a simple matter of dissolution of carbonate rock. Incoming H_2S-rich water contains at least a moderate concentration of dissolved gypsum, and oxidation of H_2S raises the sulfate content still farther. As carbonate rock dissolves, the release of calcium can force gypsum to precipitate if the influx of fresh water is not too large. Much gypsum has precipitated in such a delicate balance with carbonate dissolution that the net result resembles a direct replacement of the carbonate bedrock. Gypsum deposition can diminish the rate of cave growth by filling some of the void space in the carbonate rock. Fresh groundwater or infiltrating seepage can later carry away the gypsum, continuing to enlarge the caves long after the H_2S source has become inactive.

The texture of gypsum remnants can shed light on their origin, and therefore on the origin of the host passage or cave room. Buck *et al*. (1994) described the origin and petrology of five types of gypsum in Guadalupe caves: (1) subaerial gypsum crust that has replaced bedrock by the sulfuric acid reaction; (2) subaqueous gypsum crust of the same origin; (3) subaqueous gypsum sediment; (4) breccias of fallen gypsum blocks; and (5) evaporitic gypsum.

Gypsum replacement of calcite can take place by the following reaction:

$$2H^+ + SO_4^{2-} + CaCO_3 + 2H_2O \Leftrightarrow CaSO_4 \cdot 2H_2O + H_2O + CO_2 \qquad (5)$$

Dolomite reacts in a similar way. Where sulfuric acid is generated in contact with carbonate rock, it is difficult to achieve pH values less than about 6 because the acid is almost immediately neutralized by the carbonate. Very low pH can be reached if the acid is shielded from the carbonate rock by a rather non-reactive material such as gypsum, chert, clay, or organic material. Some water droplets isolated from the carbonate bedrock by gypsum crusts in Cueva de Villa Luz, Mexico, have pH values below 0.1 (Palmer & Palmer 1998).

Subaerial gypsum crusts form by reaction (5), which involves an approximate mole-for-mole replacement of carbonate rock (the reaction is often not perfectly balanced). The gypsum occupies a larger molar volume, so the crust expands to a greater volume than the rock it replaces. As a result the crust tends to be blistered and poorly bonded to the host rock, so it easily falls as fragments to the cave floor. In contrast, subaqueous crusts appear to have replaced the bedrock on a volumetric basis, in which each volume of carbonate rock is replaced by a roughly equal volume of gypsum. This is shown by the inheritance of textures from the original bedrock, such as bedding, pisoliths, and fossils (Fig. 12). These features are preserved almost intact, as verified by comparison with adjacent bedrock exposures (Queen 1973; Queen *et al*. 1977; Buck *et al*. 1994), although later recrystallization of the gypsum can disrupt the textures. The reaction probably involves ionic diffusion through the porous gypsum crust. Endless and Cottonwood Caves contain excellent exposures of this type of crust, which in places lines entire passages. Later dissolution along the bedrock-gypsum contact by vadose seepage often causes the gypsum crust to slump into the passage, forming a gypsum-lined tube within a larger bedrock tube.

By an odd coincidence, an almost perfect volume-for-volume replacement of limestone by gypsum can be achieved if one gypsum molecule replaces two calcite molecules, because the molar volume of gypsum is almost exactly twice that of calcite (precisely 2.02 times). This exchange can occur in the following way:

$$2H^+ + SO_4^{2-} + 2CaCO_3 + 2H_2O \Leftrightarrow CaSO_4 \cdot 2H_2O + Ca^{2+} + 2HCO_3^- \quad (6)$$

This reaction is balanced if the solution remains supersaturated with gypsum and undersaturated with calcite. The pH must remain high enough (greater than about 6.4) to suppress the tendency for H^+ to react with bicarbonate to form H_2CO_3 and CO_2. These conditions are most common in phreatic water that is close to equilibrium with carbonate rock. Typical groundwater in active sulfuric acid caves has sufficiently high pH values, 0.001-0.01 M bicarbonate, and molar Ca/SO_4 ratio about 1.0. Under these conditions, the phase relationships between gypsum and calcite, according to reaction (6), are shown in figure 13. As pH rises, the reaction can proceed to the left of the equation, allowing calcite to replace gypsum; meteoric groundwater in karst normally satisfies these conditions. Dolomite can react in a similar manner, except with a 1:1 ratio of dolomite to gypsum. Because the molar volume of gypsum is 1.15 times greater than that of well-ordered dolomite, the volume expansion during replacement tends to disrupt initial bedrock textures more than in the case of limestone.

Figure 12. Gypsum replacement of dolomite, with preservation of original bedrock textures (dolomite above, gypsum below), in the upper level of Endless Cave. Only close examination can verify the inheritance of textures by the gypsum. Width of photo is 0.5 m.

INTERPRETATION OF CAVE PATTERNS

In humid karst, caves are best interpreted in relation to the history of the river valleys into which they drain. This approach has merit in the Guadalupes, too, but the relationships are obscure. It is more appropriate to examine separately the origin of the features that make up a typical Guadalupe cave. Each cave can then be deciphered according to its individual layout and character.

CAVE ROOMS

The most impressive aspect of Guadalupe caves is the great size of their largest rooms. In humid karst, most cave rooms are formed by the intersection of two or more passages, often accompanied by breakdown. In contrast, cave rooms in the Guadalupe Mountains were formed by intense dissolution in local areas of sulfuric acid production. It is common for such a room to connect only to minor passages that seem unsuited to the task of conveying aggressive water to such a grand site. The Guadalupe Room of Carlsbad Cavern, for example, is reached by a network of narrow fissures, none of which gives the impression of large spaces beyond. The room was formed by local aggressiveness from rising H_2S, and the passages that connect it to the Main Corridor are only peripheral enlargements.

Irregular outlines, dead-end galleries, and blind alcoves are typical of Guadalupe cave rooms. Some rooms and adjacent passages have nearly horizontal floors. For example, the Big Room and adjacent Left Hand Tunnel of Carlsbad Cavern have a remarkably consistent floor elevation of 1110 m over much of their area. Some rooms have distinct notches in their walls at the level of maximum dissolution (Buck *et al*. 1994). Persistent elevations of this type, and their disregard for stratigraphic boundaries, almost certainly indicate water-table control, with aggressiveness produced at an air-water interface. Fissures are common in the floors of many cave rooms, and they are the likely sources for rising hydrogen sulfide (Fig. 14).

The oxygen demand in producing a large room cannot easily be met without plentiful air exchange with the surface, so it is not surprising that most of the largest cave rooms connect to the surface via older ascending phreatic passages. The rooms postdate the initial ascending passages, but the relict passages contribute to their enlargement by serving as conduits for oxygen exchange. In the absence of an open cave passage, air can also be exchanged in limited quantities through narrow fissures

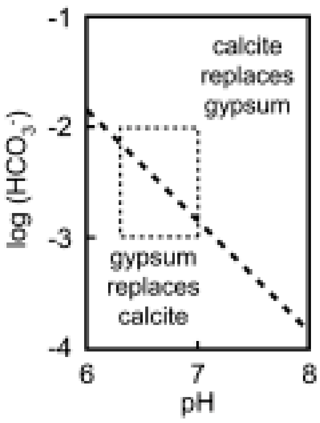

Figure 13. Stability fields for volumetric gypsum replacement of calcite (lower left) and calcite replacement of gypsum (upper right) as a function of pH and bicarbonate activity, according to reaction (6), at 25° C with molar Ca/SO_4 ratio of 1.0. For gypsum to replace calcite, $(Ca^{2+})(SO_4^{2-})$ must exceed 3.2×10^{-5}. For calcite to replace gypsum, $(Ca^{2-})(CO_3^{2-})$ must exceed 3.3×10^{-9}. The equilibrium line shifts slightly to the right as temperature decreases. The dashed rectangle shows typical conditions in present karst sulfur springs.

in the overlying bedrock. Despite the need for an oxygen supply, however, the greatest dissolution rates must have been limited to rather closed environments where high CO_2 levels could be sustained (as suggested by Fig. 11). The Main Corridor and Entrance Passage of Carlsbad Cavern provide an example of the open but indirect communication with the surface that favors the origin of large rooms. Some rooms and galleries, such as the entrance section of Cottonwood Cave, are open directly to the surface now, but probably were connected by less-direct routes before they were intersected by the present canyons.

Some rooms have uneven floors simply as the result of breakdown or gypsum accumulation. Others with irregular or sloping floors may have been generated by local mixing between H_2S-rich and oxygenated water below the water table (e.g., Prickly Ice Cube Room, Lechuguilla Cave). The presence of thick gypsum in some of them indicates either that sulfuric acid production can be very intense even below the water table, or that these rooms were formed at a dropping or fluctuating water table.

Gypsum precipitation and bedrock replacement can take place with little net increase in room volume unless the gypsum is later removed by fresh groundwater. The ceilings of major cave rooms are typically smooth and arched, and they almost invariably show evidence of gypsum replacement (Fig. 3). In some rooms large gypsum blocks still remain on the floor (e.g., the Big Room in Carlsbad). Many blocks contain smaller fragments of gypsum that have fallen from the ceiling (Hill 1987). Upward enlargement of rooms by vadose gypsum replacement has been documented in active H_2S caves such as Lower Kane Cave in Wyoming (Egemeier 1981) and Cueva de Villa Luz in Mexico (Hose & Pisarowicz 1999).

ASCENDING PASSAGES

Certain passages have remarkably steep profiles. They include inclined and vertical fissures that extend along joints and faults, as well as tubular passages controlled mainly by bedding in the back-reef strata. Both show strong evidence for having been formed (or at least initiated) by rising aggressive water.

Some fissures, also known locally as "rifts," extend downward from the floors of large rooms or passages and simply pinch downward with bottoms that are clogged with calcite crust or carbonate sediment. Examples include the route to Sulfur Shores in Lechuguilla Cave (Fig. 15) and the Four O'Clock Staircase, a 100-meter-deep vertical fissure in Virgin Cave. These fissures extend below the level of major cave enlargement and appear to be the inflow routes along which oxygenated and H_2S-rich water first began to mix. Active examples occur in Lower Kane Cave, Wyoming (Egemeier 1981), but they are narrower than the typical Guadalupe rifts. If H_2S oxidation is limited to the points where water emerges into air-filled passages or at the surface, significant enlargement does not take place deep inside the ascending fissures. Mixing between oxygen-rich and H_2S-rich flow paths below

Figure 14. Rift in the floor of the main passage of Hell Below Cave, through which an aggressive mixture of H_2S-rich water and oxygenated water rose.

the water table must have been responsible for the deep rifts in Guadalupe caves.

Many ascending passages connect different levels or serve as entrance passages to the caves (Fig. 16). Some are fissures, such as the Great White Way and the rift above Lebarge Borehole in Lechuguilla Cave (Fig. 17), while others are mainly tubular with only local fracture control. The entrance series of Carlsbad Cavern (Fig. 4), Hicks Cave (Fig. 5), and Lechuguilla Cave (Fig. 18) are all ascending passages with mainly tubular shapes. Such entrances give the superficial impression that they were once surface-water inlets, because they descend steeply from surface gullies or from the walls of canyons. The Carlsbad entrance even swallows a sinking stream during heavy rainfall. However, there is no evidence that they were vadose inputs while the caves were forming. They contain no stream entrenchment or fluting, and virtually no truly vertical shafts or coarse clastic sediment. Instead, the passage ceilings rise in a series of smooth convex-upward arcs quite distinct from the abrupt stair-step pattern typical of vadose passages. Local confinement by resistant beds can force rising passages to follow an up-dip course, accounting for the northwesterly trend of the entrance passages shown in Figures 4, 5, and 18. Abrupt discordance of such passages to the strata is common only along prominent fractures or cross-cutting structures. For example, Boulder Falls, shown in figure 18, follows a vertical breccia dike.

Like the narrow rifts described above, ascending tubes appear to have formed in one stage by aggressive solutions in which mixing of the two major water sources had already taken place. Some have enormous cross-sectional areas and vertical ranges. The descent through the entrance and Main Corridor of Carlsbad Cavern is breathtaking. The entrance series of Lechuguilla Cave (Fig. 18) rises from the Rift to the cave entrance over a vertical range of at least 200 m. The Wooden Lettuce Passage is a possible precursor to the entrance passage that extends even higher, and it is possible that the Rift itself was the original feeder, extending the vertical range still farther. There seem to be no alternate flow routes, which suggests that the entire passage formed simultaneously below the water table, although enlargement of its rooms probably took place at a later time at or near the water table.

Alternatively, some of the ascending passages may have started as narrow channels that were greatly enlarged by dissolution from their upper ends downward as the water table and zone of maximum oxidation dropped with time. This would require outflow of the water at many different levels, and large rooms that interrupt the passage profiles would correlate in elevation from one passage to another. Neither characteristic is present. Guadalupe cave development was intermittent, controlled by episodes in which H_2S-rich water was released from lower strata (as discussed later), and it is likely that the inception of a typical ascending passage took place over its entire length in a single stage, rather than in small descending increments over a long time period.

Some ascending passages are interrupted by large rooms that appear to post-date the passages. Their size and the presence of massive gypsum suggests discrete episodes in which H_2S entered and was oxidized at the water table. Examples in the entrance series of Lechuguilla Cave (Fig. 18) include Glacier Bay and the room at the base of Boulder Falls. No tra-

Figure 15. Profile through the Sulfur Shores rift, Lechuguilla Cave, from geologic leveling survey by the authors. The contact between the Capitan Limestone and Goat Seep Formation is unclear.

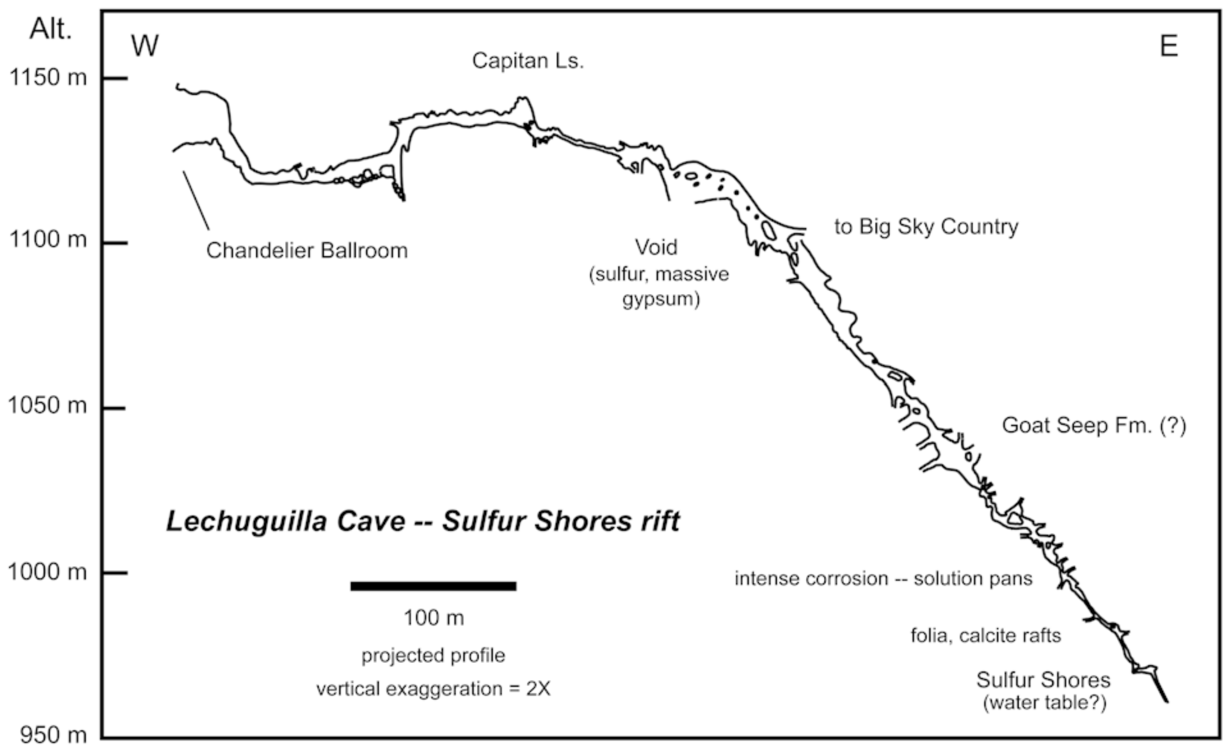

versable passages are known to lead laterally from them to the surface. Their origin apparently involved little discharge, perhaps allowing outflow to be diffuse. Much of their volume increase has taken place by later removal of gypsum by vadose seepage, a process that continues even today.

Ascending tubes must also have enlarged above the water table by sulfuric acid generated where H_2S was absorbed by moisture on walls and ceilings. This process would be enhanced when H_2S was drawn upward along wide fissures during periods of low atmospheric pressure at the surface. It may have been possible for short passages to form entirely in this way. Replacement gypsum, a likely by-product of this process, would have been easily removed by fresh infiltrating water. Rills and other gravitational dissolution features are generally absent, because (as with condensation-corrosion) the moisture rarely forms more than a capillary film. The resulting surfaces would bear many characteristics of phreatic dissolution, complicating the speleogenetic interpretation. This mechanism should be investigated more thoroughly, because it could affect the estimates of depth and percentage of phreatic dissolution in the origin of the Guadalupe caves.

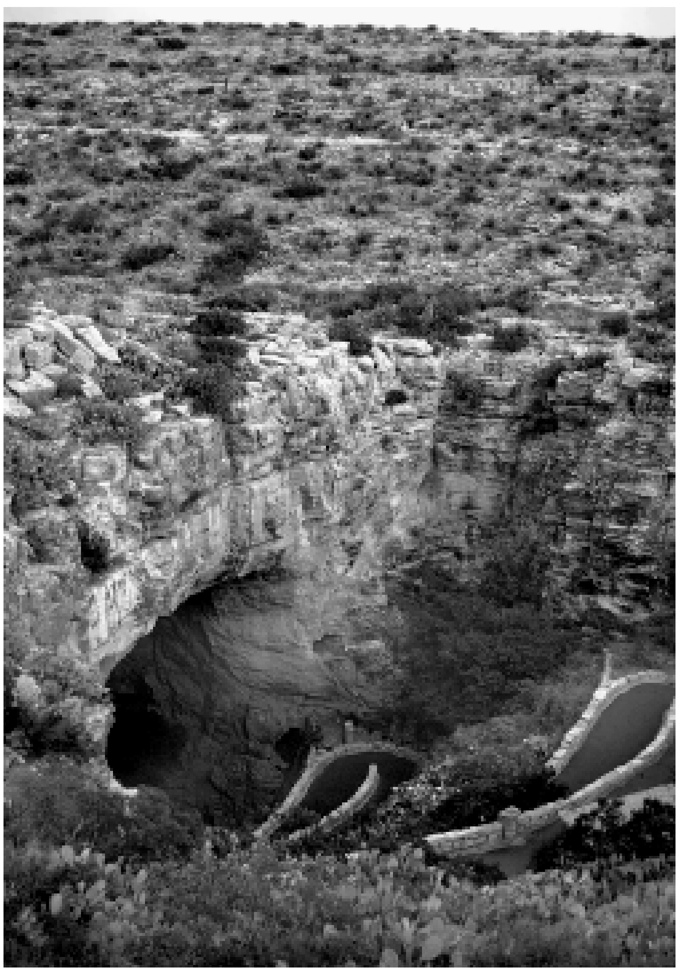

Figure 16. Entrance to Carlsbad Cavern, a former spring outlet fed by an ascending tube.

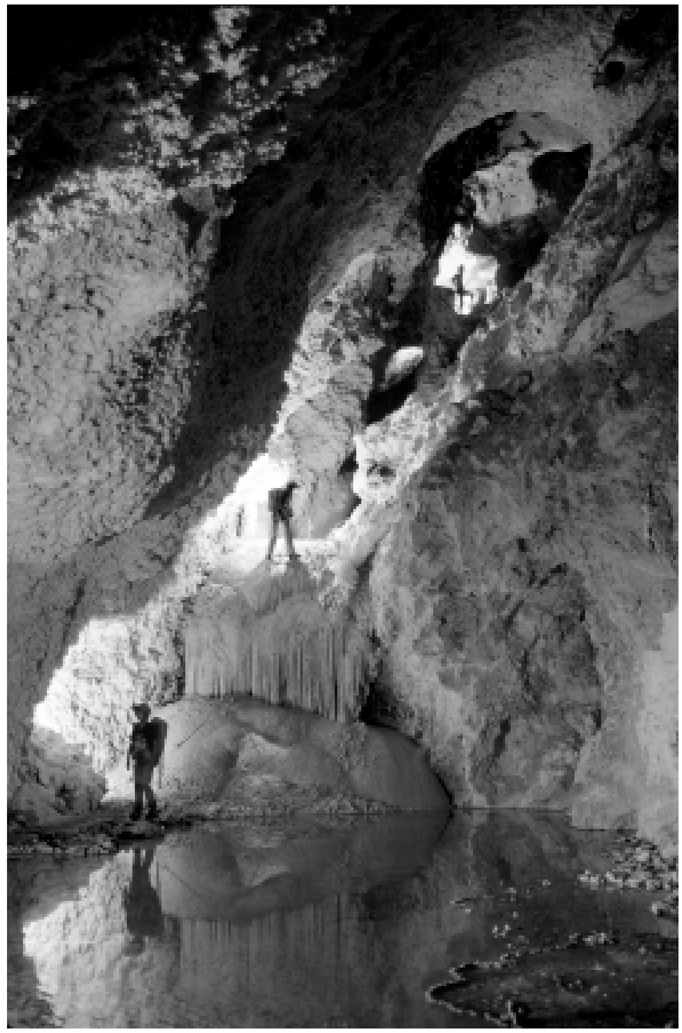

Figure 17. Lake Lebarge and the sloping fracture-controlled fissure ascending from it to higher-level passages, Lechuguilla Cave.

HORIZONTAL PASSAGES

Despite the rambling three-dimensional nature of most Guadalupe caves, certain distinct, nearly horizontal passage levels represent former water-table levels. The best documented is the Left Hand Tunnel in Carlsbad, whose floor coincides closely with that of the Big Room. Other slightly less horizontal examples, of many, include the Western Borehole in Lechuguilla Cave and the main passage of Ogle Cave (Fig. 7). Some of these tunnels once served as outlets for water from the zones of maximum cave origin, such as the outward-branching passages shown on the map of Hicks Cave (Fig. 5). They tend to diminish in size in the direction of flow because of decreasing aggressiveness. Most pinch down to fissures and spongework too narrow to traverse before reaching the surface. Cave entrances along former horizontal outflow routes at successively lower elevations, although expected, are actually quite rare.

Figure 18. Profile through the entrance passage of Lechuguilla Cave, from geologic leveling survey.

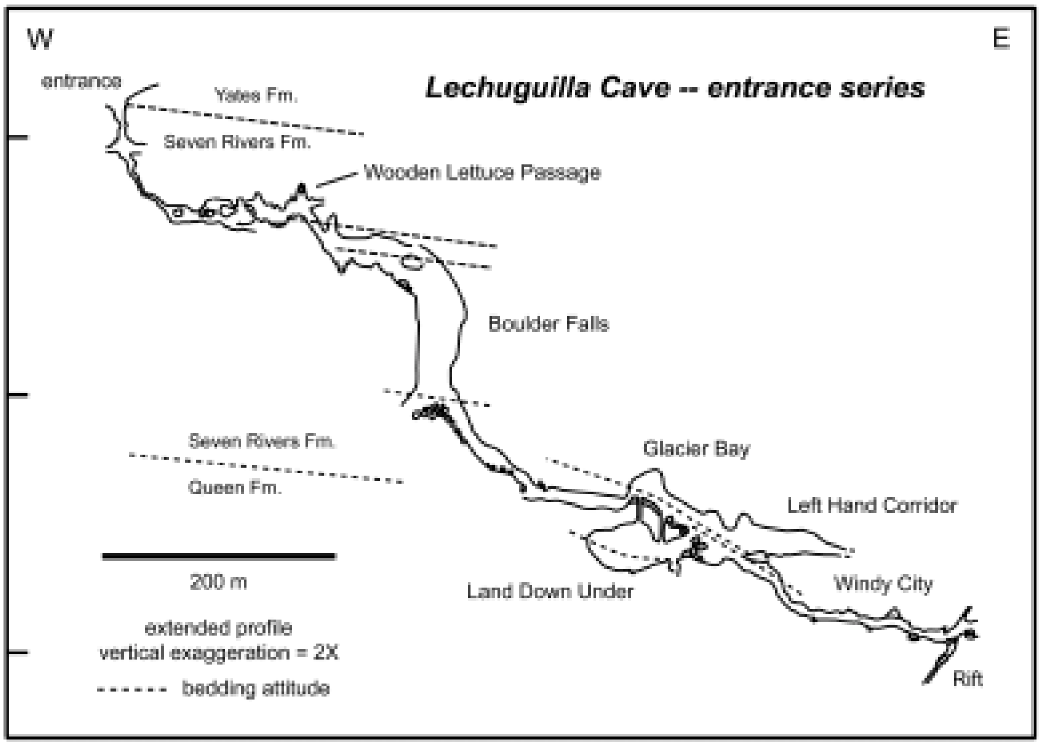

The near-horizontal trends of these passages are unaffected by stratigraphic boundaries or variations in rock texture. An example is the passage along the top of the Rift in Lechuguilla Cave, which continues southward as the E and F surveys (Fig. 19). This passage system cuts discordantly across back-reef strata, which locally have a mean dip of 7.5° SW. Water-table control is evident. Note the contrast with the entrance series, formed by ascending phreatic water, which contains sloping, stratally concordant sections (Fig. 18). The profile in figure 19 deviates from the horizontal at the southernmost extent of the F Survey. It is almost unnoticeable in the cave but is clearly shown on the expanded vertical scale of the profile. It may be the result of a mild headward steepening of the water table. Egemeier (1981) noted similar characteristics in the profile of Lower Kane Cave, Wyoming.

HORIZONTAL PARTITIONS WITHIN ROOMS AND PASSAGES

An odd characteristic of Guadalupe caves is that many of their rooms and passages are divided horizontally by thin bedrock partitions. Explorers are occasionally alarmed to find that a seemingly substantial floor is actually a frail and discontinuous shelf over a large void. In the most distinct examples, the floor of the upper level is covered with a thick deposit or replacement crust of gypsum, or there is evidence that gypsum once occupied the site.

Glacier Bay in Lechuguilla Cave is an unusual example in which a horizontal room (Land Down Under) cuts across an older sloping room (Fig. 18). The horizontal partition is about 6-8 m thick and covered with an additional 4 m of brecciated gypsum derived mostly from blocks of replaced bedrock that fell from the ceiling during cave development. The bedrock consists of silty and partly brecciated limestone and dolomite no different from that in adjacent passages, and there is no evidence that the partition consists of relatively resistant rock, nor is the partition recrystallized or dolomitized. Fluted vadose drip holes up to 2 m in diameter extend through the gypsum. Most of the holes terminate at the gypsum-bedrock contact, but a few extend all the way through the bedrock partition. Above the drip holes the ceiling shows no apparent vadose inlets such as fissures, and the drips are now inactive or nearly so.

These partitions rely on intense acidity generated at successive water-table levels. In most examples, the ceilings of both levels were enlarged upward by gypsum replacement of carbonate bedrock. During the later stage, the partition was perforated or removed entirely. While the lower level enlarged, some of the H_2S degassing from the water surface must have been absorbed by moisture on the ceiling of the upper level and prolonged the gypsum replacement of carbonate rock. Where acid drips were not entirely saturated with gypsum they could core through both the gypsum and the carbonate partition between levels.

Not every cave level relates to a former water table. Endless Cave in McKittrick Hill contains up to three superimposed labyrinths separated by bedrock partitions only a few meters thick. The resulting complexity makes a plan-view map almost indecipherable unless the overlapping tiers are depicted separately (Fig. 20). All the tiers appear to have formed simultaneously near the water table. A gypsum crust has replaced the bedrock, inheriting the bedrock textures, indicating phreatic dissolution (Fig. 12). A sequence of favorable beds and bedding-plane partings was enlarged, leaving the intervening bed remnants as partitions.

MAZES

Network and spongework mazes form parts of many Guadalupe caves, and some entire caves (e.g. Fig. 20). Mazes develop where many interconnected openings enlarge at comparable rates. This is not the way most caves form, because slight differences in flow rate or hydraulic efficiency cause larger openings to outpace the lesser ones, so that only a few reach traversable size. An effective way to form a maze is to combine high aggressiveness with short distances of flow from where the aggressiveness is produced (Palmer 1991). This criterion is amply met in the Guadalupe caves. The only major genetic difference between network and spongework mazes is the nature of the initial openings; i.e., intersecting fractures vs. intergranular pores. An impressive network maze surrounds the Left Hand Tunnel of Carlsbad Cavern (Fig. 4). Spongework is most abundant in the massive reef, which is noted for its large primary pores, and is common around the periphery of large rooms. The local term for spongework is “boneyard,” in reference to the Boneyard of Carlsbad Cavern, which contains such thin remnants that it resembles a pile of bones (Fig. 21). Hill (2000) describes early spongework of Mesozoic age, which is generally of less than traversable size. Most traversable spongework mazes were produced during the major stages of Cenozoic cave development, which in many places simply enlarged the Mesozoic pockets.

Mazes originated in mixing zones where the aggressiveness was high. In the downflow direction from these sites, where aggressiveness weakened, the passages tend to unite into single conduits, except where additional H_2S inputs boosted the local acidity. Ascending high-level tubes are least likely to have maze-like characteristics, because they represent long phreatic flow paths with rather low aggressiveness. Many mazes connect large rooms or passages, some at different levels. If the mazes were part of the main flow routes, their passages would have been enlarged to a size comparable to that of the rooms. Diffuse flow into or out of the rooms was necessary to form them.

Those caves that consist almost entirely of mazes, such as Spider Cave and the caves of McKittrick Hill (Fig. 20), were themselves the sites of greatest aggressiveness. Most are in the bedded back-reef strata, particularly the Yates Formation, and have limited vertical extent. Diffuse infiltration through silty beds may have supplied the necessary oxygen. Stratigraphic trapping of rising H_2S-rich water at and near the crest of an anticline accounts for the dense concentration of McKittrick Hill caves.

Some large rooms contain spongework in their floors and lower walls, but not in their upper walls and ceilings (for example, the New Mexico Room, Carlsbad Cavern). Ash & Wilson (1985) attributed the spongework to downward migration of H^+ ions through aggressive solutions. A simpler explanation is that the growing rooms were only partly filled with water, limiting the upward extent of spongework, and upward ceiling migration by falling of replacement rinds tended to remove incipient spongework.

VADOSE DISSOLUTION FEATURES

Although much cave enlargement in the Guadalupes took place within the vadose zone where H_2S was oxidized to sulfuric acid in moisture films, traditional vadose dissolution by descending meteoric water has been almost nil. A few forms of fresh-water vadose dissolution, though accounting for only minor cave enlargement, shed light on the local cave-forming processes:

(1) Gypsum deposits are readily dissolved by vadose water, even if the water is saturated with dissolved limestone. Rills and boreholes are produced in the gypsum by high-volume drips.

(2) Oxidation of pyrite to sulfuric acid can produce local shafts and rills in carbonate rock. An example is the Queen of the Guadalupes, a fluted shaft system that formed below a concentrated zone of pyrite weathering (Jagnow 1979).

(3) In the past, aggressive drips of sulfuric acid formed deep, narrow rills (rillenkarren) in carbonate rock (Fig. 22). The acidity of the drips is explained in the section on gypsum replacement.

(4) Condensation-corrosion occurs where warm, moist air ascends from lower levels, allowing water to condense on the walls of cooler upper levels (Queen 1981; Davis 2000). Dissolution of bedrock and speleothems is common at these condensation sites, and the dissolved minerals are drawn to zones of evaporation by capillary potential, where they precipitate as speleothems and crusts.

(5) Features that superficially resemble potholes are common in certain places, for example in the Near East and Sulfur

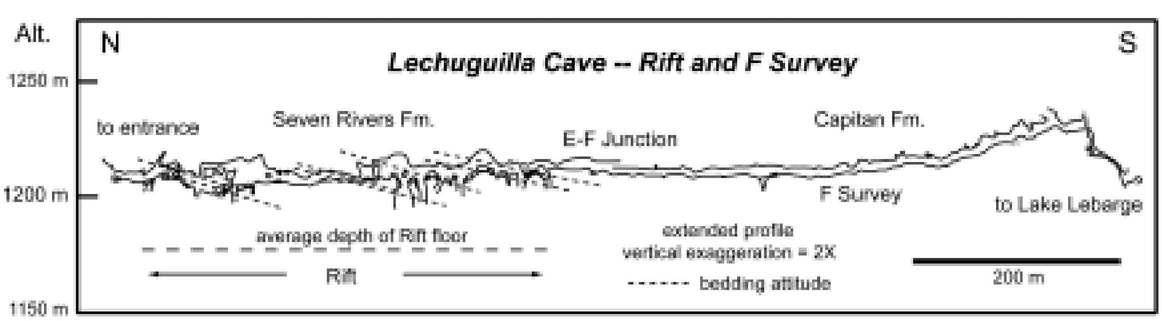

Figure 19. Profile through the Rift and related passages, Lechuguilla Cave, from geologic leveling survey.

Shores areas of Lechuguilla Cave (Fig. 15). These are not true potholes (i.e. erosional features formed by turbulent water), but simply the underground equivalent of the solution pans that form on limestone surfaces where rainwater collects in hollows. In the caves they were fed by local drips charged with sulfuric acid.

CORRELATION BETWEEN CAVES

Passages in many Guadalupe caves can be grouped into crude levels. As implied in the graph of cave age vs. elevation (Fig. 10), regional geomorphic history has played a significant role in determining the vertical layout of Guadalupe caves. One would expect the vertical arrangement of major passages and rooms to reflect the history of base-level lowering.

The real picture is not as simple as expected. Figure 23 compares the altitudes of the major rooms and passages in Carlsbad Cavern with most of those in Lechuguilla Cave. Aside from a few apparent correlations, the general picture is chaotic. Differential uplift rates are not sufficient to explain the muddle, because the two caves are close neighbors and the intervals between levels are just as mis-matched as the elevations. Portraying the vertical extent of a passage or room can be subjective because many of them taper upward and downward into smaller voids. Arbitrary decisions also had to be made as to which parts of Lechuguilla to omit, since the cave is such a complex tangle.

The Main Corridor of Carlsbad overlaps with almost every major passage and room in Lechuguilla. Distinct horizontal levels, such as the Left Hand Tunnel, floors of the Big Room and Lower Cave, Outback area, top of the Rift, Lebarge Borehole, and Western Borehole, are scattered inconsistently at many different elevations. The floor of the Big Room in Carlsbad overlaps in elevation with the Western Borehole, but the latter includes several different levels and its floor is quite irregular. A tentative correlation can also be made between the Chocolate High and the New Section in Carlsbad and the top of the Rift in Lechuguilla, but they do not include much cave volume. The Lebarge Borehole, main level of the Far East, and the Guadalupe Room match if a slight eastward slope is tolerated. But, in general, the anticipated precise matching between levels is elusive.

Because of the absence of widespread cave correlations, the confidence with which cave development can be related to regional geomorphic events is limited. However, an alternative and more dynamic view of cave evolution emerges. As the water table dropped, bursts of cave enlargement occurred at those times and places where H_2S was rising to the water table in significant quantity (Jagnow 1989). As the water table declined, episodic release of H_2S (probably during uplift and deformation) produced major rooms and passages. When these releases coincided with rather static water tables, distinct horizontal levels resulted. The greatest volumes and durations of gas escape were along the Guadalupe Escarpment, producing huge rooms and corridors such as those in Carlsbad, Ogle, and Lechuguilla Caves.

Under this scheme of cave enlargement, it was possible for neighboring caves to develop almost independently. Yet in places there was overlap between speleogenetic zones, resulting in erratic and rather unpredictable connections between

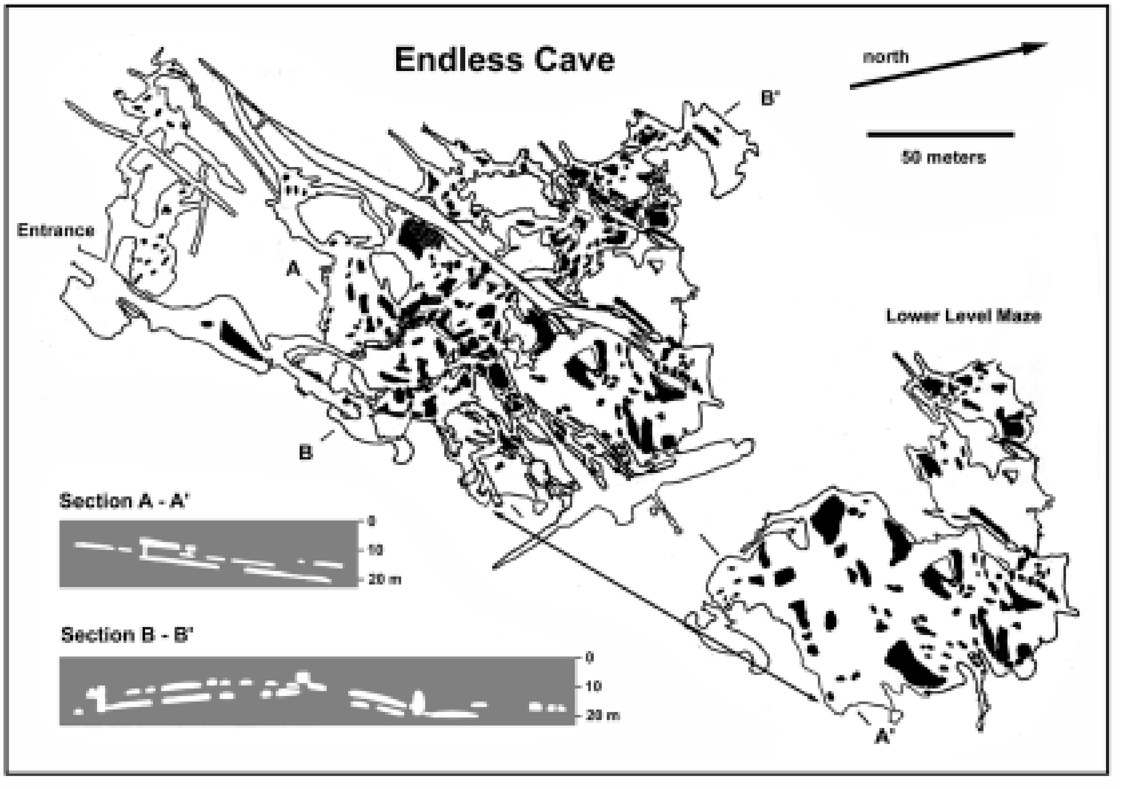

Figure 20. Map of Endless Cave, McKittrick Hill, simplified from Kunath (1978). Shaded areas on map are bedrock pillars.

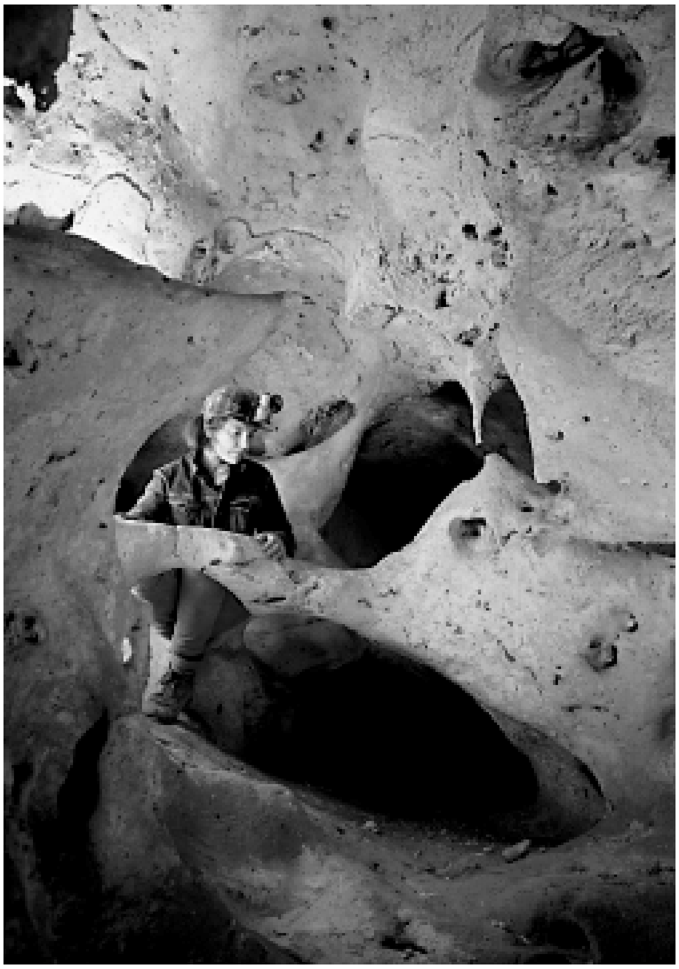

Figure 21. Spongework maze development in the Boneyard of Carlsbad Cavern.

otherwise independent caves. These connections are not necessarily traversable. Some caves, such as Spider Cave, seem isolated despite close proximity to the much larger surrounding caves (Fig. 2). Attempts by explorers to follow air movement in such caves have sometimes been frustrating. The huge air flow from several Guadalupe caves can be misleading if translated into units of cave volume, because much of it consists of passages of non-traversable size, including many fissures and pores that have undergone little if any solutional enlargement.

Certain complex Guadalupe caves were fed simultaneously by different H_2S sources. For example, the entrance series of Lechuguilla Cave was fed by water rising from the Rift area, while simultaneously (since their passages overlap in elevation) the Prickly Ice Cube Room, Underground Atlanta, and Tower Place were formed by water rising from the Sulfur Shores rift (Fig. 24). Connections between these two large areas are nearly impenetrable chutes and mazes, such as Tinseltown Maze, which were formed by minor exchange of aggressive water between the two sections as the head configuration in the aquifer changed with time.

During H_2S influxes, a given pathway would be active for a time, only to become inactive as the site of H_2S escape shifted. Some sites were active for long times, others only briefly. Some paths were occupied repeatedly, others abandoned after a single wave of activity. Although they must have varied in duration, the main episodes probably lasted at least 10^5 years to achieve such large passage and room sizes. The capricious nature of this cave development contradicts one's first impression of the Guadalupe caves as being sites of immensely stable groundwater conditions that prevailed over long periods of geologic time.

CONCLUSIONS

This paper raises as many questions as it answers. The morphology of Guadalupe caves, though well known in a general sense, could use far more quantitative evaluation. In particular, the methods for distinguishing between phreatic and vadose cave enlargement are still hazy. Further comparison with active caves of similar origin would be useful, along with a more penetrating geochemical analysis. Advances in understanding the Guadalupe caves has required a remarkable variety of researchers using tools that extend across all the sciences. And here, perhaps more than in any other cave area, the value of exploration is absolutely clear, for every new cave discovery helps to reveal more about the conditions that formed these enigmatic caves.

ACKNOWLEDGMENTS

Many thanks to Rick Olson, Richard Zopf, and Paul Rubin, who participated in the geologic field mapping. We greatly benefitted from discussions on Guadalupe cave origin with Michael Queen, Carol Hill, Marcus Buck, Donald Davis, David Jagnow, Harvey DuChene, Victor Polyak, Paula Provencio, Jim Goodbar, and Kimberley Cunningham. We greatly appreciate the cooperation of the staff at Carlsbad Caverns National Park, Lincoln National Forest, and the Bureau of Land Management office in Carlsbad, who made our work in the Guadalupe caves possible. Carol Hill, Donald Davis, Marcus Buck, and John Mylroie provided helpful reviews and editorial suggestions.

REFERENCES

Ash, D., & Wilson, W. (1985). A model for cavern development by ascending hydrogen sulfide gas for the Guadalupe Mountains, New Mexico [abs.]. *NSS Bulletin 47:* 63.

Buck, M.J., Ford, D.C., & Schwarcz, H.P. (1994). Classification of cave gypsum deposits derived from oxidation of H_2S. In Sasowsky, I.D., & Palmer, M.V. (eds.), *Breakthroughs in karst geomicrobiology and redox geochemistry*: Charles Town, WV, Karst Waters Institute, Special Publication 1: 5-9.

Cave Research Foundation (1992). *The quadrangle maps of Carlsbad Cavern, New Mexico*. New Carlisle, Ohio, Cave Research Foundation: 18 pp.

Figure 22. Rills formed by ceiling drips enriched in sulfuric acid, in Far East Series, Lechuguilla Cave. Note gypsum deposition around the drip site, apparently including mole-for-mole replacement of limestone at low pH, which involves a volume increase. Height of photo = 1.5 m.

Cunningham, K.I., Northup, D.E., Pollastro, R.M., Wright, W.G., & LaRock, E.J. (1995). Bacteria, fungi and biokarst in Lechuguilla Cave, Carlsbad Caverns National Park, New Mexico. *Environmental Geology 25(1):* 2-8.

Davis, D.G. (1980). Cave development in the Guadalupe Mountains: A critical review of recent hypotheses. *NSS Bulletin 42:* 42-48.

Davis, D.G. (2000). Extraordinary features of Lechuguilla Cave, Guadalupe Mountains, New Mexico. *Journal of Cave and Karst Studies 62*(2): 147-157.

DuChene, H.R. (1986). Observations on previous hypotheses and some new ideas on cavern formation in the Guadalupe Mountains. In Jagnow, D.H. (ed.), *Geology Field Trip Guidebook*. 1986 National Speleological Society convention, Tularosa, NM: 96-100.

DuChene, H.R. (2000). Bedrock features of Lechuguilla Cave, Guadalupe Mountains, New Mexico. *Journal of Cave and Karst Studies 62*(2): 109-119.

DuChene, H.R., & McLean, J.S. (1989). The role of hydrogen sulfide in the evolution of caves in the Guadalupe Mountains of southeastern New Mexico. In Harris, P.M., & Grover, G.A. (eds.), *Subsurface and outcrop examination of the Capitan shelf margin, northern Delaware Basin.* Society of Economic Paleontologists and Mineralogists, Core Workshop 13: 475-481.

Egemeier, S.J. (1981). Cavern development by thermal waters. *NSS Bulletin 43:* 31-51.

Egemeier, S.J. (1987). A theory for the origin of Carlsbad Caverns. *NSS Bulletin 49 (2):* 73-76.

Ehrlich, H.L. (1996). *Geomicrobiology* (3rd ed.). New York, Marcel Dekker, Inc.: 719 pp.

Harris, P.M., & Grover, G.A. (eds.) (1989). Subsurface and outcrop examination of the Capitan shelf margin, northern Delaware Basin. *Society of Economic Paleontologists and Mineralogists, Core Workshop 13:* 481 pp.

Hayes, P.T. (1964). Geology of the Guadalupe Mountains, New Mexico. *U.S. Geological Survey Professional Paper 446:* 69 pp.

Hill, C.A. (1987). Geology of Carlsbad Cavern and other caves in the Guadalupe Mountains, New Mexico and Texas. *New Mexico Bureau of Mines and Mineral Resources, Bulletin 117:* 150 pp.

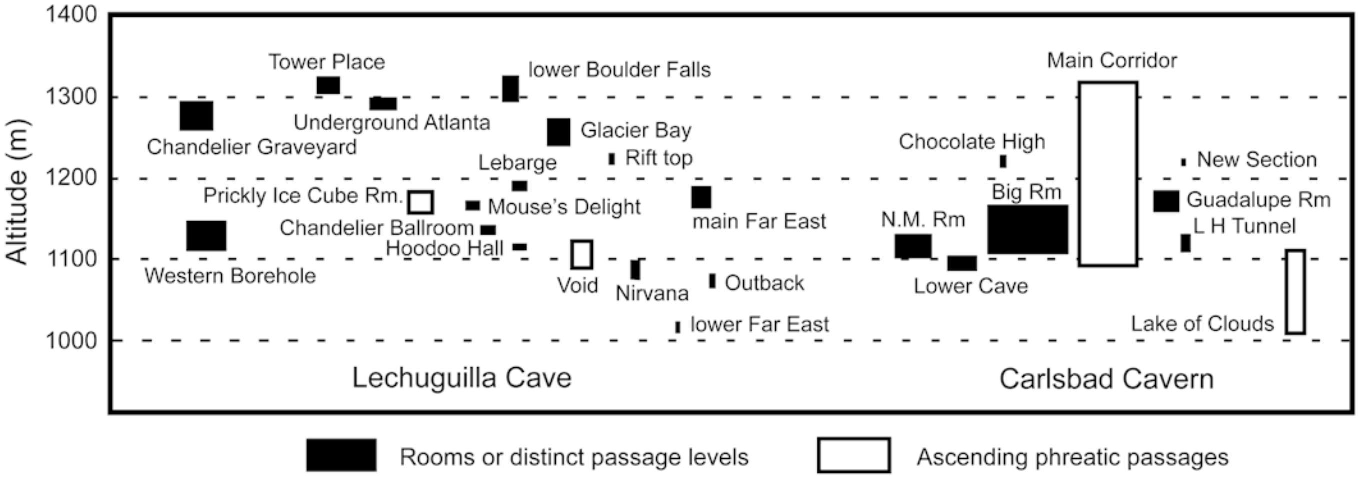

Figure 23. Elevation of major rooms and passages in Carlsbad Cavern and Lechuguilla Cave. The width of each block is proportional to the width of the room or passage. Carlsbad levels are based on data from the Cave Research Foundation (1992). Lechuguilla levels are based on geologic leveling survey, and on maps by the Lechuguilla Cave Project and Lechuguilla Exploration and Research Network.

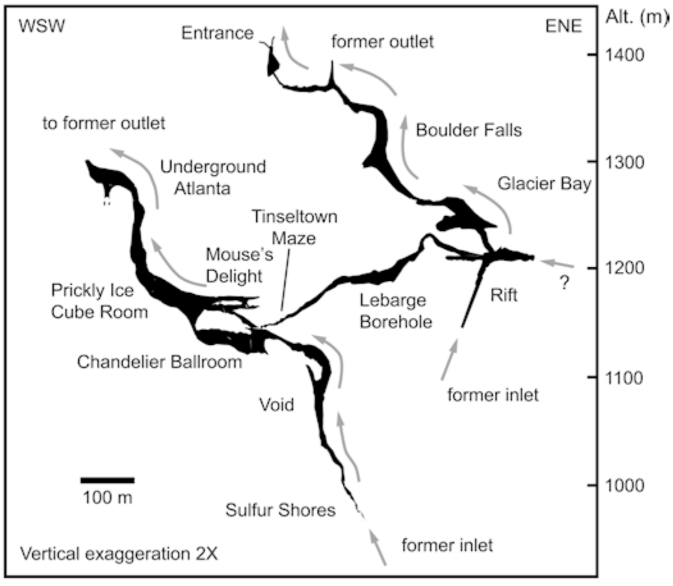

Figure 24. Projected vertical profile through part of Lechuguilla Cave (viewed from 165° with respect to true north), showing the nearly independent flow systems through the entrance series and through the Sulfur Shores - Underground Atlanta system. Based on geologic leveling survey by the authors.

Hill, C.A. (1990). Sulfuric acid speleogenesis of Carlsbad Cavern and its relationship to hydrocarbons, Delaware Basin, New Mexico and Texas. *American Association of Petroleum Geologists Bulletin 74:* 1685-1694.

Hill, C.A. (1996). *Geology of the Delaware Basin, Guadalupe, Apache, and Glass Mountains, New Mexico and west Texas.* Society for Sedimentary Geology (SEPM), Permian Basin Section, Publication 96-39: 480 pp.

Hill, C.A. (2000). Overview of geologic history of cave development in the Guadalupe Mountains, New Mexico and west Texas. *Journal of Cave and Karst Studies 62*(2): 60-71.

Hiss, W.L. (1980). Movement of ground water in Permian Guadalupian aquifer systems, southeastern New Mexico and western Texas. In Dickerson, P.W., & Hoffer, J.M. (eds.), *Trans-Pecos region*. New Mexico Geological Society, Guidebook to 31st Field Conference: 289-294.

Hose, L.D., & Pisarowicz, J.A. (1999). Cueva de Villa Luz, Tabasco, Mexico: Reconnaissance study of an active sulfur spring cave and ecosystem. *Journal of Cave and Karst Studies, 61(1):* 13-21.

Jagnow, D.H. (1979). *Cavern development in the Guadalupe Mountains.* Columbus, Ohio, Cave Research Foundation: 55 pp.

Jagnow, D.H. (1989). The geology of Lechuguilla Cave, New Mexico. In Harris, P.M., & Grover, G.A. (eds.), *Subsurface and outcrop examination of the Capitan shelf margin, northern Delaware Basin*. Society of Economic Paleontologists and Mineralogists, Core Workshop 13: 459-466.

Jagnow, D.H., & Jagnow, R.R. (1992). *Stories from stone—The geology of the Guadalupe Mountains*. Carlsbad, N.M., Carlsbad Caverns - Guadalupe Mountains Association: 41 pp.

King, P.B. (1948). Geology of the southern Guadalupe Mountains, Texas. *U.S. Geological Survey Professional Paper 215:* 183 pp.

Kunath, C.E. (1978). *The caves of McKittrick Hill, Eddy County, New Mexico*. Austin, Texas, Texas Speleological Survey: 87 pp. & 4 large-format maps.

Mylroie, J.E., Carew, J.L., & Vacher, H.R. (1995). Karst development in the Bahamas and Bermuda. *Geological Society of America, Special Paper 300:* 251-267.

Palmer, A.N. (1991). Origin and morphology of limestone caves. *Geological Society of America Bulletin 103:* 1-21.

Palmer, A.N. (1996). ***SI****—A computer program for calculating equilibria in water at low ionic strength* (Version 3.0). Oneonta, N.Y., State University of New York: software & 14 pp. manual.

Palmer, A.N., & Palmer, M.V. (1998). Geochemistry of Cueva de Villa Luz, Mexico, an active H_2S cave [abs.]. *Journal of Cave and Karst Studies 60(3):* 188.

Palmer, A.N., Palmer, M.V., & Davis, D.G. (1998). Geology and origin of Lechuguilla Cave. In Taylor, M.R., & Widmer, U. (eds.), *Lechuguilla—Jewel of the underground* (2nd ed.): Basel, Switzerland, Speleo Projects: 30-39.

Polyak, V.J., McIntosh, W.C., Güven, N., & Provencio, P. (1998). Age and origin of Carlsbad Cavern and related caves from $^{40}Ar/^{39}Ar$ of alunite. *Science 279:* 1919-1922.

Polyak, V.J. & Provencio, P. (2000). Comments on the timing, environment, and rate mechanisms of H_2SO_4-influenced speleogenesis for caves in the Guadalupe Mountains, New Mexico. *Journal of Cave and Karst Studies 62*(2): 72-74

Queen, J.M. (1973). Large-scale replacement of carbonate by gypsum in some New Mexico caves [abs.]. *National Speleological Society convention abstracts.* Bloomington, Ind.: 12.

Queen, J.M. (1981). *A discussion and field guide to the geology of Carlsbad Caverns*. Preliminary report to the National Park Service for the 8th International Speleological Congress: 64 pp.

Queen, J.M. (1994). Speleogenesis in the Guadalupes: The unsettled question of the role of mixing, phreatic or vadose sulfide oxidation. In Sasowsky, I.D., & Palmer, M.V. (eds.), *Breakthroughs in karst geomicrobiology and redox geochemistry*: Charles Town, W. Va., Karst Waters Institute, Special Publication 1: 64-65.

Queen, J.M., Palmer, A.N., & Palmer, M.V. (1977). Speleogenesis in the Guadalupe Mountains, New Mexico: Gypsum replacement of carbonate by brine mixing. *Proceedings of 7th International Congress of Speleology*. Sheffield, U.K.: 333-336.

Sarbu, S.M., Kane, T.C., & Kinkle, B.K. (1996). A chemoautotrophically based groundwater ecosystem. *Science 272:* 1953-1955.

Sares, S.W., & Wells, S.G. (1987). Geomorphic and hydrogeologic development of the Gypsum Plain Karst, Delaware Basin, New Mexico. In Powers, D.W., & James, W.C. (eds.), *Geology of the western Delaware Basin, West Texas and southeastern New Mexico*. El Paso Geological Society Guidebook 18: 98-117.

Wiggins, W.D., Harris, P.M., & Burruss, R.C. (1993). Geochemistry of post-uplift calcite in the U.S. Permian Basin. *Geological Society of America Bulletin 105:* 779-790.

Winograd, I.J., & Robertson, F.N. (1982). Deep oxygenated ground water: Anomaly or common occurrence? *Science 216:* 1227-1230.

Woods, T.L., & Garrels, R.M. (1987). *Thermodynamic values at low temperature for natural inorganic materials: An uncritical summary*. New York, Oxford University Press: 242 pp.

BEDROCK FEATURES OF LECHUGUILLA CAVE, GUADALUPE MOUNTAINS, NEW MEXICO

HARVEY R. DUCHENE
7216 E. Bentley Circle, Englewood, Colorado 80112-1197 USA

Lechuguilla is a hypogenic cave dissolved in limestones and dolostones of the Capitan Reef Complex by sulfuric acid derived from oil and gas accumulations in the Delaware Basin of southeast New Mexico and west Texas. Most of the cave developed within the Seven Rivers and Capitan Formations, but a few high level passages penetrate the lower Yates Formation. The Queen and possibly Goat Seep formations are exposed only in the northernmost part of the cave below -215 m. Depositional and speleogenetic breccias are common in Lechuguilla. The cave also has many spectacular fossils that are indicators of depositional environments. Primary porosity in the Capitan and Seven Rivers Formations was a reservoir for water containing hydrogen sulfide, and a pathway for oxygenated meteoric water prior to and during sulfuric acid speleogenesis. Many passages at depths >250 m in Lechuguilla are in steeply dipping breccias that have a west-southwest orientation parallel to the strike of the shelf margin. The correlation between passage orientation and depositional strike suggests that stratigraphy controls these passages.

Lechuguilla is a hypogenic cave that has been dissolved out of limestones and dolostones of the Capitan Reef Complex Fig. 1) by sulfuric acid derived from oil and gas accumulations in the Delaware Basin of southeast New Mexico and west Texas (Hill 1987; Palmer & Palmer 2000). Since its discovery in 1986, explorers have mapped more than 170 km of passage containing spectacular speleothems and an extraordinary assortment of other features (DuChene 1997; Hill & Forti 1997; Davis 2000). Jagnow (1989) is the only researcher who has previously written about the bedrock geology. Bedrock outcrops in Lechuguilla are superb because they have not been subjected to the chemical and mechanical weathering processes that affected surface exposures. Therefore, they provide an opportunity to view details of the Capitan Reef not readily seen on the surface.

Since 1991, members of the Lechuguilla Cave Inventory Project have been documenting the geologic, mineralogical and speleogenetic features of Lechuguilla Cave (Jagnow *et al*. 2000). Data have been collected for 159 geologic and mineralogical categories at more than 3500 survey stations spread throughout the cave (DuChene 1996). One of the goals of the Inventory Project is to better understand how Lechuguilla fits into the stratigraphic framework of the Capitan Reef Complex. The purpose of this paper is to summarize data collected on the bedrock features exposed in Lechuguilla Cave.

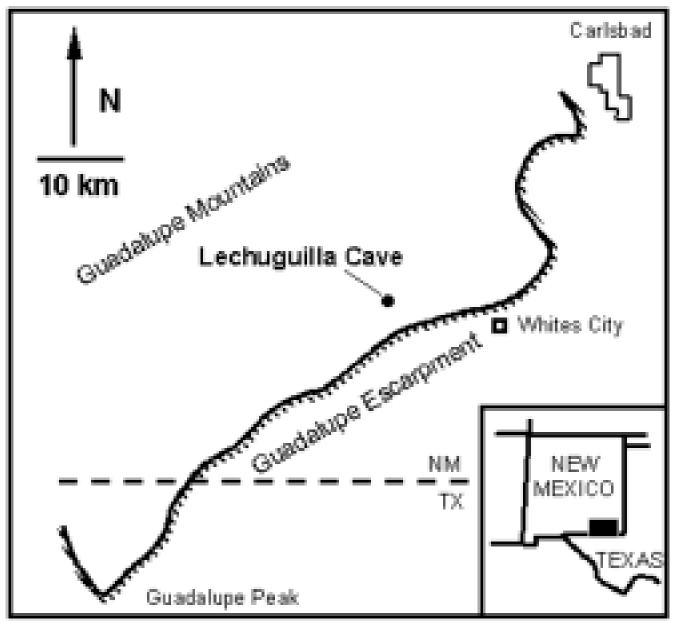

Figure 1. Location map of Lechuguilla Cave in the Guadalupe Mountains, New Mexico (from Palmer & Palmer 2000).

DEPOSITIONAL ENVIRONMENTS

Sediments of the Capitan Reef Complex deposited along a shelf and shelf margin on the periphery of the Delaware Basin in late Guadalupian (Permian) time. Within these broad divisions, Garber *et al*. (1989) recognized seven depositional environments (Fig. 2). The most landward environments are represented by coastal sabkha and playa facies (1) that grade down dip to tidal flat and shallow lagoon deposits (2). Sediments in these environments are interbedded carbonates and siliciclastics that become progressively more anhydritic up dip. The shelf grades down dip into the shelf margin comprised of a pisolite shoal (3), the immediate backreef (4), reef (5), forereef slope (6), and basin margin (7). The pisolite shoal was the highest part of the shelf profile and was located on the basinward side of the lagoon. The pisolite shoal grades into the immediate backreef comprised of bedded, highly fossiliferous packstones, grainstones and algal boundstones. Grains include fragments of mollusks, brachiopods, echinoids, and peloids.

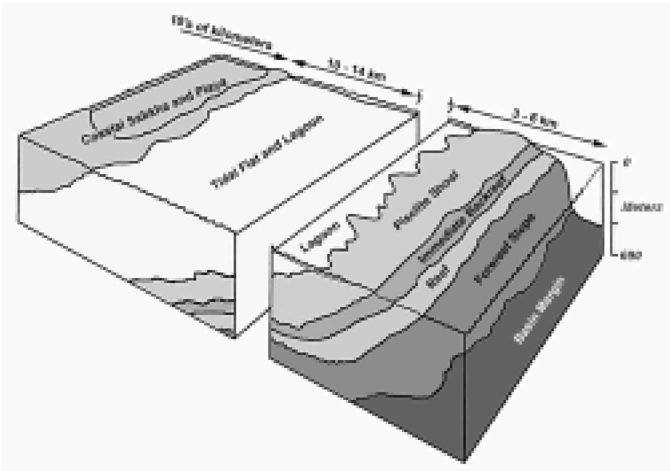

Figure 2. Schematic block diagram showing the seven depositional environments of the Capitan shelf margin: (1) coastal sabkha and playa; (2) tidal flat and lagoon; (3) pisolite shoal; (4) immediate backreef; (5) reef; (6) forereef slope; (7) basin margin. Lechuguilla Cave is developed in the immediate backreef, reef and slope. Modified from Garber *et al.* (1989).

Beds of the immediate backreef end abruptly against the massive reef.

The massive reef, 90-180 m thick, consists of sponge-algal boundstones, wackestones, packstones and grainstones. Reef-building organisms include ecologically zoned phylloid and dasycladacian algae, sponges, bryozoa, crinoids, and brachiopods. Basinward from the reef, bedded forereef slope deposits are 366-457 m thick with dips ranging from > 30° in the upper forereef to 5-10° in the lower forereef. Slope sediments include matrix-poor debris flows, grain-flows, and a minor amount of rock-fall debris (Melim & Scholle 1995). The lower slope grades into and intertongues with siliciclastic silt, sand, and carbonate debris at the basin margin.

STRATIGRAPHY

PREVIOUS WORK

Field geologists divide the rocks of the Guadalupe Mountains into formations with easily recognized characteristics that extend over wide geographic areas. (*e.g.*, King 1948; Newell *et al.* 1953). Stratigraphic studies show that backreef formations are equivalent to specific parts of the Capitan reef and to formations in the Delaware Basin, even though the lithologies change across the shelf margin (Newell *et al.* 1953; Tyrrell 1964, 1969). More recent work has focused on the specifics of deposition and diagenesis, using sequence stratigraphy to unravel the detailed geology of the Capitan Reef Complex (e.g., Fitchen *et al.* 1992; Melim & Scholle 1995; Tinker 1998; Kerans & Tinker 1999). These studies document a complex depositional history influenced by fluctuations in sea level. When sea level was high, carbonate deposition and reef building was at a maximum. When sea level was low, the upper part of the Capitan Reef Complex was emergent and subject to karst development and erosion. Wind blown siliciclastics deposition was also greater during times of low sea level (Tinker 1998).

The lithologies of the formations that crop out in Lechuguilla Cave are described briefly in this report. Formations are discussed in the order that they are encountered during a traverse of the cave from the entrance to any of the three lower level branches (Fig. 3).

BEDDED CARBONATES AND SILICICLASTICS

Carbonate and siliciclastic beds within the lower Yates, Seven Rivers and upper Queen Formations crop out throughout the upper part of Lechuguilla. Most of these outcrops are in the upper levels between the entrance and a depth of 244 m.

Yates Formation. Outside of the cave, the Yates Formation is very pale-orange to yellowish-gray, fine-grained, laminated, commonly pisolitic dolomite in beds 10-60 cm thick, alternating with grayish-orange to pale-yellowish orange, calcareous, quartz siltstone or very fine-grained sandstone, in beds 2.5-15 cm thick (Hayes & Koogle 1958). The Yates Formation conformably overlies the Seven Rivers Formation and is equivalent to the lower part of the upper Capitan Formation. Dolomite beds of the Tansill Formation conformably overlie the Yates (Fig. 3).

The Yates Formation is exposed at the entrance of Lechuguilla, in the PHD Room above the Chandelier Graveyard and in Tower Place (Figs. 3 & 4), as well as in other high level passages. The PHD Room is located at the top of a

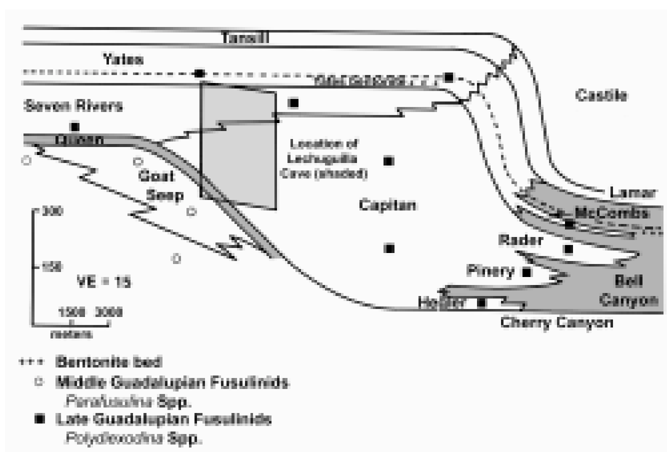

Figure 3. Schematic cross section showing location of Lechuguilla Cave within stratigraphic framework of the Guadalupe Mountains, New Mexico and Texas. Middle Guadalupian beds are characterized by *Parafusulina*; Upper Guadalupian beds by *Polydiexodina.* Note dashed correlation line within Yates, Capitan and Bell Canyon formations and position of Yates bentonite on shelf margin and in toe of slope. Shaded units are composed mostly of siliciclastics. Modified from Garber *et al.* (1989).

Figure 4. Map of Lechuguilla Cave showing localities discussed in text.

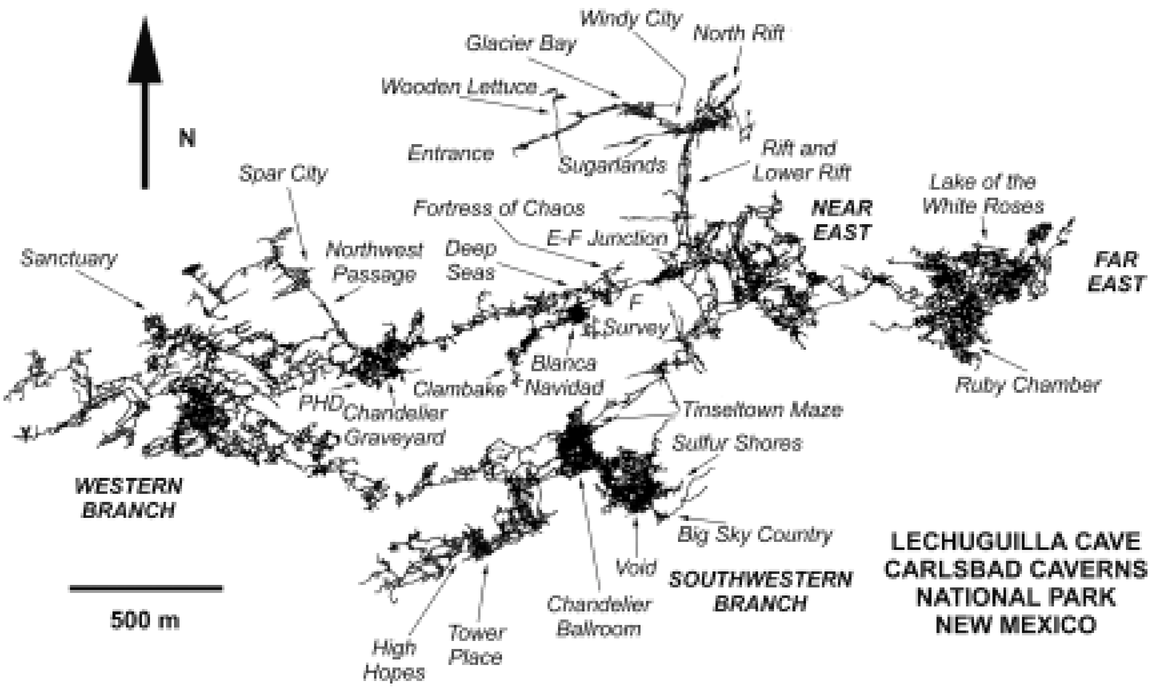

prominent, southeast-trending solution-enlarged joint that intersects a 3 m thick, pink, siltstone bed at the base of the Yates. The floor of the room is covered with siltstone breakdown blocks up to 6 m across. In Tower Place, a pinkish-orange siltstone bed ~1.5 m thick crops out on the southeast side of the room.

Seven Rivers Formation. In outcrop, the Seven Rivers Formation consists of yellowish-gray, fine-grained, commonly pisolitic dolomite in beds 30 cm to 1 m thick with rare beds of very pale-orange quartz siltstone (Hayes & Koogle 1958). These rocks grade into fossiliferous grainstones and rudstones toward the Capitan Reef. The Seven Rivers rests on the Queen Formation and is overlain by siltstone and carbonate beds of the Yates. The Seven Rivers is equivalent to the lower part of the Capitan Formation (Yurewicz 1977)(Fig. 3).

The Seven Rivers is the backreef formation that crops out throughout most of the upper part of Lechuguilla Cave. It is exposed at numerous sites between the entrance and Glacier Bay where beds stand out in relief due to differential solution. Parts of the Seven Rivers are highly fossiliferous, particularly near its contact with the massive reef. At EF Junction, which is probably less than 15 m above the massive Capitan Formation (Jagnow 1989), outcrops are composed of rudstone and consist mostly of sand-size fragments of shells and algal debris with scattered intact fossils.

Queen Formation. The Queen Formation is composed of very pale orange to yellowish-gray, fine-grained, laminated, dolomite in beds 10 cm to 1.2 m thick, interbedded with very pale-orange, silty dolomite, calcareous quartz siltstone, and very fine-grained sandstone in beds 10 cm to 1 m thick (Hayes & Koogle 1958). The Queen Formation lies conformably beneath the Seven Rivers Formation (Fig. 3). Jagnow (1989) believed that the Queen Formation is exposed in lower Windy City, Sugarlands, the North Rift, and Lower Rift. The contact between the Seven Rivers and Queen is best seen in the north part of the Rift where the Shattuck Member, a siltstone bed ~1.5 m thick, marks the contact between the Seven Rivers and Queen formations.

Capitan Formation. Field geologists in the Guadalupe Mountains traditionally divide the Capitan Formation into massive and breccia members (Hayes & Gale 1957; Hayes & Koogle 1958; Motts 1962; Hayes 1964). The massive part of the Capitan typically lacks bedding planes and is composed of light-gray, cream or white, calcitic, fossiliferous limestone with minor dolomitic limestone. The breccia member is composed mostly of fragments of reef limestone mixed with lenses and pods of siliciclastic material that were deposited in the forereef slope (Figs. 2 & 3). The contact between the massive and breccia members is gradational and indistinct at depths of 250-275 m.

Reef limestones of the massive Capitan crop out at depths of 175–275 m throughout Lechuguilla. Parts of the upper level of the Far East are developed in tan to gray, dense limestone with areas of moderate to intense fracturing (Fig. 4). In areas where the limestone is not covered with speleothemic crusts and coatings, sponge, crinoid, bryozoan, and brachiopod fossils can be seen. Locally, the reef rock contains fractures filled with calcite-cemented breccia as well as pods of fine-grained sandstone, some with ripple marks.

Breccias of the Capitan forereef slope crop out in passages and galleries below 250 m throughout the cave. Slope deposits are exposed throughout the Western Branch with particularly good examples in the Fortress of Chaos and Chandelier Graveyard. Dipping forereef beds are exposed about 30 m west of the Deep Seas Room.

Goat Seep Formation. The upper 150 m of the Goat Seep Formation is exposed on the western, faulted face of the Guadalupe Mountains (King 1948) and in North McKittrick Canyon, where it consists of light gray massive fine-crystalline to saccharoidal dolomite that is very porous in places (Hayes 1964). The formation consists of massive reef and forereef talus deposited along the shelf margin (Newell *et al.* 1953), and is mostly composed of dolomite (Hill 2000). The Goat Seep and Capitan were deposited along a prograding shelf margin that advanced as much as 6 km (King 1948). The Goat Seep shelf margin lies north of the Capitan margin in the Guadalupe Mountains, and the Goat Seep Formation is mostly adjacent to, rather than beneath, the Capitan (Fig. 3). Debris flows derived from the Goat Seep Formation intertongue with the Cherry Canyon Formation and may lie beneath part of the Capitan breccia member (Fitchen *et al.* 1992).

The Goat Seep Formation, if present at all in Lechuguilla, is likely restricted to the northernmost part of the cave. However, carbonate debris flows derived from the Goat Seep may underlie the Capitan in the area of Lechuguilla and could crop out elsewhere in the cave. No rocks similar to the Goat Seep Formation described by Hayes (1964) were observed during this study.

BEDROCK FEATURES OF LECHUGUILLA CAVE

BRECCIA DEPOSITS

Breccia is a coarse-grained rock composed of angular broken rock fragments held together by mineral cement or in a fine-grained matrix. In the Capitan Reef Complex, it resulted from both talus accumulation and solution collapse.

Breccias can be classified as crackle, mosaic and chaotic based on the amount individual clasts have been rotated and the distance they have been transported (Loucks 1999) (Table 1). Crackle breccia clasts are sharply angular, unrotated, and have not been transported from their place of origin. Mosaic breccia has poorly sorted, sharply angular clasts that are slightly rotated and have been transported no more than a few centimeters. Chaotic breccia has angular to subrounded, poorly sorted clasts of mixed lithology transported many meters.

In Lechuguilla Cave, breccias were formed by both depositional and speleogenetic processes. Depositional breccias were deposited during the growth of the Permian

Table 1. Classification of breccias in Lechuguilla Cave.

Type	Characteristics	Matrix	Occurrence	Depositional Environment	Example
			Depositional breccias		
Mosaic	Clasts sharply angular with no rounding of corners; very slight or no rotation of clasts; unsorted; well-cemented.	Calcite (predominant), silt (minor)	Fracture fill (fractures open and sub-vertical)	Tension fractures in massive reef and backreef limestone	Far East
			Collapsed beds (deposits sub-horizontal)	Bedding collapse and fragmentation due to dissolution of underlying beds	
Chaotic	Clasts angular to subrounded, poorly sorted, mixed lithologies		Large masses parallel to dip of forereef slope	Forereef slope	Fortress of Chaos
	Clasts angular to subrounded, poorly to moderately sorted, mixed lithologies including bedded pisolitic limestone and siltstone; moderately imbricate; well cemented.	Calcite (predominant), silt (minor)	Channel fill	Passes and channels through reef	Approach to Chandelier Graveyard
			Speleogenetic breccias		
	Characteristics	**Matrix**	**Occurrence**	**Depositional Environment**	**Example**
Crackle	Clasts sharply angular and unrotated; surfaces not chemically altered; lithology identical to surrounding bedrock	Calcite, gypsum, or may be uncemented	Ceilings and walls of passages and galleries	Ceilings and walls of passages and galleries	Passage walls and ceilings of Tinseltown Maze
Mosaic	Clasts sharply angular with no rounding of corners; very slight or no rotation of clasts; unsorted; uncemented to well-cemented	Gypsum	Wedging where gypsum is crystallizing in compression fractures	Compression fractures where dissolved gypsum is migrating downward through bedrock	Void
		Uncemented	Collapse of compression-fractured rock into passage	Open passages currently in the process of stabilization or collapse	Void
Chaotic	Clasts sharply angular; surfaces chemically unaltered except where facing original passage; unsorted; clasts show evidence of rotation due to falling from ceiling or wall; lithology identical to surrounding bedrock.	Uncemented	Passage and gallery floors. Clasts may be isolated or in large piles	Secondary fill ("breakdown") in passages and galleries.	Fortress of Chaos

Figure 5. Chaotic breccia near Blanca Navidad Hall, Lechuguilla Cave. Photo by Dan Legnini.

Figure 6. Fissure filled with breccia cemented with sparry calcite, Far East, Lechuguilla Cave. Photo by Kathy Sisson-DuChene.

(Guadalupian) Capitan Reef Complex and are part of the bedrock. Speleogenetic breccias, also known as breakdown, form during the air-filled, vadose stage of cave formation due to the following factors: (1) removal of buoyant support when the water level lowers below a passage horizon; (2) base level back flooding; (3) undercutting by free-surface streams; (4) crystal wedging processes, and (5) earthquake activity (Ford & Williams 1989). In Lechuguilla, (1) and (4) were the foremost factors. Davies (1949) was the first to classify breakdown in caves, and more recently, Loucks (1999) presented a classification for recognizing speleogenetic breakdown in paleokarst.

Chaotic breccia is the most common type of depositional breccia in Lechuguilla Cave. It crops out in passages below 250 m in the Capitan forereef slope where it consists of poorly sorted clasts up to a meter or more in diameter cemented together by gray or brown, coarsely crystalline calcite. Typical examples crop out in the Fortress of Chaos, Chandelier Graveyard and the approach to Blanca Navidad Hall (Fig. 5). Chaotic breccia with smaller clasts fills many fractures in massive reef limestone. Most fracture filling breccia is cemented by gray calcite (Fig. 6), but some has a matrix of reddish-brown fine-grained sandstone.

Depositional mosaic breccia is rare in Lechuguilla, occurring in backreef beds where non-speleogenetic dissolution of evaporites in Guadalupian time caused overlying beds to collapse. It also occurs in massive reef limestone where rocks are broken when they fall into fractures and depositional voids. In Spar City and the northern end of Wooden Lettuce Passage, “ghost breccia” is formed where clasts of chaotic breccia have been completely dissolved, leaving only the coarsely crystalline calcite matrix.

The most common type of speleogenetic breccia in Lechuguilla is breakdown, found throughout the cave. Breakdown fragments range from a few millimeters to several meters in diameter and litter the floors of most large passages and galleries. Most breakdown accumulations are uncemented, but in some areas, calcite flowstone binds the clasts together. Speleogenetic crackle breccia is common in the Chandelier Ballroom and the Void where the massive reef limestone is shattered, but where many fragments remain in place. A good example of speleogenetic mosaic breccia crops out at the east end of the Tinseltown Maze where the bedrock is shattered and clasts have been rotated by gypsum crystal wedging.

FRACTURES AND FRACTURE FILL

Many vertical fractures in Lechuguilla are filled with siliciclastic sediment ranging from coarse silt to very fine-grained sand. Hayes (1964) described fractures of this type as “Type 1 sandstone dikes” that formed when tension cracks caused by settling of the reef were filled with sand.

Type 1 sandstone dikes exposed in Lechuguilla Cave occur at depths ranging from 125-345 m, but they are concentrated between 200 and 250 m in the lower part of the Seven Rivers Formation (Fig. 7). Most of the sandstone in the dikes is stained pink or pinkish-orange, but in some fractures it is colorless to white. Regardless of color, the sandstone is friable and disaggregates at the slightest touch. It is common for sand to fall from fractures and accumulate in piles along walls or on passage floors.

Type 1 sandstone dikes are common in the F Survey and in Big Sky Country above the Void. One dike in Big Sky Country is 2 m-wide and filled with sandstone that ranges from colorless to beige and displays liesegang banding (nested bands caused by rhythmic precipitation within a fluid-saturated rock). A sample of the siliciclastic material from this fracture

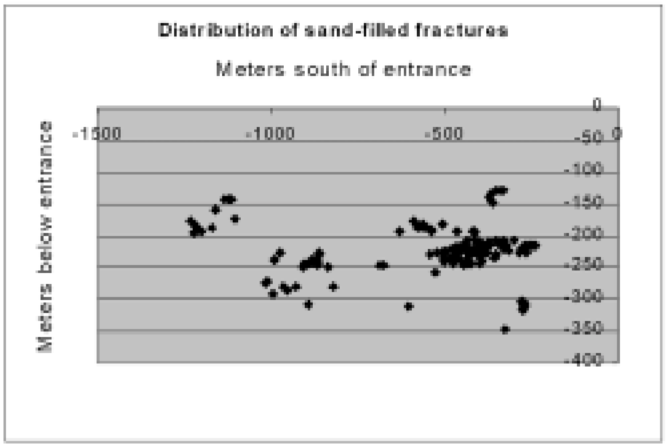

Figure 7. Distribution of sand-filled fractures in Lechuguilla Cave. Y-axis is depth below entrance; X-axis is distance south (or north) of entrance.

is composed of uncemented, colorless to white, subangular to subrounded, non-calcareous, coarse silt to very fine-grained sand (W. B. Hanson, pers. comm. 1989).

Fractures filled with breccia are also common in the massive Capitan reef limestone in Lechuguilla. Most of this fracture-filling breccia is cemented with sparry calcite (Fig. 6), but there are a few places where breccia clasts are mixed with sand.

Paleontology

The Capitan reef was built by marine organisms that had skeletons composed of minerals, predominantly calcium carbonate. Principal frame-building organisms include calcareous sponges, encrusting calcareous algae, and bryozoans (Newell *et al.* 1953; Cronoble 1974; Wood 1999). Fossils of many of these organisms are common in the bedrock of Lechuguilla Cave. They lived where environmental conditions were best suited to their needs for food, clean water, and oxygen. Consequently, when these organisms are found in place, they are excellent indicators of the environment at the time they were alive.

Most fossils in Lechuguilla have been broken into sand-size fragments that accumulated in voids in the Capitan Reef and in the backreef lagoon. However, many intact fossils are exposed where the bedrock is not covered by mineral coatings and crusts. Common fossils include brachiopods, bryozoans, crinoid columnals, echinoid spines, gastropods, pelecypods, scaphopods, cephalopods and porifera. table 2 summarizes the habitats of the more common fossil groups observed in Lechuguilla Cave. For discussions of the paleontology and paleoecology of the Capitan Reef Complex, see Newell *et al.* (1953), Cronoble (1974), Babcock (1977), Wood *et al.* (1994) and Wood (1999).

Table 2. Distribution of biota in the Capitan Reef Complex (after Newell *et al.* 1953).

Category	Most common habitat
Algae	reef
Brachiopoda	immediate backreef, reef and proximal slope
Bryozoa	reef and proximal slope
Porifera	reef
Fusulinidae	reef
Cephalopoda	all
Gastropoda	backreef
Pelecypoda	backreef, reef and proximal slope

Algae

Calcareous algae are sediment-binding and encrusting organisms that were important to the stabilization of sediment within the massive reef facies of the Capitan Formation. The upper Capitan Formation contains an abundant and diverse calcareous algal flora, including skeletal phylloid algae. In contrast, the lower Capitan, which is equivalent (at least in part) to the Seven Rivers Formation (Fig. 3), contains only a hemispherical form of alga (Babcock's form C) and a problematic alga *Archeolithoporella* in any abundance (Babcock 1977). *Archeolithoporella* is an encrusting skeletal alga(?) that played an important role in binding and stabilizing sediment within the reef (Newell *et al.* 1953; Achauer 1969; Cronoble 1974; Babcock 1977; Wood 1999).

Brachiopoda

Brachiopods are solitary marine invertebrates that may be attached or unattached to the substrate. They are characterized by two bilaterally symmetrical calcareous or chitinophosphatic valves. In the Capitan, brachiopods are most common in the immediate backreef, reef and proximal slope, but they are found in most marine environments. Most of the brachiopods in the reef are cemented to the substrate, but pedunculate types are also represented, particularly along the seaward margin (Newell *et al.* 1953).

Many brachiopod shells in Lechuguilla are composed of crystalline calcite that is less soluble than the surrounding bedrock, and dissolution has caused the fossils to stand out in relief on passage walls and ceilings. In some cases, the shells are broken, revealing the internal spiral structures of the brachiopod. Particularly fine specimens up to 5 cm across and similar to *Neospirifer* sp. are exposed in Spar City where they are associated with crinoid columns, sponges, bryozoans, and a straight-coned nautiloid. An excellent example of a rare, complete *Leptodus* sp. is exposed in the Sanctuary (B. Luke, pers. comm. 1997; Fig. 8). Because of their fragility, and because the ventral valve of *Leptodus* was securely attached to the reef substrate, the shells tend to break up after the animal dies, and the ventral valve is more likely to be preserved (Newell *et al.* 1953: 66 & 194). Other brachiopod fossils, some with internal structures exposed, are present in the Clambake Room (L. Doran, pers. comm. 1999).

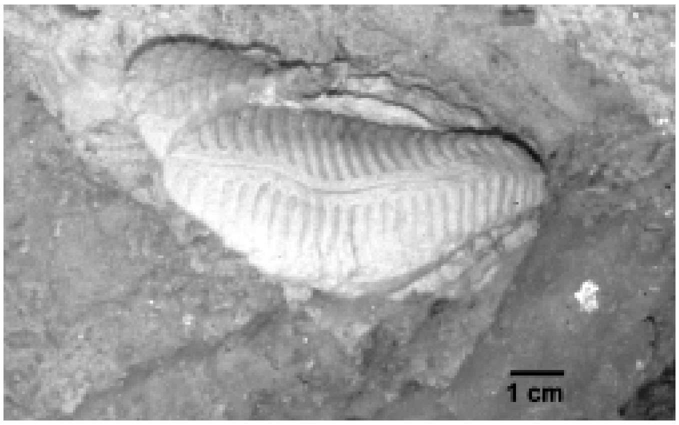

Figure 8. *Leptodus* sp. in Sanctuary, Lechuguilla Cave. Photo by John Lyles.

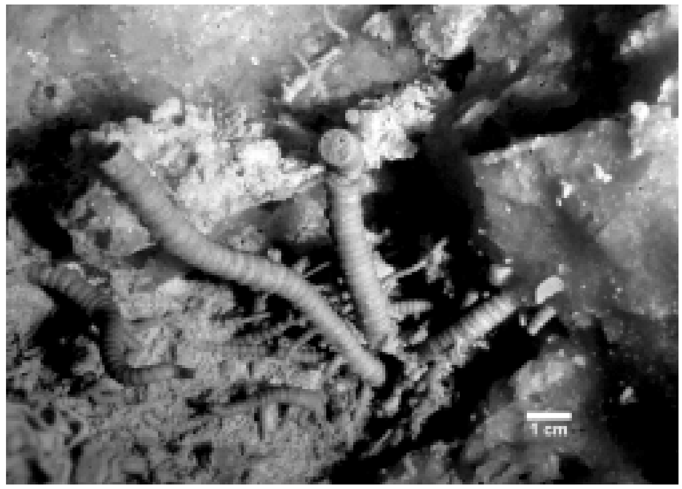

Figure 9. Crinoid column segments, Clambake Room, Lechuguilla Cave. Photo by Dave Bunnell.

BRYOZOA

Bryozoans are attached colonial invertebrates with calcareous skeletons. They occur in branching forms that superficially resemble modern branching corals, and as fenestrate varieties that have small window-like openings between branches arranged in a reticulate pattern. Fragments of fenestrate bryozoans are common in the massive Capitan as well as in debris flows within the forereef slope. Good examples of bryozoans are present in the Void and numerous other sites in Lechuguilla Cave. For a discussion of the role of fan shaped and branching bryozoa as frame builders of the Capitan Reef, see Wood *et al.* (1994, 1999)

ECHINODERMATA

Echinoderms are solitary, bottom-dwelling marine organisms characterized by an endoskeleton formed of plates or ossicles composed of crystalline calcite and having bilateral-radial symmetry. Crinoidea (crinoids) and Echinoidea (echinoids), subphyla of Echinodermata, are common in the Capitan Reef Complex.

Crinoids are attached or unattached echinoderms characterized by five-fold symmetry, a body that is enclosed by calcareous plates, and a stem (or column) composed of individual, button-like segments. The most common crinoid fossils in Lechuguilla are individual columnals and 1-3 cm long segments of the column. However, longer branched segments are present in Spar City and in the Clambake Room (Linda Doran, pers. comm. 1999).

Echinoids, or sea urchins, are characterized by subspherical shape, interlocking calcareous plates, and movable appendages or spines. Because they are composed of plates, echinoid skeletons break apart after the death of the animal so that complete fossils are rare. Echinoid spines are bulbous with a convex indentation at the attached (proximal) end, tapering to a blunt or pointed tip. Excellent echinoid spines 4-5 cm long have been found in the Clambake Room (Fig. 10). Echinoid spines are commonly associated with gastropods, suggesting that they occupied the same ecological niche (Newell *et al.* 1953).

FUSULINIDAE

Fusulinids are foraminifers belonging to the suborder Fusulinina, family Fusulinidae, and are characterized by a multichambered elongate calcareous microgranular test typically having the shape of a grain of wheat. They are common in reef and slope sediments and are used by paleontologists to date and correlate Paleozoic strata.

Fusulinids are widely distributed in the bedrock of Lechuguilla Cave, but most have been recrystallized so that they are useless for age correlation. One usable sample was collected at a depth of 331 m on the route from the Ruby Chamber to Lake of the White Roses. The bedrock in this area dips of 20°-25° and is comprised of highly fossiliferous and brecciated limestone. These fusulinids are all an advanced species of *Parafusulina*, having all of the characteristics of *Polydiexodina* except the multiple tunnels. They have been transported and abraded, which is consistent with their position within forereef slope deposits. The *Parafusulina* fossils are probably of lower Capitan age indicating that these slope deposits are equivalent to the Queen or Seven Rivers formations.

GASTROPODA

Gastropods (snails) are mollusks in which most species have an asymmetric, helically coiled shell with the apex pointed away from the aperture (Fig. 11). Bellerophontid gastropods, however, have a planispirally coiled shell. Gastropods are most common in sediments of the immediate backreef but are found throughout the shelf margin.

Some of the most spectacular fossils in Lechuguilla are large bellerophontid gastropods found at numerous sites in the Seven Rivers Formation. The most “famous” of these is “The Flying Potato,” in the F Survey near the E-F Junction (Fig. 12). This specimen has a width of 190 mm and a height of 115 mm. It is one of many bellerophontid gastropods in the lower part of the Seven Rivers Formation exposed in the walls and ceiling

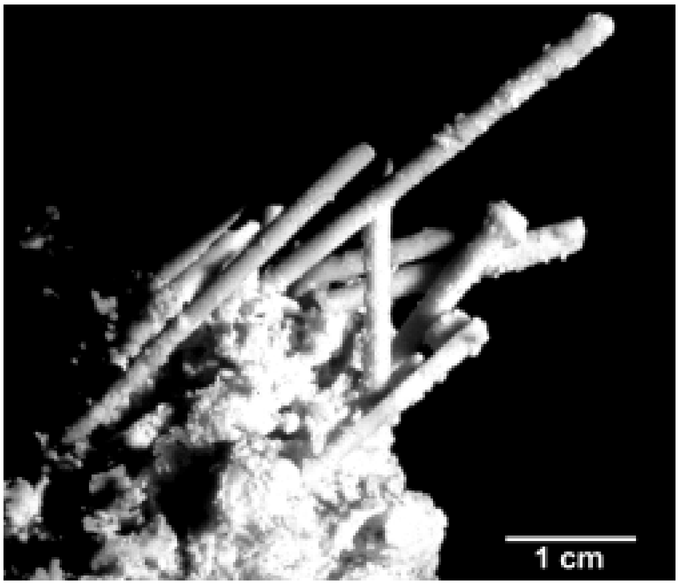

Figure 10. Echinoid spines, Clambake Room, Lechuguilla Cave. Photo by Dave Bunnell.

Figure 11. Helically coiled gastropods near station F5, F survey, Lechuguilla Cave. Photo by David Jagnow.

of the F Survey. At the time of its discovery, the "Flying Potato" was the largest known bellerophontid gastropod in the world (Kues & DuChene 1990).

Pelecypoda

Pelecypods (clams) are mollusks with symmetrical mirror-image valves. They are found in the backreef, reef and forereef slope of the Capitan Reef Complex but are most common in the proximal lagoon and nearby reef. Newell *et al.* (1953) identified 24 varieties of pelecypod from the Capitan Formation.

Pelecypods have been reported from numerous stations in the Void in Lechuguilla Cave.

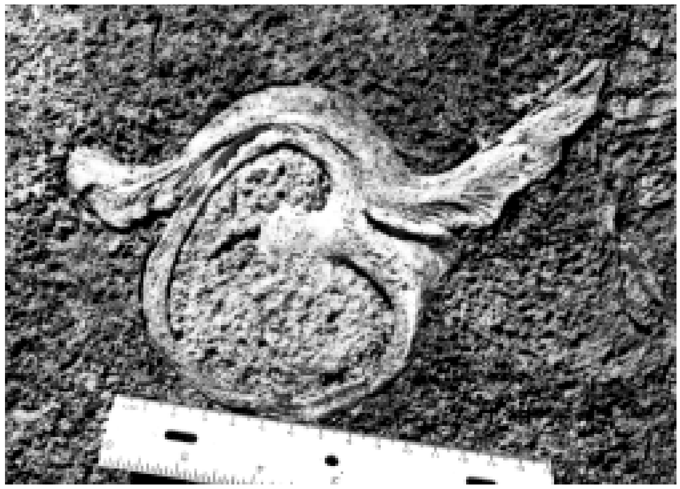

Figure 12. Bellerophontid gastropod at station F5, F survey, Lechuguilla Cave. Photo by David Jagnow.

Cephalopoda

Cephalopod shells are the straight, curved or coiled skeletons of marine mollusks that are divided into chambers connected by a siphuncle. Modern cephalopods include octopi, squid, cuttlefish and *Nautilus*.

Most of the cephalopod fossils found in Lechuguilla are coiled ammonoids ranging up to 15 cm across. Typical examples are found in the Rift, in High Hopes, and in a fissure in Clambake Room (Fig. 13). One example of a straight-coned nautiloid has been found in Spar City (Fig. 14). This specimen is 16 cm long with an aperture ~1.5 cm across. It is associated with branching crinoid columnals, sponges and large neospiriferid brachiopods, all of which are coated black.

Porifera

Sponges belong to the phylum Porifera, which consist of many-celled aquatic invertebrates characterized by an internal skeleton of silica or calcium carbonate. Sponges are most commonly found in growth position in the massive reef, but they are also found in transported blocks within the forereef slope and in patch reefs in the backreef lagoon.

Common varieties seen the Capitan Formation in Lechuguilla are *Lemonia*, *Amblysiphonella*, *Cystaulites*, *Guadalupia*, and *Girtycoela.* They are illustrated in Newell *et al.* (1953) and Bebout and Kerans (1993).

Discussion

In the limestones of the Guadalupe Mountains, the mixing of connate water rich in hydrogen sulfide with oxygenated meteoric water is essential for sulfuric acid speleogenesis (Davis 1980; Hill 1987; Palmer & Palmer 2000). Aside from geochemical processes, major factors that controlled the location, development and morphology of cave passages were the location of porous and permeable rock along the Capitan shelf margin, structure and stratigraphy, and the depth of the water

Figure 13. Ammonoid, Clambake Room, Lechuguilla Cave. Photo by Dave Bunnell.

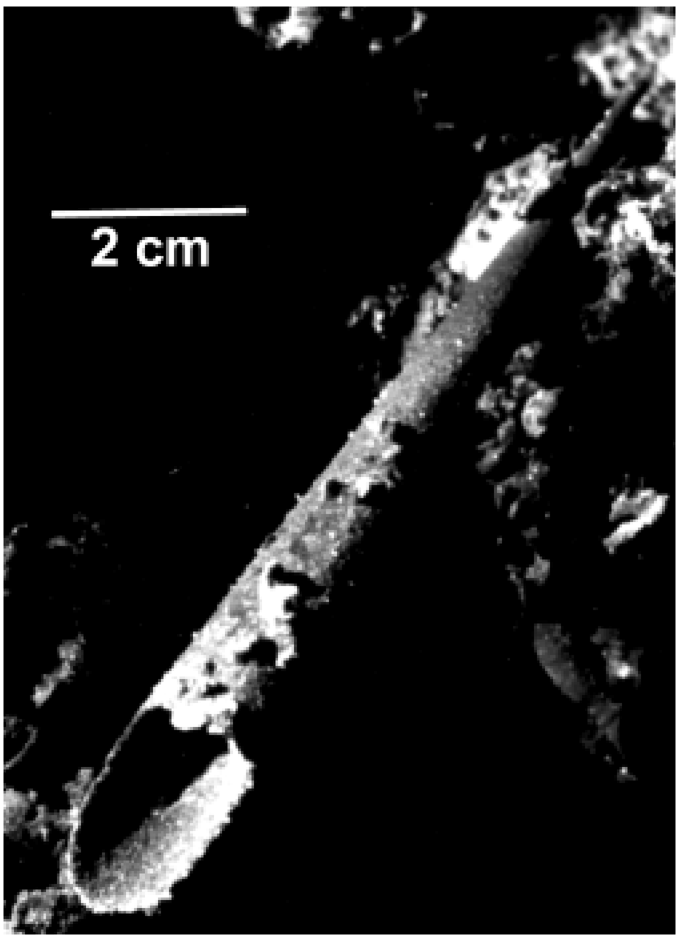

Figure 14. Straight-coned nautiloid, Spar City, Lechuguilla Cave. Photo by Tim Stone.

table during speleogenesis.

STRATIGRAPHY AND RESERVOIR CHARACTERSTICS

Most of Lechuguilla Cave developed in the immediate backreef facies of the lower part of the Seven Rivers Formation, and in the massive reef and forereef slope environments of the Capitan Formation. Immediate backreef sediments are porous rudstones and packstones that become progressively more abundant toward the reef. These rocks have high interstitial porosity where pores have not been filled with calcite or anhydrite cement. Porosity tends to increase toward the shelf margin where water circulation winnowed finer grained material from the sediment.

The massive Capitan is composed of carbonate precipitated by reef flora and fauna and held together by encrusting organisms such as *Archeolithoporella*. Irregular voids, fractures, and cavities are common, resulting from random growth and collapse of reef structures in a dynamic environment. Massive reef limestones have excellent porosity and permeability where not filled with post-depositional cements.

Much of the sediment that was deposited in the forereef slope of the Capitan was produced in the massive reef. Slope detritus is coarsest near the top of the slope, and becomes progressively finer toward the toe of the slope. Large fragments of reef material have the same porosity and permeability as the massive reef. Finer grained material near the top of the slope can also have excellent porosity.

Together, the immediate backreef, massive reef and forereef slope deposits of the Seven Rivers and Capitan Formations form an elongate, tabular lithosome as much as 6 km wide, hundreds of kilometers long, and 600 m thick. This body of rock is the most seaward part of the Capitan shelf margin and is where primary porosity and permeability are best developed. It comprises a significant part of the Capitan aquifer of Hiss (1980) and contains Lechuguilla and most of the other caves in the Guadalupe Mountains. To the east in the Delaware Basin, the Capitan aquifer is both a reservoir for groundwater and a path for hydrodynamic flow. In the past, prior to the erosion events that exhumed and dissected the Guadalupe Mountains, it is likely that the Capitan-Seven Rivers lithosome was continuous to the western escarpment of the uplift (DuChene & Martinez 2000).

Primary matrix porosity in the Capitan-Seven Rivers lithosome is important to speleogenesis because it provided the reservoir in which water with dissolved hydrogen sulfide was stored; i.e., if the lithosome did not have well-developed primary porosity, sulfuric acid speleogenesis could not have taken place. The permeability of the lithosome allowed oxygenated meteoric water to move freely through the reservoir to sites where caves were being formed. Reservoirs with intergranular or intercrystalline porosity have more surface area than those with fracture porosity. This means that there is more surface area where sulfuric acid can react with bedrock, implying that dissolution could occur at a faster rate and in a larger volume of bedrock. Passages and galleries developed where the reservoir has intergranular porosity should have wider cross sections than passage developed along fractures. Examples of galleries formed in porous bedrock are the large, mostly tubular, northeast-trending passages in the Western and Southwestern branches of Lechuguilla Cave. Passages developed along fractures include the Rift and the Northwest Passage.

STRUCTURAL AND STRATIGRAPHIC CONTROL OF CAVE PASSAGES

The map of Lechuguilla Cave (Fig. 4) shows two major passage orientations with a primary west-southwest trend parallel to the shelf margin and a secondary trend more or less perpendicular to it. These trends can be correlated with joint patterns mapped by King (1948: Plate 21) for the Guadalupe Mountains. Many north- and northwest-trending passages such as the Rift and the Northwest Passage, and some northeast-trending passages such as the route to Sulfur Shores, are clearly controlled by joints. These passages are narrow compared to their height, have >150 m of vertical relief, and die out with depth. They extend across formation boundaries and connect upper and lower levels of the cave.

In contrast, many northeast-trending passages and galleries are developed at depths of 250–300 m in south-dipping breccias and debris flows of the Capitan forereef slope. These passages parallel depositional strike of the slope and do not cross formation boundaries. Passages are roughly tubular in cross section with floors covered by breakdown blocks composed of depositional breccia. Some galleries, such as the Deep Seas Room, have elliptical cross sections with the long axis sloping to the south. These factors strongly suggest that bedding within the forereef slope controls the shape and orientation of many passages in the lower level of Lechuguilla.

Stratigraphy was not the only control on passage formation. The position of the water table and the porosity of the bedrock were other critical factors that determined where speleogenesis took place. Major levels occur at depths of 150-220 m and 250-300 m, indicating that there were at least two speleogenetic episodes. During the first, the water table was probably located at a depth near 150 m, above the contact between the Seven Rivers and Capitan formations. Bedding, joints, fractures and sandstone dikes in the lower Seven Rivers and Upper Capitan controlled passage morphology and orientation at that level. During the second episode, the water table was probably at a depth of 210 m near the transition between the massive and forereef slope members of the Capitan. Speleogenesis took place along the upper part of the water table in south-dipping beds of the slope (Palmer & Palmer 2000).

CONCLUSIONS

Based on paleontologic and stratigraphic data from outcrops in Lechuguilla, most of the cave is developed in the immediate backreef facies of the Seven Rivers Formation and the reef and forereef slope facies of the Capitan Formation. This porous lithosome parallels the Capitan shelf margin and extends from the western escarpment of the Guadalupes northeast to the border between New Mexico and Texas. The Capitan-Seven Rivers lithosome was the original reservoir where water containing hydrogen sulfide was stored prior to and during sulfuric acid speleogenesis, and it was the avenue for eastward migration of oxygenated meteoric water. Because mixing of hydrogen-sulfide water with oxygenated water occurred within the lithosome, it was the site of the major speleogenetic events that formed Lechuguilla Cave.

The strike, dip, porosity, and stratigraphic character of beds in the Capitan forereef slope control the orientation and morphology of many passages below -250 m in Lechuguilla. These passages trend northeast, parallel to the shelf margin, and were formed when the water table was near the transitional contact between massive reef limestones and beds of the forereef slope.

ACKNOWLEDGMENTS

This report would not be possible without the cooperation of the National Park Service at Carlsbad Cavern. Special thanks go to Ronal Kerbo, Dale Pate, Jason Richards and Stan Allison for expediting the many inventory expeditions required for basic data collection. The process of gathering information would have been impossible without the enthusiastic cooperation of dozens of cavers who volunteered their time in support of the project. Comments and suggestions by Carol Hill, Ira Sasowsky, Donald Davis, and an anonymous reviewer resulted in significant improvement of this paper. This work was supported by grants from the National Park Service.

REFERENCES

Achauer, C.W. (1969). Origin of Capitan Formation, Guadalupe Mountains, New Mexico and Texas. *American Association of Petroleum Geologists Bulletin 53 (11)*: 2314-2323.

Babcock, J.A. (1977). Calcareous algae, organic boundstones, and the genesis of the upper Capitan Limestone (Permian, Guadalupian), Guadalupe Mountains, west Texas and New Mexico. In Hileman, M.E., & Mazzullo, S.J. (eds.), *Upper Guadalupian facies Permian Reef Complex Guadalupe Mountains New Mexico and West Texas*. Society of Economic Paleontologists and Mineralogists, Permian Basin Section Publication 77-16: 3-44.

Bebout, D.G. & Kerans, C. (1993). *Guide to the Permian Reef Geology Trail, McKittrick Canyon, Guadalupe Mountains National Park, west Texas.* Bureau of Economic Geology, University of Texas, Austin: 48 pp.

Cronoble, J.M. (1974). Biotic constituents and origin of facies in Capitan reef, New Mexico and Texas. *The Mountain Geologist 11(3)*: 95-108.

Davis, D.G. (1980). Cave development in the Guadalupe Mountains: A critical review of recent hypotheses. *NSS Bulletin 42(3)*: 42-48.

Davis, D.G. (2000). Extraordinary features of Lechuguilla Cave, Guadalupe Mountains, New Mexico. *Journal of Cave and Karst Studies 62*(2): 147-157.

Davies, W.E. (1949). Features of cave breakdown. *Bulletin of the National Speleological Society 11*: 34-35.

DuChene, H.R. (1996). Interim Report, April 1–September 30, 1996. Lechuguilla Cave Geological and Mineralogical Inventory Project. Unpublished Report to Carlsbad Caverns National Park: 22 pp.

DuChene, H.R. (1997). Lechuguilla Cave, New Mexico, U.S.A. In Hill, C. A. & Forti, P., *Cave minerals of the world, 2nd Ed.* Huntsville, AL. National Speleological Society: 343-350.

DuChene, H.R. & Martinez, R. (2000). Post-speleogenetic erosion and its effect on cave development in the Guadalupe Mountains, New Mexico and west Texas. *Journal of Cave and Karst Studies 62(*2): 75-79.

Fitchen, W.M., Gardner, M.H., Kerans, C., Little, L., Sonnenfeld, M.D., Tinker, S.W. & Wardlaw, B.W. (1992). Evolution of platform and basin architecture in mixed carbonate-siliciclastic sequences: Latest Leonardian through Guadalupian, Delaware Basin (abs.). *American Association of Petroleum Geologists 1992 Annual Convention Official Program*: 41.

Ford, D.C. & Williams, P. (1989). *Karst geomorphology and hydrology*. Unwin Hyman, London: 601 pp.

Garber, R.A., Grover, G.A., & Harris, P.M. (1989). Geology of the Capitan shelf margin-subsurface data from the northern Delaware Basin. In Harris, P.M. & Grover, G.A. (eds.), *Subsurface and outcrop examination of the Capitan shelf margin, northern Delaware Basin.* Society of Economic Paleontologists and Mineralogists Core Workshop No. 13: 3-269.

Hayes, P.T. (1964). Geology of the Guadalupe Mountains: *U. S. Geological Survey, Professional Paper 446*: 69 pp.

Hayes, P.T. & Gale, B.T. (1957). Geology of the Carlsbad Caverns East Quadrangle, New Mexico. *U. S. Geological Survey Geological Quadrangle Map GQ-98.* Scale 1:62,500.

Hayes, P.T., & Koogle, R.L. (1958). Geology of the Carlsbad Caverns West Quadrangle, New Mexico-Texas. *U. S. Geological Survey Geological Quadrangle Map GQ-112.* Scale 1:62,500.

Hill, C.A. (1987). Geology of Carlsbad Cavern and other caves in the Guadalupe Mountains, New Mexico and Texas. *New Mexico Bureau of Mines and Mineral Resources Bulletin 117,* 150 p.

Hill, C.A. (2000). Overview of geologic history of cave development in the Guadalupe Mountains, New Mexico and west Texas. *Journal of Cave and Karst Studies 62(*2): 60-71.

Hill, C.A., & Forti, P. (1997). *Cave minerals of the world, 2nd Ed.* Huntsville, AL. National Speleological Society: 463 pp.

Hiss, W.L. (1980). Movement of ground water in Permian Guadalupian aquifer systems, southeastern New Mexico and West Texas. *New Mexico Geological Society Guidebook, 31st Field Conference, Trans-Pecos Region:* 289-294.

Jagnow, D.H. (1989). The geology of Lechuguilla Cave, New Mexico. In Harris, P.M. & Grover , G.A. (eds.), *Subsurface and outcrop examination of the Capitan shelf margin, northern Delaware Basin*. Society of Economic Paleontologists and Mineralogists Core Workshop No. 13: 459-466.

Jagnow, D.H., Hill, C.A., Davis, D.G., DuChene, H.R., Cunningham, K.I., Northup, D.E. & Queen, J.M. (2000). History of sulfuric acid theory of speleogenesis in the Guadalupe Mountains, New Mexico and west Texas. *Journal of Cave and Karst Studies 62*(2): 54-59.

Kerans, C. & Tinker, S.W. (1999). Extrinsic stratigraphic controls on development of the Capitan Reef Complex. In Saller, A.H., Harris, P.M., Kirkland, B.L. & Mazzulo, S.J. (eds.), *Geologic framework of the Capitan Reef.* Society of Economic Paleontologists and Mineralogists Special Publication No. 65: 15-36.

King, P.B. (1948). Geology of the southern Guadalupe Mountains, Texas: *U.S. Geological Survey Professional Paper 215*: 183 pp.

Kues, B.S. & DuChene, H.R. (1990). The largest Paleozoic bellerophontid gastropod. *Journal of Paleontology 64(3)*: 478-479.

Loucks, R.G. (1999). Paleocave carbonate reservoirs: Origins, burial-depth modifications, spatial complexity, and reservoir implications. *American Association of Petroleum Geologists Bulletin 83(11)*: 1795-1834.

Melim, L.A., & Scholle, P.A. (1995). The forereef facies of the Permian Capitan Formation: The role of sediment supply versus sea-level changes. *Journal of Sedimentary Research B65(1)*: 107-118.

Motts, W.S. (1962). Geology of the West Carlsbad Quadrangle, New Mexico. *U.S. Geological Survey Geological Quadrangle Map GQ-167*. Scale 1:62,500.

Newell, N.D., Rigby, J.K., Fischer, A.G., Whiteman, A.J., Hickox, J.E. & Bradley, J.S. (1953). *The Permian Reef Complex of the Guadalupe Mountains region, Texas and New Mexico.* San Francisco, W. H. Freeman: 236 pp.

Palmer, A.N & Palmer, M.V. (2000). Hydrochemical interpretation of cave patterns in the Guadalupe Mountains, New Mexico. *Journal of Cave and Karst Studies 62(*2): 91-108.

Tinker, S.W. (1998). Shelf-to-basin facies distributions and sequence stratigraphy of a steep-rimmed carbonate margin: Capitan depositional system, McKittrick Canyon, New Mexico and Texas. *Journal of Sedimentary Research 68(6)*: 1146-1174.

Tyrell, W.W., Jr. (1964). Petrology and stratigraphy of near-reef Tansill-Lamar strata, Guadalupe Mountains, Texas and New Mexico. In Moore, G.E. & Wilde, G.L., (eds.), *Geology of the Capitan Reef Complex of the Guadalupe Mountains.* Roswell Geological Society Guidebook: 66-82.

Tyrrell, W.W., Jr. (1969). Criteria useful in interpreting environments of unlike but time-equivalent carbonate units (Tansill-Capitan-Lamar), Capitan Reef Complex, West Texas and New Mexico. In Friedman, G. M., (ed.), *Depositional environments in carbonate rocks.* Society of Economic Paleontologists and Mineralogists Special Publication 14: 80-97.

Wood, R. (1999). Paleoecology of the Capitan Reef. In Saller, A.H., Harris, P.M., Kirkland, B.L. & Mazzulo, S.J. (eds.), *Geologic framework of the Capitan Reef.* Society of Economic Paleontologists and Mineralogists Special Publication No. 65:129-137.

Wood, R., Dickson, J.A.D, & Kirkland-George, B. (1994). Turning the Capitan Reef upside down: A new appraisal of the ecology of the Permian Capitan reef, Guadalupe Mountains, Texas and New Mexico. *Palaios 9:* 422-427.

Yurewicz, D.A. (1977). The origin of the massive facies of the Lower and Middle Capitan Limestone (Permian), Guadalupe Mountains, New Mexico and west Texas: In Hileman, M. E., & Mazzullo, S. J. (eds.). *Upper Guadalupian facies Permian Reef Complex Guadalupe Mountains New Mexico and west Texas.* Society of Economic Paleontologists and Mineralogists, Permian Basin Section Publication 77-16: 45-92.

CLAYS IN CAVES OF THE GUADALUPE MOUNTAINS, NEW MEXICO

VICTOR J. POLYAK
Department of Earth and Planetary Sciences, University of New Mexico, Northrop Hall, 200 Yale Blvd, Albuquerque, New Mexico 87131 USA
NECIP GÜVEN
Department of Geosciences, Texas Tech University, P.O. Box 41053, Lubbock, Texas 79409-1053 USA

The origins of clay minerals in the caves of the Guadalupe Mountains, New Mexico are categorized as (1) detrital, (2) inherited from the weathering of dolostone and siltstone, and (3) authigenic. Clay minerals found in these caves include hydrated halloysite, kaolinite, dickite, illite, montmorillonite, illite-smectite mixed-layers, palygorskite, and trioctahedral smectite. The detrital clay minerals are montmorillonite, illite, dickite and kaolinite. The clay minerals inherited from the bedrock by condensation-induced weathering (in wall residues) are illite and dickite. Cave-authigenic clay minerals include hydrated halloysite (endellilte), trioctahedral smectite, montmorillonite, and probably palygorskite. Hydrated halloysite formed by the alteration of illite, montmorillonite, illite-smectite mixed-layers, kaolinite, or dickite during sulfuric acid-related speleogenesis. Trioctahedral smectite precipitated with Mg-carbonate minerals in dolomite crusts and huntite moonmilk. Montmorillonite formed in saturated ledge deposits of redistributed wall residues. Less clear is the origin of palygorskite in laminated silt and clay deposits in Carlsbad Cavern.

Clays in caves are most often related to surface stream-transported sediments and soils. Clays can also be inherited from the weathering of bedrock cave walls. Clay minerals may also form in caves, although there have been relatively few reports of clay authigenesis as indicated by Hill & Forti (1997). The study of cave clays and their associated minerals has the potential to yield information about clay genesis, the geologic history of the caves, and perhaps even the regional geologic history. The Guadalupe Mountains of southeastern New Mexico contain two world-renowned caves, Carlsbad and Lechuguilla, as well as other caves of geologic interest. The clay mineralogy and clay origin in these caves are summarized below.

THE CAVES AND CLAY-BEARING SEDIMENTS

The study area includes the caves of the Guadalupe Mountains in New Mexico (Fig. 1). Clay samples were collected in Carlsbad Cavern from the Big Room, Left Hand Tunnel, Guadalupe Room, Boneyard (near Lunchroom), New Mexico Room, Lower Devils Den, Nooges Realm, Green Clay Room, and Lower Cave. Samples were collected in Lechuguilla Cave from Apricot Pit, Boulder Falls, Glacier Bay, Lake Lebarge, The Great Beyond, and Tinseltown. Other samples were collected from Barranca, Cottonwood, Dry, Endless, Hell Below, Madonna, Spider, Three Fingers, Virgin, and Wind caves.

The cave deposits studied include (1) recent cave muds, (2) solution cavity fillings, (3) joint and fracture fillings, (4) pockets of altered bedrock, (5) floor deposits, (6) wall residues, (7) laminated silt deposits, (8) Permian clay beds in dolostone bedrock, and (9) clay-bearing carbonate speleothems.

Cave muds. Mud introduced into the caves from surface runoff accounts for relatively small-sized cave deposits in the Guadalupe Mountains. The largest, most recent mud deposits occur in Barranca, Cottonwood, Hidden, Madonna, Three Fingers, and Virgin caves. Old mud deposits occur in Endless Cave and in the Guadalupe Room of Carlsbad Cavern. All of these appear to result from short-lived flooding events when surface canyons dissected the cave systems. For example, the entrance to Cueva de la Barranca is located directly in the bot-

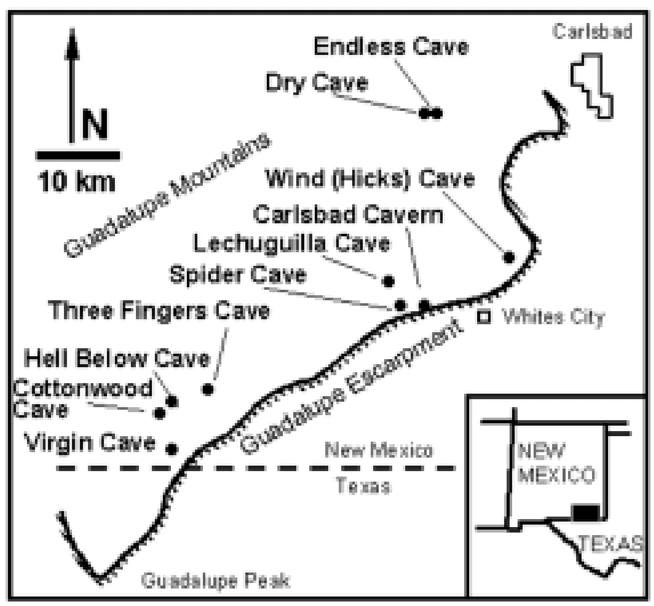

Figure 1. Location map showing general locations of caves in the Guadalupe Mountains pertinent to this study.

tom of a canyon. Accumulation of mud will continue in Cueva de la Barranca until down-cutting of the canyon progresses and positions the cave entrance on the slope above the flood level of the canyon. With the exception of Hidden Cave, the mud deposits in these caves are generally thin (<0.5 m thick). Samples of mud were collected from Barranca, Carlsbad, Cottonwood, Endless, Madonna, Spider, and Virgin caves.

Solution cavity fillings. Solution cavity (spongework) fillings are mostly exhibited in Carlsbad Cavern. Spongework, a network of irregular, interconnected solution cavities, is filled or partially filled with clay-rich sediments in Lower Cave, the Boneyard, and the Green Clay Room of Carlsbad Cavern. Less obvious solution cavity fillings have been observed in Cottonwood and Lechuguilla caves. These green, red, and brown clays filling the cavities are commonly laminated.

Joint and fracture fillings. Joint and fracture fillings sometimes consist of clay-rich material that is similar in appearance and texture to solution cavity fillings described above. Carlsbad Cavern and Lechuguilla Cave contain numerous joint and fracture fillings. Some of these deposits may be altered small siltstone/sandstone "dikes" similar to those described by Jagnow (1977) and Hill (1996).

Pockets of altered bedrock. Bedrock pockets are usually black due to manganese mineralization, and commonly contain blue hydrated halloysite (endellite) nodules. These pockets are products of the sulfuric acid-related speleogenesis (Polyak & Güven, 1996). The pockets of altered bedrock range in diameter from 5 cm to 1 m. They have been observed in Carlsbad, Cottonwood, Endless, Lechuguilla, and Virgin caves. Pockets of altered bedrock are widely distributed within these caves. In Carlsbad and Lechuguilla caves, pockets are observed where bedrock in the caves has been protected from water; these areas are coincident with the occurrence of gypsum blocks.

Floor and ledge deposits from autochthonous sediments. Floor and ledge deposits are numerous and diverse in the Guadalupe caves. These sediments have been derived from within the caves and have not been transported by water. The clay mineralogy in these deposits can vary considerably. Good examples of this type of sediment are deposits in Spider Cave, which consist of autochthonous wall residues that have gently fallen and accumulated on the floor and ledges. In Carlsbad Cavern, some floor deposits consist of fallen bedrock pocket materials and solution cavity fillings. Floor deposits of bluish-white hydrated halloysite (endellite) occur in the New Mexico Room of Carlsbad Cavern and in Endless Cave.

Wall residues. Wall residues appear to have formed by the alteration of bedrock. The residue left behind from weathered dolostone bedrock has been referred to as "condensation-corrosion" residue (Hill, 1987; Cunningham *et al*. 1995). In Lechuguilla Cave, many of these residues are black from manganese enrichment. In other Guadalupe caves, wall residues are commonly brown and clay-rich. Hill (1987) suggested that these residues are inorganic in origin and due to condensation and corrosion. However, Cunningham *et al.* (1995) suspected that biochemical and biomechanical alteration of the bedrock plays a major role in the origin of the wall residues. Wall residues occur in Cottonwood, Endless, Hell Below, Lechuguilla, Spider, and Wind caves.

Laminated silt deposits. Carlsbad Cavern is perhaps the only cave that contains significant volumes of laminated quartz-rich silt. Large quantities of silt are located in Lower Devils Den, Left Hand Tunnel, the Big Room, and Lower Cave. The laminated silts to which we refer are equivalent to the orange-silt banks of Left Hand Tunnel reported by Hill (1987). The silt deposits are up to 3 m thick in some areas. They differ from the cave muds by having a coarser texture, detrital calcite and dolomite, and lesser clay content. The laminated silts from Lower Cave and Left Hand Tunnel contain 10-40% clay, 30-50% silt, 25-35% fine sand, and <4% medium sand.

Permian clay beds. Beds of clay within and parallel to the bedding of dolostone have been observed in four caves (Cottonwood, Dry, Endless, and Spider). All of these clay beds are less than 0.3 m thick and occur in the caves only in backreef units in the upper Seven Rivers Formation near the contact with the Yates Formation. These clay beds are probably an exposed Permian shale unit.

Clays associated with carbonate speleothems. Clay minerals and magnesium silicates have been found in some carbonate speleothems such as dolomite and huntite moonmilk and crusts (Polyak & Güven 1997).

METHODS

Samples were dispersed in deionized water to collect the clay-fraction for X-ray diffraction (XRD) and electron microscopy analyses. Both powder and particle-oriented diffraction patterns were obtained from the clay-fractions. Samples were examined with a JEOL JEM 100CX analyzing electron microscope, which allows scanning electron microscopy (SEM), transmission electron microscopy (TEM), scanning transmission electron microscopy, and energy dispersive X-ray (EDX) microanalysis. Semiquantitative and quantitative chemical analyses were determined by EDX microanalysis.

CLAY MINERALS IN GUADALUPE CAVES

The clay minerals in caves of the Guadalupe Mountains are kaolinite, dickite, hydrated halloysite (endellite), illite, montmorillonite, trioctahedral smectite, and palygorskite. Mixed-layers of illite and smectite also occur in these caves.

Kaolinite [$Al_2Si_2O_5(OH)_4$] is the major constituent of a thin clay bed in backreef dolostone near the contact of the Seven Rivers and Yates formations, exposed in the walls of Cottonwood, Dry, and Endless caves. Kaolinite is also a minor constituent in cave muds and detrital cave sediments in all of the study area caves. Crystals are anhedral to euhedral, micron- to submicron-sized platelets (<4 µm in diameter). Kaolinite

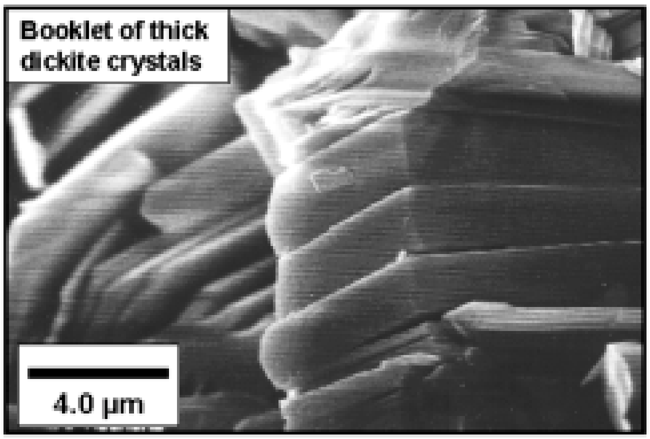

Figure 2. Thick platelets of dickite crystals from a Spider Cave ledge deposit. Booklets of dickite are well preserved after low-energy transport from the bedrock to wall residue to the ledges.

from the Cottonwood Cave clay bed is well crystallized.

Dickite [$Al_2Si_2O_5(OH)_4$], a polymorph of kaolinite, occurs as authigenic pods in the Permian backreef dolostones throughout the Guadalupe Mountains adjacent to the Capitan reef (Polyak & Güven 1995; Polyak 1998). In the caves, it is found disseminated in ledge and floor deposits, and is abundant in weathering-induced wall residues. Dickite crystals are thick, relatively large euhedral platelets (Fig. 2), with diameters up to 100 µm. Millimeter-sized pods are moderately abundant in the dolostone (in the caves and on the surface) and are sometimes found in ledge and floor deposits, and in wall residues in the caves. Dickite occurs in Cottonwood, Endless, Hell Below, Three Fingers, Spider, Virgin, and Wind caves. It has also been reported in Lechuguilla Cave (Palmer & Palmer 1992).

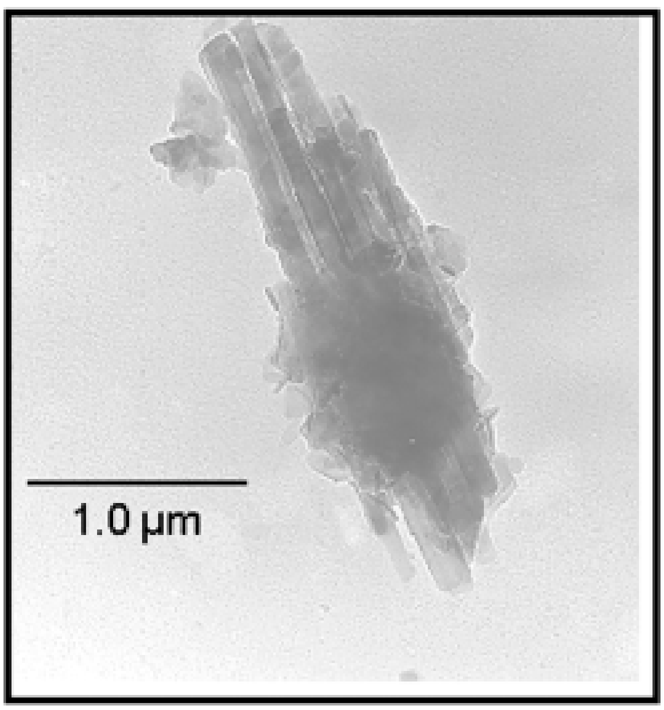

Figure 3. TEM image of illite particle from wall residue (illite laths extend from illite lamella, Wind Cave sample).

Illite is disseminated within the backreef dolostone adjacent to the Capitan reef. In the caves, it is a major constituent of brown wall residues and ledge and floor deposits of these wall residues. Illite is also a minor component in cave muds, and laminated silt and clay deposits. Illite particles occur as lamellar aggregates and euhedral to subhedral laths (Fig. 3). The laths represent authigenic crystals in the dolostone, whereas the aggregates are probably Permian detrital particles (Polyak 1998). The composition of the illite has been estimated from EDX microanalysis of several platelets and aggregates as $K_{0.90}$ $(Al_{1.60}Mg_{0.25}Fe_{0.15})$ $(Si_{3.25}Al_{0.75})O_{10}(OH)_2$. The random powder XRD patterns of two relatively pure illite samples (<1-µm fractions of wall residues from Spider and Three Fingers caves) are comparable to Marblehead illite (Clay Mineral Society source clay). The particle-oriented patterns show a moderate degree of crystallinity (crystallinity index >0.5°2θ, consistent with a diagenetic grade of illite; Weaver 1989).

Montmorillonite was reported by Davies (1964), Friesen (1967, 1970), and Hill (1987) as the major component of green, red, and brown clays in Lower Cave and other areas of Carlsbad Cavern. As Friesen noted, most of these clays are located below the 200-m depth level of Carlsbad Cavern. Montmorillonite is also a major constituent of the <2-µm fraction of laminated silts and clays in Carlsbad Cavern. It is abundant in cave muds, and it is found in saturated ledge and floor deposits of Spider Cave. Montmorillonite particles in the green and brown clays of Carlsbad Cavern are predominantly rounded oval-shaped lamellar aggregates, and poorly developed thin films (Fig. 4). The composition of montmorillonite in these cave deposits is probably somewhat aluminous as indicated by EDX microanalysis of several aggregates and whole rock analysis of green clay from Carlsbad Cavern. A formula has not yet been established for these samples due to inclusions of illite, kaolinite, iron oxides, and aluminum hydroxides within the aggregates. The chemical composition for montmorillonite is: $(E)_{x+y}$ $(Al_{2-y}Mg_y)$ $(Si_{4-x}Al_x)O_{10}(OH)_2 \cdot nH_20$; where E is the interlayer cation (i.e., Na, K, Ca), y and x are octahedral and tetrahedral substitutions, and y>x (Güven 1988). Montmorillonite in the clays of Lower Cave, laminated silts of Left Hand Tunnel and Lower Cave, and in the cave muds is associated with lesser amounts of illite and trace amounts of kaolinite. XRD patterns indicate that the proportions of montmorillonite to illite to kaolinite are similar in most of these deposits.

Palygorskite $(Mg, Al)_2Si_4O_{10}(OH) \cdot 4H_2O$) was reported by Davies (1964) from Lower Cave, Carlsbad Cavern as a pink, calcite-hardened clay. Palygorskite also occurs as disseminated fibers in brown and green clay from Lower Cave, and in laminated silt from Left Hand Tunnel and Lower Cave.

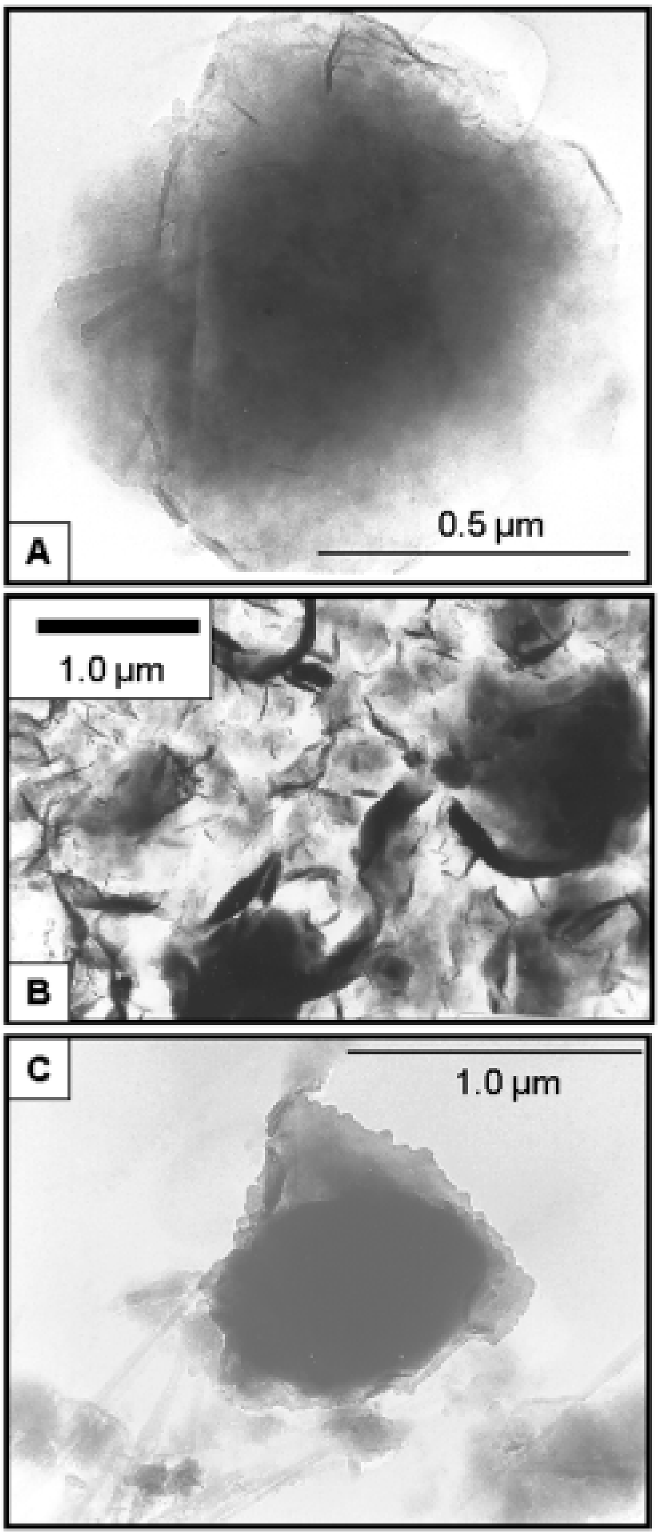

Figure 4. TEM images of montmorillonite films and aggregates. (A) Aggregate of films from green clay in Green Clay Room. (B) Films and rounded lamellar aggregates from brown clay in Lower Cave. (C) Oval-shaped lamellar aggregate from laminated silt in Lower Cave.

Palygorskite is associated with montmorillonite, illite, and kaolinite in the <2-µm fraction of these deposits. TEM micrographs show fibers of palygorskite radiating from oval-shaped montmorillonite aggregates (Fig. 5). SEM images show palygorskite fibers diseminated in the clay-rich matrix of the laminated silt, and sometimes concentrated along quartz grain surfaces.

Illite-smectite mixed-layers and kaolinite are the main constituents of a clay bed in Endless and Dry caves. This clay bed is probably a thin Permian shale unit, exposed in the cave walls, which was truncated by sulfuric acid-related speleogenesis. The clay is a mixture of random and regular interstratified illite-smectite, and the illite/smectite is approximately 70-80% (Polyak 1998).

Trioctahedral smectites (probably a stevensite and minor amounts of saponite) are found associated with Mg-carbonate speleothems (Polyak & Güven 1997). Crystals occur as fibers, ribbons, and films. Aggregates of these form filaments that intertwine with dolomite, huntite, and magnesite crystals in crusts and moonmilk (Fig. 6). The smectite is intimately associated with quartz or opal, and in some settings, uranyl vana-

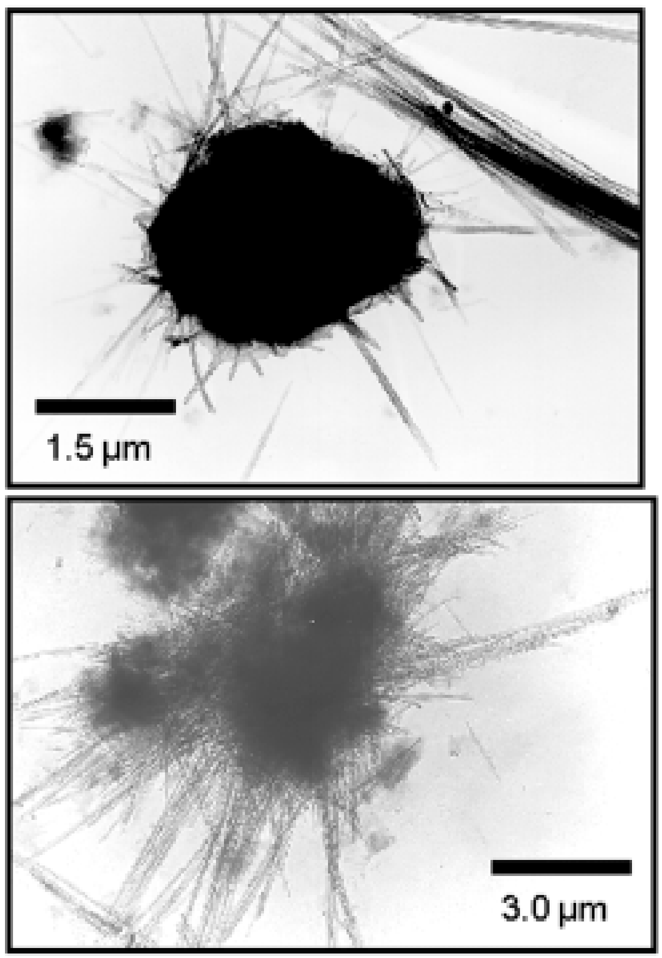

Figure 5. TEM images of palygorskite fibers radiating from montmorillonite aggregates.

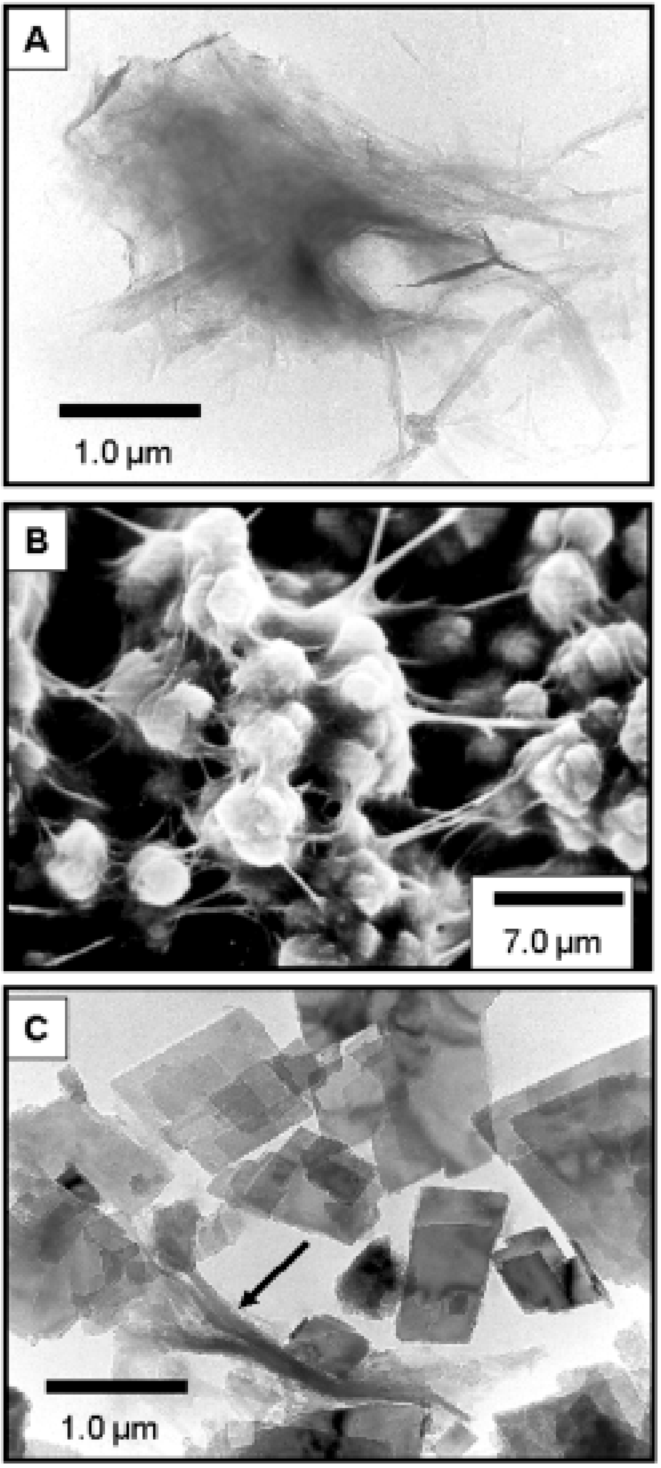

Figure 6. TEM images of trioctahedral smectite lamellae and fiber-like particles. (A) Insoluble residue after Na-acetate digestion of dolomite crust (Christmas Tree Room, Carlsbad Cavern). (B) SEM photograph of smectite filaments intertwined with dolomite rhombs (from same room as A). (C) Filaments consist of fiber-like smectite in huntite moonmilk (plates are huntite, Hell Below Cave, after Polyak & Güven 2000).

dates. From EDX microanalysis of several films and fiber aggregates, the approximate formula for one phase of trioctahedral, poorly crystallized smectite in these caves is $(Ca,Na,K)_{0.55}(Mg_{2.90}Al_{0.10})(Si_{3.95}Al_{0.05})O_{10}(OH)_2 \bullet nH_2O$.

Hydrated halloysite $[Al_2Si_2O_5(OH)_4 \bullet 2H_2O]$ (endellite) is the most colorful clay mineral in the Guadalupe Mountains. It can be white to blue, or it can also have tints of brown and red. The blue hydrated halloysite is distinct in appearance; however, amorphous opal from Cottonwood Cave was found to display a similar blue color. Hydrated halloysite was first reported in caves of the Guadalupe Mountains by Davies & Moore (1957). Hill (1987) reported the hydrated halloysite (endellite) in Carlsbad, Cottonwood, and Endless caves as the by-product of sulfuric acid-related speleogenesis. Hydrated halloysite crystals from these caves are tubular and generally less than 1.0 µm in length and 0.05 µm in diameter (Fig. 7). Hydrated halloysite occurs in pockets of altered bedrock, in white alteration rims around solution cavity fillings, in some floor deposits, and in black wall residues (Polyak & Güven 1996). It can be intimately associated with alunite, natroalunite, gibbsite, hydrobasaluminite, and hydrous iron and manganese

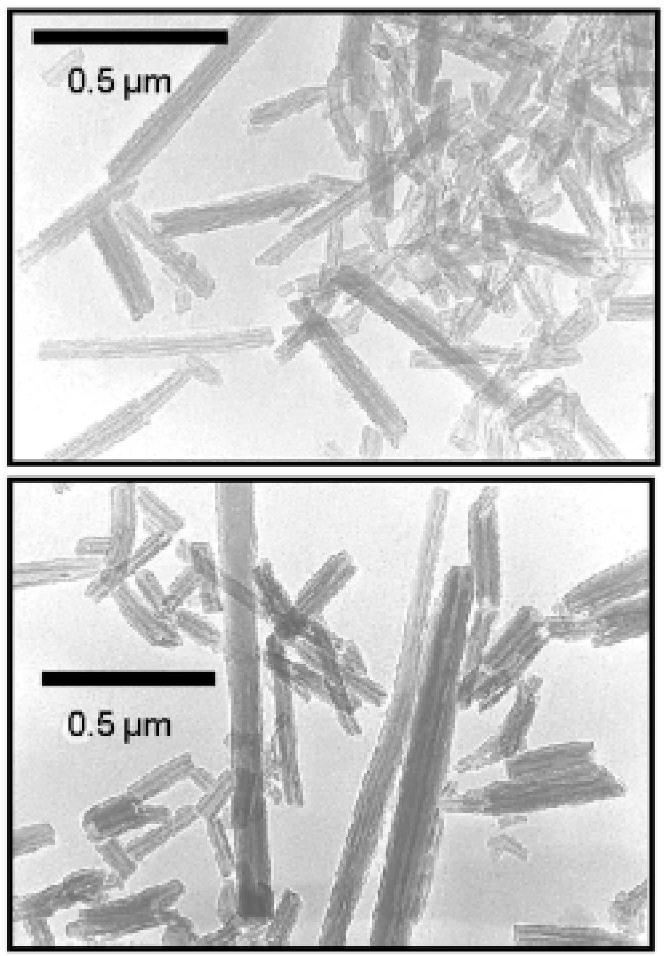

Figure 7. TEM image of hydrated halloysite (endellite) tubes (Virgin Cave).

oxides (Provencio *et al*. 1998).

DISCUSSION

The origin of clays in caves is placed in three categories: (1) detrital; (2) inherited from bedrock by weathering; and (3) cave-authigenic.

DETRITAL ORIGIN FOR CLAYS

Detrital clays are introduced into caves by streams or seeping waters, and consequently, they are constituents of muds, silts, sands, or gravels. In caves of the Guadalupe Mountains, detrital sediments are not abundant or widespread. In all of these detrital deposits, the clay minerals are montmorillonite with minor amounts of illite and kaolinite. The clay mineralogy of the laminated clay and silt deposits in Left Hand Tunnel and Lower Cave of Carlsbad Cavern is consistent with that of soils of the southwestern and midwestern U.S.A. (Allen & Hajek 1989; Borchardt 1989). This and other reasons suggest that the laminated silt and clay deposits of Carlsbad Cavern are detrital in origin, rather than autochthonous prior to, or from, speleogenesis as Hill (1987) reported. In all of these mud, silt, and clay deposits, montmorillonite is the major clay component.

CLAYS INHERITED FROM WEATHERING OF THE BEDROCK

Condensation-induced weathering of the dolomitic bedrock along cave walls and ceilings can dissolve the carbonate components of the bedrock, and form a layer containing predominantly acid-insoluble materials (condensation-corrosion residue). These residues are normally brown (color derived from goethite) on dolostone, and contain abundant illite and dickite. The same mineralogy occurs from dissolving samples of dolostone bedrock with Na-acetate or HCl, showing that the illite and dickite in the wall residues are inherited from the bedrock by condensation-induced weathering. In Spider Cave, dickite crystals in white pods in the wall residues are arranged in booklets. This arrangement of euhedral crystals gives a false indication that the dickite is cave-authigenic. Translocation and preservation of the dickite booklets from the cave walls to the ledges demonstrate that these deposits formed in a low-energy weathering environment.

CAVE-AUTHIGENIC CLAYS

Clay mineral authigenesis in caves is normally difficult to demonstrate. Cave sediments of detrital origin usually contain more than one clay mineral. Understanding the origin of the cave clays therefore requires extensive studies of the clays in the cave sediments, in the bedrock, and in soil, fluvial, and alluvial sediments above the caves. The following are examples of clay mineral authigenesis in caves of the Guadalupe Mountains.

Trioctahedral smectite. Trioctahedral smectite (stevensite and probably minor saponite) occurs with dolomite and huntite in carbonate speleothems such as crusts and moonmilks. Amorphous and poorly developed Mg-bearing silicates occur in other carbonate speleothems such as aragonite crust and aragonite/calcite stalagmites. These silicates formed in a Mg-rich carbonate setting with Mg-calcite, aragonite, dolomite, and huntite. Authigenesis of trioctahedral smectite in carbonate speleothems took place because the precipitation of calcite and aragonite extracted Ca and increased the Mg/Ca ratio in water films. As a consequence, this process increased the pH and alkalinity (increase in Na, K, and probably $[CO_3^{2-}]/[HCO^{3-}]$). Poorly crystallized trioctahedral smectite then formed under these Mg-rich and alkaline conditions (Polyak & Güven 2000).

Montmorillonite. In Spider Cave, montmorillonite is forming in ledge and floor deposits from eroded wall residues. The wall residues above a preexisting water line and above the ledge and floor deposits contain illite and dickite, while those below the water line contain abundant montmorillonite. Montmorillonite authigenesis took place when the ledge and floor deposits were submerged by floodwater, or when the sediments were later saturated with condensate water after the floodwater level descended (Polyak 1998).

Palygorskite. Suarez *et al*. (1994) showed palygorskite fibers radiating from lamellar micromicas, and they argued that the palygorskite fibers could not be detrital. Palygorskite fibers radiate from smectite aggregates in the laminated silt and clay samples collected from Left Hand Tunnel and Lower Cave in Carlsbad Cavern (Fig. 5). It is unlikely that these fibers could have survived transport from the surface, and palygorskite is not a clay constituent of the carbonate bedrock. So it is probable that it formed in a carbonate-alkaline environment produced by drip waters that saturated the silt and clay deposits, or by detrital grains of calcite and dolomite occurring in the laminated silt. The carbonate-alkaline environment containing aluminum and silicon (from abundant montmorillonite and illite) is conducive to palygorskite authigenesis (Jones & Galan 1988).

Hydrated halloysite. Hydrated halloysite is the product of the H_2SO_4-speleogenesis-related alteration of montmorillonite (Hill 1987), illite, illite-smectite mixed-layers, dickite, and kaolinite (Polyak & Güven 1996; Polyak *et al*. 1998). It may be considered a cave-authigenic mineral, but more specifically it is a speleogenetic by-product mineral. Good examples of this type of alteration are exhibited in the Green Clay Room of Carlsbad Cavern, and in Endless Cave. Alunite or natroalunite usually occurs with hydrated halloysite. In Cottonwood Cave, hydrated halloysite is associated with hydrobasaluminite (Polyak & Provencio 1998).

CONCLUSION

Clays are not abundant in caves of the Guadalupe Mountains. Most are detrital in origin (muds and silts), and contain montmorillonite, illite, and kaolinite. Condensation-related wall residues are made up of insoluble residues of the bedrock, which usually contain abundant dickite and illite. Authigenesis of clay minerals in these caves occurs in only a few settings. Authigenic montmorillonite occurs in saturated ledge deposits in Spider Cave. Authigenic palygorskite is found in laminated silt deposits and in the clay deposits of Carlsbad Cavern. The two more common and most obvious cave-authigenic clay minerals are trioctahedral smectite (stevensite) and hydrated halloysite (endellite). Trioctahedral smectite is authigenic in Mg-carbonate speleothems such as huntite moonmilk and dolomite crust. Hydrated halloysite is a primary speleogenetic by-product; it formed from the alteration of montmorillonite, illite, kaolinite, dickite, or illite-smectite mixed-layers during the sulfuric acid-related origin of these caves.

ACKNOWLEDGMENTS

We thank Ransom Turner of Lincoln National Forest, Dale Pate and Jason Richards of Carlsbad Caverns National Park, and Jim Goodbar of the Carlsbad District, Bureau of Land Management for field assistance and for permission to collect samples. We also thank Carol A. Hill, Annabelle Foos, and Donald G. Davis for their reviews of our manuscript.

REFERENCES

Allen, B.L. & Hajek, B.F. (1989). Mineral occurrence in soil environments. In Dixon J.B. & Weed S.B. (eds.). *Minerals in soil environments.* Madison, WI. Soil Science Society of America: 199-278.

Borchardt, G. (1989). Smectites. In Dixon J.B. & Weed, S.B. (eds.). *Minerals in soil environments.* Madison, WI. Soil Science Society of America: 675-727.

Cunningham, K.I., Northup, D.E., Pollastro, R.M., Wright, W.G., & LaRock, E.J. (1995). Bacteria, fungi and biokarst in Lechuguilla Cave, Carlsbad Caverns National Park, New Mexico. *Environmental Geology 25*: 2-8.

Davies, W.E. (1964). Attapulgite from Carlsbad Caverns, New Mexico. *U.S. Geological Survey Professional Paper 501-C*: C82-C83.

Davies, W.E., Moore, G.W. (1957). Endellite and hydromagnesite from Carlsbad Caverns. *Bulletin of the National Speleological Society 19*: 24-27.

Friesen, W.B. (1967). Explanation of analytical data, X-ray analysis of clay materials-Carlsbad Caverns. Unpublished report in files of Carlsbad Caverns National Park: 13 pp.

Friesen, W.B. (1970). A study of the clay deposits of Carlsbad Caverns, New Mexico. Unpublished report in files of Carlsbad Caverns National Park: 19 pp.

Güven, N. (1988). Smectites. In Bailey, S.W. (ed.). *Hydrous Phyllosilicates. Reviews in Mineralogy, Mineralogical Society of America 19*: 497-559.

Hill, C.A. (1987). Geology of Carlsbad Cavern and other caves in the Guadalupe Mountains, New Mexico and Texas. *New Mexico Bureau of Mines and Mineral Resources Bulletin 117*: 150 pp.

Hill, C.A. (1996). Geology of the Delaware Basin, Guadalupe, Apache, and Glass mountains, New Mexico and west Texas. *Permian Basin Section-Society for Economic Palaeontology and Mineralogy Publication 96-39*: 480 pp.

Hill, C.A. (2000). Overview of geologic history of cave development in the Guadalupe Mountains, New Mexico and west Texas. *Journal of Cave and Karst Studies 62*(2): 60-71.

Hill, C.A. & Forti, P. (1997). *Cave minerals of the world. 2nd edition*. Huntsville, AL. National Speleological Society: 463 pp.

Jagnow, D.H. (1977). *Geologic factors influencing speleogenesis in the Capitan Reef Complex, New Mexico and Texas*. Unpublished MS thesis, University of New Mexico, Albuquerque: 203 pp.

Jones, B.F. & Galan, E. (1988). Sepiolite and palygorskite. In Bailey, S.W. (ed.). *Hydrous phyllosilicates*. *Mineralogical Society of America, Reviews in Mineralogy 19*: 631-674.

Palmer, A.N. & Palmer, M.V. (1992). Geochemical and petrologic observations in Lechuguilla Cave, New Mexico (abs.) In Ogden, A.E. (ed.), *Friends of Karst Meeting: Proceedings*. Tennessee Tech University, Cooksville, TN: 25-26.

Polyak, V.J. (1998). *Clays and associated minerals in caves of the Guadalupe Mountains, New Mexico*. Unpublished Ph.D. dissertation, Texas Tech University, Lubbock, TX: 190 pp.

Polyak, V.J. & Güven, N. (1995). *Dickite in caves of the Guadalupe Mountains in New Mexico*. (abs.) 32nd Annual Meeting of the Clay Minerals Society, Program and Abstracts, Baltimore, MD: 100.

Polyak, V.J. & Güven, N. (1996). Alunite, natroalunite and hydrated halloysite in Carlsbad Cavern and Lechuguilla Cave, New Mexico. *Clays and Clay Minerals 44*: 843-850.

Polyak, V.J. & Güven, N. (1997). Trioctahedral smectite in Mg-carbonate speleothems (abs.). *Texas Journal of Microscopy 28*: 11.

Polyak, V.J. & Güven, N. (2000). Authigenesis of trioctahedral smectite in magnesium-rich carbonate speleothems in Carlsbad Cavern and other caves of the Guadalupe Mountains, New Mexico. *Clays and Clay Minerals 48*: 317-321.

Polyak, V.J. & Provencio, P. (1998). Hydrobasaluminite and aluminite in caves of the Guadalupe Mountains, New Mexico. *Journal of Cave and Karst Studies 60(1)*: 51-57.

Polyak, V.J., McIntosh, W. C., Güven, N. & Provencio, P. (1998). Age and origin of Carlsbad Cavern and related caves from $^{40}Ar/^{39}Ar$ of alunite. *Science 279*: 1919-1922.

Provencio, P., Polyak, V.J., & Mosch, C.J. (1998). By-products of H_2S/H_2SO_4 speleogenesis (abs.). *Journal of Cave and Karst Studies 60 (3)*: 188.

Suarez, M., Robert, M., Elsass, F., & Pozas, J. M. M. (1994). Evidence of a precursor in the neoformation of palygorskite–new data by analytical electron microscopy. *Clay Minerals 29*: 255-264.

Weaver, C.E. (1989). Clays, muds, and shales. *Developments in Sedimentology 44*, Elsevier, New York: 818 pp.

Jeffrey R. Forbes - Geochemistry of Carlsbad Cavern pool waters, Guadalupe Mountains, New Mexico. *Journal of Cave and Karst Studies 62*(2): 127-134.

GEOCHEMISTRY OF CARLSBAD CAVERN POOL WATERS, GUADALUPE MOUNTAINS, NEW MEXICO

JEFFREY R. FORBES
Daniel B. Stephens & Associates, 6020 Academy NE, Albuquerque, NM 87109, USA

Water samples collected from 13 pools in Carlsbad Cavern were analyzed to determine the concentrations of major ions. Air temperature, relative humidity, and carbon dioxide concentration of the cave atmosphere were also measured. Large differences in water quality exist among different cave pools, with some pools containing very fresh water, while others are brackish, with total dissolved solids concentrations up to 5000 mg/L. Brackish water pools appear to be associated with those portions of the cave where evaporation rates are high and/or soluble minerals are present. Geochemical speciation modeling showed that some pools are close to saturation with respect to the common cave minerals aragonite, calcite, gypsum, and hydromagnesite.

A tracer test was performed using a non-toxic bromide salt to estimate the leakage rates of selected pools. Pool volumes calculated based on dilution of the bromide tracer were up to 550 m³. The tracer test results were used to calculate mean residence times for the water in each pool. Calculated mean residence times based on bromide tracer loss rates ranged from less than a year for Rookery Pool and Devil's Spring to 16 years for Lake of the Clouds. Calculated pool leakage rates ranged from 2 L/day to over 100 L/day. The pools with the highest leakage rates appear to be Rookery Pool, Green Lake, and Lake of the Clouds.

The long residence times indicated by the tracer tests suggest that the pools evaporate more water than they leak. However, evaporation should result in an accumulation of dissolved chloride and other solutes in the pools, which for most pools does not appear to be the case. Taken together, these observations suggest that the pools are recharged primarily by infrequent precipitation events, separated by long periods of slow evaporation and minimal leakage.

Carlsbad Cavern, located in southeastern New Mexico, U.S.A., contains numerous pools of standing water ranging from small shallow puddles to Lake of the Clouds, with an estimated volume of approximately 550 m³. This report summarizes the results of a two-year water chemistry study of 13 of the pools selected throughout the cave (Fig. 1). The main objectives of the study were to determine how pool water quality varies from one pool to another, and to track water quality changes in a particular pool over time.

The cave pools in Carlsbad Cavern are recharged by drip water that enters through the cave ceiling. Water is lost from the pools by a combination of evaporation from the pool surface, leakage from the bottom, and overflow from the perimeter. Flowing streams are not observed in the cave, except possibly following infrequent intense precipitation events. Detailed geologic information and maps of Carlsbad Cavern and the surrounding Guadalupe Mountains can be found in Jagnow (1977) and Hill (1987).

The pools investigated during this study lie at depths ranging from approximately 150 m to 316 m below the main entrance. Lake of the Clouds is the deepest known point in the cave. All of the pools in Carlsbad Cavern are perched, and dripwater moving downward accumulates in each pool as a result of the low permeability of the pool bottom. The elevation of the regional groundwater table is believed to be some 30 m below the lake level at Lake of the Clouds (Hill 1987).

Some of the pools sampled during this study have been affected by human activities. For example, there are reports that some pools (e.g. Mirror Lake, Longfellows Bathtub) were refilled in the past with water from the Park drinking water supply, which is obtained from Rattlesnake Springs located 8 km to the southwest (Bowen 1998). Furthermore, Caldwell (1991) reported that hypochlorite bleach was used in past restoration activities around some of the pools. Therefore, the data reported here serve primarily to document current condi-

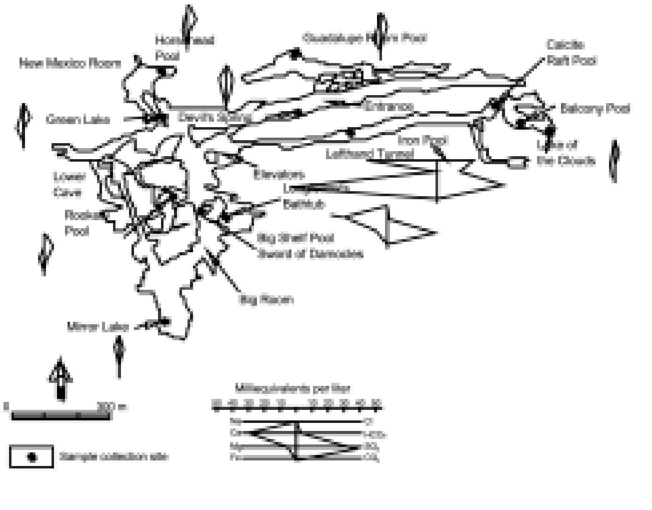

Figure 1. Sample locations in Carlsbad Cavern.

Table 1. Summary of Carlsbad Cavern Pool Water Quality.

NM = not measured

***TDS too low and charge balance error too high, possibly due to presence of ions that were not analyzed.**

Sample Location	Date	Air Temp (C)	Air RH (%)	Air CO2 (ppm)	Water pH	Water Temp (C)	EC (μS/cm @ 25C)
Balcony Pool	1/22/95	19.4	95	NM	8.19	18.5	795
Big Shelf Pool	4/8/95	NM	NM	NM	NM	14.4	1680
	9/24/95	12.6	NM	NM	NM	14.7	1710
	11/12/95	NM	NM	NM	NM	14.6	1710
Calcite Raft Pool	1/22/95	18.9	95	530	8.27	18.3	1150
	4/9/95	18.6	97	NM	8.34	18.1	1150
	9/25/95	18.2	NM	NM	7.64	18.2	1125
	11/12/95	NM	NM	NM	NM	18.0	1120
Devils Spring	8/6/94	13.3	95	NM	7.87	11.0	770
	10/8/94	13.6	92	750	8.11	12.6	755
	1/21/95	10.7	71	NM	8.50	9.5	740
	4/8/95	12.2	91	NM	8.72	10.7	760
	9/24/95	NM	NM	NM	7.86	12.1	760
	11/12/95	NM	NM	NM	NM	11.0	760
Green Lake	8/6/94	13.9	97	NM	8.12	13.5	505
	10/8/94	14.2	97	1000	8.01	13.6	520
	1/21/95	13.6	88	330	8.62	13.3	480
	4/8/95	13.9	92	NM	9.14	13.1	485
	9/24/95	NM	NM	NM	8.04	13.5	490
	11/12/95	NM	NM	NM	NM	13.5	485
Guadalupe Rm	8/6/94	NM	NM	NM	NM	NM	520
Horsehead Pool	8/6/94	16.1	97	NM	8.33	15.5	420
	10/8/94	16.4	97	1000	7.92	16.0	415
	1/21/95	16.1	98	570	8.46	15.9	400
	4/8/95	16.4	97	NM	8.38	15.7	400
Iron Pool	3/12/94	16.3	NM	NM	8.67	NM	11300
	8/7/94	16.4	92	NM	8.84	15.5	11100
	10/9/94	16.1	92	800	8.34	15.8	9440
	1/22/95	16.1	90	400	8.64	15.7	9830
	4/9/95	16.4	97	NM	8.78	15.6	10800
	9/25/95	NM	NM	NM	8.30	15.7	9340
	11/12/95	NM	NM	NM	NM	15.6	10000
Lake of Clouds	8/7/94	19.4	95	NM	NM	18.5	405
	10/9/94	19.6	96	800	7.72	19.2	400
	1/22/95	19.7	95	670	8.45	19.0	385
	4/9/95	19.4	95	600	8.71	19.0	385
	11/12/95	NM	NM	NM	NM	19.0	392
Longfellows Bathtub	8/7/94	15.3	94	NM	NM	14.0	2630
	10/8/94	15.3	92	1000	7.46	14.6	2590
	1/21/95	14.7	89	370	7.91	14.1	2440
	4/8/95	14.7	92	NM	8.01	13.9	2570
	9/24/95	13.0	NM	NM	7.23	14.4	2560
	11/12/95	NM	NM	NM	NM	14.2	2550
Mirror Lake	10/8/94	15.6	94	1200	7.64	15.3	335
	1/21/95	15.3	95	330	8.44	14.9	315
	4/8/95	15.0	97	NM	8.38	14.7	345
	9/24/95	13.2	NM	NM	7.59	14.8	355
	11/12/95	NM	NM	NM	NM	14.8	355
Rookery Pool	8/7/94	14.3	95	NM	NM	13.0	475
	10/9/94	14.2	97	900	8.09	14.0	420
	1/21/95	13.9	96	400	8.69	13.6	435
	4/9/95	14.4	94	NM	8.40	13.4	450
	9/24/95	12.4	NM	NM	8.27	13.7	475
	11/12/95	NM	NM	NM	NM	13.8	525
Sword of Damocles Pool	4/8/95	NM	NM	NM	NM	13.5	1550
	9/24/95	12.0	NM	NM	NM	14.0	1580
	11/12/95	NM	NM	NM	NM	13.8	1540

tions, but do not necessarily reflect pool water quality prior to anthropogenic impacts.

PREVIOUS STUDIES

Several prior studies of water quality have been done in Carlsbad Cavern. As part of his PhD dissertation, Thrailkill (1965, 1971) performed a thorough investigation of speleothem precipitation based primarily on chemical analysis of drip and seep water samples collected along flow paths. He reported major ion concentrations from about 50 sample locations throughout the cave, including one-time sampling of several of the same pools investigated here (Mirror Lake, Green Lake, and Rookery Pool). Thrailkill's field assistant, Boyer (1964), wrote an excellent report on drip and pool water chemistry as it pertains to carbonate mineral precipitation.

Two studies by McLean (1971, 1976) were done to determine the potential causes of the drying of cave pools in Carlsbad Cavern. In addition to measurements of air temperature and air flow, pool water-level hydrographs were prepared,

TDS	Calcium	Magnesium	Sodium (All concentrations in mg/L)	Potassium	Chloride	Sulfate	Bicarbonate	Chg. Bal. Error (%)	Ionic Strength (molal)
NM	70	39	NM	NM	7	25	135	NM	NM
NM	NM	NM	NM	NM	NM	NM	NM	NM	NM
NM	NM	NM	NM	NM	NM	NM	NM	NM	NM
NM	NM	NM	NM	NM	NM	NM	NM	NM	NM
NM	94	60	NM	NM	16	45	135	NM	NM
NM	NM	NM	NM	NM	NM	NM	NM	NM	NM
NM	NM	NM	NM	NM	NM	NM	NM	NM	NM
NM	NM	NM	NM	NM	NM	NM	NM	NM	NM
630	87	45	24	1.8	30	140	305	1.8	0.013
571	84	29	21	1.8	30	145	260	-4.0	0.011
NM	76	39	NM	NM	30	160	270	NM	NM
NM	NM	NM	NM	NM	NM	NM	NM	NM	NM
NM	NM	NM	NM	NM	NM	NM	NM	NM	NM
NM	NM	NM	NM	NM	NM	NM	NM	NM	NM
447	31	48	8	0.4	10	22	325	-1.7	0.008
420	30	46	8	0.4	10	24	305	-1.2	0.008
NM	30	46	NM	NM	9	22	275	NM	NM
NM	NM	NM	NM	NM	NM	NM	NM	NM	NM
NM	NM	NM	NM	NM	NM	NM	NM	NM	NM
NM	NM	NM	NM	NM	NM	NM	NM	NM	NM
439	25	52	15	0.7	20	48	280	0.4	0.009
406	25	45	7	0.5	10	17	305	-3.3	0.008
379	24	42	7	0.4	10	17	275	-1.7	0.007
NM	24	35	NM	NM	7	19	240	NM	NM
NM	NM	NM	NM	NM	NM	NM	NM	NM	NM
NM	15	440	NM	NM	840	2500	665	NM	NM
5971	25	1140	910	220	820	2000	860	28.0	0.14
4390	24	860	820	200	670	1040	775	36.0	0.11
NM	24	795	NM	NM	500	1650	665	NM	NM
NM	NM	NM	NM	NM	NM	NM	NM	NM	NM
NM	NM	NM	NM	NM	NM	NM	NM	NM	NM
NM	NM	NM	NM	NM	NM	NM	NM	NM	NM
327	37	38	5	1.1	15	13	220	9.7	0.007
305	30	32	5	1.1	10	10	220	3.3	0.006
NM	30	32	NM	NM	7	12	220	NM	NM
NM	NM	NM	NM	NM	NM	NM	NM	NM	NM
NM	NM	NM	NM	NM	NM	NM	NM	NM	NM
2671	608	67	9	1.1	15	1850	120	-6.0	0.051
2277	516	70	9	1.1	10	1520	150	-3.7	0.045
NM	516	58	NM	NM	14	1750	110	NM	NM
NM	NM	NM	NM	NM	NM	NM	NM	NM	NM
NM	NM	NM	NM	NM	NM	NM	NM	NM	NM
NM	NM	NM	NM	NM	NM	NM	NM	NM	NM
298	47	14	6	0.5	10	27	195	-3.4	0.006
NM	47	7	NM	NM	7	29	150	NM	NM
NM	NM	NM	NM	NM	NM	NM	NM	NM	NM
NM	NM	NM	NM	NM	NM	NM	NM	NM	NM
NM	NM	NM	NM	NM	NM	NM	NM	NM	NM
392	31	49	NM	NM	10	NM	305	NM	NM
411	30	46	5	0.4	10	18	305	-1.3	0.008
NM	24	42	NM	NM	7	17	240	NM	NM
NM	NM	NM	NM	NM	NM	NM	NM	NM	NM
NM	NM	NM	NM	NM	NM	NM	NM	NM	NM
NM	NM	NM	NM	NM	NM	NM	NM	NM	NM
NM	NM	NM	NM	NM	NM	NM	NM	NM	NM
NM	NM	NM	NM	NM	NM	NM	NM	NM	NM
NM	NM	NM	NM	NM	NM	NM	NM	NM	NM

and limited water quality data were also reported. McLean showed that the primary cause of excessive pool evaporation was the unrestricted air flow up the elevator shafts during winter. In response to McLean's work, revolving doors were installed at the bottom of each elevator shaft in 1972 to reduce the convective air flow, and drying of the cave pools.

Williams (1983) correlated rainfall patterns at Carlsbad Cavern with pool water levels and drip rates in the cave. Drip rates into some cave pools (e.g. Green Lake) increased significantly following storm events, but the drip response was found to lag from 2 to 5 weeks behind the associated precipitation event. Pool water levels showed similar responses and lags of 6 to 14 weeks. The lag times were taken as evidence of considerable water storage in the vadose zone.

Ingraham *et al.* (1990) and Chapman *et al.* (1992) investigated the stable isotopic composition and tritium activity of water samples collected from drips and pools in Carlsbad Cavern, including some of the same pools sampled during this study (Horsehead Pool, Rookery Pool, Lake of the Clouds). Their data indicate that the pools investigated leak more water than they evaporate, and that the travel time for water through the vadose zone from the surface to the main cave level range between 17 and 36 years. S.J. Lambert (pers. comm.) also performed extensive stable isotopic analyses of drip and pool water samples from Carlsbad Cavern, but reached the quite different conclusion that vadose zone travel times may be as little as 3 weeks to 3 months, depending on the intensity of precipitation events.

Caldwell (1991) reported the results of chemical and microbiological tests performed on pool water samples collected throughout Carlsbad Cavern in 1981. The main focus of this study was to compare the water quality of pools affected by visitor activities with those that had not been affected. The report concluded that oranges and other organic debris deposited in particular cave pools by visitors had created anoxic conditions that altered the natural microbiology of these pools.

Brooke (1996) performed a water quality study in Carlsbad Cavern to identify anthropogenic impacts on cave water quality, with an emphasis on correlating such impacts with specific surface sources (e.g. sewer, parking lot, visitor center, etc.). For example, elevated dissolved nitrate concentrations in the eastern portion of the cave (Left Hand Tunnel) were attributed to some combination of sewerline leaks and bat guano from overlying portions of the cave. Van der Heijde *et al.* (1997) summarized Brooke's work, and attempted to identify areas of the cave most susceptible to impacts by release of contaminants at the surface.

METHODS

Water samples from 13 pools throughout Carlsbad Cavern (Fig. 1) were collected and analyzed periodically for pH, temperature, electrical conductivity (EC), alkalinity, and the concentrations of major and trace inorganic solutes. The temperature, relative humidity, and carbon dioxide concentration of the cave air adjacent to each of the pools was also measured. Water temperature (±0.1°C) and pH (±0.01 unit) were measured in the cave using an Orion 250A pH meter, and EC was determined using a Horiba ES-12 conductivity meter (±2 percent). EC values were corrected from field temperature to 25°C by applying a 2 percent per degree C temperature coefficient, as described in APHA (1992). Wet and dry bulb air temperatures were determined to the nearest 0.1°C using a research-grade sling psychrometer, and percent relative humidity (RH) was calculated from these values. The precision of RH values is approximately ±1 percent up to a maximum of 95 percent RH, above which the sling psychrometer becomes unreliable. Absolute barometric pressure was measured to the nearest 5 mbar using a Casio watch barometer. Carbon dioxide concentrations in the cave air were measured using Draeger colorimetric tubes (Draeger 1992).

Analysis of water samples was performed as follows. Total alkalinity was determined in the cave by acid titration using a Hach kit to the bromcresol green-methyl red colorimetric endpoint. Concentrations of calcium, magnesium, and chloride were determined later on clear, unfiltered water samples by colorimetric titration. Calcium and magnesium were titrated using CalVer colorimetric indicator chloride was titrated using a silver nitrate endpoint indicator and sulfate was determined turbidimetrically with barium chloride (Hach 1992). Bromide was determined by ion-selective electrode (ISE), with selected samples verified using ion chromatography. Sodium and potassium concentrations were determined by flame atomic emission spectroscopy. The precision of the major ion analyses is approximately ±10 percent. For samples for which all major ions were determined, total dissolved solids (TDS) concentrations were calculated as the sum of dissolved ions.

The geochemical equilibrium speciation code PCWATEQ (Plummer *et al.* 1976) was used to determine the distribution of dissolved species in the pool waters, as well as the saturation indices of common cave minerals. The Davies equation option was used in the model runs, and the ionic strengths of the pool waters (Table 1) were low enough (<0.2) to be successfully handled by the code. Input data included field temperature, pH, and the concentrations of the major ions as determined in the laboratory. The code also calculates CO_2 partial pressure in the water, which provides a useful comparison to CO_2 concentrations determined in the cave air.

A tracer test was performed using a non-toxic bromide salt to estimate the leakage rates of selected pools. Crystalline NaBr was oven-dried at 105°C for 24 hours. Based on the estimated volume of each pool, an aliquot of NaBr (weighed to 0.1g) was added such that the resulting bromide ion concentration in the pool would be approximately 10 mg/L, assuming zero initial Br concentration. Based on ISE analyses of pool water samples collected prior to addition of the tracer, this assumption is valid, as initial Br concentrations were all less than 0.1 mg/L. For each pool, the weighed quantity of NaBr was dissolved in approximately 500 mL of deionized water. The concentrated solution was poured into the pool, and the water mixed using a canoe paddle. Water samples were collected periodically over time and analyzed for bromide ion concentrations to monitor the disappearance of the tracer resulting from leakage or overflow of the pool. The dissolved bromide ion is generally believed to behave as a "conservative tracer" in water, meaning that it travels unretarded with the water, and that its concentration varies only as a result of simple dilution or evaporation processes.

RESULTS

Table 1 shows the results of field and laboratory tests performed on water samples collected from the various cave pools in Carlsbad Cavern. For samples with complete major ion analyses, charge balance errors expressed as percentages were calculated as:

$$CBE = 100\ (meq_{cations} - meq_{anions}) / (meq_{cations} + meq_{anions})$$

Charge balance errors were generally within acceptable ranges (<5%), with the exception of a few saline samples from Iron Pool.

POOL WATER QUALITY

The concentrations of major ions were found to vary significantly among the pools. Most of the pool waters can be classified as very fresh water (TDS 200 to 500 mg/L) of the calcium-magnesium-bicarbonate type. Fresh water pools include Devils Spring, Green Lake, Horsehead Pool, Lake of the Clouds, Mirror Lake, and Rookery Pool. Stiff water quality diagrams were prepared to illustrate differences in water types among the different pools (Fig. 1).

Values of pH ranged between 7 and 9, with most values being close to 8.5. For a particular pool, the lowest pH values generally occur during late summer or early autumn, which corresponds to the period of maximum stagnation of the cave atmosphere, and hence the highest carbon dioxide concentrations in the cave air (McLean 1971).

Somewhat unusual is the observation that in some pools, magnesium concentrations equal or exceed those of calcium (e.g. Lake of the Clouds, Rookery Pool). This situation is probably attributable both to the high magnesium content of the dolomitic rocks in which the cave is developed, as well as the tendency for the magnesium/calcium ratio to increase in the cave waters as a result of evaporation and precipitation of calcite (Thrailkill 1971).

Two of the pools (Longfellows Bathtub and Iron Pool) were found to contain much higher concentrations of dissolved ions. Longfellows Bathtub contained elevated concentrations of calcium and sulfate, with calculated TDS concentrations of about 2500 mg/L. These observations are consistent with the dissolution of gypsum, which is present nearby in the cave (Hill 1987; her sheet 2).

Iron Pool is a small, but interesting, yellow-green-colored pool in Left Hand Tunnel. Iron Pool contains the most saline water of any of the pools studied. The water in this pool is a magnesium-sulfate type brine, with calculated TDS values ranging between 4000 and 6000 mg/L. Although only about 0.5 m deep, the water in Iron Pool is chemically stratified, with less dense, less saline water near the surface, and more saline water at the bottom. The elevated magnesium concentrations are probably at least partially attributable to dissolution of hydromagnesite “moonmilk”, which is abundant in this portion of Left Hand Tunnel (Thrailkill 1971). Evaporation appears to be responsible for the high concentrations of other major ions measured in Iron Pool (e.g. sodium, potassium, chloride). It is not known what gives Iron Pool its characteristic color, but the color cannot be due to dissolved iron, which was below detection limits. The unacceptably high positive charge balance error for samples from the Iron Pool suggests the presence of another major anion that was not determined during this study (probably nitrate), although poor analytical precision for these samples may also be a factor.

The TDS of the pool waters does not correlate with depth beneath the land surface. In fact, the pool at the lowest elevation in the cave (Lake of the Clouds) is among the pools containing the lowest concentrations of dissolved solutes. The locations of brackish or saline pools appears instead to correlate with those locations in the cave where evaporation rates are high and/or soluble minerals are present, such as gypsum or hydromagnesite.

Based on the similarity of EC measurements for successive monitoring dates at a particular pool (Table 1), only very small changes in water quality were observed during the course of this study. This, in turn, suggests that any water quality changes during the 1994-95 study period were occurring quite slowly. However, it is quite possible that more rapid changes in pool water quality could occur in response to unusually heavy precipitation events. Indeed, rapid filling of cave pools has been reported following periods of heavy rainfall (McLean 1994). Comparing the major ion concentrations determined in this study with those reported previously by Thrailkill (1965) and Caldwell (1991), the results for particular pools appear quite similar. This suggests, but does not prove, that large changes in water quality have not occurred in most of the pools over a period of three decades.

The chloride concentration of most of the pool waters is surprisingly low, generally between 5 and 20 mg/L. If pool water evaporates slowly over time, but the pool does not leak, then a gradual increase in chloride concentration over time should be expected. The only pool that contains elevated chloride concentrations is Iron Pool (Cl^- = 840 mg/L). Because all other pools contain relatively low chloride levels, this suggests that chloride and other solutes are being carried away from the pools, either by leakage through pool bottoms, or overflow along the edges. This conclusion is supported by previous data reported by Thrailkill (1965) for some of the same pools (Mirror Lake, Green Lake), which indicates only minor change in chloride concentration over the past 30 years.

The chloride and bromide concentrations in Rookery Pool (4.3 and 0.06 mg/L) and in the nearby drip water that recharges the pool (5.2 and 0.07 mg/L) were similar, indicating little evaporative concentration of solutes in the pool. Given that the relative humidity above the pool is ~92 percent, and, thus, evaporation is occurring, we can infer that the evaporation rate from the pool surface is small compared with the leakage rate of water through its bottom, as discussed below.

GEOCHEMICAL MODELING

Table 2 shows calculated mineral saturation indices for selected minerals and water samples. Values greater than zero indicate mineral supersaturation, whereas values less than zero indicate undersaturation. The model results indicate that most of the pools are saturated or slightly supersaturated with respect to calcite and aragonite. The water in Longfellows Bathtub is at saturation with respect to gypsum, which is not surprising given the presence of this mineral. Based on the model results, the water in Iron Pool is somewhat supersaturated with respect to hydromagnesite, which is reasonable

Table 2. Mineral Saturation Index Calculated Using PCWATEQ

Location	Sample Date	Calculated Log PCO_2 (dissolved, in atm)	$SI_{aragonite}$	$SI_{calcite}$	SI_{gypsum}	$SI_{hydromagnesite}$
Devils Spring	8/6/94	-2.5	+0.38	+0.53	-1.4	-11.
Green Lake	8/6/94	-2.7	+0.31	+0.46	-2.6	-8.5
Horsehead Pool	8/6/94	-2.9	+0.43	+0.58	-2.7	-7.2
Iron Pool	8/7/94	-3.3	+0.70	+0.85	-1.5	+1.8
Lake of the Clouds	10/9/94	-2.4	-0.14	+0.01	-2.9	-11.
Longfellows Bathtub	10/8/94	-2.4	+0.22	+0.37	0.0	-14.
Mirror Lake	10/8/94	-2.4	-0.13	+0.02	-2.2	-14.
Rookery Pool	10/9/94	-2.7	+0.25	+0.40	-2.6	-8.8

given the abundance of this mineral in the moonmilk that lines the floor of this portion of Left Hand Tunnel.

CAVE ATMOSPHERE

The carbon dioxide concentration of the cave atmosphere above the pools ranges from that of fresh outside air ($10^{-3.5}$ atm = 350 ppm) to approximately 5 times greater than atmospheric. The lowest carbon dioxide concentrations in cave air are observed during the winter months when cold dense outside air sinks into the natural entrance, thereby freshening the cave atmosphere (McLean 1971). Based on the geochemical modeling, the partial pressures of carbon dioxide in the pool waters themselves are 2 to 10 times greater than those of the cave atmosphere (Table 2), suggesting that the pools represent a continuous source of carbon dioxide to the cave air. This is in accordance with previous observations by McLean (1971). Relative humidity (RH) of the cave air follows similar seasonal trends, with the lowest RH values occurring in winter, when pulses of cold, dense, dry air sink into the Natural Entrance.

TRACER TEST

The results of the bromide tracer test are shown in table 3. Pool volumes calculated from dilution of the bromide tracer ranged from <1 m³ for Sword of Damocles Pool to 550 m³ for Lake of the Clouds. The volume of Lake of the Clouds was undoubtedly even larger in the past, as evidenced by the large subaqueous mammillary concretions (clouds) that are now exposed far above lake level (Hill 1987). Calculated volumes for most of the other pools are in the range of 10 to 50 m³.

Mean residence times were calculated from the bromide tracer test results for each pool. The residence time may be thought of as the average time that a water molecule spends in the pool, assuming steady state conditions. Steady state implies that pool volume remains constant over time, or stated differently, inflow equals outflow.

Mean residence times were calculated using the loss of bromide over time (Table 3). Residence times ranged from less than a year for Rookery Pool and Devils Spring to 16 years for Lake of the Clouds. Figure 2 shows an example plot of the bromide tracer data for Devils Spring. In this plot, C/C_0 represents the ratio of the bromide concentration in the pool at any given time to its initial (or highest) concentration following addition of the bromide tracer. When the natural log of C/C_0 is plotted versus time, a straight line should result whose slope is proportional to the mean residence time. The time required for loss of half of the tracer initially present ($C/C_0 = 0.5$ or $\ln C/C_0 = -0.69$) is equivalent to the mean residence time.

In general, the calculated residence times were much longer than expected. In addition, some of the pools showed anomalous tracer test results that appeared puzzling at first. For example, bromide concentrations at Lake of the Clouds climbed steadily for the first 100 days following introduction of the tracer, then declined slowly thereafter. This was due to our inability to achieve thorough initial mixing of the tracer in this large lake. Instead, the bromide tracer slowly diffused throughout Lake of the Clouds, effectively delaying the onset of the test.

For any reservoir in steady state, it can be shown that the mean residence time is equal to the turnover time (T_0), which is defined as the ratio of the volume of the reservoir to its flux rate into or out of the reservoir:

$T_0 = V/Q$
where: V is pool volume (L)
Q is inflow rate or outflow rate (L/s)

Because we have calculated the pool volumes based on the initial dilution of the bromide tracer, it is possible to estimate the inflow rate (or outflow rate) by solving for Q in the equa-

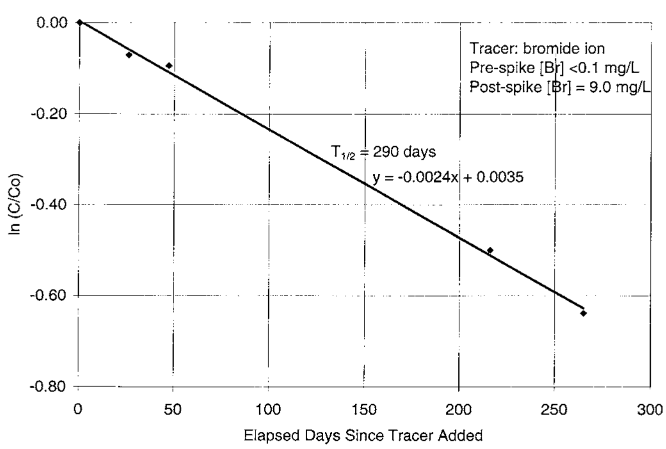

Figure 2. Plot of bromide tracer data for Devils Spring.

Table 3. Bromide Tracer Test Results.

Pool Name	Mass NaBr (g)	Date Tracer Introduced	Sample Date	Elapsed Days	Br Conc. (mg/L)	C/Co	ln(C/Co)	Est. Pool Volume (m3)	Br Loss Rate (yr-1)	Mean Res. Time (yrs)	Est. Leakage Rate (L/day)
Big Shelf Pool	75	2/19/95	2/23/95	3	12.4	1.00	0.00	6	0.07	9.3	2
			2/26/95	6	12.3	0.99	-0.01				
			3/5/95	13	12	0.97	-0.03				
			4/8/95	47	11.9	0.96	-0.04				
			9/24/95	216	11.6	0.94	-0.07				
			11/12/95	265	11.6	0.94	-0.07				
Devils Spring	200	2/19/95	2/20/95	0	8.9	1.00	0.00	22	0.9	0.8	75
			3/18/95	26	8.3	0.93	-0.07				
			4/8/95	47	8.1	0.91	-0.09				
			9/24/95	216	5.4	0.61	-0.50				
			11/12/95	265	4.7	0.53	-0.64				
Green Lake	340	2/19/95	2/23/95	3	7.8	1.00	0.00	44	0.6	1.2	100
			2/26/95	6	7.7	0.99	-0.01				
			3/5/95	13	7.9	1.01	0.01				
			3/18/95	26	7.7	0.99	-0.01				
			4/8/95	47	7.7	0.99	-0.01				
			9/24/95	216	5.9	0.76	-0.28				
			11/12/95	265	5.1	0.65	-0.42				
Lake of the Clouds	1200	4/9/95	4/9/95	0	0.2	0.09	-2.40	550	0.04	16	94
			4/17/95	8	0.7	0.32	-1.15				
			4/23/95	14	1	0.45	-0.79				
			5/6/95	27	1.4	0.64	-0.45				
			5/29/95	50	1.9	0.86	-0.15				
			11/12/95	217	2.2	1.00	0.00				
			12/8/96	609	2.1	0.95	-0.05				
Longfellows Bathtub	300	2/19/95	2/20/95	0	17.8	1.00	0.00	17	NM	NM	NM
			2/23/95	3	18.6	1.04	0.04				
			2/26/95	6	19	1.07	0.07				
			3/5/95	13	20.5	1.15	0.14				
			3/18/95	26	21	1.18	0.17				
			4/8/95	47	21.1	1.19	0.17				
			9/24/95	216	20.5	1.15	0.14				
			11/12/95	265	17.4	0.98	-0.02				
Mirror Lake	150	2/19/95	2/23/95	3	14.9	1.00	0.00	10	0.3	2.3	12
			2/26/95	6	14.2	0.95	-0.05				
			3/5/95	13	14.3	0.96	-0.04				
			9/24/95	216	12.6	0.85	-0.17				
			11/12/95	265	11.7	0.79	-0.24				
Rookery Pool	400	2/19/95	2/23/95	3	12.2	0.91	-0.09	30	1	0.7	117
			2/26/95	6	12.4	0.93	-0.08				
			3/5/95	13	13.4	1.00	0.00				
			4/8/95	47	12.6	0.94	-0.06				
			9/24/95	216	7.6	0.57	-0.57				
			11/12/95	265	6.3	0.47	-0.75				
Sword of Damocles Pool	13	2/19/95	2/23/95	3	16.5	1.00	0.00	0.8	0.9	0.8	3
			2/26/95	6	16.2	0.98	-0.02				
			3/5/95	13	14.9	0.90	-0.10				
			4/8/95	47	13.6	0.82	-0.19				
			9/24/95	216	10.7	0.65	-0.43				
			11/12/95	265	8.5	0.52	-0.66				

tion above. Leakage rate values calculated in this manner for each pool are shown in table 3, and range from 2 L/day to over 100 L/day. The pools with the highest leakage rates appear to be Rookery Pool, Green Lake, and Lake of the Clouds. Given its large volume, however, the leakage rate of Lake of the Clouds is remarkably low, possibly attributable to sealing of the pool bottom by precipitation of subaqueous calcite.

The long residence times indicated by the tracer tests would suggest that the pools evaporate more water than they leak. However, evaporation should result in an accumulation of dissolved chloride and other solutes in the pools, making them progressively more saline with time. Except for Iron Pool, this does not appear to be the case, and most of the pools contain very fresh water, with no buildup of salts. This is consistent with the stable isotopic composition of the water, which indicates little evaporative concentration of heavy isotopes (Ingraham *et al.* 1990; Chapman *et al*. 1992). Taken together, these observations suggest that the pools are recharged primarily by infrequent precipitation events, separated by long quiescent periods of slow evaporation and minimal leakage.

CONCLUSIONS

Chemical analysis of water samples collected from pools in Carlsbad Cavern reveals large differences in water quality among the different pools sampled, but little change in water quality for a particular pool during the two-year study period during 1994-95. While most pools contain fresh water of the calcium-magnesium-bicarbonate type, brackish water is found in some pools where evaporation rates are high and/or soluble evaporite minerals are present. Bromide tracer tests suggest mean water residence times in the pools ranging from less than one year to 16 years. The relatively long residence times for some pools indicate that leakage rates are slow. However, the low concentrations of dissolved ions observed in most of the pools demonstrate that leakage or overflow rates are sufficient to prevent evaporative buildup of solutes in these pools over time.

ACKNOWLEDGMENTS

The author is very grateful to the following cavers for assistance in collecting the pool water samples and performing field measurements: Cindy Brustad, Jay Brustad, Harry Burgess, Jackie Burgess, Sharon Chong, Scott Christenson, Fred Douglas, Eileen Graham, Lois Gronseth, Debra Harrison, Peter Hollings, Lee Hopwood, Pat Jablonsky, Cece Jimenez, John Leland, Jennie McDonough, Esty McLane, John McLean, Dave Milligan, Ray Nance, Michael Queen, Jason Richards, Linda Starr, and Doug Warner. Sharon Chong assisted the author in performing the laboratory analyses. Dale Pate and Jason Richards of Carlsbad Cavern National Park provided logistical assistance and encouragement. Daniel B. Stephens & Associates, Inc. provided financial and technical support, and the use of field and laboratory instruments. The author also appreciates the constructive comments of June Mirecki, Carol Hill, and Donald Davis, who reviewed the manuscript.

REFERENCES

American Public Health Association (APHA) (1992). Standard methods for the analysis of waste and wastewater. Method 2510 (Electrical Conductivity): 2-43 to 2-47.

Bowen, E. (1998). Hydrogeology of Rattlesnake Springs, independent study paper as partial fulfillment of MS degree in Hydrology, New Mexico Tech, Socorro: 171 pp.

Boyer, P. S. (1964). Analysis of cave waters from Carlsbad Caverns. Senior thesis, Dept. of Geology, Princeton University, May 1, 1964: 58 pp.

Brooke, M. (1996). *Infiltration pathways at Carlsbad Cavern National Park determined by hydrogeologic and hydrochemical characterization and analysis.* MS thesis, Colorado School of Mines.

Caldwell, D. E. (1991). Limnological survey of cavern pools. Unpublished report to Carlsbad Caverns National Park: 31 pp.

Chapman, J.B., Ingraham, N.L. and Hess, J.W. (1992). Isotopic investigation of infiltration and unsaturated zone flow processes at Carlsbad Cavern, New Mexico. *Journal of Hydrology 133*:343-363.

Draeger Company (1992). Draeger Detector Tube Handbook, 8th Edition, National Draeger, Inc.: 318 pp.

Hach Company (1992). *Water Analysis Handbook, 2nd Edition*: 831 pp.

Hill, C.A. (1987). Geology of Carlsbad Cavern & other caves in the Guadalupe Mountains, New Mexico and Texas. *New Mexico Bureau of Mines & Mineral Resources, Bulletin 117*: 150 pp.

Ingraham, N.L., Chapman, J.B. and Hess, J.W. (1990). Stable isotopes in cave pool systems: Carlsbad Cavern, New Mexico, U.S.A. *Chemical Geology 86*:65-74.

Jagnow, D.H. (1977). Geologic factors influencing speleogenesis in the Capitan Reef complex, New Mexico & Texas. MS thesis, University of New Mexico: 197 pp.

McLean, J.S. (1971). The microclimate of Carlsbad Caverns. *U.S. Geological Survey Open-File Rept. 71-198:* 67 pp.

McLean, J.S. (1976). Factors altering the microclimate in Carlsbad Caverns. *U.S. Geological Survey Open-File Rept. 76-171:* 55 pp.

Plummer, L.N., Jones, B.F., and Truesdell, A.H. (1976 revised 1978, 1984). WATEQF, a FORTRAN IV version of WATEQ, a computer program for calculating chemical equilibria of natural waters. U.S. Geological Survey Water Resources Investigations paper 76-13.

Thrailkill, J.V. (1965). *Studies of the excavation of limestone caves and the deposition of speleothems, Pt. 2: Water chemistry and carbonate speleothem relationships in Carlsbad Caverns, New Mexico*. PhD dissertation, Princeton University: 193 pp.

Thrailkill, J.V. (1971). Carbonate deposition in Carlsbad Caverns. *Journal of Geology 79:*683-695.

Van der Heijde, Paul K.M., Kolm, K.E., Dawson, H., and Brooke, M. (1997). Determining water infiltration routes from structures located above Carlsbad Cavern, Carlsbad Caverns National Park, New Mexico, International Ground Water Modeling Center Rept. GWMI 97-01: 88 p.

Williams, P.W. (1983). The role of the subcutaneous zone in karst hydrology. *Journal of Hydrology 61:*45-67.

H.J. Turin and M.A. Plummer - Lechuguilla Cave pool chemistry, 1986-1999. *Journal of Cave and Karst Studies 62*(2): 135-143.

LECHUGUILLA CAVE POOL CHEMISTRY, 1986-1999

H.J. TURIN

Los Alamos National Laboratory, Los Alamos, NM 87545 USA turin@lanl.gov

M.A. PLUMMER

New Mexico Institute of Mining and Technology, Socorro, NM 87801 USA

In May 1986, cavers dug into Lechuguilla Cave, in southeastern New Mexico, USA. Subsequent exploration and research have demonstrated that Lechuguilla is a world-class cave, both in size and in speleological importance. Of particular interest to hydrologists and geochemists are the numerous isolated pools throughout much of the cave. Since 1986, close to 200 water samples have been collected and subjected to over 2000 individual analyses. Results of these analyses are collected and published here for the first time.

Dominant cations in the pool waters are calcium and magnesium; dominant anions are bicarbonate and sulfate. These characteristics reflect the limestone/dolomite host bedrock of the cave, modified to varying degrees by the cave's massive gypsum deposits, associated with the cave's early development. The overall chemistry of the water can be explained by a small number of geochemical processes, starting with evaporation and concentration of local rainfall, and dissolution of soil CO_2 and local bedrock. Within the cave, excess CO_2 is degassed, leading to precipitation of $CaCO_3$ and increased Mg^{2+}:Ca^{2+} ratios. In some areas of the cave, infiltrating water encounters and dissolves gypsum, leading to increased $CaCO_3$ precipitation and increased SO_4^{2-}:HCO_3^- ratios. In at least one location, massive evaporation has created a magnesium sulfate brine. Geochemical characteristics seem to confirm that the pool located at Lechuguilla's current deep point is actually the regional aquifer, suggesting that the cave's maximum air-filled depth has been reached.

In May 1986, a team of cavers digging in a guano cave a few kilometers west of Carlsbad Cavern broke through into cave passage, thus setting off one of the most remarkable events in American cave discovery and speleology—the exploration of Lechuguilla Cave. Within a week over 1050 m of cave had been surveyed to a depth of over 210 m (Bridges 1988). Lechuguilla quickly appeared on lists of the world's longest caves and is currently the deepest known limestone cave in the United States. The rate of discovery and surveying of Lechuguilla has been truly astounding, and exploration continues to this day. The cave had a total surveyed length of over 170 km and depth of 475 m as of November 2000. Due in large part to the stewardship of the National Park Service and the foresight of the caving community, science has been a part of exploration of Lechuguilla Cave since the beginning. Important studies in the fields of geology (Polyak *et al*. 1998), speleogenesis (Hill 1995, 2000; Jagnow *et al*. 2000), mineralogy (Polyak & Güven 1996, 1999; DuChene 1997), cave biology (Northup *et al*. 1992), cave microbiology (Cunningham *et al*. 1995), geomicrobiology (Dotson *et al*. 1999; Spilde *et al*. 1999; Northup *et al*. 2000), and microclimatology (Cunningham & LaRock 1991) have all been conducted within the cave.

One of the most striking aspects of Lechuguilla, located beneath the semi-arid Chihuahuan desert, is the large number of pools scattered throughout much of the vertical and horizontal extent of the cave (Fig. 1). With few exceptions, the pools show neither obvious interconnections nor visible inflow or outflow other than flowstone seeps and ceiling drips. The pools, therefore, generally represent isolated samples of vadose-zone water infiltrating along separate and independent flow paths. As early as June 1986, the potential geochemical significance of these pools was recognized, and the first sampling and analysis program was initiated. Since then, seven different researchers have collected close to 200 pool and drip-water samples from the cave and have performed over 2000 analyses.

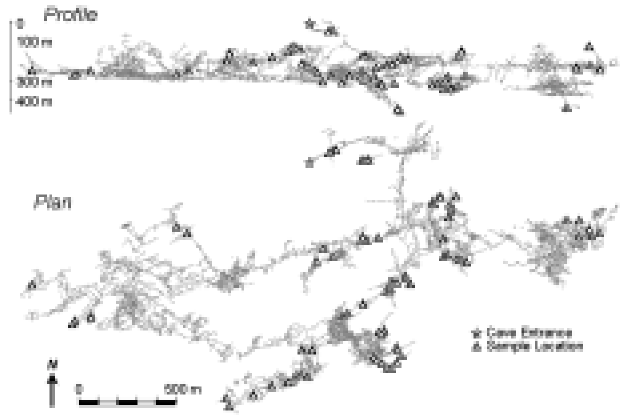

Figure 1. Map of Lechuguilla Cave, showing cave entrance and sample locations.

GEOLOGIC SETTING

Lechuguilla Cave lies within the Permian Capitan Reef Complex of the Guadalupe Mountains in southeastern New Mexico and west Texas. These same rocks host nearby Carlsbad Cavern and numerous smaller caves. The geology and speleogenesis of these caves have been described at length by Hill (1987). The upper passages of Lechuguilla penetrate the backreef rocks of the Artesia Group, while the main cave rooms are within the massive Capitan reef (Palmer *et al.* 1991). While the Capitan reef in the Guadalupe Mountains is a relatively pure limestone, the overlying backreef deposits include a mixture of limestone, sandstone, and dolomite. As the water analyses reveal, the dolomite has a profound effect on the local water geochemistry.

Sulfuric acid speleogenesis theories for the Guadalupe Mountain caves were first proposed in the early 1970s and are now widely accepted as the primary mechanism of cave formation (Jagnow *et al.* 2000). Hill (1987) amassed an impressive collection of geologic, geochemical, and isotopic evidence that points to oxidation of hydrogen sulfide migrating from Delaware Basin oil and gas fields as the source of the sulfuric acid that dissolved the limestone and dolomite, forming the caves. Hill's report was published just as Lechuguilla Cave was first being explored; Lechuguilla's massive gypsum deposits, formed by the reaction of sulfuric acid and limestone, provided further confirmation of this theory, as well as a major control on pool chemistry. In fact, the combination of limestone and dolomite bedrock and gypsum cave deposits together explains the wide variations in water chemistry within the cave.

WATER SAMPLING PROGRAMS

Seven different researchers have conducted water chemistry studies in Lechuguilla Cave; their results are presented in Tables 1-3. In some cases the researcher associated sample locations with established survey stations. This has the great advantage of being a permanent and recoverable site identifier, readily capable of being computer plotted onto cave maps and being correlated to mineralogical maps. Unfortunately, the vast majority of water sample locations have only been identified by descriptions based on informal cave feature names. These names are not standardized and are not readily available in the computerized survey databases. Furthermore, names have already changed in the short history of Lechuguilla exploration; Bitter Water Pool, Briny Pool, and Gorilla Piss Pool all refer to the same small puddle! With the help of other Lechuguilla surveyors and scientists, we have attempted to assign survey stations to all of the sampling locations. Any future samplers are strongly encouraged to tie their locations into the established survey system.

SAMPLE SETS:

GO Samples. Gregg Oelker, formerly of Montgomery Laboratories (Pasadena, CA), collected or coordinated the collection of 58 samples from the cave and three water supply samples between June 1986 and April 1990. pH and alkalinity titrations were conducted within 48 hours; remaining major-ion and trace-element analyses were performed on appropriately preserved (but unfiltered) samples using a variety of analytical techniques (ion chromatography, ion-specific electrode, atomic absorption/emission) in accordance with EPA protocols by Montgomery Laboratories. The results of these analyses were collated in an unpublished report (Oelker 1990). Oelker did not assign sample identification numbers; the numbers used in this paper (GO-1 through GO-61) correspond to their order in his report.

KC Samples. Kimberley I. Cunningham, formerly with the U.S. Geological Survey (Lakewood, CO), determined sulfate concentrations of six pools in April 1989. In-cave measurements were conducted using a Hach kit; reported values are the average of at least three analyses and are estimated to be precise to within 1 mg/L.

AP Samples. Arthur Palmer of the State University of New York-Oneonta and Margaret Palmer (Oneonta, NY) collected 17 samples between August 1988 and June 1994. pH and temperature measurements were conducted in the cave; remaining analyses were conducted in Oneonta and at the Illinois State Water Survey. Sample numbers shown are Palmer's, with the "AP" prefix added. The three 1988 Pellucidar samples were collected in support of an investigation of the formation of subaqueous helictites; these results were published by Davis *et al.* (1990). The remaining analyses have not been previously published.

WW Samples. Win Wright of the United States Geological Survey (Durango, CO) collected ten samples in October 1989 and February 1990. pH and temperature measurements and alkalinity titrations were conducted in the cave at the sampling site; additional analyses were conducted by the U.S. Geological Survey. The sample numbers shown in the tables were assigned by the authors. These data are published here for the first time.

DN Samples. Diana Northup of the University of New Mexico (Albuquerque, NM) coordinated the collection of 22 water samples in 1991 and 1992. In a few cases, in-cave pH measurements were made; other analyses were conducted at the University of New Mexico. Northup's research area is in microbiology rather than chemistry, and that directed her choice of analyses. Results of the 1991 analyses were presented in an unpublished report (Northup *et al.* 1992); the 1992 data are presented here for the first time.

JT Samples. Jake Turin (senior author of this paper) of Los Alamos National Laboratory (Los Alamos, NM) collected 27 cave water samples and one local aquifer sample between June 1992 and November 1999. pH and temperature were measured at the sample site using an in-cave calibrated pH meter and digital thermometer; alkalinity titrations, ion chromatography and ICP/AES (inductively-coupled plasma/atomic emission spectroscopy) analyses were performed on filtered and pre-

Table 1. Identification and description of cave and aquifer samples. The abbreviated table appearing here demonstrates the format of the full table, available on the internet at http:www.caves.org/pub/journal/volume62.htm.

Sample ID	Date Collected	Location Description	LCP/LEARN Survey Station	Field pH	Field T(C)
GO-1	6/1/86	Lake Lechuguilla	A10	8	
KC-1	4/16/89	Sulfur Shores	FNM13		
AP-LG1	7/89	Lake Louise, rafts, mam. pool	EC58	7.92	20.3
WW-2	2/25/90	Bitter Pool (Briny Pool)	FK5	8.25	
DN-MB-10	10/14/91	Lost Pecos River	MB10		
JT-LC92-01	6/6/92	Sugarlands	CA12	8.5	19.2
HD-LB1a	1/15/96	Liberty Bell Room: 1st pool from entrance	A9	8.54	

served samples at Los Alamos National Laboratory. These data are published here for the first time.

HD Samples. Helen Dawson of the Colorado School of Mines (Golden, CO) collected 58 samples between January 1996 and April 1997. pH measurements were made in the field using either a pH meter or pH indicator paper, field anion measurements were made using Hach kits, and cations were measured at the Colorado School of Mines by ICP/AES. One aspect of Dawson's work was repeated sampling of the same pool to determine temporal trends. While she used the same sample identification for each analysis, we have appended lower-case letters to her sample identifications to differentiate different sampling episodes. These data are published here for the first time.

Aquifer Samples. Eleven analyses of water samples from the regional Capitan aquifer are included in the tables for comparison purposes. These analyses include three samples collected by Oelker, one collected by Turin, and seven analyses published by Hill (1987: Table 2). The latter are given a "CH" prefix in the tables.

ANALYTIC RESULTS AND DISCUSSION

Eleven water samples from the regional aquifer and 197 samples of cave pool and drip water are listed and described in table 1, together with pH and temperature values where available. Location descriptions are as provided by the original researcher; corresponding survey stations are listed when possible. Figure 1 shows the cave pool sample locations, table 2 lists major-ion analyses and calculated saturation indices where appropriate, and table 3 lists trace element and minor-ion analyses. Note that only applicable samples appear in table 2 and table 3; i.e. a sample that was not analyzed for trace elements will not appear in table 3. Of the available data, the GO, WW, and JT sample sets have the most complete and directly comparable analyses. Excluding the Briny and Dilithium Pool samples, these three sets include 90 different samples.

In addition to the chemical analyses presented in this paper, a small number of Lechuguilla pool samples have been collected for stable isotope (Hill 1996: 321 & 452; Wright unpub. data) and tritium analysis (Turin & Plummer 1995; Wright unpub. data). A discussion of these results is outside the scope of the present paper. We are currently involved in a major new isotopic study of Lechuguilla pools; the older results and new results will be presented and discussed in a future publication.

MAJOR-ION ANALYSES

The major ions found in Lechuguilla cave pool water include Ca^{2+}, Mg^{2+}, Na^{+}, K^{+}, HCO_3^{-}, Cl^{-}, SO_4^{2-}, and NO_3^{-}. The other major dissolved constituent present is SiO_2. These nine parameters are listed in table 2, together with TDS (total dissolved solids) and, when possible, calculated SI (saturation indices) for calcite, dolomite, gypsum, quartz, and chalcedony, and calculated PCO_2 (partial pressure of CO_2).[1] Mean values and coefficients of variation for the eight major ions and silica for the 90 GO, WW, and JT samples are shown in table 4. All available analyses are plotted on a modified Piper diagram in figure 2. This plot differs from the familiar Piper diagram in that the cation axes have been rearranged to emphasize variations in the Mg:Ca ratio, and NO_3^{-} has been combined with Cl^{-} on the anion axes.[2] Figure 3 shows a plot comparing calcite and dolomite SI values for both cave pool and aquifer samples. Note that several of the AP alkalinity values are markedly lower than most other researchers' results. This phenomenon, possibly attributable to differences in analytical methods, has caused many of the AP points to appear as outliers, above and to the right of the bulk of the samples in the central field of figure 2, and below and to the left in figure 3.

[1] The SI and PCO2 values were calculated using the SI program (based on the Debye-Hückel equation) for almost all of the samples; PHRQPITZ (based on the Pitzer equation and the MacInnes convention), was used for the three samples collected from the Briny Pool (samples GO-20, WW-2, and JT-LC95-02). In order to calculate SI values, relevant ion concentrations, pH, and temperature are all required. If no temperature was recorded, a value of 18.5°C (the average pool temperature measured for the JT cave samples) was assumed for cave samples, and a value of 23.0°C (the measured value for White City Well sample JT-LC94-06) was assumed for aquifer samples. If a pH or relevant ion concentration value was missing, SI values were not calculated. In two cases, reported values were judged extremely unlikely (the pH value of GO-33 and the Ca^{2+} concentration for DN-PL); these samples are not plotted nor are SI values reported.

[2] For a number of WW samples, alkalinity values were not available; for some DN samples, the reported alkalinity values were judged unreliable and for some AP samples no $Na^{+} + K^{+}$ values were available. In these cases, missing values were estimated by charge balance; the estimated values are italicized in table 2. Note that these estimated values are used only for Figure 2; they were not considered reliable enough for SI calculations.

Table 2. Major-ion analyses and saturation indices (SI) of cave and aquifer samples. Values estimated by charge balance are italicized. SI is expressed as (2/n) log(IAP/Ksp), where n is the number of ions per mineral formula (e.g. 2 for calcite, 4 for dolomite). The abbreviated table appearing here demonstrates the format of the full table, available on the internet at http:www.caves.org/pub/journal/volume62.htm.

Sample ID	Ca^{2+}	Cl^-	K^+	Mg^{2+}	Na^+	NO_3^-	SiO_2	SO_4^{2-}	Total Alk. as HCO_3^-	TDS (calc.)	SI Calcite	SI Aragonite	SI Dolomite	SI Gypsum	SI Quartz	SI Chalcedony	log P_{CO_2}
	(mg/L)										(2/n) log(IAP/K_{sp})						(atm)
GO-1	38.6	4.3	0.7	43.3	3.8	4.4	12.2	45	275	425	0.45	0.30	0.57	-2.2	0.36	0.06	-2.6
KC-1								17.5									
AP-LG1	40.08			27.47													
WW-2	60	4100	650	5400	4500	3900		23300	1,190	43100	0.43	0.24	1.65	-0.9			-2.6
DN-HB-1	23	3.0	0.62	29.5	4.75	3.32		19.5	61	145	-0.07	-0.22	0.08	-2.7			-2.6
JT-LC92-01	22.9	2.74	1.54	28.2	3.41	48.7	11.8	16.5	161	286	0.54	0.39	0.69	-2.8	0.32	0.03	-3.3
HD-LB1a	23	10	0.90	64.1	2.19	10.6	8.19	50.0	342	510	0.82	0.67	1.15	-2.4	0.17	-0.12	-3.1

Table 3. Trace-element and minor-ion analyses of cave and aquifer samples. The abbreviated table appearing here demonstrates the format of the full table, available on the internet at http:www.caves.org/pub/journal/volume62.htm.

Sample ID	Al	As	B	Ba	Br	Cr	Cs	Cu	F	Fe	Li	Mo	NH_4	Ni	Pb	PO_4	Rb	Sr	V	Zn	TOC	DOC
											(mg/L)											
GO-1	<0.1	<0.002	<0.025	0.16		<0.01		<0.02	0.23	<0.02		<0.01		<0.02	<0.002			0.16		<0.02		
WW-2										12												
DN-MB-10																					1.78	1.70
JT-LC92-01	<0.1	<0.05	0.14	0.28	0.02				0.36	<0.01	0.02		<0.05			<0.05		0.13		<0.01		
HD-LB1a	<0.02	<0.05	0.028	0.084		<0.005		<0.002			<0.002	<0.01		<0.01		0.08		0.094	0.004	<0.002	1	

The dominant cations in the cave pools are calcium and magnesium and the dominant anions are carbonate, bicarbonate and sulfate, reflecting the calcite and dolomite host bedrock and the gypsum deposits within the cave system. The distribution of these major ions is a product of the geochemical processes that affect local precipitation as it moves downward into the cave system. These processes, including evaporation, root-zone CO_2 enrichment, bedrock and gypsum dissolution, CO_2 degassing and speleothem precipitation, are described in detail in the geochemical evolution section below.

Although carbonate and gypsum elements dominate the chemistry of the pools, other major species are present as well, including silica, potassium, sodium, chloride and nitrate. Silica is derived from detrital sand and silt within the bedrock, especially in the backreef facies of the Artesia Group Yates Formation, which either contains or overlies most of the cave (Hill 1987; Palmer *et al*. 1991). The relatively low CV (Table 4) and clustering of SI values near zero (Table 2) suggest that silica concentrations are controlled by chalcedony solubility. No obvious bedrock sources of potassium, sodium, or chloride overlie the cave, and it is likely that these ions are derived from local atmospheric input, concentrated to varying degrees by evaporation both in the near-surface soil and in the cave itself. Table 5 shows averaged precipitation concentrations (reflecting both precipitation and dry fallout) and enrichment factors, calculated as the ratio of average pool concentration to average precipitation concentration. Enrichment factors for these three relatively nonreactive ions are similar, ranging from 27 to 36. Their nonreactive behavior is further demonstrated by their similar degree of variability (Table 4) and by positive correlations between the three (Na-Cl $r^2 = 0.52$; Na-K $r^2 = 0.41$).

Table 4. Mean concentrations and coefficients of variance for major ions and silica for 90 GO, WW, and JT samples (excluding Briny and Dilithium Pools).

Constituent	Average Concentration (mg/L)	Coefficient of Variation
Ca^{2+}	34.1	29%
K^+	0.9	44%
Mg^{2+}	36.9	29%
Na^+	3.7	41%
Cl^-	3.6	47%
NO_3^-	6.9	100%
SO_4^{2-}	42.6	97%
Total Alk. (as HCO_3^-)	234.1	22%
SiO_2	11.3	28%

Nitrate's reactive behavior is revealed by its low enrichment factor (Table 5) and high variability (Table 4). Two possible sources for nitrate in the cave pools are atmospheric deposition and in-cave biological activity, both natural and anthropogenic. Nitrate's relatively low enrichment factor suggests that some atmospheric nitrate is lost during infiltration, perhaps in the root zone. An in-cave nitrate source is indicated by high nitrate levels (>20 mg/L) found in areas with known guano deposits (Sugarlands, samples JT-LC92-01 and DN-SU), heavily traveled near-surface sites (Lake Lechuguilla, samples GO-1 to GO-5, and the Liberty Bell, samples GO-55 and GO-56), and a pool near a popular cave camping site that shows signs of microbiological colonization (Pink Dot Pool,

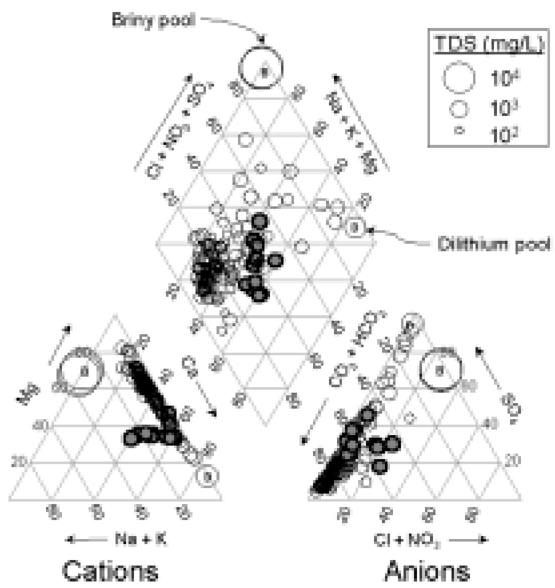

Figure 2. Piper diagram of water sample chemistry data with symbols proportional to log (TDS) for Lechuguilla cave pools (open circles) and aquifer samples (solid circles).

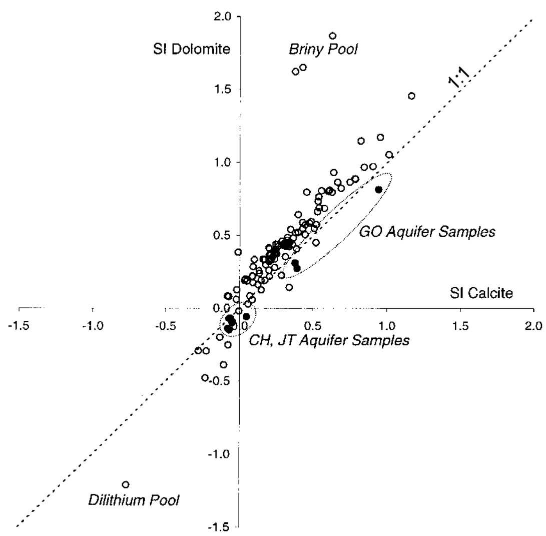

Figure 3. Plot of saturation index (SI) for calcite versus SI for dolomite. Cave samples are shown as open circles and aquifer samples as solid circles.

HD-46A samples). The spotty nature of these occurrences is reflected in the very high overall variability in nitrate concentrations (Table 4).

TRACE ELEMENT ANALYSES

Results of trace-element analyses with at least one detection are shown in table 3. In addition to these analyses, the JT, GO, and HD sample sets were analyzed for additional constituents shown in table 6; none of these additional analyses resulted in detectable concentrations at the detection levels shown in the table. (Iron concentrations reported for the WW samples were significantly higher than those reported by other investigators, even when the same pool was sampled. This suggests that there may be an analytical problem with these samples.)

Table 5. Mean precipitation concentration at Guadalupe Mountains National Park, 1984-1997. Atmospheric deposition concentrations measured at Guadalupe Mountains National Park by the National Atmospheric Deposition Program (1998).

Constituent	Mean Concentration (mg/L)	Enrichment Factor (pool/precipitation)
Ca^{2+}	0.454	75
K^{+}	0.024	36
Mg^{2+}	0.039	954
Na^{+}	0.106	35
$NH_4{}^{+}$	0.222	0
Cl^{-}	0.135	27
$NO_3{}^{-}$	0.774	9
$SO_4{}^{2-}$	1.124	38
pH	5.258	

Most of the trace-element analyses resulted in non-detects, but a few interesting patterns emerge. Trace elements that were consistently detected include barium, fluoride, and strontium. All three of these elements have been associated with local sulfur and Mississippi Valley-type ore deposits (Hill 1996). Of these three, fluoride and strontium showed a positive correlation ($r^2 = 0.77$), and both appeared somewhat correlated to silica ($r^2 = 0.74$ for F, $r^2 = 0.51$ for Sr). This suggests that there may be a silicate mineral source of both fluoride and strontium in the pool waters. (The correlation does not appear to reflect similar geochemical behavior—if this were the case, fluoride and chloride would correlate closely, but their r^2 is only 0.29). Barium showed no significant ($r^2 > 0.10$) correlation with any other species.

Table 6. Additional trace elements and minor ions not detected in any analyses. Detection limits (mg/L) are given in parenthesis.

JT	GO	HD
Ag (0.005 - 0.05)	Ag (0.01)	(13 samples in table 3)
Cd (0.0002 - 0.002)	Be (0.005)	Ag (0.003)
Co (0.002)	Cd (0.003)	Cd (0.002)
I (0.01 - 0.02)	Co (0.025)	Co (0.005)
Mn (0.01)	Hg (0.001)	Mn (0.015)
$NO_2{}^{-}$ (0.02 - 1)	Mn (0.02)	Ti (0.001)
S_2O_3 (0.01 - 0.1)	Se (0.002)	
Sb (0.0002 - 0.1)	Ti (0.002)	
	Tl (0.005)	

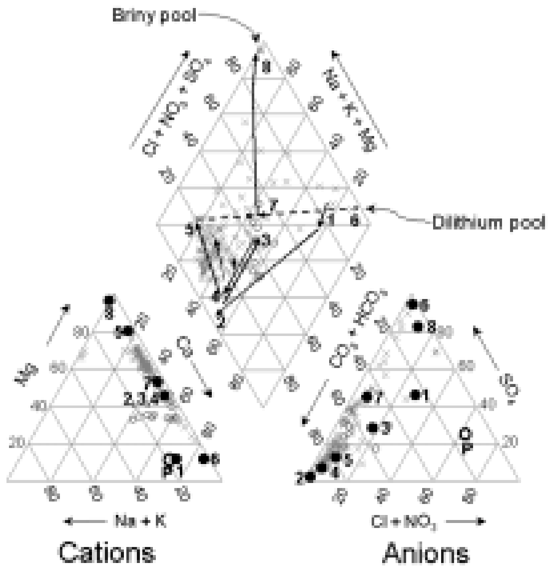

Figure 4. Piper diagram illustrating the modeled geochemical evolution of cave pool water. Refer to text for explanation.

TIME-SERIES ANALYSES

During the 14 years of analyses presented in this paper, numerous pools were sampled more than once. While this should provide an opportunity to look for water chemistry trends, that task is complicated by problems with pool identification caused by inconsistent use of survey station IDs and pool names, and the inevitable variability introduced by different sampling and analytical methods. When the data are carefully evaluated, most of the pools with repeated samplings show either constant chemistry (within 10-20%), or inconsistent "noisy" signals, with concentrations bouncing up and down.

One notable exception is Lake Lechuguilla, which was sampled eight times between 1986 and 1997 (samples GO-1 to GO-5 and HD-LL1a, b & c). The major-ion analyses for these samples are presented in table 7. Between 1986 and 1990, the pool showed a major increase in sulfate and nitrate concentrations, balanced by a slight increase in calcium and a decrease in alkalinity. This trend reversed itself between January 1996 and April 1997, with the latest samples returning to near-1986 values. Lake Lechuguilla is relatively close to both the cave entrance and the ground surface, and has experienced major water-level changes over the last decade. The chemical changes cannot be attributed to evaporative concentration, because chloride levels have not varied along with nitrate and sulfate. The changes may reflect the natural variability of precipitation chemistry, the introduction of pedogenic sulfate and nitrate, or human contamination. This phenomenon merits further monitoring and research.

GEOCHEMICAL EVOLUTION OF POOL CHEMISTRY

The major-ion geochemistry of the Lechuguilla pools is summarized in two plots: the modified Piper diagram (Fig. 2) and a plot comparing saturation indices for calcite and dolomite (Fig. 3). These plots suggest that the samples can be divided into four populations: Capitan aquifer water (including Lake of the White Roses), typical cave pool water, Briny Pool water, and Dilithium Pool water. The first two categories demonstrate the range of geochemical processes that determine the chemistry of water as it moves from the surface down toward the water table, while the last two examples are special cases; end-members of a particular process.

AQUIFER SAMPLES

The eleven aquifer analyses presented in table 2 break down into two distinct groups. The JT and CH analyses show water that is in equilibrium with calcite and dolomite, with an elevated PCO_2 of $10^{-1.8}$ atm. These points cluster close to the origin of figure 3. The GO samples, on the other hand, are supersaturated with respect to calcite and dolomite, show a lower PCO_2 of $10^{-2.8}$ – $10^{-2.2}$ atm, and extend upward from the origin of Figure 3 along a 1:1 line. This difference is due to degassing of the GO samples between sampling and analysis. The JT and CH analyses more accurately reflect actual aquifer conditions.

The aquifer water originates as precipitation at the ground surface. As the water infiltrates through the soil and root zone, evapotranspiration concentrates the dissolved ions, elevated biogenic CO_2 levels in the root zone force CO_2 into solution, and the resulting carbonic acid-enhanced water dissolves cal-

Table 7. Major-ion analyses of Lake Lechuguilla, 1986-1997.

Sample ID	Date Collected	Ca^{2+}	Cl^-	K^+	Mg^{2+}	Na^+ mg/L	NO_3^-	SiO_2	SO_4^{2-}	Total Alk. (HCO_3^-)
GO-1	6/1/86	38.6	4.3	0.7	43.3	3.8	4.4	12.2	45	275
GO-2	3/30/88	31.1	4.2	0.9	42.7	4.4	4.3	12.0	52	250
GO-3	10/24/88	28.9	4.2	0.9	39.5	3.2	6.2	10.3	47	232
GO-4	6/1/89	41.1	4.1	0.9	49.8	4.3	11.9	12.0	130	202
GO-5	4/7/90	77.2	5.5	1.6	58.5	4.5	38.5	12.0	250	183
HD-LL1a	1/15/96	35	10	1.31	39.3	3.69	8.4		100.0	220
HD-LL1b	6/9/96						6.2		56.3	351
HD-LL1c	4/3/97		10				5.3		67.7	

cite and dolomite as it moves downward through the rock. The result is the high-PCO_2, calcite/dolomite-saturated water exemplified by the JT and CH aquifer samples. These samples show an average Mg:Ca molar ratio of 0.68, close to the predicted ratio of 0.78 for a calcite/dolomite equilibrated solution at 23°C, a measured aquifer sample temperature (Mg:Ca molar ratios at different temperatures were predicted using PHREEQC; Parkhurst 1995).

TYPICAL POOLS

Cave pool water starts in the same way as the aquifer water, as precipitation infiltrating through soil, evaporating, and dissolving CO_2, calcite, and dolomite. Before this water reaches the water table, however, it encounters cave passage with lowered CO_2 levels due to mixing with atmospheric air. As a result, CO_2 pressures in the cave (mean = $10^{-2.7}$ atm) are typically less than the $10^{-1.8}$ atm value of the aquifer samples but greater than the atmospheric level of $10^{-3.5}$ atm. Infiltrating water entering the cave thus degasses CO_2 and tends to become supersaturated with respect to carbonate minerals. The degree of supersaturation reached is largely a function of the difference between the soil-zone CO_2 pressure encountered during infiltration, which may be highly variable, and the CO_2 pressure within the cave. Supersaturation of calcite and dolomite occurs in a 1:1 ratio as a result of CO_2 degassing and most of the pool samples fall along that line in a plot of the saturation index of dolomite versus saturation index of calcite (Fig. 3). Evaporation of pool water would also cause supersaturation along a 1:1 line, but would lead to a correlation between saturation and chloride concentration. With the exception of the Briny Pool (discussed below), no such correlation exists.

Both calcite and dolomite are supersaturated in most of the pool samples showing that precipitation and re-equilibration is not instantaneous, and that kinetic factors determine observed chemistry. Although both calcite and dolomite precipitation are rate-limited, dolomite precipitation is particularly slow (Appelo & Postma 1996; Hill & Forti 1997). As a result, calcite preferentially precipitates, decreasing the degree of supersaturation of calcite relative to that of dolomite and increasing the Mg:Ca molar ratio of the water beyond the predicted equilibrium ratio of 0.90 at 18.5°C, the average cave pool temperature. Most of the pool samples have Mg:Ca molar ratios greater than one (mean, excluding Briny Pool samples, equals 1.9) and plot left of the 1:1 line on figure 3.

In some cave passages, water also encounters gypsum, formed during the original sulfuric acid dissolution of the cave (Hill 2000). Dissolution of gypsum adds both calcium and sulfate to the water, which can cause supersaturation and subsequent precipitation of calcite via the common-ion effect and incongruent dissolution of dolomite, if present. This precipitation mechanism has been identified as the source of subaqueous helictites in a number of Lechuguilla pools (Davis *et al.* 1990; Davis 2000). The lack of correlation between Mg and SO_4 in our data suggests that most water/gypsum interactions occur below dolomite bedrock horizons.

LAKE OF THE WHITE ROSES

The current deep point of Lechuguilla is Lake of the White Roses, in the cave's Far East section. The 30-m depth of this pool and its surveyed location relative to local groundwater elevations have led to speculation that the pool is, in fact, a window on the regional Capitan aquifer. The pool's chemistry, represented here by 3 samples (GO-53, WW-10 & DN-MNBX), supports this hypothesis. The samples' average Mg:Ca molar ratio of 0.82 more closely resembles the average aquifer sample ratio of 0.68 than the average cave pool (neglecting the Briny Pool) ratio of 1.9, and the calculated PCO_2 value of sample GO-53 of $10^{-1.7}$ atm is much closer to the average aquifer value of $10^{-1.8}$ atm than the average cave pool (without the Briny Pool) value of $10^{-2.7}$ atm.

DILITHIUM POOL

The Dilithium Pool (sample GO-37) is named for the spectacular selenite (gypsum) crystals that have apparently grown within the pool. It represents an extreme case of gypsum dissolution in Lechuguilla; it is the only pool in the cave that is gypsum-saturated and is, in fact, slightly supersaturated in gypsum. Despite the high Ca concentration, the very low alkalinity (73 mg/L HCO_3^-) reported for the pool indicates that it is undersaturated with respect to calcite (SI = -0.77). This combination of gypsum supersaturation and calcite undersaturation is somewhat enigmatic. The Dilithium Pool is in a small chamber beneath a large room containing massive gypsum deposits, affording ample opportunity for feed water to become gypsum-saturated. Supersaturation could then be triggered by cooling, evaporation, or dissolution of a non-gypsum calcium or sulfate phase. Cooling of water at equilibrium with calcite and gypsum would produce the observed direction of changes in saturation, but a sufficient cooling mechanism is not obvious. Evaporation would tend to increase the saturation of both gypsum and calcite, and would result in elevated chloride concentrations. On the contrary, the Dilithium Pool chloride concentration is the lowest in the cave. On the senior author's 1992 visit to the Dilithium Pool, selenite needles appeared to be growing from pockets of mineral debris that had fallen into the pool from walls of the chamber. A sample of this debris was collected from the walls and analyzed by X-ray diffraction. It consisted primarily of quartz and calcite, with minor amounts of unidentified sulfate phases. Dissolution of this material could thus cause gypsum supersaturation, but cannot explain the calcite undersaturation.

None of these explanations is wholly satisfactory, and the Dilithium Pool problem merits further investigation. One possibility that cannot be dismissed is analytical error. A small error in the alkalinity measurement may explain the puzzling calcite undersaturation, while an error in the chloride measurement could restore evaporation as a valid explanation. Both alkalinity and chloride concentrations are low relative to the sulfate concentration, making this a challenging water to analyze accurately. Only one sample from the Dilithium Pool has been analyzed and explanations for the existing results will likely remain speculative until confirmatory analyses are produced.

BRINY POOL

The Briny Pool (samples GO-20, WW-2, JT-LC95-02) (formerly called the Bitter Water Pool) represents another extreme in the range of chemical composition seen in the Lechuguilla samples. On the basis of both chemistry and morphology, it has previously been interpreted as the highly evaporated remnant of a much larger pool (Davis *et al.* 1990). The concentration of chloride in the pool suggests that as much as 99.99 percent of the original water has evaporated from that pool. Again, because of the kinetic barrier to dolomite precipitation, this has led to extensive supersaturation of dolomite (SI = 1.72) relative to calcite (SI = 0.48) and the highest Mg:Ca ratio (159) of the cave pool samples.

While many of the pools in nearby Carlsbad Cavern show evaporation effects due to the large natural entrance (Forbes 2000), with the exception of the Briny Pool, the pools of Lechuguilla, with no present-day natural entrance, show little evidence of evaporation. The presence of a ringtail skeleton near the Briny Pool suggests that at one time, there may have been a natural entrance nearby. An investigation into the mechanism and timing of such a major evaporation episode and its possible connection to a former cave entrance seems worthwhile.

GEOCHEMICAL MODELING

To illustrate the dominant processes in the geochemical evolution of the pool water, we performed a series of simple experiments with the geochemical modeling program PHREEQC (Parkhurst 1995). Results are summarized as a series of connected paths on the Piper diagram (Fig. 4). These simulations are intended to demonstrate the processes that produce "typical" Lechuguilla water, rather than any one specific pool. As discussed earlier, the different pools represent different independent flowpaths from the ground surface. Each flow path will have slightly different evaporation, bedrock, trace mineral, and PCO_2 characteristics, leading to the observed variability in chemistry.

The starting solution for the model was the average composition of local precipitation (Table 5). This composition is marked with a "P" on figure 4. In step 1, the composition of the precipitation was adjusted to reflect presumed plant uptake of nitrate in the root zone by decreasing the nitrate concentration to match the average cave-pool nitrate:chloride ratio. We then equilibrated the solution with calcite and dolomite bedrock (step 2) and represented evapotranspiration by removing sufficient water to match the average chloride concentration in the cave pools (step 3). Uptake of CO_2 in the root zone was simulated by increasing PCO_2 level to $10^{-1.5}$ atm while maintaining calcite/dolomite equilibrium (step 4). Note that although we modeled steps 1-4 sequentially and plotted them as such, in reality they all occur more or less simultaneously during infiltration.

As the water enters the cave, it degasses CO_2, becoming supersaturated with respect to carbonate minerals, and begins precipitating calcite. As discussed earlier, this is a kinetically limited process. Because our simple model does not account for kinetics, we've simulated this process by decreasing PCO_2 to the average cave level, while maintaining equilibrium with calcite, but not dolomite (step 5). Three different step 5 arrows are shown on figure 4, representing different starting points, corresponding to slightly different soil PCO_2 levels. Note that these step 5 pathways traverse the bulk of the cave pool samples. The location of the different pools along the step 5 pathways reflects different degrees of calcite precipitation. At this point, we've simulated the major characteristics of the typical cave pool; simulating the chemistry of the Dilithium Pool and the Briny Pool required additional processes.

The Dilithium Pool chemistry differs from the other pools by its gypsum saturation. This pool was simulated by equilibrating the composition produced at the end of step 5 with gypsum (step 6). This point closely corresponds to the actual Dilithium Pool point (Fig. 4). The Briny Pool composition reflects a major evaporation episode; such a process is difficult to simulate using PHREEQC, which is limited to relatively dilute solutions. Furthermore, our simulation exercise was restricted to major ions and minerals and did not include minor minerals, such as celestite, magnesite, or hydromagnesite that are known to occur in Lechuguilla (DuChene 1997), and which will become important under high-evaporation conditions. Nevertheless, we explored the limits of our simulation by simulating the evaporation of a mixture of 92.5% "typical" pool water and 7.5% Dilithium Pool water. This mixing is shown in figure 4 as step 7, and the ensuing evaporation is step 8. As can be seen, this pathway moves in the general direction of the Briny Pool composition, but the simulated Briny Pool has higher magnesium and sulfate concentrations than the actual pool. Inclusion of additional magnesium and sulfate minerals in the simulation would help remedy this discrepancy.

CONCLUSIONS

The data presented here represent a major compilation of chemical analyses from one of the best-studied and most geochemically diverse caves in the world. The chemistry of the water is initially determined by precipitation chemistry, the bedrock that hosts the cave, and the gypsum deposits that date from the sulfuric acid formation of the caves. The water is then modified by present-day geochemical processes, including speleothem deposition, evaporation, and interaction with biological activity. Together, these processes result in diverse chemical compositions that reveal the complexity of the cave geochemical environment. The authors hope that these data will provide other researchers with the raw material for more in-depth analysis and characterization of cave processes.

ACKNOWLEDGMENTS

The authors express their profound gratitude to our colleagues who graciously shared their data for this paper. We also thank our numerous caver friends who lugged the JT samples out of the cave with us, and Ron Kerbo, David Ek, Dale Pate, and the staff of the Carlsbad Caverns National Park Cave Resources Office who permitted and enthusiastically supported these expeditions. This manuscript was vastly improved by review comments by Carol Hill, Carol Wicks, and Donald Davis. The senior author thanks Wes Myers, Fraser Goff, and the Laboratory-Directed Research and Development Program of Los Alamos National Laboratory for their support, and Bill Peachey, without whom none of this would have ever begun.

REFERENCES

Appelo, C.A.J. & Postma, D. (1996). *Geochemistry, groundwater and pollution*. Rotterdam. A.A. Balkema: 536 pp.

Bridges, R.A. (1988). The exploration of Lechuguilla Cave. *National Speleological Society News 46*(10): 372-376.

Cunningham, K.I. & LaRock, E.J. (1991). Recognition of microclimate zones through radon mapping, Lechuguilla Cave, Carlsbad Caverns National Park, New Mexico. *Health Physics 61*(4): 493-500.

Cunningham, K.I., Northup, D.E., Pollastro, R.M., Wright, W.G. & LaRock, E.J. (1995). Bacteria, fungi and biokarst in Lechuguilla Cave, Carlsbad Caverns National Park, New Mexico. *Environmental Geology 25*(1): 2-8.

Davis, D.G. (2000). Extraordinary features of Lechuguilla Cave, Guadalupe Mountains, New Mexico. *Journal of Cave and Karst Studies 62*(2): 147-157.

Davis, D.G., Palmer, M.V. & Palmer, A.N. (1990). Extraordinary subaqueous speleothems in Lechuguilla Cave, New Mexico. *NSS Bulletin 52*: 70-86.

Dotson, K.E., Schelbe, R.T., Spilde, M.N., Crossey, L.J. & Northup, D.E. (1999). Geochemistry and mineralogy of corrosion residue, Lechuguilla and Spider Caves, Carlsbad Caverns National Park, NM: Biogeochemical processes in an extreme environment. *Geological Society of America Abstracts with Programs 31*(7): A-154.

DuChene, H.R. (1997). Lechuguilla Cave, New Mexico, U.S.A. In C. A. Hill & P. Forti (eds.), *Cave minerals of the world. 2nd ed*. Huntsville, AL. National Speleological Society: 343-350.

Forbes, J.R. (2000). Geochemistry of Carlsbad Cavern pool waters, Guadalupe Mountains, New Mexico. *Journal of Cave and Karst Studies 62*(2): 127-134.

Hill, C.A. (1987). Geology of Carlsbad Cavern and other caves in the Guadalupe Mountains, New Mexico and Texas. *New Mexico Bureau of Mines & Mineral Resources, Bulletin No. 117:* 150 pp.

Hill, C.A. (1995). Sulfur redox reactions: Hydrocarbons, native sulfur, Mississippi Valley-type deposits, and sulfuric-acid karst in the Delaware Basin, New Mexico and Texas. *Environmental Geology 25*(1): 16-23.

Hill, C.A. (1996). *Geology of the Delaware Basin, Guadalupe, Apache, and Glass Mountains, New Mexico and West Texas.* Permian Basin Section - SEPM, Publication No. 96-39*:* 480 pp.

Hill, C.A. (2000). Overview of geologic history of cave development in the Guadalupe Mountains, New Mexico and west Texas. *Journal of Cave and Karst Studies 62*(2): 60-71.

Hill, C.A. & Forti, P. (1997). *Cave minerals of the world. 2nd ed*. Huntsville, AL. National Speleological Society: 463 pp.

Jagnow, D.H., Hill, C.A., Davis, D.G., DuChene, H.R., Cunningham, K.I., Northup, D.E. & Queen, J.M. (2000). History of sulfuric acid theory of speleogenesis in the Guadalupe Mountains, New Mexico and west Texas. *Journal of Cave and Karst Studies 62*(2): 54-59.

National Atmospheric Deposition Program (1998). National Atmospheric Deposition Program (NRSP-3)/National Trends Network, NADP Program Office, Illinois State Water Survey, Champaign IL.

Northup, D.E., Carr, D.L., Crocker, M.T., Hawkins, L.K., Leonard, P. & Welbourn, W.C. (1992). Lechuguilla Cave Biological Inventory. Unpubublished Report, Carlsbad Caverns National Park files: 177 pp.

Northup, D.E., Dahm, C., Melim, L.A., Spilde, M.N., Crossey, L.J., Lavoie, K.H., Mallory, L.M., Boston, P.J., Cunningham, K.I. & Barns, S.M. (2000). Evidence for geomicrobiological interactions in Guadalupe caves. *Journal of Cave and Karst Studies 62*(2): 80-90.

Oelker, G.L. (1990). The Lechuguilla Cave Water Study. Unpubublished Report, Carlsbad Caverns National Park files*:* unnumbered pp.

Palmer, A.N. (1996). *Instructions for Use of SI Program, Version 3.01.* State University of New York, Oneonta, Unpub. Report: unnumbered pp.

Palmer, A.N., Palmer, M.V. & Davis, D.G. (1991). Geology and origin of Lechuguilla Cave. In M.R. Taylor (ed.), *Lechuguilla - Jewel of the underground.* Basel. Speleo Projects: 22-31.

Parkhurst, D.L. (1995). User's guide to PHREEQC - A computer program for speciation, reaction-path, advective-transport, and inverse geochemical calculations. *U.S. Geological Survey, Water-Resources Investigations Report No. 95-4227:* 143 pp.

Plummer, L.N., Parkhurst, D.L., Fleming, G.W. & Dunkle, S.A. (1988). A computer program incorporating Pitzer's equations for calculation of geochemical reactions in brines. *U.S. Geological Survey, Water-Resources Investigations Report No. 88-4153:* 310 pp.

Polyak, V.J. & Güven, N. (1996). Alunite, natroalunite, and hydrated halloysite in Carlsbad Cavern and Lechuguilla Cave, New Mexico. *Clays and Clay Minerals 44*(6): 843-850.

Polyak, V.J. & Güven, N. (1999). Authigenesis of a trioctahedral smectite in magnesium carbonate speleothems in caves of the Guadalupe Mountains, New Mexico. *Geological Society of America Abstracts with Programs 31*(7): A-154.

Polyak, V.J., McIntosh, W.C., Güven, N. & Provencio, P. (1998). Age and origin of Carlsbad Cavern and related caves from $^{40}Ar/^{39}Ar$ of alunite. *Science 279*: 1919-1922.

Spilde, M.N., Shearer, C.K. & Sharp, Z. (1999). Biogenic corrosion of bedrock at Lechuguilla and Spider Caves, Carlsbad Caverns National Park, NM: A stable isotope and trace element analysis study. *Geological Society of America Abstracts with Programs 31*(7): A-155.

Turin, H.J. & Plummer, M.A. (1995). Tritium in Lechuguilla Cave pool water: Implications for recharge processes. *Geological Society of America Abstracts with Programs 27*(6): 95.

Joyce Lundberg, Derek C. Ford, and Carol A. Hill - A preliminary U-Pb date on cave spar, Big Canyon, Guadalupe Mountains, New Mexico. *Journal of Cave and Karst Studies 62*(2): 144-148.

A PRELIMINARY U-Pb DATE ON CAVE SPAR, BIG CANYON, GUADALUPE MOUNTAINS, NEW MEXICO, USA

JOYCE LUNDBERG
Department of Geography, Carleton University, Ottawa K1S5B6 CANADA, jlundber@ccs.carleton.ca
DEREK C. FORD
School of Geography and Geology, McMaster University, Hamilton, L8S4K1 CANADA
CAROL A. HILL
17 El Arco Drive, Albuquerque, NM 87123-9542 USA, carolannhill@cs.com

U-Pb dating of a football-sized, dogtooth spar, calcite crystal collected from a cave in Big Canyon, Guadalupe Mountains, New Mexico, USA, gave an age estimate of 87 - 98 Ma for calcite deposition. This Upper Cretaceous (Laramide) date is important because: (1) it implies that there may have been a major karsting episode in the Guadalupe Mountains in the Laramide; (2) it implies that the Laramide was a time of heating and deeply circulating hydrothermal water; (3) it relates to the possible time of regional uplift above sea level of the Guadalupe Mountains along with the rest of the western United States; and (4) it relates to a time of possible hydrocarbon maturation and migration in the Delaware Basin.

Spar (or "geode") caves are lined with dogtooth and/or nailhead spar calcite crystals. In the Guadalupe Mountains, these can be small, individual caves or small to large rooms intercepted by later, larger, sulfuric acid cave passages. They can range from a few meters up to tens of meters or more in size, but most are (on the average) about 5 m. From fluid-inclusion temperature data (~30-85ºC), spar crystals in the Guadalupe Mountains are known to have precipitated from low-temperature hydrothermal water (Crysdale 1987; Hill 1987). Hill (1996) thought that spar in Guadalupe caves was Miocene (Basin and Range) because isotopically similar spar fills Basin and Range fault zones along the western escarpment of the Guadalupe Mountains.

The spar sample dated in this study (Sample 97CAH) was collected from a small (12 m long x 2 m wide) cave located in Big Canyon, Guadalupe Mountains (Fig. 1). It is a "football"-size crystal 40 cm long and 18 cm in diameter (at its center) that grew as a single crystal over time, from inside outward. The outermost 1 cm of the crystal is an opaque, white crust, probably the result of sub-aerial weathering, but its bulk interior consists of tight, inclusion-free, translucent calcite that can be assumed to have functioned as a system closed to any infiltration or leakage after its precipitation.

U-PB ANALYSES

In principle, the decay of ^{238}U to stable ^{206}Pb (and the decay of the rare isotope, ^{235}U to ^{207}Pb) function as chronometers that can be applied to all kinds of cave calcites. However, there has been little application of this method in karst studies hitherto because Pb is very widespread in nature and it is difficult to find speleothem samples that do not have significant amounts of it (common Pb) incorporated into the growing calcite; this background "noise" masks the U-Pb decay signal in perhaps

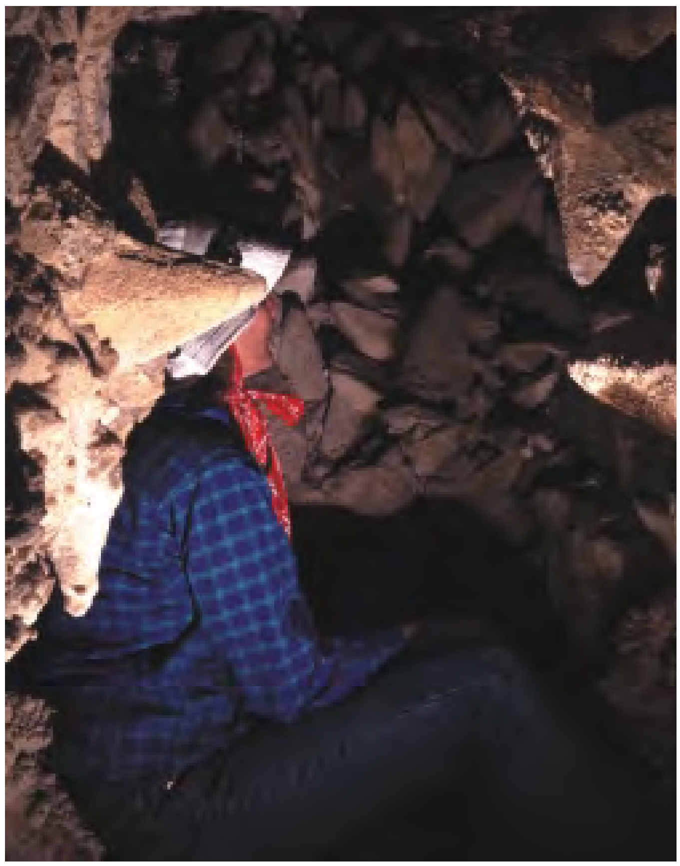

Figure 1. Dogtooth spar crystals lining a small "geode" cave in the area of Big Canyon, Guadalupe Mountains. Some of the spar crystals are as large as footballs. Photo by Alan Hill.

the majority of instances. This serious problem can sometimes be avoided by working with calcites that display big variations in U content from point to point. This causes the ratios of parent ^{238}U or daughter ^{206}Pb to non-radiogenic ^{204}Pb ($^{238}U/^{204}Pb$; $^{206}Pb/^{204}Pb$) in a sample to vary: the slope of the line drawn through a plot of results from varying sub-samples establishes the age (Ludwig 1977). For reviews of U-Pb dating of secondary calcites in caves and elsewhere see Smith *et al.* (1991) and Richards *et al.* (1996).

Two sets of three sub-samples of ~0.5 gm each were taken at intervals of 3-4 cm from the center to the inner (unweathered) edge of the crystal. In a clean room at McMaster University, the samples were dissolved and passed through ion exchange columns in 0.7M HBr form and the Pb extracted with 6M HCl. The U fraction was processed through a 7.5M HNO_3 column and extracted with 0.7M HBr. Isotopic ratios were measured by thermal ionization mass spectrometry on a VG 354 machine with a Daly detector in peak jumping mode. The Pb fraction was loaded with silica gel and run at 1400ºC, and corrected for fractionation using measured ratios from the NBS981 standard. The U fraction was run on a double filament, correcting for fractionation by using the average fractionation factor measured in natural uranium runs on the mass spectrometer during the preceding year. One of the central sub-samples failed to run. The analytical data for the remaining five sub-samples are given in table 1.

RESULTS

The mean age of the Big Canyon spar sample calculated with the $^{238}U/^{206}Pb$ dating equation is 91.3 Ma, plus or minus a two standard deviation error margin of 7.8 Ma. The age obtained with the $^{235}U/^{207}Pb$ equation we calculated conservatively as 108±46 Ma; Urs Klötzli, a U-Pb dating specialist who refereed the work, derived a more precise estimate of 95±7.3 Ma from our data. The lower intercept on a simple $^{207}Pb/^{206}Pb$ v. $^{238}U/^{206}Pb$ concordia plot yields an age of 86±12 Ma; using the calculated ratios of common Pb in the sub-samples to refine the isochron regression Klötzli obtained a more reliable lower intercept of 90.7±2.8 Ma.

It will be seen that these five age estimates are very close together, placing within one standard deviation of each other. Thus, the arithmetic mean age of spar sample 97CAH can be placed between 87 and 98 Ma with confidence. Because of the common Pb problem, it is probably infeasible to determine the difference in age between the oldest and youngest parts of the crystal; however, from the isochrons, this is likely to be much less than the range of 11 million years cited above.

DISCUSSION

The Upper Cretaceous date on the Big Canyon cave spar is important that these are the first "hard" data that specifically relates to Laramide events in the Guadalupe Mountains. Since the spar lines cave passages, it implies that spar caves are also at least this old; that is, there was possibly a major karst episode in the Guadalupe Mountains in the Laramide. This makes sense since a major uplift of an area should initiate karst dissolution in carbonate rocks. If this date is correct, then it strongly suggests that at least some spar-lined cave passages formed much earlier than has previously been supposed.

Fluid-inclusion temperatures of the spar also suggest that Guadalupe spar caves were formed by hydrothermal water. This in turn implies that a magmatic heat source existed below the Guadalupe Mountain-Delaware Basin area in the Laramide, and may have been responsible for regional uplift. This same heat source could also relate to the maturation and migration of hydrocarbons, and answer some pertinent questions concerning the timing of oil and gas migration into some of the big fields of the Delaware Basin area.

From an inter-regional perspective, this new information on the possible timing of the Guadalupe Mountain uplift may also relate to the "Alvarado Ridge" – a postulated north-trending Laramide continental arch that extended from Mexico to Wyoming (Eaton 1987). Thus, this one date reaches beyond purely speleogenetic considerations.

CONCLUSIONS

The U-Pb date adopted here should be considered preliminary for two reasons:

(1) Only one U-Pb date has so far been obtained on a spar crystal from a Guadalupe cave.

(2) It now appears from these very limited data that there may be (at least) two spar depositional episodes in the Guadalupe Mountains: one of Laramide age and one of Basin

Table 1. U-Pb analytical data for speleothem 97CAH.

Sub-sample	U (ug/g)	Pb (ug/g)	$^{238}U/^{204}Pb$	$^{206}Pb/^{204}Pb$	$^{235}U/^{204}Pb$	$^{207}Pb/^{204}Pb$
97CAH-FT	2.03±0.66*	0.11±0.29*	1504±0.7*	37.58±0.25*	10.91±0.69*	16.29±0.26*
97CAH-FM	0.22±0.62	0.13±0.17	101±0.7	19.10±0.14	0.73±0.68	15.30±0.14
97CAH-FB	0.07±0.62	0.52±1.43	7.3±1.4	17.06±1.22	0.05±1.37	14.48±1.10
97CAH-08	0.73±0.66	0.02±0.12	3725±0.7	70.43±0.11	27.02±0.73	17.88±0.13
97CAH-04	0.70±0.62	0.04±1.14	1219±1.3	32.54±1.00	8.84±1.28	16.13±1.10

* all error margins are quoted to two standard deviations.

and Range age. Spar crystals from other caves should now be dated to establish whether the cave spar linings are all of Laramide age.

Considering the importance of this one date to the understanding of regional, petroleum, and speleogenetic events, it is hoped that this dating program can be continued in the future.

ACKNOWLEDGMENTS

Lincoln National Forest gave permission to collect the (already broken) spar sample. Thanks to Denise Mruk Cox, Kurt Cox, Alan Hill, and Ransom Turner for helping to collect the sample. U-Pb dates were obtained in the McMaster University U-dating laboratory, aided by a research grant to Ford from the Natural Sciences and Engineering Research Council of Canada. The authors are indebted to Urs Klötzli (University of Vienna), and Art and Peggy Palmer (SUNY Oneonta), for their prompt and helpful refereeing of this late addition to the Guadalupe Symposium. Lincoln National Forest has requested that the name and location of the cave be kept secret. Inquiries should be made to Cave Specialist Ransom Turner, Lincoln National Forest, Federal Building, Carlsbad, NM 88220.

REFERENCES

Crysdale, B.L. (1987). *Fluid inclusion evidence for the origin, diagenesis and thermal history of sparry calcite cement in the Capitan Limestone, McKittrick Canyon, West Texas*: Unpublished MS thesis, University of Colorado: 78 pp.

Eaton, G.P. (1987). Topography and origin of the southern Rocky Mountains and Alvarado Ridge. In Coward, M.P. *et al.* (eds.). *Continental extensional tectonics*. Geological Society of America Special Publication 28: 355-369.

Hill, C. A. (1987). *Geology of Carlsbad Cavern and other caves in the Guadalupe Mountains, New Mexico and Texas*. New Mexico Bureau of Mines and Mineral Resources Bulletin 117: 150 pp.

Hill, C.A. (1996). *Geology of the Delaware Basin: Guadalupe, Apache and Glass Mountains, New Mexico and west Texas*. Society of Economic Paleontologists and Mineralogists, Permian Basin Section, Publication no. 96-39: 480 pp.

Ludwig, K. (1977). Effect of initial radioactive-daughter disequilibrium on U-Pb isotope apparent ages of young minerals. *Journal of Research of the United States Geological Survey, 5*: 663-667.

Richards, D.A., Bottrell, S.H., Cliff, R.A. & Strohle, K-D. (1996). U-Pb dating of Quaternary age speleothems. In Lauritzen, S-E. (ed.). *Climate change: The karst record.* Karst Waters Institute Special Publication 2: 136-137.

Smith, P.E., Farquhar, R.M & Hancock, R.G. (1991). Direct radiometric age determination of carbonate diagenesis using U-Pb in secondary calcite. *Earth and Planetary Science Letters, 105*: 474-491.

Donald G. Davis - Extraordinary features of Lechuguilla Cave, Guadalupe Mountains, New Mexico. *Journal of Cave and Karst Studies 62*(2): 147-157.

EXTRAORDINARY FEATURES OF LECHUGUILLA CAVE, GUADALUPE MOUNTAINS, NEW MEXICO

DONALD G. DAVIS
441 S. Kearney St., Denver, Colorado 80224-1237 USA (dgdavis@nyx.net)

Many unusual features are displayed in Lechuguilla Cave, Guadalupe Mountains, New Mexico, U.S.A. Early speleogenic features related to a sulfuric acid origin of the cave include acid lake basins and subterranean karren fields. Speleogenetic deposits, also products of sulfuric acid origin, include gypsum "glaciers" and sulfur masses. Features related to convective atmospheric phenomena in the cave include corrosion residues, rimmed vents, and horizontal corrosion/deposition lines. Speleothems of nonstandard origin include rusticles, pool fingers, subaqueous helictites, common-ion-effect stalactites, chandeliers, long gypsum hair, hydromagnesite fronds, folia, and raft cones. Other unusual features discussed are silticles and splash rings.

This paper was originally developed as a poster presentation for the Lechuguilla Cave geology session at the 1996 National Speleological Society Convention in Salida, Colorado. It is intended to convey an overview and basic understanding of the cave's remarkable suite of geologic features, some of which are virtually unique to this cave. Others were previously known but much better-developed and/or more abundant in Lechuguilla than elsewhere. Categories described here represent the peculiar things that make explorers experience Lechuguilla Cave as different from other caves. Following are the ones that seem particularly significant.

Lechuguilla Cave is a huge, bewilderingly complex, three-

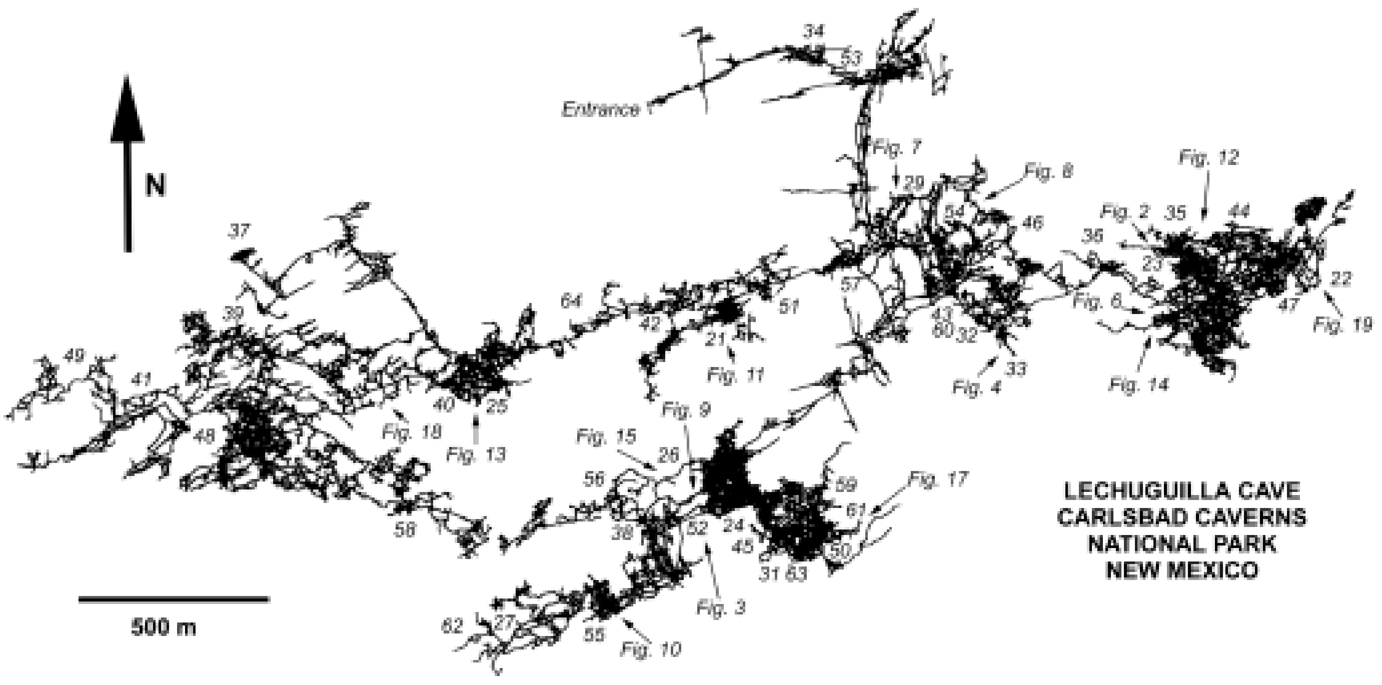

Figure 1. Line plot of Lechuguilla Cave. Guide to map locations: Nos. 2-18 are locations of figures in this paper; higher numbers below are named localities mentioned in the text. Blanca Navidad-19 Boundary Waters-20, Bryce Canyon-21, Chandelier Ballroom-22, Chandelier Graveyard-23, Darktown-24, Death Valley-25, East Rift-26, Emperors Throne Room-27, FLI Room-28, FUNC Survey-29, Ghost Town-30, Ghostriders Balcony-31 Glacier Bay-32, Glacier Way-33, Grand Illusion-34, Here be Dragons-35, Hoodoo Hall-36, Jackpot-37, Jewel Box-38, Keel Haul-39, Lake Louise-40, Lake of the Blue Giants-41, Lake of the White Roses-42, Land of the Lost-43, Land of Fire and Ice-44, MBF Survey-45, Mental Breakdown-46, Northern Exposure-47, Pearlsian Gulf-48, Pellucidar-49, Prickly Ice Cube Room-50, Rim City-51, Rusticles-52, Shangri-La-53, Shelobs Lair-54, Snow Whites Passage-55, Southern Climes-Stratosphere Room-57, Stud Lake-58, Sulfur Shores-59, Vesuvius-60, The Void-61, Western Borehole-62.

dimensional maze, 475 m deep, with more than 170 km of surveyed passage (Fig. 1). It fits the pattern defined by Palmer (1991) as a "ramiform maze," which is characteristic of caves of hypogenic (rising-fluid) origin. The cave consists largely of the following three morphologic elements: (1) large rooms and galleries; (2) intricate "boneyard" intergrading with breakdown or underlying larger voids; and (3) deep, rift-like, usually slanting slots, which also may underlie larger spaces. The rifts and some boneyard pits were probably feeder vents for ascending hydrogen-sulfide-rich fluids, which, upon mixing with oxygenated groundwater and/or reaching the water-table interface with air, developed sulfuric acid and dissolved the larger chambers. The input points probably moved eastward and downward over time as the Guadalupe Mountains were tilted during the late Tertiary and Quaternary periods (Hill 2000; Palmer & Palmer 2000).

Lechuguilla Cave, because it is deep and protected by its small entrance cross-section and tight siltstone caprock from rapid influx of surface water and air, has a geothermally-driven temperature gradient in which the present average temperature of the highest (entrance) part is about 2°C lower than its lowest parts. In the more vertical sections of the cave, this gradient drives convectional unidirectional airflow loops that cause evaporation in warmer areas and condensation in cooler. This process, which was probably more intense in the past, has contributed to unusual suites of interrelated, corrosive and depositional features in the cave.

Early Speleogens

Acid Lake Basins

An acid lake basin may be thought of as a "negative rimstone pool," where a pond of aggressive water once stood, eating away its floor and undercutting parts of the limestone walls (Fig. 2). A distinct line marking the ancient water surface was thereby created. At least five examples have been recognized in Lechuguilla Cave, the most impressive being in the East Rift in the Eastern Branch, and near the Pearlsian Gulf in the Southwestern Branch. I am not aware of identical cases, confined to limited basins, reported from any other cave, but aggressive water, at the top of a phreatic zone or floodwater zone, is known to form solution-beveled flat ceilings and wall notches in other caves (Ford & Williams 1989). Such wall notches, on a larger scale than the restricted basins mentioned here, were recently recognized in the Keel Haul to Northern Exposure area of Lechuguilla's Western Branch.

The East Rift acid lake basin has conical orifices in the pool floor, which seem to have been source vents for corrosive fluids and/or gases. Above the water line, upward-facing surfaces are grooved by fields of rillenkarren, suggesting rapid condensation of highly aggressive films of trickling moisture. This topic is considered further in the next section. At some of these basins, the rillenkarren are overlain by several centimeters of granular gypsum, implying that the sulfuric acid cave development process was still active when the cave had drained at least to the level of the acid lake in each area.

Subterranean Rillenkarren

Subterranean rillenkarren are spectacular deeply-grooved fields of limestone bedrock (Fig. 2), and are cave analogs of the rillenkarren that more commonly develop from rain and snow on surface karst exposures (Sweeting 1973). Such features have been noted in thermal caves such as Lower Kane Cave, Wyoming, but those in Lechuguilla Cave and Carlsbad Cavern are the best-developed examples known to the author.

The cave rillenkarren were not formed by infiltrating surface water. The ceilings overhead are usually smoothly rounded and show no signs of water influx. The karren usually cluster around floor joints, or small openings connecting to lower-level chambers (which commonly are floored with calcite-raft deposits). They are not active today, but seem to date from a time when the regional water table was lowering, and when the temperature gradient was relatively high. This drove a "distillation-retort" effect. High evaporation at the water level caused the calcite rafts to accumulate, and condensation of the rising vapor at cooler levels attacked the bedrock and breakdown, etching the karren fields and resupplying dissolved calcite to the water below as the condensate trickled back down (Davis 1982, 1995).

Subterranean rillenkarren have thus far been noted in the Guadalupe caves only in Lechuguilla, Carlsbad Cavern, and Mudgetts Cave (a small cave near Lechuguilla) - not in any of the otherwise similar caves elsewhere in these mountains. Lechuguilla and Carlsbad are also by far the largest Guadalupe caves known. This suggests that the presence of rillenkarren is related to a particularly high intensity of the sulfuric acid cave-development process, which might have generated temperatures high enough to drive sufficient evaporation/condensation to produce rillenkarren. The present temperature in these areas is about 20°C. The paleotemperature has not been determined, but was probably not above 35°C (Palmer & Palmer 2000). The elevated temperatures may have been caused by exothermic reactions involved in generation of hydrogen sulfide and its oxidation to sulfuric acid.

Speleogenetic Deposits

Gypsum "Glaciers"

Lechuguilla Cave contains thousands of tons of massive or laminated gypsum, which accumulated where groundwater flow was not strong enough to carry away all of the sulfate produced by the sulfuric acid reaction with the limestone when the cave was enlarging (Hill 1987). These gypsum deposits are up to 10 m thick.

Gypsum beds in Lechuguilla have been dissolved away from large areas of the cave by later seeping and dripping surface water, or by fresh-water reflooding below -290 m. The best-preserved remnants, in dry rooms and alcoves, are at least 30 m long in some places, and strongly resemble miniature ice glaciers. The similarities include "bergschrund" gaps at the upper edge of the mass; pits and "crevasses" in the body (Fig. 3), and "bergs" calving from the lower edge. These effects are produced by dissolution pitting and by undermining at the contact with moist underlying rock, rather than by mass flow and melting as in true glaciers. At least one good example can be seen in every branch of the cave, the best being in the following chambers: Glacier Bay, Land of Fire and Ice, Prickly Ice Cube Room, Blanca Navidad, and Stratosphere Room.

SULFUR MASSES

In most areas of the cave, hydrogen sulfide from oil and gas deposits oxidized completely to sulfuric acid (Hill 2000), which in turn attacked the limestone, enlarging the cave and forming gypsum deposits. Locally, however, the oxidation process stopped at elemental sulfur, which occurs as lemon-yellow pods and stringers up to 1 m thick embedded in larger masses of gypsum (Fig. 4). The sulfur, which may be massive, granular, or platy, has been exposed locally by dissolution of the surrounding gypsum. The deposits seem to be spontaneously oxidizing very slowly: one can smell sulfurous gases in the air up to about 60 m from some sulfur localities.

DuChene (1997) has noted that these sulfur deposits occur in places where fine-grained sandstone layers form the ceiling and/or walls: perhaps the sandstone had inhibited oxygenation or had stalled completion of the reaction chain by preventing all sulfur from oxidizing as quickly as it would in contact with carbonates. Massive and crystalline sulfur is also found in Cottonwood Cave (Davis 1973), and small deposits occur in Carlsbad Cavern, but Lechuguilla Cave may contain more sulfur than all other known caves in the world combined. There are deposits in all three branches of the cave. The best are in passages off Ghost Town, Ghostbusters balcony, the Void, and near the Blanca Navidad chamber.

In other parts of Lechuguilla Cave and Carlsbad Cavern are much smaller, yellow-crystalline encrustations, which for many years were also assumed by observers to be sulfur. These crystals have been determined to be tyuyamunite and metatyuyamunite, uranium-vanadium minerals that were mobilized in groundwater and redeposited in the caves (DuChene 1997; Hill & Forti 1997).

ATMOSPHERIC SPELEOFACTS

I use here the umbrella term "speleofacts," which encompasses both speleothems and speleogens (Lange 1959), because some of the entities described unite both speleogenic and speleothemic elements sharing a common geometry.

CORROSION RESIDUE

In many places in Lechuguilla Cave, where currents of warm, moist air rise from deeper levels and impinge on walls and ceilings, the bedrock is attacked by condensation, leaving a lacy mat of insoluble residue up to 2.5 cm or more thick (Fig. 5). When heavy enough, this residue can fall in patches to the floor, leaving sticky dark-colored splotches. Corrosion residue is composed largely of iron, manganese, and aluminum compounds, or silica where on siltstone matrix (Cunningham *et al*. 1995). The color ranges from dark brown (most common) to reddish, orange, yellow and black, depending on the substrate which may be limestone, siltstone, or vein calcite.

Similar residues occur in other caves having sufficient relief and temperature gradients to drive convective airflow cells (e.g., Wind Cave and Jewel Cave, South Dakota). But, as with other features considered in this paper, corrosion residues seem more profoundly developed in Lechuguilla Cave than elsewhere. The Lechuguilla corrosion residues have been found to host a dense population of microorganisms. The extent to which the microbes may be actually responsible for creating the residue, or may simply be using the residue network as a convenient habitation substrate, is not yet clear. Nor is their food source. The microbes are believed to be chemolithoautotrophic (using inorganic energy sources), because no substantial amount of organic matter comes from outside, because the nearest relatives of organisms isolated from the residues are chemolithoautotrophic, and because organisms cultured from residue samples produced iron and manganese oxides (Northup *et al*. 2000). However, the hypothesis that the microorganisms are oxidizing iron or manganese in the bedrock raises questions, as these walls have been in the zone of oxidation for millions of years and should be already fully oxidized. Cunningham *et al*. (1995) suggested that the bacteria may be utilizing traces of sulfur-compound gases dissolving into the condensate from the impinging air stream. This could explain why corrosion residues are not so well developed in caves less rich in sulfur.

RIMMED VENTS

Rimmed vents are a composite speleogen/speleothem, having one side corroded and the other encrusted. In Lechuguilla Cave, the encrustation may be composed of calcite, aragonite, or gypsum, and rarely hydromagnesite. The corroded side may be coated with corrosion residue. The rims may form ear-like projections from the walls of passages, as in Rim City in the entrance passage series, and above the Grand Illusion in the Far East (symposium back cover), but are more often seen at constrictions or intersections between passages, or around impenetrably small holes in floors. They were originally recognized as distinct entities in the Caverns of Sonora, Texas (Burch 1967), and then in Jewel Cave (Conn & Conn 1977) and elsewhere, but as with many other unusual speleofacts, they are probably more abundant and larger in Lechuguilla than at any other site reported. Some gypsum rims in Lechuguilla's Far East are up to 1 m high and extend for up to 5 m along the edge from which they grow.

The mechanism of rim formation is not well understood, but they are believed to develop via simultaneous condensation and evaporation in response to humidity gradients across a wall projection. The encrusted sides normally face the surface or the entrance (i.e., a source of cooler, drier air), while the corroded sides face the warmer, moister cave interior. The moisture condensing on the corroded side is assumed to dissolve the substrate there, then move by wicking action to the other side, where evaporation redeposits the material as a rim. In some places, aragonite rims form along walls and ceiling while gypsum rims grow on the floor at the same site, suggesting that slightly drier and therefore denser air tends to follow the floor.

The "Stingray Eyes" are tiny vents, rimmed with hydromagnesite, in the floor of the "Rusticles" area of the Near East. Hydromagnesite rims also occur in the FUNC Survey in the Southwestern Branch. As far as I know, hydromagnesite rims have been recognized only in Lechuguilla Cave.

HORIZONTAL CORROSION/DEPOSITION LINES

These strikingly horizontal boundaries have evaporative deposits such as gypsum crust and aragonite frostwork below, and bare corroded wall above (Fig. 6). If it were not that associated deposits are not subaqueous, they could easily be mistaken for water lines (in fact, a water line and an atmospheric line are juxtaposed within 2 m of each other in the Lake of the Blue Giants chamber). Corrosion lines are well developed in certain long passages and large chambers, such as Snow Whites Passage, the East Rift, Glacier Way, and Death Valley.

Corrosion/deposition lines mark long-term stratification of air in these chambers. A thermometer test above and below the line in Glacier Way did not reveal a measurable temperature difference. However, humidity stratification alone (more humid air being lighter, and therefore drifting to the top) would probably account for the air separation. As with rimmed vents, the result is condensation attack above the line, seepage of condensate downward, and evaporative redeposition below. Hill (1987) also measured higher CO_2 concentration along the ceiling of Left Hand Tunnel in Carlsbad Cavern, showing that air stratification can also enhance corrosion of the upper walls.

SPELEOTHEMS OF UNCONVENTIONAL ORIGIN

"BIOTHEMS"

Rusticles. These bizarre, eccentric stalactites and columns (Fig. 7) are largely confined to a limited area of the Near East of Lechuguilla Cave, although they also have been reported from an obscure passage off the route to the Lake of the White Roses deep point in the Far East. The cores are composed of iron oxide minerals which, as seen under the microscope, consist of fossil microbial casts. The outer shells are composed of calcite crust. The rusticles appear to have grown underwater where reduced iron-rich fluid was trickling from above into standing water, giving rise to subaqueous streamers of iron-mineral sheaths of iron-oxidizing bacteria (Davis *et al*. 1990). These streamers were originally very fragile; had they not been encrusted with calcite before the basin drained, they would probably have disintegrated and disappeared.

The name "rusticles" was borrowed from accounts of the discovery of the wreck of the ship *Titanic*, which was found to be draped with submarine iron-rust stalactites of similar appearance and, probably, origin. Stalactiform deposits in Fairy Cave, Colorado (another cave of hypogenic sulfide-related origin), are interpreted here as subaqueous rusticles, but they are far less spectacularly developed there. Rusticles should not be confused with subaerial iron dripstone which is common in other caves (Hill & Forti 1997).

The pool finger complex. In several old pool basins in Lechuguilla Cave are fields of stalactiform fingers, up to 50 cm long, that evidently grew underwater. They are commonly interconnected by parabolic u-loops. Unlike the rusticles, they are made of solid calcite, without more than traces of iron or other constituents. They resemble rusticles, however, in seeming to be based on encrustation of bacterial streamers, fossilized fragments of which in places may be seen underneath the fingers. They are best developed in basins that were at the lower end of a series of flowstone slopes and ponds; the feeder flowstone may itself contain fossilized bacterial strings as can be seen above the MBF survey locality (Davis 1990). With the possible exception of some nontypical fingers in Stud Lake, they are not active today, and the identity and food source of the bacteria involved are not known. Northup *et al*. (2000) discuss the connection of bacteria and pool fingers in this issue.

In one location off the FLI Room (Fig. 8), the fingers are accompanied by web-like sheets that have been called "webulites." Aside from being based on calcification of biaxial organic sheets rather than uniaxial strings, their origin is the same.

In some places, pool fingers are transitional to the longer-known subaqueous palisade-like speleothem called "chenille spar." Pool fingers and related forms are not unique to Lechuguilla Cave; they are also known from Nevada, northern New Mexico, Colorado, Arizona, Wyoming, and elsewhere. However, it was the particularly well-developed occurrence in Lechuguilla Cave that was first given the "pool finger" name (in Davis *et al*. 1990), and that led to their being classified as a distinct speleothem type by Hill & Forti (1997).

COMMON-ION EFFECT SPELEOTHEMS

Subaqueous helictites. When solutions of different chemicals mix, if they contain one ion that is the same, this may trigger crystallization of the less soluble species. Until the discovery of peculiar new speleothems in Lechuguilla Cave, this "common-ion effect" had been recognized as a factor in speleothem deposition only in a few cases, including growth of calcite flowstone in gypsum caves (Hill & Forti 1997: 142), and growth of the speleothems in subglacial Castleguard Cave in Canada (Atkinson 1983).

Then, subaqueous helictites - wormlike speleothems with tiny central canals (no previously recognized subaqueous speleothem had been known to have that structure), were found in Lechuguilla Cave. They were first seen in a large room called Pellucidar, then subsequently in about 30 other locations (Fig. 9). Within Lechuguilla Cave some are still submerged, whereas others are "dead" in dry basins. This discovery was unique; all helictites previously known had been assumed to have grown in air, from capillary seepage of moisture from the wall.

The subaqueous helictite sites share one property: the basins in which they grew were invariably fed by flowstone that ran under gypsum deposits in such a way as to dissolve gypsum into the water feeding the pool. This suggested that the common ion effect is responsible for subaqueous helictites: trickles of calcium-sulfate-enriched water flow into pools already saturated with calcium carbonate, introduce excess calcium ions, and cause rings of calcite to precipitate around the entry points. This confines the gypsum-bearing influx to tiny canals and extends the resulting growth into helictitic form. Analyses of the inflowing and ambient water (Davis *et al*. 1990) in the Pellucidar pool are consistent with this hypothesis.

Confirmed examples of subaqueous helictites of the Lechuguillan type remain almost confined to Lechuguilla Cave, probably because gypsum is excessively abundant there, and few other caves have gypsum in contact with active calcite flowstone. Other, less spectacular, subaqueous helictites have been reported from nearby Endless and Virgin Caves, New Mexico, in localities also well supplied with gypsum (Mosch 1996.)

"Helictite bushes" in Wind Cave, South Dakota, have also been recognized as being subaqueous in origin (Davis 1989a, 1991), but these are considerably different from the Lechuguillan helictites. They have large internal canals, and the water source was from below, not from gypsum-enriched flowstone seepage. Helictite bushes may be more closely related to submarine "smokers" than to the subaqueous helictites of Lechuguilla Cave.

Common-ion-effect stalactites. Subaqueous helictites are not the only Lechuguillan speleothems that involve the common-ion effect. As might be expected, it also seems to be significant in subaerial calcite deposition. The most prominent such case is that of certain aberrant stalactites. These stalactites tend to be isolated below sources of gypsum-enriched seepage. They are lumpy, wavy, and irregular, rather than smoothly contoured as is typical of normal stalactites. This may reflect uneven concentration of calcium ions, from incomplete mixing of the stringy source flows.

The most spectacular example of a presumed common-ion-effect stalactite is the Gripping Hand group (Fig. 10) near the Blanca Navidad room in the Western Branch (Davis & Petrie 1994). This group consists of a flattened, branching stalactitic mass about 4 m long, which resembles a giant moose antler. It feeds a pool containing subaqueous helictites.

Common-ion-effect stalactites smaller than the Gripping Hand occur in the Chandelier Graveyard, Here Be Dragons, and the Far East. In the Far East, some have their tips spread out into flattened pads. This may mean that they dipped into standing water, with the gypsum mixing causing a shelfstone ring to form before the rest of the water was sufficiently saturated to grow shelfstone around the entire passage (Fig. 11).

EVAPORATIVE SPELEOTHEMS

"Chandelier" stalactites and stalagmites. Evaporative conditions have long prevailed in much of Lechuguilla Cave, so it is not surprising that speleothems of evaporative origin are plentiful. These include relatively common forms such as aragonite frostwork, and more unusual types composed of gypsum.

The most imposing forms of gypsum may be classed as stalactites. Most of these are coarsely crystalline and eccentric, lacking central canals, and of much more complex outline than calcite stalactites. This is probably because gypsum tends to precipitate in crystals that are large with respect to the size of the speleothem. The cave's most famous feature is elaborately branching selenite "chandeliers," which have grown up to about 6 m long in the Chandelier Ballroom. Smaller ones are found in other parts of the cave (front cover). Chandelier stalactites are not unique to Lechuguilla. Others about as large exist in Cupp-Coutunn Cave, Turkmenistan (Maltsev 1997), and smaller examples have been noted elsewhere in New Mexico and in Wyoming, Colorado, and Utah (Hill & Forti 1997).

As with several other characteristic Lechuguillan features, the Chandelier Ballroom's extraordinary chandeliers seem to owe their development to airflow convection driven by temperature gradient, the convection in turn driving an evaporation/condensation cycle. In a maze level about 25 m above the Ballroom, condensation slowly dissolves massive floor gypsum. The resulting seepage evaporates after seeping into the Ballroom, depositing chandelier crystals.

Gypsum stalagmites and columns, usually hollow, are also common in Lechuguilla Cave. Some of these stalagmites also radiate chandelier-style selenite crystal arms downward and outward, like fossilized Christmas trees (Fig. 12). The best examples are up to 4.5 m high, in the Chandelier Graveyard. These "chandemites" are rarer, and some think more bizarre in appearance, than chandelier stalactites.

Long gypsum hairs. The chandeliers are amazingly massive gypsum growths, but Lechuguilla is also notable for incredibly delicate ones. The apogee of this is its superlong gypsum hairs. These can be almost invisibly thin, in places gently spiraling, and up to at least 6 m long. They were first seen near Lake Louise, and later found in larger sizes and numbers in Darktown (Fig. 13). The areas where they are well developed are lined with mammillary calcite crust. This substrate presumably has exactly the right pore size and structure to extrude the hairs.

In some places, including Land of the Lost and Shelobs Lair, aggregates of hairs form cottony, cloudlike puffs that move in the slightest breeze. Other relatively common gypsum forms, including flowers and needles, reach exceptional size - more than 1 m in drier parts of Lechuguilla Cave.

Hydromagnesite fronds. Hydromagnesite is often associated with aragonite and gypsum in evaporative parts of Lechuguilla Cave. It is commonly seen as moonmilk, "sand," and "krinkle blisters," and less often as balloons and intermediate forms. An uncommon form (previously undescribed to the author's knowledge) is curving, featherlike fronds, first noted in the Boundary Waters section of the Far East, and subsequently in the Southern Climes (Fig. 14) and Mental Breakdown areas of the Western Branch. When occurring singly, these are up to 10 cm long. In one case, many radiate from a single stem and curve upward, forming a 10 cm "tree", resembling an aragonite bush except for a chalky appearance and curving branches. Whether this is a pure hydromagnesite form, or is based on an aragonite core, is unknown.

Folia

Folia are sloping, contoured, interleaved shelves, normally composed of calcite (but rarely of mud, halite, or sulfur; Hill & Forti 1997), that cover overhanging walls and ceilings. In Lechuguilla Cave, folia are found almost exclusively within about 37 vertical meters of the present water table surface at the Lake of the White Roses and Sulfur Shores (Fig. 15), the deepest points of the cave. The details of folia development are not well understood, but appear to represent a water-table equivalent of shelfstone. Shelfstone maintains a distinct horizontal level because it is controlled by a fixed, perched overflow point. Folia shelves are sloping and overlapping because the calcite accretion attempts to follow the irregular fluctuations of a calcite-saturated water table. (A subaqueous interpretation has also been proposed - see Green 1996.) Unlike shelfstone, calcite folia are invariably associated with deposits of calcite rafts. They are usually found in caves of hypogenic (rising-water) origin, and are known from Nevada, Utah, Arizona, and Colorado, as well as New Mexico and Europe (Hill & Forti 1997). In Lechuguilla Cave, the level at which folia growth begins probably marks the time at which the final withdrawal of aggressive groundwater occurred.

Raft Accumulations and Cones

Calcite rafts develop as thin sheets on the surface of quiet, supersaturated water. They are fairly widely distributed in caves around the world, but are exceptionally abundant in parts of Lechuguilla Cave, where they form deep floor accumulations. Such deposits probably gathered as the groundwater surface drained past the lower levels of the cave, and seepage from above collected in increasingly isolated and restricted basins from which it evaporated. They may be, in part, the evaporative result of evaporation/condensation cycles in which condensation was causing corrosion effects such as rillenkarren at higher levels - in other words, another "distillation-retort" effect. There are at least two generations of old calcite rafts in Lechuguilla Cave: an older one represented by partly redissolved truncated raft cones in the Jackpot and Shangri-La rooms, and a younger one best developed in the Western Borehole. Only at the water table, and a few other pools, are rafts now actively growing in the cave.

When drops of water fall from fixed ceiling points above raft-covered water surfaces, the impacts may cause rafts to sink. Others drift into the resulting gaps and are sunk in turn, creating symmetrical stalagmite-like raft piles (called cave cones) beneath the water, 3 m or more high in places. When exposed by a declining water level, they may become encrusted or overgrown with aragonite frostwork. Encrusted raft piles can usually be distinguished from true stalagmites by their conical (rather than parabolic or cylindric) shape, reflecting the angle of repose of the heaped rafts. In some cases, however, the rafts are cemented together as they accumulate, forming towers much steeper than the angle of repose (Fig. 16).

Other Features

"Silticles"

Where flowstone-depositing seepage has access to fine sediment, and where it flows over ledges, the sediment may become cemented into comb-like fringes of stalactiform growths up to 25 cm long. The sediment is usually silt, but it may also be hydromagnesite moonmilk, as seems to be the case in the example shown in figure 17. Unlike true stalactites, silticles lack central canals and commonly taper to sharp points. They are prevalent in caves of the Guadalupe Mountains but have received little attention in the literature. Few, if any, of those in Lechuguilla Cave seem to be active today; they date from wetter times when water influx washed preceding deposits of loose silt or moonmilk over ledges.

Splash Rings

When water drops fall on cave floors, the splash rebound may spray out as a symmetrical corona around the impact point, falling in a partial or complete circle or ellipse up to 2 m in diameter. Depending on the water composition and the substrate, this may create either negative (speleogenic) or positive (speleothemic) rings on the floor. In Lechuguilla Cave, negative rings incised into gypsum (Fig. 18) and residual sediment are relatively common, the best display being in the Blanca Navidad room (one such incised ring has been seen in a calcite raft deposit). In the Vesuvius area of the cave, two positive splash rings have developed as raised welts on otherwise smoothly contoured flowstone (Davis 1989b).

Conclusions

On first impression, the features discussed in this paper seem heterogeneous and unrelated except that they all happen to be unusual characteristics of this one peculiar cave. On closer examination, however, many of them can be seen to be interrelated to each other by way of their dependence on the unusual origin of the cave from rising water charged with hydrogen sulfide and sulfuric acid (Palmer & Palmer 2000), or on convective airflow loops driven by the strong temperature gradient generated by the cave's large vertical relief.

Acknowledgments

My thanks to Harvey DuChene, who provided the accompanying photographs from his archive of pictures by many photographers, and digitized the location map; to Carol Hill and George Moore, who reviewed the draft and gave many useful suggestions; to the explorers of Lechuguilla Cave, without whom we would know none of this; and to the U.S. National Park Service managers who have expedited our studies.

REFERENCES

Atkinson, T.C. (1983). Growth mechanisms of speleothems in Castleguard Cave, Columbia Icefields, Alberta, Canada. *Arctic & Alpine Research 15*(4): 523-536.

Burch, J. (1967). Modification by chalkification. *Texas Caver 12*(1): 3-4, 16.

Conn, H. & Conn, J. (1977). *The Jewel Cave Adventure*. Zephyrus Press, Teaneck, NJ: 238 pp.

Cunningham, K.I., Northup, D.E., Pollastro, R.M., Wright, W.G. & LaRock, E.J. (1995). Bacteria, fungi and biokarst in Lechuguilla Cave, Carlsbad Caverns National Park, New Mexico. *Environmental Geology 25*: 2-8.

Davis, D.G. (1973). Sulfur in Cottonwood Cave, Eddy County, New Mexico. *Bulletin of the National Speleological Society 35*(3): 89-95.

Davis, D.G. (1982). Rims, rills and rafts: Shaping of cave features by water condensation from air (abs.). *Cave Research Foundation Annual Report 24*: 29.

Davis, D.G. (1989a). Helictite bushes - A subaqueous speleothem? *NSS Bulletin 51*(2): 120-124.

Davis, D.G . (1989b). Lechuguilla Cave: the ongoing saga. *Rocky Mountain Caving 6(2)*: 29-32.

Davis, D.G. (1990). The nation's deepest: Lechuguilla of the Guadalupes. *Rocky Mountain Caving 7*(2): 14-15.

Davis, D.G. (1991). Wind Cave helictite bushes as a subaqueous speleothem: Further observations. *Geo² 19*(1): 13-15.

Davis, D.G. (1995). Rims, rills and rafts: Shaping of cave features by atmospheric water exchange. *Geo² 22*(2): 23-29, 32.

Davis, D.G. & Petrie, G. (1994). Chipping away at the barrier. *Rocky Mountain Caving 11*(2): 8-11.

Davis, D.G., Palmer, A.N. & Palmer, M.V. (1990). Extraordinary subaqueous speleothems in Lechuguilla Cave, New Mexico. *NSS Bulletin 52*(2): 70-86.

DuChene, H.R. (1997). Lechuguilla Cave, New Mexico, U.S.A. In Hill, C.A. & Forti, P. (eds.). *Cave Minerals of the World, 2nd Ed*. National Speleological Society, Huntsville, AL: 343-350.

Ford, D.C. & Williams, P.W. (1989). *Karst Geomorphology and Hydrology*. Chapman and Hall, London: 601 pp.

Green, D.J. (1996). The origin of folia (abs.) *National Speleological Society Convention Program with Abstracts*. Salida, CO, Aug. 5-9: 41.

Hill, C.A. (1987). Geology of Carlsbad Cavern and other caves in the Guadalupe Mountains, New Mexico and Texas. *New Mexico Bureau of Mines & Mineral Resources, Bulletin 117*: 150 pp.

Hill, C.A. (2000). Overview of geologic history of cave development in the Guadalupe Mountains, New Mexico and west Texas. *Journal of Cave and Karst Studies 62*(2): 60-71.

Hill, C.A. & Forti, P. (1997). *Cave Minerals of the World, 2nd ed*. National Speleological Society, Huntsville, AL: 463 pp.

Lange, A.L. (1959). Introductory notes on the changing geometry of cave structures. *Cave Studies 11*: 69-90.

Maltsev, V. (1997). Cupp-Coutunn Cave, Turkmenistan. In Hill, C.A. & Forti, P. (eds.). *Cave Minerals of the World, 2nd ed*. National Speleological Society, Huntsville, AL: 323-328.

Mosch, C.J. (1996). Subaqueous helictites, Virgin Cave, New Mexico (abs.): *Journal of Cave and Karst Studies 58*(3): 209.

Northup, D.E., Dahm, C.N., Melim, L.A., Spilde, M.N., Crossey, Lavoie, K.H., Mallory, L.M., Boston, P.J., Cunningham, K.I. & Barns, S.M. (2000). Evidence for geomicrobiological interactions in Guadalupe caves. *Journal of Cave and Karst Studies 62*(2): 80-90.

Palmer, A.N. (1991). Origin and morphology of limestone caves. *Geological Society of America Bulletin 103*: 1-21.

Palmer, A.N & Palmer, M.V. (2000). Hydrochemical interpretation of cave patterns in the Guadalupe Mountains, New Mexico. *Journal of Cave and Karst Studies 62*(2): 91-108.

Sweeting, M.M. (1973). *Karst Landforms*. Columbia Univ. Press, New York, 356 pp.

Back cover (*Journal* page 50**): "The Ear" - gypsum rim, Far East. Photo by David Harris, Harris Photographic.**
Front cover(*Journal* page 158**): Chandelier stalactite, Western Branch (Jewel Box). Photo by David Harris, Harris Photographic.**

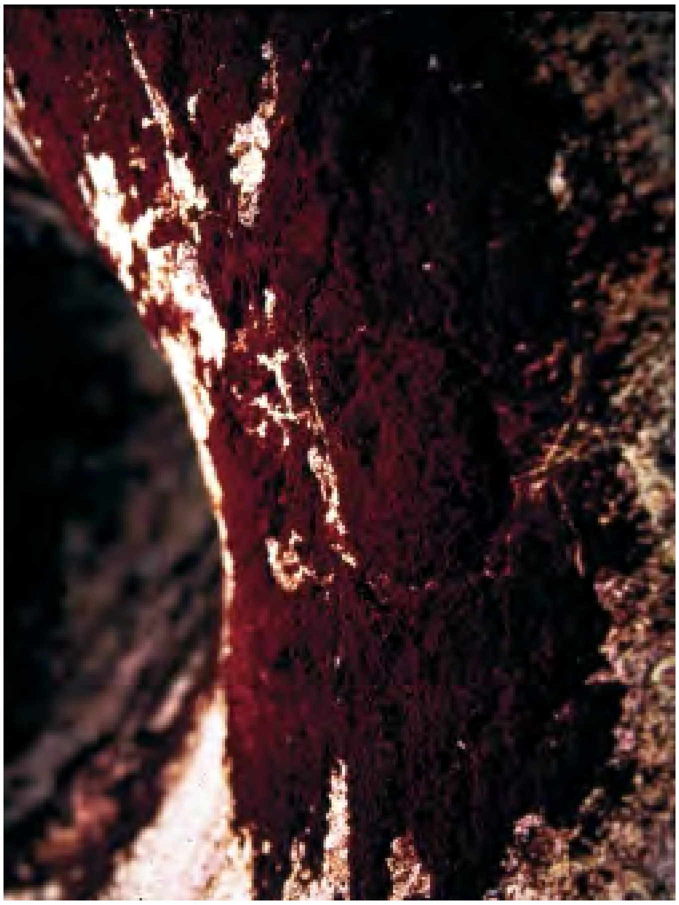

Figure 2 (Top Left). Acid lake undercut and rillenkarren above, in Far East (Bryce Canyon). Rillenkarren are more than 1 m high. Photo by Kathy Sisson-DuChene.
Figure 3 (Top Right). "Crevasse" in gypsum "glacier," Prickly Ice Cube Room. Photo by David Harris, Harris Photographic.
Figure 4 (Bottom Left). Sulfur mass, Near East (Ghostriders balcony). Photo by Kathy Sisson-DuChene.
Figure 5 (Bottom Right). Corrosion residue coating wall, Land of the Lost vicinity. Area shown ~1 m high. Photo by David Harris, Harris Photographic.

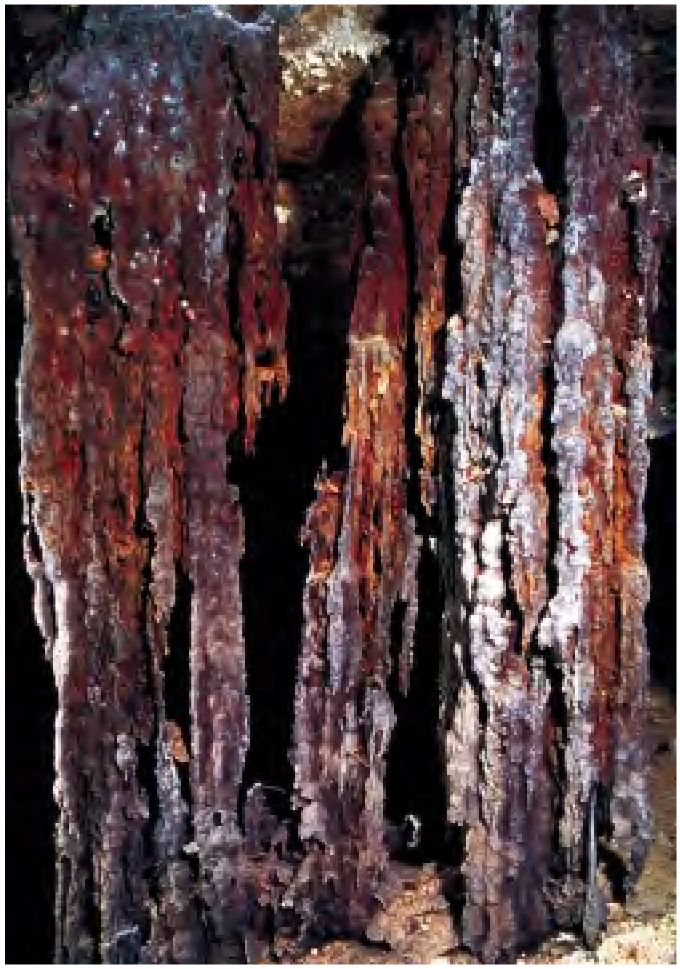

Figure 6 (Top Left). Stratified air line, Near East (Emperors Throne Room). Photo by Nick Nichols.
Figure 7 (Top Right). Rusticles, Near East. Area shown ~1 m high. Photo by David Harris, Harris Photographic.
Figure 8 (Bottom Right). Pool fingers, Southwestern Branch (FLI room). Fingers ~0.3 m long. Photo by David Harris, Harris Photographic.

Figure 9 (Bottom Left). Subaqueous helictites ~0.3 m long, in High Hopes. Photo by David Harris, Harris Photographic.
Figure 10 (Top Left - Next Page). The Gripping Hand (Blanca Navidad Room). Note caver for scale. Photo by David Harris, Harris Photographic.

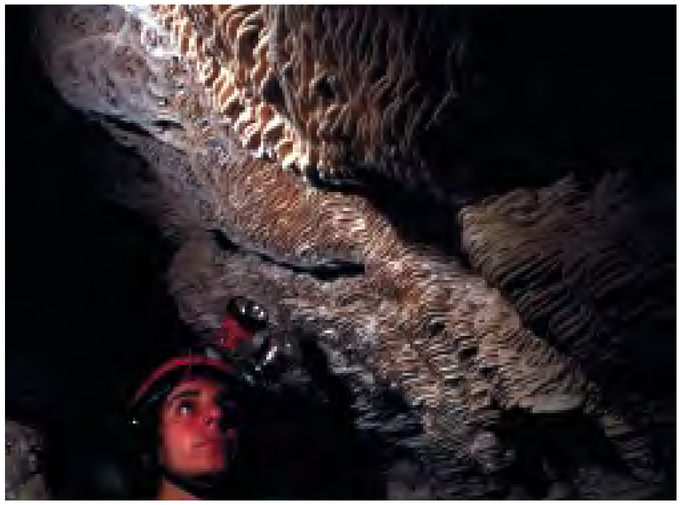

Figure 11 (Top Right - Previous Page). Common-ion-effect stalactite with rimstone pad (Far East). Photo by David Harris, Harris Photographic.

Figure 12 (Bottom Left - Previous Page). Chandelier stalagmite, Far East. Photo by Kathy Sisson-DuChene.

Figure 13 (Bottom Right - Previous Page). Long gypsum hair, Southwestern Branch (Darktown). Visible section ~0.3 m long. Photo by Larry McLaughlin.

Figure 14 (Top Left). Hydromagnesite fronds, Rock 'n Rillen Room (Western Branch). Longest ~7 cm long. Photo by Peter Bosted.

Figure 15 (Top Right). Folia, Sulfur Shores. Photo by Dick LaForge.

Figure 16 (Middle Left). High-angle raft cones, encrusted with aragonite (Hoodoo Hall). Height up to ~5 m above basal slope. Photo by David Modisette.

Figure 17 (Bottom Right). Silticles, Far East (Boundary Waters). Area shown ~0.7 m high. Photo by David Harris, Harris Photographic.

Figure 18 (Bottom Left). Small negative splash ring in gypsum, Chandelier Graveyard. Photo by Peter Bosted.

National Speleological Society
2813 Cave Avenue
Huntsville, Alabama 35810-4431